Geologia Croatica
Journal of the Croatian Geological Survey
and the Croatian Geological Society

2026 | 79/1 | 69–128 | 35 Figs. | 5 Suppls. | www.geologia-croatica.hr

Source rocks of the External Dinarides, Croatia

Tamara Troskot-Čorbić[1,*] and Damir Takač[2]

[1,*] INA-Industrija nafte, d.d., Exploration & Production, E&P Laboratory, Lovinčićeva 4, Zagreb, Croatia, retired; (*corresponding author: troskottamara@gmail.com)
[2] INA-Industrija nafte, d.d., retired, Nova Cesta 28, Zagreb, Croatia; (dambato@gmail.com)

doi: 10.4154/gc.2026.02

Crossref Similarity Check

Article history:
Manuscript received: April 3, 2025
Revised manuscript accepted: October 1, 2025
Available online: February 25, 2026

Keywords: Dinarides, source rocks, petroleum potential, asphalt, migrabitumen

Abstract

The External Dinarides, with an abundance of both autochthonous and allochthonous organic matter, have been the subject of sustained petroleum exploration by INA – *Industrija nafte, d.d.* (INA), Croatia's national oil company, since the 1960s. To evaluate the residual hydrocarbon potential, a comprehensive suite of geochemical analyses, encompassing over 5,000 samples from drill cores, cuttings, outcrops, and formation fluids, have been performed. These investigations have delineated potential source rocks within various stratigraphic horizons and established critical genetic linkages between these source rocks and generated hydrocarbons, thereby refining the understanding of the region's petroleum systems. This article synthesizes INA's key findings derived from the extensive source rock data analysis, offering valuable insights into the remaining hydrocarbon prospectivity of the External Dinarides.

1. INTRODUCTION

The External Dinarides form a complex fold-and-thrust belt along the northeastern Adriatic margin and comprise a thick stratigraphic succession from the Carboniferous to the Quaternary (VLAHOVIĆ et al., 2005). Diverse depositional conditions across the region have resulted in significant variations in the type and abundance of organic matter which occurs as thin laminae, thicker layers, dispersed matter within the mineral matrix, and migrated bitumen in cracks and cavities. These diverse occurrences define the two primary types of organic-rich rocks in the Dinarides: laminated carbonates containing indigenous organic matter (kerogen and associated bitumen), and bituminous dolomites and limestones containing allochthonous, migrated, or degraded hydrocarbons. Both types were identified long ago and were called by geologists "the primary and secondary bituminous rocks".

Abundant oil seeps throughout the External Dinarides, both coastal and inland, have been documented since the 13th century. Bitumen-asphalt was exploited, and traded, leading to the establishment of bitumen mines in the 18th and 19th centuries (ŠEBEČIĆ, 1995, 1996). Extensive surveying of surface bitumen occurrences commenced in the 20th century (MARGETIĆ, 1950). Notably, the "bituminous girodal schists" of Baljevac, Korenica, and the "Lemeš Formation" (Jurassic deposits in Lika, Knin, Svilaja, and Dinara) were exploited (FURLANI, 1910; MARGETIĆ, 1950; VELIĆ, 2007). Extensive regional mapping described the "Lemeš Formation" (POLŠAK et al., 1977, 1978) and similar rocks on Mount Poštak (GRIMANI et al., 1972, 1975), identifying algal shale with source rock potential and the dominance of sapropel-type kerogen (JACOB et al., 1983; ŠEBEČIĆ & ERCEGOVAC, 1983). ŠEBEČIĆ (1979a, 1979b, 1980, 1982, 1983, 1984) and ŠEBEČIĆ et al. (1988, 1989, 1990) extensively characterized these bituminous rocks.

The widespread presence of asphalt, bitumen, oil shale, and coal spurred petroleum exploration by INA from the 1960s onwards. Altogether, 17 exploration wells were drilled across the onshore Dinarides and islands, a limited number given the region's size, indicating that the Dinarides, particularly the Lika region, remained largely unexplored. International companies, including AMOCO, ECL, and Shell, have also participated in exploration, most recently with INA's collaboration with GEPlan in 2018. INA's Exploration and Production (E&P) Laboratory conducted field prospecting, sampling, and organic geochemical analyses.

Since the petroleum potential of the Dinarides is closely linked to the Adriatic Sea (Adriatic Basin), especially the Adriatic Carbonate Platform (VLAHOVIĆ et al., 2005), the data from both regions are considered to predict the distribution of source rocks and other geological formations.

Historically, oil and gas exploration in Croatia focused on the Pannonian and Adriatic basins. The 1973 discovery of the Ivana gas field in the Adriatic Basin spurred extensive exploration, with over 176 wells drilled and 22 gas fields discovered (MALVIĆ et al., 2011). These fields were developed through a long-standing partnership between Croatia's INA and Italian energy majors ENI and EDISON. Since becoming the sole operator in the late 2018, INA has maintained an annual production output of approximately 200 to 250 million m^3 (INA, Annual reports, 2024–2025). Exploration in the Southern Adriatic and the Dinarides has been less successful, with non-commercial hydrocarbon indications in wells such as Ravni kotari-3, Kate-1, Vlasta-1, and Melita-1, contrasting with the Northern Adriatic.

Despite limited commercial success, the Dinarides are considered to have significant hydrocarbon potential, as explained in studies such as BARIĆ et al. (2003) and GRANDIĆ et al. (2004). Research was focused on the Adriatic offshore and the broader Peri-Adriatic region, particularly on Cretaceous sediments and anoxic events (BARIĆ, 1988; BARIĆ et al., 1988; GUŠIĆ & JELASKA, 1990, 1993; JENKYNS, 1991; MOLDOWAN et al., 1992; JERINIĆ et al., 1994; ŠPANIĆ et al., 1995; COTA & BARIĆ, 1998; BARIĆ & COTA, 1999, 2003; BARIĆ & TARI, 2005; FIKET et al., 2008; GRANDIĆ et al., 1997, 1999, 2001, 2002a, 2002b, 2004, 2013, 2014; GRANDIĆ, 2010; COTA et al., 2015; VELIĆ et al., 2015). This body of work suggests substantial potential for future hydrocarbon discoveries, driving petroleum exploration in Croatia beyond the Pannonian and Adriatic basins.

The broader Mediterranean region contains diverse petroleum provinces with varied source rocks (ZAPPATERRA, 1994). A petroleum system, comprising the geological elements and processes of hydrocarbon generation, migration, and accumulation, is characterized by active source rocks, migration pathways, reservoirs, traps, seals, and overburden (MAGOON & DOW, 1994; DEMAISON & HUIZINGA, 1994). The widespread surface occurrences of asphalt and oil seeps in the Dinarides, the Dalmatian Asphalt Hydrocarbon Zone, as defined by ZAPPATERRA (1994), indicate a working petroleum system. BARIĆ et al. (2003) identified two petroleum systems in the Adriatic offshore: a Plio-Pleistocene system in the north with commercial biogenic gas production, and a second, hypothetical Jurassic – Cretaceous carbonate system in the central part of the Adriatic where accumulations have yet to be discovered. Studies of Italian hydrocarbons (MATTAVELLI & NOVELLI, 1990; MATTAVELLI et al., 1991; KATZ et al., 2000) and those in Greek and Albanian basins (RIGAKIS & KARAKITSIOS, 1998; PRIFTI & MUSKA, 2013), along with Dinarides-focused research (JACOB et al., 1983; BARIĆ et al., 1988; ŠPANIĆ et al., 1995; COTA & BARIĆ, 1998; BARIĆ, 2006; VELIĆ, 2007; FIKET et al., 2008; BLAŽEKOVIĆ SMOJIĆ et al., 2009; TROSKOT-ČORBIĆ, 2011; VELIĆ et al., 2015; VITZTHUM et al., 2021), suggest active source rocks and the elements for hydrocarbon accumulation. However, a comprehensive synthesis of the petroleum system elements for the entire External Dinarides is still needed. While preliminary results have been presented at conferences (e.g., BARIĆ & COTA, 2003; BARIĆ & TARI, 2005; ŠPANIĆ et al., 1995; ŠPANIĆ & TROSKOT-ČORBIĆ, 2013; TROSKOT-ČORBIĆ & ŠPANIĆ, 2010; TROSKOT-ČORBIĆ et al., 2005, 2015; TROSKOT-ČORBIĆ, 2019), a synthesis is still to be completed. Although there have been no commercial discoveries to date in the Dinarides and much of the Adriatic region, the presence of source rocks and hydrocarbon indicators offer a promising future exploration. Unpublished internal INA studies and detailed interpretations of organic facies in the Upper Jurassic deposits of Gorski Kotar, Lika, and Dalmatia (TROSKOT-ČORBIĆ, 2011) underpinned the recent Dinarides bidding round by the Croatian Hydrocarbon Agency (CHA) in 2020 – 2023 (TAKAČ et al., 2021).

This paper aims to address this gap by providing a comprehensive interpretation of over 5000 borehole and outcrop samples. The objectives are to: (a) evaluate the hydrocarbon potential of the External Dinarides; (b) identify and verify the potential source rocks across multiple stratigraphic levels; (c) establish genetic correlations between source rocks and hydrocarbons; and (d) assess the overall petroleum system/systems.

2. GEOLOGICAL SETTING

2.1. Geotectonic position

The Dinarides belong to the complex tectonic system of the Mediterranean realm, shaped by the interaction of the African and Eurasian plates (Fig. 1). Following the Variscan orogeny, the Mediterranean area was characterized by rifting (CARMINATI & DOGLIONI, 2005).

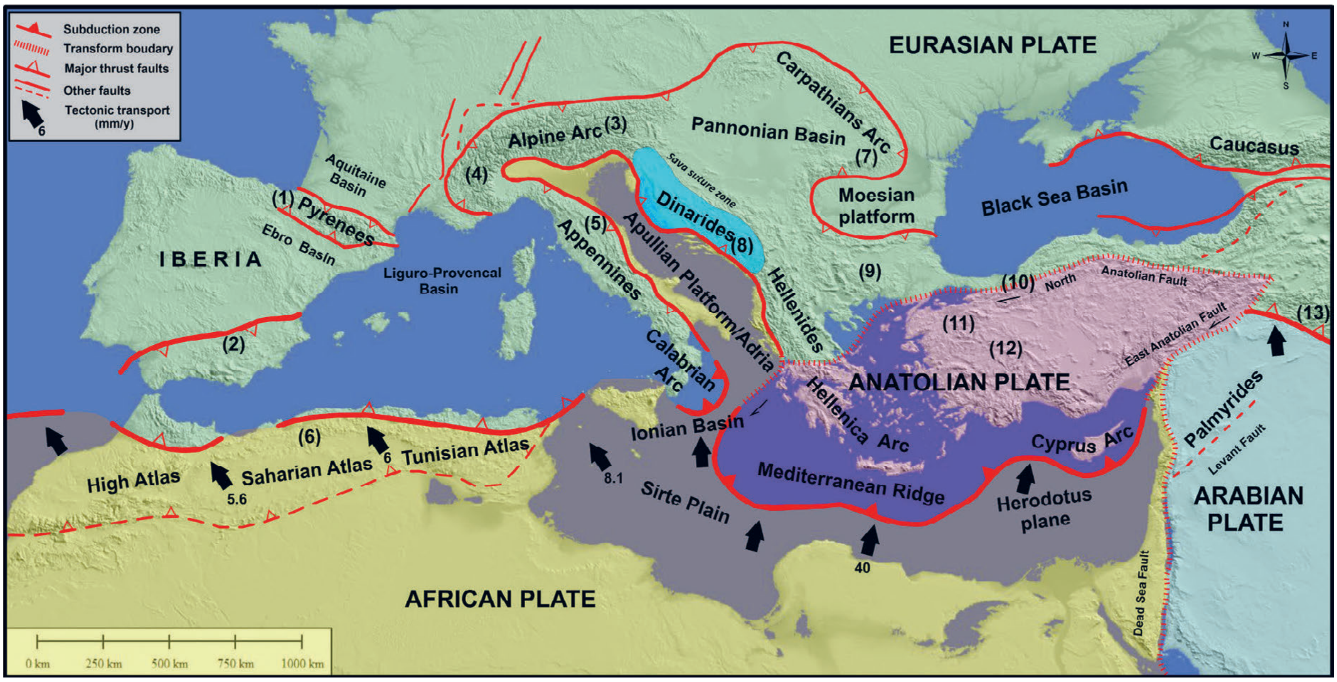

Figure 1. A simplified tectonic map of the Mediterranean region showing plate boundaries, collision zones, and directions of extension and tectonic transport. The main collision zones are numbered: (1) Pyrenees, (2) Betics, (3) Eastern Alps, (4) Western Alps, (5) Apennines, (6) Maghrebides, (7) Carpathians, (8) Dinarides – Albanides – Hellenides, (9) Balkanides, (10) Intra-Pontide Suture Zone, (11) Izmir – Ankara – Erzincan Suture Zone, (12) Inner Tauride Suture, (13) Bitlis – Zagros Suture (modified after CHAMOT-ROOKE et al., 2005; DILEK, 2006).

During the Mesozoic, various carbonate platforms formed along passive continental margins (VLAHOVIĆ et al., 2005). In the Late Mesozoic, subduction zones dominated the Mediterranean (Cimmerian, Dinarides, and Alps – Betics from east to west), reversing extension and consuming Tethyan oceanic lithosphere and adjacent continental margins (CARMINATI & DOGLIONI, 2005; CARMINATI et al., 2012). These events resulted in mountain and plateau building, magmatism, foreland and hinterland deformation, foreland flexures and sedimentary basin evolution, escape tectonics, orogenic collapse, lithospheric-scale extension, and the opening of small ocean basins (DILEK, 2006). These events were influenced by collision magnitudes, continental margin geometry, and mantle dynamics (DEWEY et al., 1986; JOLIVET et al., 1999; SPAKMAN & WORTEL, 2004). Most of the colliding continental blocks had Gondwanan affinity, with their tectonic history involving Tethyan seaway evolution and relative motions between Eurasia and Gondwana (DILEK & MOORES, 1990; DILEK et al., 1999). Opening of the ocean basins led to continental fragment rifting from Eurasia, Iberia, and Africa (Gondwana), forming separate platforms and basins (DERCOURT et al., 1986, 2000). The resulting continental and oceanic lithosphere were consumed by subduction zones accommodating Africa – Eurasia convergence since the Middle Jurassic (GAINA et al., 2013; HANDY et al., 2010, 2015; SCHMID et al., 2008).

The Mediterranean region's turbulent geological history includes several Messinian salinity crises. Africa – Eurasia convergence and glacio-eustatic sea level fall isolated the Mediterranean, leading to episodic desiccation and evaporite precipitation (RYAN et al., 1971; KASTENS et al., 1990). Messinian evaporitic deposition occurred in isolated basins, differing from pre-Messinian basins with hemipelagic facies (CAVAZZA & WEZEL, 2003). Reconnection with the Atlantic Ocean occurred 5.33 million years ago through the Strait of Gibraltar, with the "Zanclean flood" filling grabens with ocean water. Rapid river incision near Gibraltar caused slope retreat and eventual Atlantic overflow. The Mediterranean refilling likely took less than 1000 years (HSÜ et al., 1973). Another major flood occurred in the eastern Mediterranean, likely through southeastern Sicily (MICALLEF et al., 2018). The Zanclean mega-flood's erosional signature is smaller in the Sicily Channel (shallow water carbonates) than in the Strait of Gibraltar (flysch) (GARCIA-CASTELLANOS et al., 2009). Pliocene Trubi Formation marls mark the end of the Messinian desiccation and the return to normal marine sedimentation (DECIMA & WEZEL, 1973; CITA & MCKENZIE, 1986).

Several major collision zones occurred: (1) the Pyrenees between Africa and Europe, (2) the Betics between Africa and Iberia, (3) the Eastern Alps between Adria and Eurasia, (4) the Western Alps between Adria and Eurasia, (5) the Apennines between Adria and the Apenninic platform, (6) the Maghrebides between Africa and Europe, (7) the Carpathians between Pannonian basin and East European Platform, (8) the Dinarides – Albanides – Helenides between Adria and Pelagonia/Eurasia, (9) the Balkanides between the Moesian platform/Rhodope and Strandja Massif, (10) the Intra-Pontide Suture Zone between Sakarya and Western Pontides, (11) the Izmir-Ankara-Erzincan Suture Zone, (12) the Inner Tauride Suture, and (13) the Bitlis – Zagros Suture between Arabia and Eurasia (Fig. 1; DILEK & MOORES, 1990). The Alps and Apennines most significantly influenced development of the Dinarides.

The Alps were formed during two collisional events: the Adria – Eurasia collision in the Eastern Alps (Cretaceous), and the Adria – Eurasia collision in the Western Alps (Tertiary), involving Apulian and Eurasian crust imbrication and strike-slip deformation from Apulia's counterclockwise rotation (COWARD & DIETRICH, 1989; DEWEY et al., 1989; DILEK et al., 1999; DILEK, 2006; STAMPFLI & BOREL, 2004).

The Apennines resulted from the collision of Adria's western passive margin with the Apenninic platform and Europe along a west-dipping subduction zone (DOGLIONI et al., 1999). The deformation front migrated north-eastward, eastward, and south-eastward, with significant shortening (80 – 200 km), uplift (up to 2.5 km), and subsidence (up to 5 km) (CAVAZZA et al., 2004).

The Adriatic plate (Adria), where Mesozoic – Early Tertiary carbonates were deposited, is interpreted either as a single plate or as a collage of several (BOSELLINI, 2002; VEZZANI et al., 2010; VLAHOVIĆ et al., 2005; KORBAR, 2009). Adria's relationship with Africa is debated, with some considering them to be continuous unit (MUTTONI et al., 2001; SCHETTINO & TURCO, 2011) and others to be separated by an oceanic realm. GPS data indicate Adria's slow movement away from Africa (DEVOTI et al., 2008). The Dinarides development involved Upper Permian – Miocene tectonic events, including the Oligo-Miocene fold-thrust belt formation from Adria – Eurasia convergence that actually took place from the Middle Jurassic (SCHMID et al., 2020; VAN HINSBERGEN et al., 2020). Restoring Adria's north-directed displacement and Southern Alps shortening requires a 20° counterclockwise rotation, and is supported by palaeomagnetic, seismotectonic, and GPS data (ANDERSON & JACKSON, 1987; CALAIS et al., 2001; BATTAGLIA et al., 2004; WEBER et al., 2006). Formation of the Dinarides involved south-directed thrusting, ongoing shortening, transpression, and thrusting (USTASZEWSKI et al., 2008). The Sava suture zone, formed by the Tisza – Dacia Mega-Unit convergence with Adria, separates the Dinarides and Tisza – Dacia (SCHMID et al., 2008; USTASZEWSKI et al., 2010). Neotethyan closure along the Sava Zone occurred in the Maastrichtian to Early Palaeogene (PAMIĆ, 1993, 2002), with Early Miocene syn-rift sediments sealing Mid-Eocene thrusting (TARI, 2002).

2.2. Evolution of the Dinarides

The Dinarides mountain range is characterized by a thick sequence of sedimentary rocks spanning the Upper Palaeozoic, Mesozoic, and Palaeogene periods, with localized occurrences of Miocene lacustrine sediments. Obducted ophiolites and volcanic formations are also present, primarily concentrated in the northern part of the Adriatic microplate. Most of the sedimentary rocks originated from the vast Adriatic Carbonate Platform (AdCP) (VLAHOVIĆ et al., 2005). In contrast, the ophiolites and volcanic formations are linked to significant

Figure 2. A map showing the present-day distribution of the Adriatic Carbonate Platform (AdCP) deposits, delineated by outcrop and offshore well data (southwestern platform margin after GRANDIĆ et al., 1999; northeastern platform margin after DRAGIČEVIĆ & VELIĆ, 2002) (modified after VLAHOVIĆ et al., 2005).

tectonic events, notably the collision of the Adriatic plate with Europe-derived units at the end of the Cretaceous. Earlier, during the latest Jurassic to earliest Cretaceous period, Triassic – Jurassic ophiolites were obducted onto the distal Adriatic passive margin (PAMIĆ, 1993). As the Dinarides in Croatia are predominantly composed of carbonate sediments derived from the AdCP, their geotectonic evolution is intrinsically linked to the long-term evolution of this platform over at least 300 million years, including its foundational basement (Fig. 2).

The base of the AdCP, and consequently of the Dinarides, is composed of Upper Carboniferous and Lower Permian siliciclastic deposits, transitioning upwards into Middle Permian to Middle Triassic mixed carbonate and clastic deposits. These formed on an extensive epeiric platform along the northern margin of Gondwana (VLAHOVIĆ et al., 2005). Evidence of Middle to Upper Permian sabkha evaporites also exists (ŠUŠNJARA et al., 1992; TIŠLJAR, 1992). Middle Triassic volcanism, occurring across the broad epeiric carbonate platform, and a regional Middle/Late Triassic emersion event were consequences of broader regional events associated with Middle Triassic continental rifting (CHANNELL et al., 1979). This rifting event is considered to mark the initial breakup of the Adriatic plate (PAMIĆ et al., 1998), leading to the regional extension and development of deep normal faults that formed half-graben structures (LOWRENCE et al., 1995). These half-grabens provided the structural framework for a large, shallow-marine, isolated carbonate platform within the Southern Tethyan realm, where thick Upper Triassic sequences of early and late diagenetic dolostones accumulated (VLAHOVIĆ et al., 2005). A subsequent disintegration event occurred during the Toarcian. The formation of a trough connecting the Ionian Basin with the Umbria-Marche and Belluno pelagic basins, characterized by deep-marine deposition, represented the initial stage in the development of the present-day Adriatic Sea (BERNOULLI, 1971, 2001; VLAHOVIĆ et al., 2005). This newly formed entity is identified as the Adriatic Carbonate Platform (AdCP, VLAHOVIĆ et al., 2005). Concurrently, the future northeastern margin of the platform experienced emergence and subsidence (GUŠIĆ & BABIĆ, 1970; ŠIKIĆ & BASCH, 1975; DRAGIČEVIĆ & VELIĆ, 2002). This tectonic activity coincided with the Toarcian Oceanic Anoxic Event (OAE), and it is likely that the anoxic conditions slowed deposition and contributed to the drowning of tectonically subsided portions of the former platform (JENKYNS & CLAYTON, 1986; JENKYNS, 1988; PÁLFY & SMITH, 2000; JONES & JENKYNS, 2001). Middle Jurassic tectonic activity resulted in local uplifts, short-lived emersions, and the deposition of thin carbonate breccia beds in Istria (MARINČIĆ & MATIČEC, 1991), with similar short emersion events recorded at various Middle Jurassic intervals.

Synsedimentary tectonics played a major role in shaping the complex palaeogeography and depositional patterns during the Kimmeridgian and Tithonian (MATIČEC, 1989; TIŠLJAR et al., 1994, 2002; VELIĆ et al., 1994, 2002a, 2002b). While significant parts of the platform remained as restricted lagoonal environments, other areas were uplifted, emerged, and underwent karstification, leading to the localized formation of bauxites (e.g., western Croatia, western Bosnia, eastern Herzegovina, and western Montenegro). In the central part of the platform, these tectonic movements led to the formation of relatively shallow intraplatform troughs with deeper depositional settings, such as in Gorski Kotar or extending from Bihać towards the southeast (Croatia and western Bosnia, e.g., Poštak Mountain and the Knin area). This latter trough was connected to the open Tethyan realm and therefore contains deposits with greater pelagic influence, including limestones with chert, radiolarians, and ammonites – known as the Lemeš Deposits (also called, Lemeš Beds, Lemeš Layers, Lemeš Formation, Lemeš Facies, *Die Lemeš-schichten*, FURLANI, 1910; CHOROWICZ & GEYSSANT, 1972). By the end of the Jurassic, a new compressional/transpressional tectonic regime led to the formation of small pull-apart basins, local emersions, and facies differentiation. These compressional tectonics within the platform area were likely associated with the initiation of subduction northeast of the platform (VLAHOVIĆ et al., 2005). The Jurassic/Cretaceous transition in the central parts of the platform was marked by a brief period of emergence, observed in western and southern Croatia, western Bosnia, and parts of Montenegro, sometimes accompanied by bauxite occurrences (e.g., Dinara Mountain; VELIĆ et al., 2002a). The Lower Cretaceous is characterized by shallow-water environments and numerous short-lived emersions resulting from the interplay of tectonics and eustatic sea-level changes (MATIČEC et al., 1996). A regionally significant event occurred during the Lower Aptian, marked by the partial drowning of the platform. This is evidenced by massive mudstones and oncolites (e.g., Istria, Biokovo Mountain, Korčula Island) or well-bedded orbitolinid limestones with *Hedbergella* and *Saccoccoma* (e.g., Velika Kapela Mountain, VELIĆ & SOKAČ, 1978). This Lower Aptian event correlates well with the Early Aptian Oceanic Anoxic Event (OAE-1a, JENKYNS, 1980; JONES & JENKYNS, 2001). The transition from the Lower to Upper Cretaceous is largely characterized by thick late-diagenetic dolostones and heavily recrystallized limestones, sometimes preserving relics of early-diagenetic dolostones and tectogenic-diagenetic breccias (VLAHOVIĆ et al., 2005). The Late Cretaceous was the most complex period in the platform's history, representing its full maturity and the onset of its disintegration (VELIĆ et al., 2002a). Three key factors drove facies diversity: near continuous synsedimentary tectonic activity with varying local impacts, eustatic sea-level fluctuations, and the extensive development of rudist communities, which produced substantial amounts of carbonate material. The interplay of these factors resulted in diverse local geological responses. Around the Cenomanian/Turonian boundary, a temporary drowning of the platform occurred across a significant portion of its extent (GUŠIĆ & JELASKA, 1990, 1993; FUČEK et al., 1991; JELASKA et al., 1994; TIŠLJAR et al., 2002; VLAHOVIĆ et al., 2005). The northeastern platform margin was emergent from the Late Cenomanian (locally even the earliest Cenomanian) until the Late Santonian, with the formation of local bauxite deposits in Slovenia, Croatia, and Bosnia and Herzegovina (ŠPARICA, 1981; BUSER, 1987; DRAGIČEVIĆ & VELIĆ, 2002). This event correlates with the Cenomanian/Turonian Oceanic Anoxic Event (OAE-2, SCHLANGER et al., 1987; JENKYNS, 1985, 1991; JONES & JENKYNS, 2001). The final disintegration of the platform in the Late Cretaceous was driven by the interaction of eustatic sea-level changes and local tectonic controls. Compression, increasing in intensity from the Late Santonian/Early Campanian, led to the formation of several small, elongated troughs separated by shallower areas that were either completely emergent or covered by shallow sea (DRAGIČEVIĆ, 1987; VELIĆ et al., 2002a). Troughs located near the northeastern platform margin are characterized by continuous carbonate-clastic, flysch-type deposition from the Maastrichtian to the Palaeocene (DRAGIČEVIĆ & VELIĆ, 2002; VELIĆ et al., 2002a). Deeper-marine deposition with pelagic influences from the adjacent Budva-Cukali trough was recorded in the Split – Dubrovnik intraplatform trough during the Campanian, Maastrichtian, and Early Palaeogene (JELASKA et al., 2000). The Cretaceous – Palaeogene transition was marked by a period of emersion (of varying duration) across the entire AdCP, often associated with bauxite formation. In most areas, the oldest Palaeogene deposits are of Eocene age, although Maastrichtian and Palaeocene strata have been documented in some localities in SW Slovenia (DROBNE et al., 1989; JURKOVŠEK et al., 1996) and southern Croatia (GUŠIĆ & JELASKA, 1990). The Eocene – Oligocene flexural foreland basin system of the External Dinarides developed following the Palaeocene regional emergence phase, driven by southwestward propagating thrusting (BALLING et al., 2021). During the Palaeogene, these foreland basins were filled with various deposits: (1) Liburnian deposits – Palaeocene to Eocene freshwater to brackish limestones, with a limited distribution; (2) Foraminiferal limestones – predominantly Lower to Middle Eocene foramol-type limestones representing a range of environments from restricted inner platform (Miliolid limestones) to shallower and deeper shoreface (Alveolina and Nummulite limestones) and relatively open carbonate ramps (Discocyclina limestones); (3) Transitional beds – Middle Eocene deeper marine clayey mudstones and "Globigerina marls"; and (4) Flysch – mainly Middle Eocene to Lower Oligocene, extending up to the Lower Miocene in some places (VLAHOVIĆ et al., 2005). The continuation of compressional tectonics, with maximum stress oriented southwest-northeast, resulted in the final uplift of the Dinarides during the Oligocene – Miocene, giving them their characteristic northwest-southeast ('Dinaric') strike (VLAHOVIĆ et al., 2005).

The margins of the AdCP, which constitute the Dinarides, are largely covered. The southwestern margin is now submerged beneath the recent Adriatic Sea deposits. The northeastern platform margin is exposed in the Žumberak and Samoborska Gora Mountains north of Karlovac, although it is mostly obscured by overthrusted Palaeozoic – Triassic deposits, Late Cretaceous – Palaeogene flysch, or Neogene and Quaternary deposits (JELASKA, 1973, 1987; ŠPARICA, 1981; DRAGIČEVIĆ & VELIĆ, 1994, 2002; PAMIĆ et al., 1998).

2.3. Tectonic units of the Dinarides

The Dinarides fold-thrust belt, a prominent northwest-southeast trending orogen stretching approximately 700 km in length and 300 km in width, lies between the Southern Alps to the northwest and the Albanides to the southeast. Its formation is characterized by top-southwest shortening of a thick sequence of Mesozoic to Cenozoic sediments, with the internal parts also incorporating low-grade metamorphic Palaeozoic rocks of Gondwanan origin. This deformed sequence represents the Adriatic passive margin that once faced the northern branch of the Neotethys (SCHMID et al., 2020). The Dinarides are fundamentally divided into two genetically distinct parts: the External (Outer or Karst) Dinarides located along the Adriatic Sea, primarily consisting of remnants of the AdCP and its underlying basement, and the Inner (or Internal) Dinarides, situated between the External Dinarides and the Pannonian Basin, composed of rocks from both passive and active continental margin settings, including ophiolites (Fig. 3; PAMIĆ et al., 1998).

The External Dinarides are characterized by very thick (locally >8 km) Palaeo-Mesozoic platform carbonates belonging to the AdCP. This continuous sequence is interrupted along its southeastern margin by a deep-water Triassic – Cretaceous embayment known as the Budva unit in Montenegro (GORIČAN, 1994; BERNOULLI, 2001; VLAHOVIĆ et al., 2005; PICOTTI & COBIANCHI, 2017). The development of the Dinarides has been marked by several key geotectonic events throughout its geological history. The External Dinarides can be further subdivided into four main units (nos. 1 to 4 on Fig. 3; SCHMID et al., 2020).

1. The Adriatic Plate (no. 1 on Fig. 3): This unit often refers to the Istrian and Apulian carbonate platforms, framed by the external thrust belts of the Southern Alps, Dinarides, and Apennines. During its collisional interaction with the Alpine and Dinaridic orogens to the north and east, this part of the Adriatic plate acted as a rigid indenter (CHANNELL et al., 1979; SCHMID & KISSLING, 2000; PINTER et al., 2005). Also known as the Istrian Karst, it exhibits a significant hiatus between Cretaceous and Palaeogene carbonates, generally increasing from northeast to southwest (KORBAR, 2009). Structurally, this part of the platform forms a gentle anticline composed of over 2000 metres of thick Mesozoic carbonate deposits, ranging in age from the Middle Jurassic to the Eocene. Palaeogene Foraminiferal limestones and flysch unconformably overlie this Mesozoic sequence.
2. The Dalmatian Zone (no. 2 on Fig. 3): This zone is thrust over the undeformed Adriatic plate along a frontal thrust that is covered by the seafloor to the west and southwest of the outer islands. It is characterized by a nearly complete Cretaceous and Palaeogene carbonate sequence. Relatively narrow, it encompasses most of the

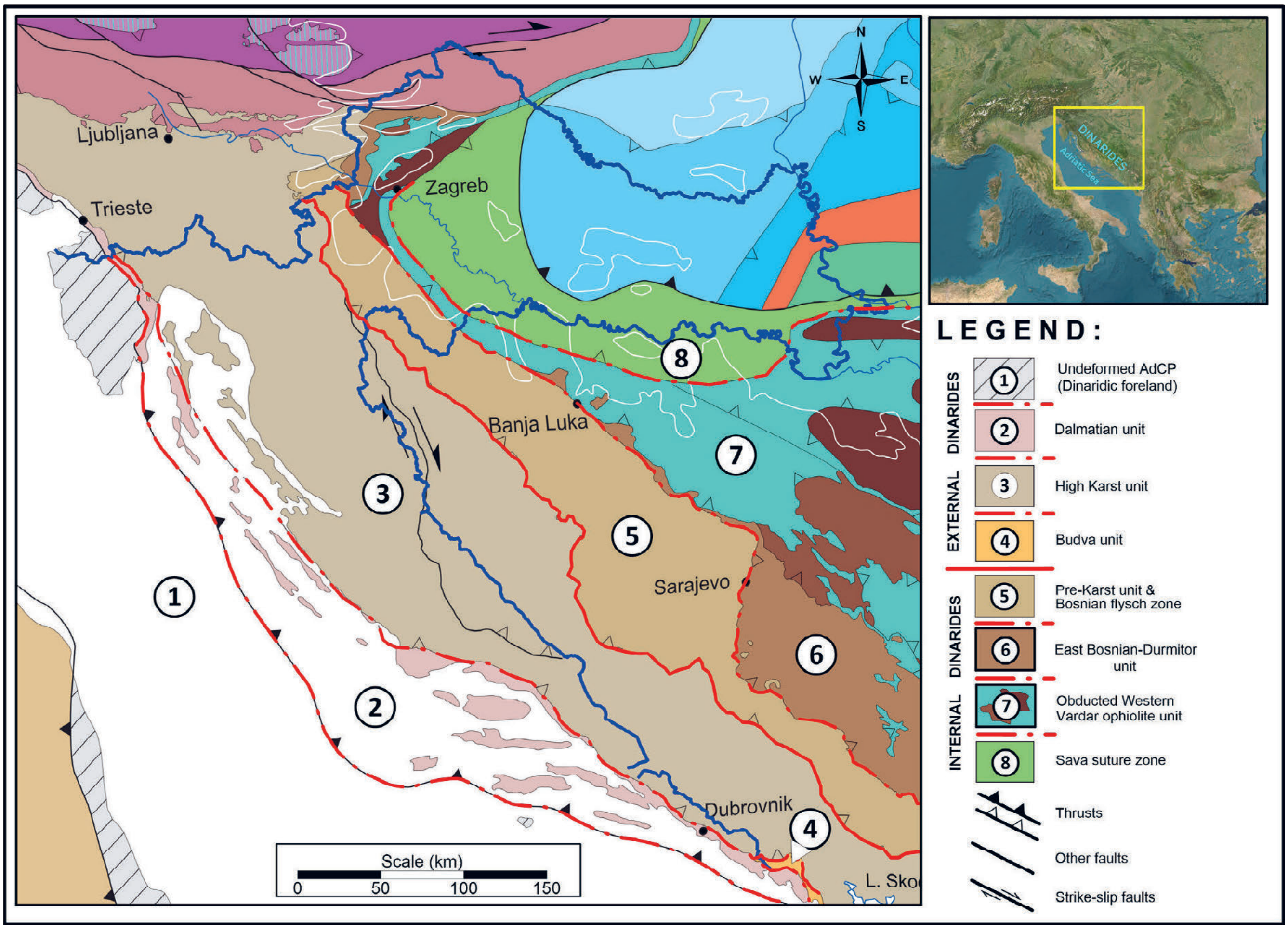

Figure 3. A tectonic map of the Dinarides showing key structural units (modified after SCHMID et al., 2008, 2020; USTASZEWSKI et al., 2008).

Adriatic islands and parts of the onshore area around Montenegro, Dubrovnik, Split, and the western half of the island of Cres. Deep exploratory drilling in the central Adriatic have encountered the layers of this zone. The Dalmatian zone is generally overlain by the High Karst unit, likely the last major thrust zone formed during the Dinarides' tectonic evolution.

3. The High Karst Unit (no. 3 on Fig. 3): This unit of the External Dinarides is defined by Late Triassic – Cretaceous carbonate platform facies and Palaeogene syn- and post-orogenic sediments. It overlies the Dalmatian zone along a thrust zone extending for more than 500 km, except in the southernmost area of Montenegro, where it overlies the Budva zone. Thrusting within this unit occurred primarily during the Late Eocene to Early Oligocene (the "Dinaridic phase" of the Southern Alps), evidenced by the accumulation of flysch-type sediments in a developing flexural foreland basin from the Middle to Late Eocene (TARI, 2002) and even into the Late Miocene (DE CAPOA et al., 1995). Later, the Split – Karlovac fault system, a 350-kilometre-long dextrally transpressive transverse fault located entirely within the High Karst unit, became active and affected Miocene-age strata in intra-montane basins (CHOROWICZ, 1975).
4. The Budva Unit (Montenegro) (no. 4 on Fig. 3): Situated in the southeasternmost part of the Dinarides coast, the Budva unit in Montenegro has a sedimentary record starting with Lower Triassic continental deposits (GORIČAN, 1994). These are followed by the upper part of Lower Triassic carbonates deposited on a carbonate ramp that experienced drowning in the Late Anisian. This drowning event was associated with normal faulting and rifting, accompanied by sub-volcanic intrusions, volcanic flows, tuffs, and radiolarites, ultimately leading to open marine deposition of predominantly deep-water limestones (ČADJENOVIĆ et al., 2008; VAN UNEN et al., 2019).

The Internal Dinarides consist of a stack of composite nappes, comprising continental units from the more distal Adriatic margin (SCHEFER et al., 2010; GAWLICK et al., 2017) that overlie obducted Western Vardar ophiolites (Fig. 3). These nappes formed through the sequence thrusting following the latest Jurassic obduction, primarily during the Late Cretaceous to Cenozoic orogeny (SCHMID et al., 2008). Obduction was succeeded by convergence between Adria and Eurasia, resulting in the northeastward subduction of remnant oceanic lithosphere beneath Europe-derived units (SCHMID et al., 2020; VAN HINSBERGEN et al., 2020). The continent-continent collision led to Maastrichtian – Palaeocene deformation and metamorphism of Upper Cretaceous trench deposits in the Sava Suture Zone (USTASZEWSKI et al., 2010) and subsequent nappe-stacking within the Internal Dinarides (SCHMID et al., 2020). The final closure of the Neotethyan oceanic basins along the Sava Zone occurred between the Maastrichtian and Early Palaeogene (PAMIĆ, 1993, 2002). This timing is supported by the observation that Early Miocene syn-rift sediments of the Pannonian Basin System overlie Middle Eocene siliciclastics that were affected by the final stages of post-collisional thrusting (TARI, 2002). Consequently, the Internal Dinarides are believed to have remained attached to the Tisza – Dacia Mega-Unit during the last 20 million years. The Internal Dinarides can be further divided into four main units (nos. 5 to 8 on Fig. 3, SCHMID et al., 2008).

1. The Pre-Karst and Bosnian Flysch Unit (no. 5 on Fig. 3): The Pre-Karst unit represents a palaeogeographic realm considered transitional between the carbonate platforms of the High Karst Unit and the more internal Bosnian Flysch, which is characterized by Late Jurassic to Cretaceous flysch deposits. The external parts of the Pre-Karst Unit show Jurassic – Cretaceous transitional platform-slope facies. From the Mid-Jurassic onward, breccias were shed northeastward from the High Karst palaeogeographic domain towards the more distal parts of the Adria passive continental margin, which had submerged during the Early Jurassic. The Bosnian Flysch comprises latest Jurassic to Cenozoic flysch-type deposits that exhibit variations in depositional age, palaeotectonic environment, and source area, both in strike and dip directions. In the most internal zones of these units, flysch deposition began during the Late Jurassic, becoming progressively younger towards the more external parts, where it commenced variably during the latest Cretaceous or even the Palaeogene. This flysch, containing radiolaritic pelagic intervals, formed at the leading edge of the Western Vardar Ophiolitic Unit during its obduction onto the Adria passive margin, the most distal parts of which were evidently transformed into an active margin during the Late Jurassic (SCHMID et al., 2008).
2. The East Bosnian – Durmitor Thrust Sheet (no. 6 on Fig. 3): This is a composite tectonic unit. Its lower part consists of Palaeozoic and Mesozoic formations that detached from the Adriatic passive margin during Cenozoic times. Its upper part is composed of the Western Vardar Ocean ophiolites, obducted during the Late Jurassic to earliest Cretaceous. The Palaeozoic to Mesozoic sequence culminates with Middle to Upper Jurassic radiolarites, deposited after an early Middle Jurassic drowning event (RADOIČIĆ et al., 2009; VISHNEVSKAYA et al., 2009). The northeast-southwest striking external thrust contact of this unit with the Bosnian flysch is significantly deflected to a north-south orientation in the Sarajevo area due to post-middle Miocene dextral strike-slip movements (VAN UNEN et al., 2019).
3. The Western Vardar Ophiolite Unit (no. 7 on Fig. 3): This unit represents the ophiolites that were obducted onto the Adria margin. It consists of a high-grade metamorphic sole, typically underlying the obducted ultramafic massifs. The ophiolitic mélange beneath the metamorphic sole, as well as younger strata that post-date obduction and are structurally part of this unit, are also included (SCHMID et al., 2008). Two additional units, the Drina – Ivanjica and Jadar – Kopaonik units, are surrounded by the Western Vardar Ophiolite Unit and can be considered integral parts of this broader complex. The

Drina – Ivanjica thrust sheet represents even more distal parts of the Adriatic passive margin. It was likely emplaced in Early to Mid-Cretaceous times on top of the East Bosnian – Durmitor thrust sheet and passively carried the previously obducted Western Vardar ophiolites (SCHMID et al., 2008). The Jadar – Kopaonik thrust sheet comprises a non-metamorphic Palaeozoic basement (Jadar block), overlain by Permian Bellerophon limestones, followed by a Triassic succession similar to that of the Drina – Ivanjica thrust sheet (DIMITRIJEVIĆ, 1997). The low-grade metamorphosed Palaeozoic to Mesozoic rocks form a tectonic window (Kopaonik block) within this unit.

4. The Sava Suture Unit (no. 8 on Fig. 3): Located at the northernmost edge of the Dinarides, the Sava Suture Unit marks the boundary between the upper plate Tisza and Dacia Mega-Units to the northeast and southeast, respectively, and the lower plate Internal Dinarides (SCHMID et al., 2008). Originally interpreted as a Late Cretaceous to Early Palaeogene volcanic (back-)arc basin, this belt of ophiolitic, magmatic, and metamorphic rocks was active until the Mid-Eocene collision between the Dinarides and the Tisza Block (PAMIĆ et al., 2002).

3. SAMPLES AND METHODS

From the 1980s onward, INA conducted a comprehensive organic geochemical study on over 5,000 samples. These samples, collected from boreholes (cores, sidewall cores, and cuttings) and surface outcrops, represent all the stratigraphic units within the Dinarides and Adriatic region (Fig. 4). All samples were subjected to rigorous quality control procedures. For the numerous surface samples, the potential impact of weathering was carefully evaluated, as secondary oxidation can significantly reduce organic carbon and bitumen content in organic reach rocks (CLAYTON & SWETLAND, 1978; WAPLES, 1985; LITTKE, 1993).

Petrographic and biostratigraphic analyses were performed to determine rock type and age. Organic geochemical investigations focused on laminated and fine-grained limestones and shales containing indigenous organic matter (kerogen and associated bitumen), as well as dolostones and limestones with migrated bitumen filling pores, fissures, and cavities.

The primary objectives of the organic geochemical study were to assess the quantity, quality, and thermal maturity of the organic matter present in the samples. Standard geochemical methods were employed for this evaluation.

Total organic carbon content (TOC, wt. %) was measured for all samples using Leco carbon analysers (Leco IR 212 and Leco C744) after acid removal of carbonates. Samples exceeding 0.5% TOC for clastic rocks and 0.3% TOC for carbonates (PALACAS, 1984; HUNT, 1995) were selected for further detailed analysis, following source rock evaluation criteria outlined by PETERS & CASSA (1994).

Selected samples underwent Rock-Eval pyrolysis using a Rock-Eval 6 instrument (ESPITALIÉ et al., 1985; ESPITALIÉ & BORDENAVE, 1993). The key Rock-Eval parameters (S_1, S_2, S_3, T_{max}, HI, OI, PI) are presented in the appendices. Standard diagrams illustrating these parameters are included in the figures. Due to the extensive Rock-Eval dataset, only TOC values derived from this method are presented in Appendices A-E.

Organic petrography, including vitrinite reflectance (VR, $\%R_o$), was performed according to established procedures (STACH et al., 1982; TAYLOR et al., 1998). Microscopic examination of organic matter concentrates (obtained after HCl/HF/$ZnCl_2$ treatment) was conducted using transmitted, blue-fluorescent, and reflected light microscopy (Olympus BH-2, Olympus BX-51, Leitz MPV-3, and Zeiss Axio Imager with MSP 210). Vitrinite reflectance (VR, $\%R_o$, random values with measurement statistics) was measured in oil immersion (50x magnification) in incident non-polarized light at 546 nm, calibrated against standards with known reflectance values. Vitrinite reflectance values were converted to peak palaeotemperatures using the formula by BARKER & PAWLEWICZ (1994): $T_{peak} = (\ln Rr + 1.68) / 0.0124$, with additional support from graphs and tables in RAINER et al. (2016) and BOSTICK (1979). When VR was measured on solid bitumen, mean random reflectance was calculated using JACOB's (1989) equation: $\%R_o = 0.618 * \%R_b + 0.40$ where $\%R_b$ represents bitumen reflectance (BR). Maceral descriptions followed the STACH et al. (1982) and TAYLOR et al. (1998) classifications. An internal Thermal Alteration Index (TAI) to VR ($\%R_o$) correlation scale was used: 1^+<0.35; 2^- 0.35 – 0.45; 2 0.45 – 0.55; 2^+ 0.55 – 0.70; 3^- 0.70 – 0.95; 3 0.95 – 1.25; 3^+ 1.25 – 2.00; 4^- 2.00 – 3.00; 4>3.00.

The sulphur content of kerogen, bitumen, and oil was determined using Leco SC 132 and Leco SC-144DR sulphur analysers via infrared detection after combustion in a pure oxygen environment at 1350 °C.

Stable carbon isotope analyses were performed using a Finnigan MAT delta E mass spectrometer, following SOFER's (1980) procedures. Carbon isotope ratios ($^{13}C/^{12}C$) are reported in ‰ relative to VPDB (Vienna Pee Dee Belemnite standard).

Selected samples underwent Soxhlet extraction using dichloromethane/methanol (72 hours) or chloroform (36 hours for aged samples). Extractable Organic Matter (EOM) concentrations (in ppm) were determined after solvent evaporation. The extracts were fractionated into saturated hydrocarbons (alkanes), aromatic hydrocarbons, NSO-compounds (resins), and asphaltenes using column liquid chromatography and further fractionated using an Agilent Solid Phase Extraction (SPE) unit with a silica gel stationary phase to isolate saturated hydrocarbons by n-hexane elution.

Gas chromatography (GC) analysis was performed on an Agilent 7890A instrument using a 50 m × 0.25 mm i.d. DB-petro column with a film thickness of 0.5 μm and helium carrier gas. The analysis employed a constant flow mode and a flame ionization detector. The oven temperature gradually increased, starting at 35 °C for 10 min, ramping to 40 °C at 1 °C/min, reaching 320 °C at 8 °C/min, and maintaining this temperature for 60 minutes.

Gas chromatography-mass spectrometry (GC-MS) was conducted using an Agilent 7890A GC coupled with an Agilent MS 5975C mass spectrometer (MS). The GC 7890A was fitted with a 30 m × 0.25 mm i.d. HP-5MS column, with a film thickness of 0.25 μm and using helium as the carrier gas. The

GC oven temperature was ramped from 60 °C to 145 °C at 15 °C/min, increased to 315 °C at 2 °C/min, and maintained at this temperature for 15 minutes. The mass spectrometer operated in electron impact (EI) mode at 70 eV, allowing for the identification of various compounds within the separated fractions. Specific biomarkers (terpanes, steranes, phenanthrenes, and methylphenanthrenes) were identified based on characteristic fragments and mass ranges, following established references (PETERS et al., 2005a, 2005b and references therein).

The outcomes of these extensive organic geochemical analyses enabled the delineation of potential source rocks and the documentation of allochthonous hydrocarbon occurrences across various stratigraphic levels. Furthermore, established genetic correlations clarified the relationships between specific hydrocarbons and their corresponding source rocks, providing valuable insights into their potential and quality, and ultimately aiding in the identification of optimal exploration targets.

4. RESULTS AND DISCUSSION

4.1. Carboniferous source rocks characterisation

Carboniferous shales from the Lika area exhibit promising organic matter enrichment (sample locations 16, 49, 59, 67, 79, 98, 105, 120 on Fig. 4; Suppl. 1, Table S1).

Shales in the Bruvno area show elevated organic matter content. In the Bruvno-1 well, marls and shales contain total organic carbon (TOC) ranging from 0.49% to 0.89%,

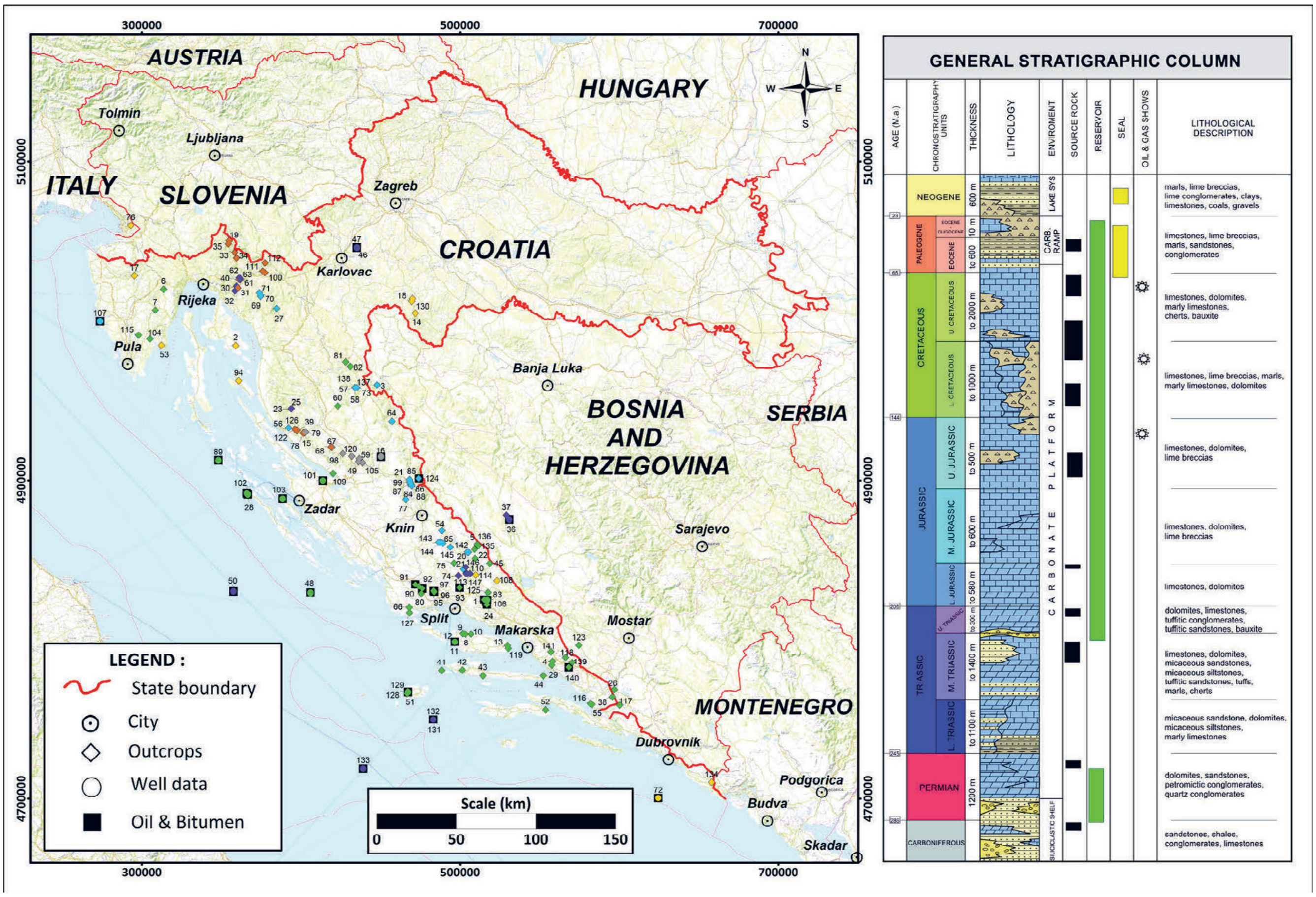

Figure 4. The spatial distribution of sampling locations for organic-rich carbonates and shales in the External Dinarides, displayed on a map with a generalized stratigraphic column illustrating lithology and petroleum system elements. Numeric labels on the map correspond to the alphabetical listing of sample locations provided below: (1) Akrap-Duboki Dolac, (2) Baška, (3) Bihać-Zavalje, (4) Biokovo-Duga Njiva, (5) Bitelić-Jelinjak, (6) Boljun, (7) Bolobani, (8) Brač-Brizi, (9) Brač-Mirca, (10) Brač-Škrip, (11, 12) Brač-1 well, (13) Brač-Sumartin, (14) Brezovo Polje, (15) Brušane, (16) Bruvno-1 well, (17) Buzet-Sovinjsko brdo, (18) Buzeta, (19) Čabar-Ravnice, (20) Dabar, (21) Dimići, (22) Dinara-Bitelić, (23) Donje Pazarište, (24) Donji Dolac-Okruglica, (25) Donje Pazarište-Jovanović potok, (26) Dračevo, (27) Drežnica-Jasenak, (28) Dugi otok-1 well, (29) Duge Njive, (30) Fužine-Bajer, (31) Fužine, (32) Fužine-Željeznička stanica, (33) Gerovo-Klukov, (34) Gerovo-Razloge, (35) Gerovo-Tršće, (36) Glamoč-1 well, (37) Glamoč-Busija, (38) Glušci, (39) Griči, (40) Homer, (41) Hvar-Pakleni otoci, (42) Hvar-Milna, (43) Hvar-Pitve, (44) Hvar-Sućuraj, (45) Kamešnica-Bili brig, (46, 47) Karlovac-2 well, (48) Kate-1 well, (49) Klarića Vrelo, (50) Kornati more-1 well, (51) Komiža, (52) Korčula-Krkmača, (53) Koromačno, (54) Kozjak, (55) Kremena-Ljubić potok, (56) Kubus, (57, 58) Koreničko Vrelo, (59) Ličko Cerje, (60) Ljubovo, (61) Lokve-Homer, (62) Lokve-Lazac, (63) Lokve-Špičunak, (64) Mamac, (65) Maovice, (66) Marina-Trogir, (67, 68) Marunovac, (69) Matić Poljana 1a, (70) Matić Poljana 1b, (71) Matić Poljana 1c, (72) Melita-1 well, (73) Milanović Draga, (74) Muć, (75) Ogorje-Milešina, (76) Padričano, (77) Palanka, (78) Paljež, (79) Pikovac, (80) Plišivica, (81) Plitvice-Hajduk Mlin, (82) Plitvice, (83) Poljica-1 well, (84) Poštak-Halda, (85) Poštak-Dimići, (86) Poštak-Dimići I, (87) Poštak-Škundrići, (88) Poštak-Vištice, (89) Premuda-1 well, (90) Primorski Dolac, (91-92) Primorski Dolac-Preslo, (93) Prugovo, (94) Rab-Lopar, (95) Radošić-Lastva, (96) Radošić-Ninčevića, (97) Radošić-Tenderi, (98) Raduč, (99) Rastičevo, (100) Ravna gora, (101) Ravni kotari-2 well, (102) Ravni kotari-3 well, (103) Ravni kotari-4 well, (104) Rebići, (105) Ričice, (106) Rošca, (107) Rovinj-1 well, (108) Ruda, (109) Seline, (110) Sinj, (111) Skrad-Most, (112) Skrad-Rastoke, (113) Sutina, (114) Sutina-Sinj, (115) Šajini, (116) Slivno Ravno-Kremena, (117) Srijetež, (118) Stilja-Vukmir, (119) Sumartin, (120) Sv.Rok-Lotići, (121) Svilaja, (122) Takalice, (123) Tihaljina-Zasjede, (124) Torbički Vagan, (125) Trilj, (126) Velika Draga, (127) Vinišće, (128) Vis-1 well, (129) Vis-Komiža, (130) Vladića Mlin, (131-132) Vis-1 well, (133) Vlatka-1 well, (134) Vodovađa, (135) Vrdovo-Bršič, (136) Vrdovo-Golo Brdo, (137) Vrelo-Milanovića Draga, (138) Vrelo-Zubovića Draga, (139) Vrgorac, (140) Vrgorac-Orlić, (141) Vrgorac-Kozica, (142) Vrlika-Dabar, (143) Vrlika-Lemeš, (144) Vrlika-Maovice, (145) Vrlika-Otišić, (146) Zelovo, (147) Zelovo-Sutinske Staje.

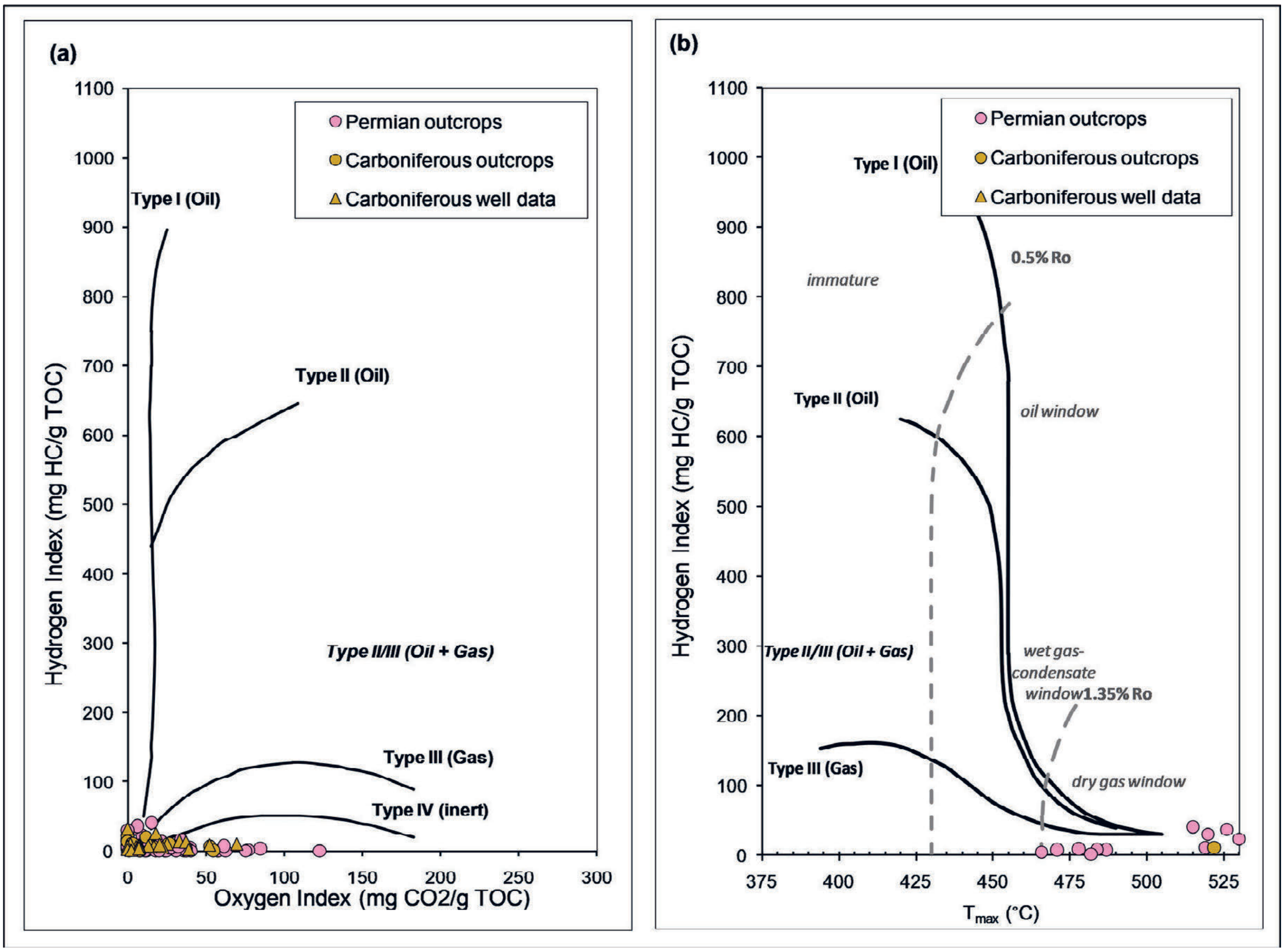

Figure 5. Source rock characterization of Carboniferous and Permian marls and shales using Rock-Eval pyrolysis data: **a** Hydrogen index (HI) *versus* oxygen index (OI) crossplot showing organic matter type distribution; **b** Hydrogen index (HI) *versus* T_{max} crossplot illustrating thermal maturity trends.

exceptionally reaching 4.08% in the uppermost sample. The organic matter in these samples is classified as predominantly terrestrial, gas-prone kerogen type III (Fig. 5), mainly composed of vitrinite macerals. The stable carbon isotope ratio of kerogen in the organic carbon-rich shale ($\delta^{13}C_{Ker.}$ -31.94‰, VPDB) supports a terrestrial origin. High thermal maturity, indicated by T_{max} > 500 °C, TAI 4$^-$, and VR > 2%R_o, suggests the organic matter has reached metagenesis. Vitrinite reflectance values indicate a maximum temperature exposure for these Carboniferous source rocks ranging from 200 to 220 °C,

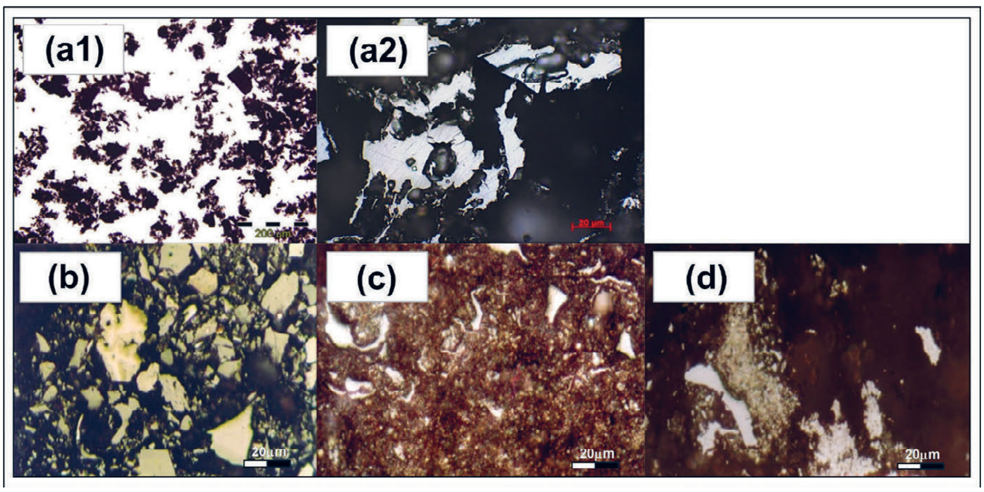

Figure 6. Photomicrographs of organic matter from Carboniferous and Permian carbonates and shales. **a** Pikovac shale: Thermally altered amorphous organic matter with high-reflecting vitrinite (VR 4.41%R_o) shown in transmitted white light **a1** and reflected white light with oil immersion **a2**; **b** Tršće-Sokolica siltite: Anisotropic vitrinite (VR 1.83%R_o) under reflected white light with oil immersion; **c** Brušane dark mudstone: Vitrinite (VR 2.07%R_o) in thermally altered amorphous organic matter, with pyrobitumen (BR>3%R_b) in pores and fractures (reflected white light, oil immersion); **d** Griči dark limestone: Vitrinite (VR 2.11%R_o) within thermally altered amorphous organic matter (reflected white light, oil immersion).

with a maximum of 245 °C (RAINER et al., 2016; BOSTICK et al., 1979; BARKER & PAWLEWICZ, 1994).

Similarly, shales from Pikovac, Marunovac, Ričice, and Ličko Cerje also exhibit elevated TOC content, generally ranging from 0.70% to 2.17%, with one exceptional sample reaching 14.30%. However, these shales show no evidence of free or generated hydrocarbons. The kerogen type is classified as III to IV (Fig. 5). Pyrolysis and microscopic analyses reveal a highly thermally altered stage, with T_{max} values exceeding 500 °C, a TAI of 4, and VR greater than 4%R_o, indicating a transition into the metamorphic stage. The maceral composition is dominated by vitrinite and inertinite, along with highly altered amorphous organic matter (Fig. 6a1, a2). Consequently, these shales possess no remaining hydrocarbon generation potential. The maximum temperature range to which these rocks were exposed is estimated to be higher than 220 to 245 °C, potentially reaching 260 – 270 °C (RAINER et al., 2016; BOSTICK et al., 1979; BARKER & PAWLEWICZ, 1994). Thermal maturity data indicate that Middle Triassic volcanism was a significant thermal event in the region's evolution. ŚRODOŃ et al. (2018) determined that the thermal climax occurred during the Late Cretaceous and Palaeocene, due to burial under high palaeogeothermal gradients. They estimated the thickness of the eroded sedimentary column overlying the Carboniferous rocks of the broader Bruvno area to be approximately 7 to 8 km.

4.2. Permian source rocks characterisation

Elevated organic matter content was observed in Permian clastic rocks and carbonates from Gorski kotar and Velebit Mountain (sample locations 15, 19, 31, 33 – 36, 39, 40, 63, 68, 78, 100, 111 – 112, 122, 126 on Fig. 4; Suppl. 1, Table S2).

In Gorski kotar, Permian shales (Homer, Lokve, Fužine, Mrzla Vodica, Ravna Gora, Gerovo, Čabar, Tršće, Skrad) have TOC ranging from 0.50% to 6.24%. The kerogen is type III to IV (Fig. 5), consisting primarily of thermally altered vitrinite and inertinite macerals (Fig. 6b). These shales exhibit a high degree of thermal alteration, reaching the catagenetic to metagenetic stage (T_{max} > 466 °C, TAI 3^+ to 4^-, VR 1.65 to 2.75%R_o). Consequently, they are not considered prospective for hydrocarbon exploration.

Similarly, Permian shales from Velebit Mt. (Brušane area (Takalice), Griči, Velika Draga, Marunovac) have elevated TOC (0.52% to 7.61%) and are highly thermally altered, reaching initial metagenesis (T_{max} > 482 °C, TAI 4^-, VR > 2%R_o). The kerogen is type III, possibly II/III, and consists mainly of unstructured amorphous organic matter with vitrinite and pyrobitumen particles (Fig. 6c, d). The stable carbon isotope ratios measured in two samples of bitumen (Griči and Velika Draga $\delta^{13}C_{Bit.}$ -24.76 and -28.04‰, VPDB, respectively) support the assumption of thermally altered kerogen type II/III. The presence of insoluble, highly reflective pyrobitumen, cata-impsonite (bitumen reflectance BR > 3.5%R_b, corresponding to VR >2.5%R_o, calculated using the conversion of JACOB (1989)), suggests these rocks generated hydrocarbons. These shales are interpreted as exhausted source rocks, having generated hydrocarbons between the end of the Triassic and early Jurassic, before the Dinarides' formation.

Upper Permian rocks from the Istrian Plateau (Rovinj-1 well) have low organic matter content and lack source rock characteristics (COTA & BARIĆ, 1998).

4.3. Triassic source rocks characterisation

Elevated organic carbon (TOC) content was found in Triassic shales from Gorski kotar, and in shales and mudstones from the volcano-clastic-carbonate complex in Velebit, Svilaja Mountains, on the island of Vis and in the Glamoč area, Bosnia and Herzegovina (B&H) (sample locations 23, 25, 30, 32, 36 – 37, 47, 50, 61 – 61, 74, 110, 113, 132 – 133, 146 – 147, on Figs. 4, 7; 8; Suppl. 2, Tables S1–S3). However, their hydrocarbon potential and the origin of their organic matter vary.

In Gorski kotar, TOC in Triassic shales (0.57 to 0.86%) is of terrestrial origin (Suppl. 2, Table S1). The kerogen is type III to IV (Fig. 8a–c), with predominantly vitrinite and inertinite macerals (Fig. 9a, b). High thermal alteration (VR 1.74 to 2.51%R_o, TAI>3^+, the absence of fluorescence) places these shales in a transitional stage between catagenesis and metagenesis, making them unsuitable for hydrocarbon generation (Fig. 8d).

Shales in the Velebit Mt. (Donje Pazarište area) have similar TOC values (0.30% to 0.89%; Suppl. 2, Table S1) and also lack hydrocarbon generation potential due to high thermal maturity (T_{max} > 480 °C, TAI 4^-, VR 1.84 to 2.52%R_o, absence of fluorescence), placing them in a transitional catagenesis/metagenesis stage (Fig. 8d). While Rock-Eval suggests type III to IV kerogen (Fig. 8a–c), other data indicate a mixed, predominantly marine (algal and bacterial) origin with minor terrestrial input (kerogen type III/II). This is supported by variable organically bound sulphur (0.34 – 6.34%) and stable carbon isotope ratios ($\delta^{13}C_{Ker.}$ -22.62‰ to -24.43‰, VPDB; $\delta^{13}C_{Bit.}$ -23.51‰ to -25.88‰, VPDB; Suppl. 2, Table S2, and in a diagram after SOFER (1984), Fig 10.), and the presence of amorphous organic matter with minor vitrinite, inertinite, and traces of pyrobitumen (Fig. 9c; TAYLOR et al., 1998; JACOB, 1985). These rocks, representing the oldest deep marine strata in the External Dinarides (SMIRČIĆ et al., 2020), contain algal and bacterially degraded organic matter, with some terrestrial input, deposited in anoxic marine conditions. They are considered inactive source rocks, having experienced maximum temperatures above 180 °C (BARKER & PAWLEWICZ, 1994; BOSTICK, 1979; RAINER et al., 2016), with hydrocarbon generation and expulsion likely occurring in the late Jurassic to early Cretaceous, before Dinaride formation. The remaining organic matter is unreactive carbon residue.

Triassic black limestones and calcareous shales in the Zelovo – Sutine and Muć area of Svilaja Mt. also have elevated total organic carbon (TOC) content, generally ranging from 0.40 to 3.23%, reaching up to 4.21% (Suppl. 2, Table S1). The kerogen is type III to IV and thermally altered (Fig. 8a–c). Maceral composition is dominated by amorphous organic matter, with varying proportions of vitrinite and inertinite (up to 20%). Traces of pyrobitumen suggest the possible presence of higher-quality kerogen type II, and gas and oil generation (Fig. 9d, f; JACOB, 1985). The absence of fluorescence and the low sulphur content are notable. Multiple lines of evidence indicate a mixed origin for the organic matter in these rocks, with a significant terrestrial contribution. Stable carbon isotope ratios of kerogen, bitumen, and saturated and aromatic hydrocarbons support this interpretation (Fig. 10a; SOFER, 1984; Suppl. 2, Table S2). Gas chromatography (GC) and gas chromatography-mass spectrometry (GC-MS) of extracted bitumen (SMIRČIĆ et al., 2018, 2020) further corroborate a mixed origin. The bitumen molecular distribution shows normal alkanes dominating over isoprenoids (Pr/nC_{17}, $Ph/nC_{18} < 1$), and a Carbon Preference Index (CPI) close to 1, indicative of mature bitumen. A Pr/nC_{17} *versus* Ph/nC_{18} cross-plot also suggests a mixed, predominantly terrestrial source (Fig. 10b; CONNAN & CASSOU, 1980). GC-MS reveals a dominance of hopanes over steranes (Fig. 11a1, a2; Suppl. 2, Table S3), indicating a pronounced role for bacteria in bitumen formation (OURISSON et al., 1979; ROHMER, 1993). The dominance of C_{29} homologues in C_{27} – C_{29} regular steranes points to a significant contribution from higher plants and bacteria (VOLKMAN et al., 1986; VOLKMAN, 1988). The initial organic matter deposition likely occurred in a shallow marine setting, with substantial terrestrial input and intensive bacterial processing (Fig. 12a; HUANG & MEINSHEIN, 1979). The presence of gammacerane suggests a marine, stratified water column (SINNINGHE DAMSTE et al., 1995), and the distribution of C_{31} – C_{35} homohopanes indicates reduced oxygen levels. While pristane generally dominates over phytane (Pr/Ph>1), suggesting an oxic environment or greater terrestrial input, this may be influenced by maturity (DIDYK et al., 1978). Vitrinite reflectance (VR 1.14 to 1.31%R_o), the thermal alteration index (TAI>3), and pyrobitumen reflectance (BR ≈1.6%R_b, corresponding to 1.38%R_o; JACOB, 1989) indicate a high degree of thermal maturity, reaching higher catagenesis. Sterane ratios (20S/(20S+20R) 0.39 – 0.42, ββ/(ββ+αα) 0.56 – 0.57) also suggest a main to late stage of oil generation (MACKENZIE et al., 1982; SEIFERT & MOLDOWAN, 1978, 1980, 1986; MACKENZIE & MAXWELL, 1981). These limestones and shales have therefore lost their hydrocarbon generation potential, having experienced maximum temperatures of 130 – 150 °C (BARKER & PAWLEWICZ, 1994; BOSTICK, 1979; RAINER et al., 2016), and are considered to be the primarily exhausted source rocks.

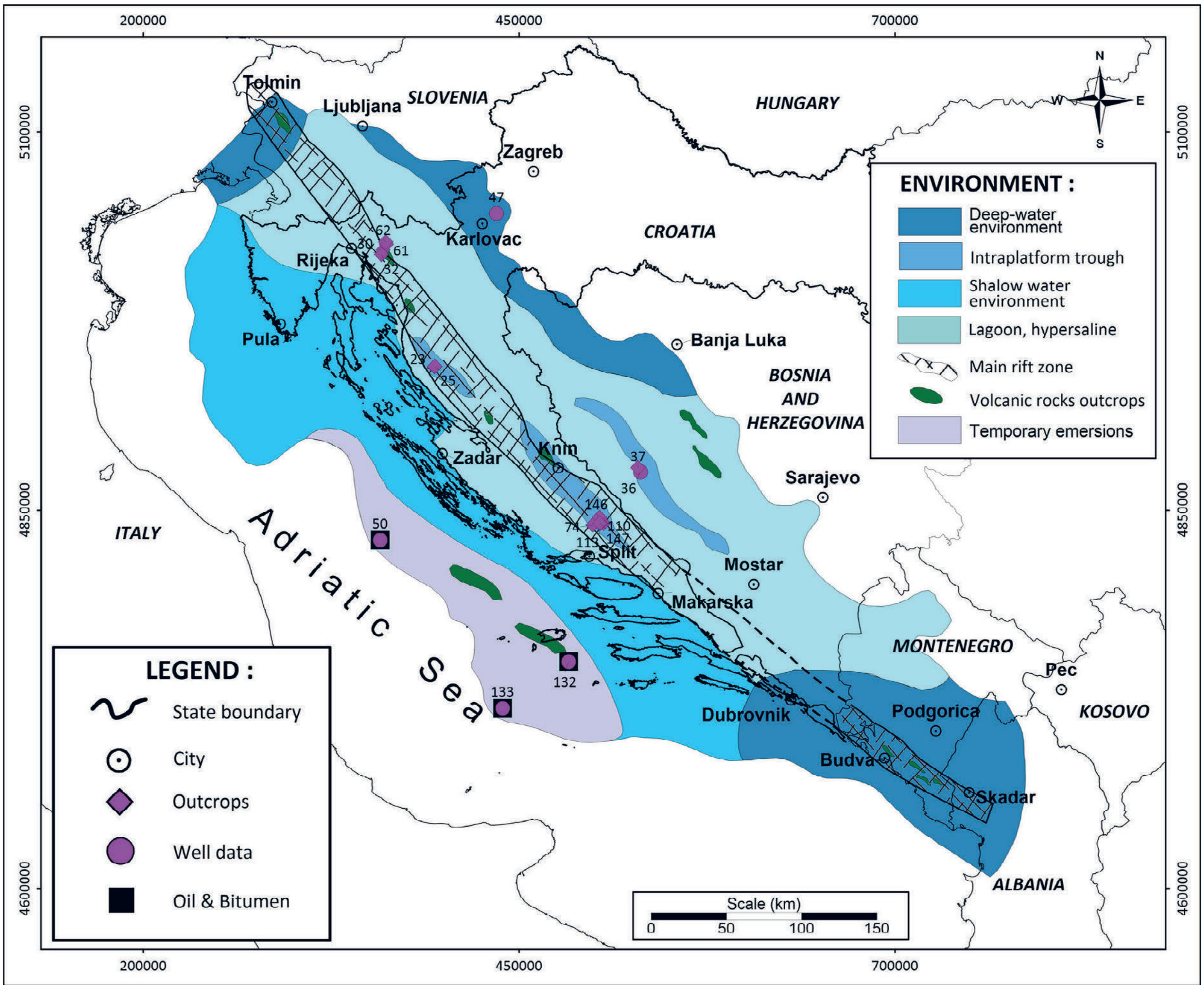

Figure 7. The spatial distribution of the sample locations of organic-rich carbonates and shales on a schematic Middle Triassic palaeogeographical map of the AdCP (Adriatic Carbonate Platform) showing the main sedimentary environments (modified after VELIĆ et al., 2002b and TARI, 2002). Sample location names are provided in Figure 4.

Ladinian calcite-rich shales outcropping in the Glamoč area in Bosnia and Herzegovina have elevated total organic carbon (TOC) contents (1.12 to 2.25%), demonstrating fair to good hydrocarbon potential (S_2 up to 5 mg HC/g rock; Suppl. 2, Table S1). The kerogen is of mixed types II and III, indicating the potential for both oil and gas generation (Fig. 8a–d). Thermal maturity, as indicated by T_{max} values (T_{max} ≤435º), suggests an early stage of maturation (diagenesis to early catagenesis), with palaeotemperatures (Tp) below 80 °C.

The Middle to Upper Triassic marls and limestones in the Glamoč-1 well (interval 1590 – 2160 m) also have increased TOC (0.5 to 2.6%; Suppl. 2, Table S1). However, their

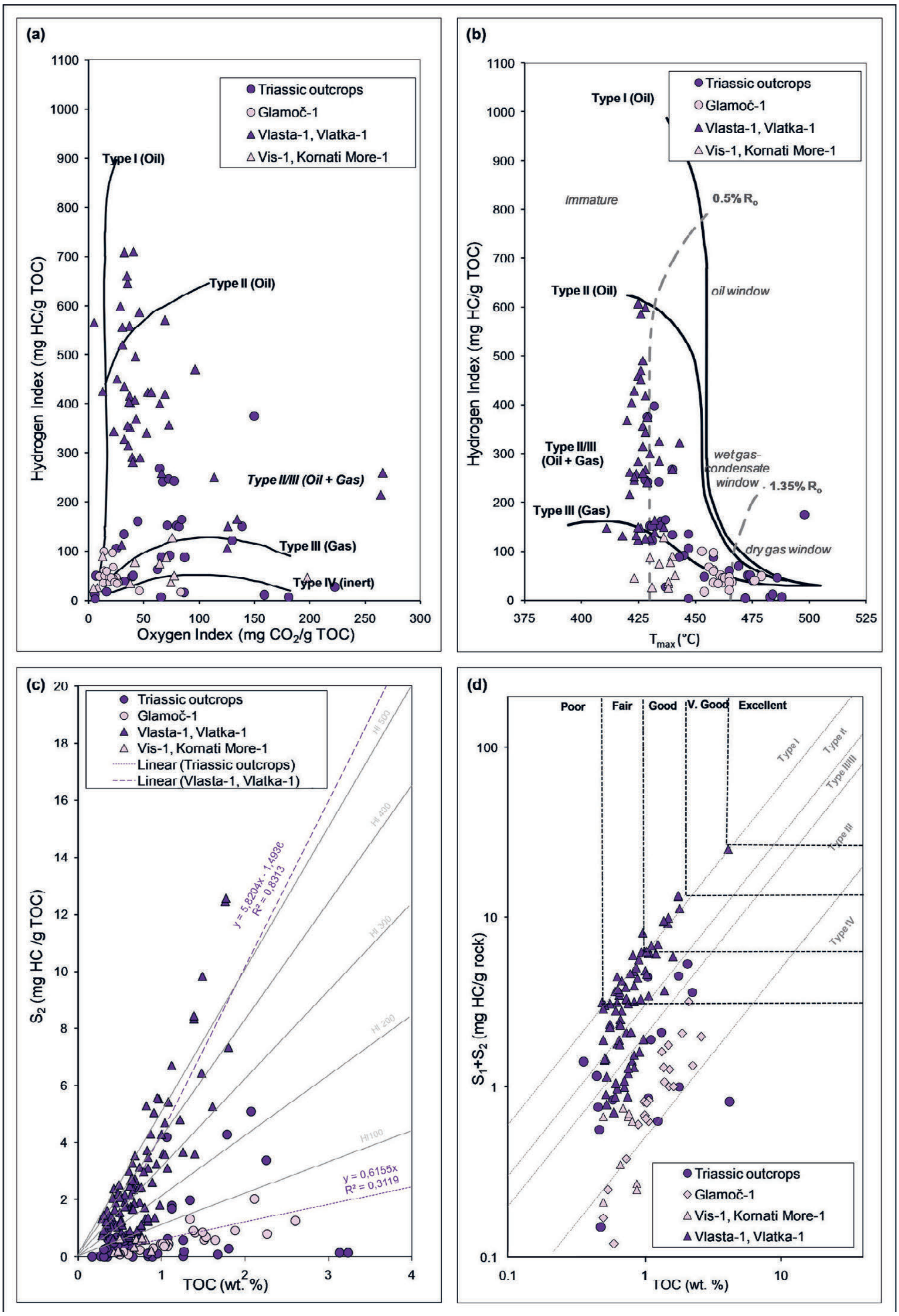

Figure 8. Source rock characterization of Triassic carbonates, marls, and shales using Rock-Eval pyrolysis data: **a** Hydrogen Index (HI) *versus* Oxygen Index (OI) crossplot showing organic matter type classification; **b** Hydrogen Index (HI) *versus* T_{max} crossplot illustrating thermal maturity levels and trends; **c** Generative Potential (S_2) *versus* Total Organic Carbon (TOC) crossplot with superimposed average Hydrogen Index (HI) trends, indicating hydrocarbon generation potential; **d** Source rock quality assessment using a crossplot of Petroleum potential (S_1+S_2) *versus* Total Organic Carbon (TOC).

generative potential is generally poor (S_1+S_2 ≤ 2 mg HC/g rock), due to higher thermal maturity (T_{max} > 450 °C, VR > 1.15%R_o). The maceral composition of the isolated organic matter is dominated by thermally altered amorphous organic matter with up to 15% vitrinite, inertinite, and pyrobitumen particles (Fig. 9d). The presence of pyrite and pyrite framboids suggests anoxic conditions during organic matter deposition. Stable carbon isotope ratios of bitumen, saturated, and aromatic hydrocarbons ($\delta^{13}C_{Bit.}$ -27.90‰ to -28.90‰, $\delta^{13}C_{Sat.}$ -28.06‰ to -29.34‰, $\delta^{13}C_{Aro.}$ -27.18‰ to -28.84‰, VPDB, respectively) indicate marine organic matter (Fig. 10a; SOFER, 1984). The n-alkane distribution of the extract is unimodal, with a maximum in the lower hydrocarbon range and a CPI close to 1, indicating higher maturity. The Pr/nC_{17} and Ph/nC_{18} ratios range from 0.43 to 0.82 and 0.52 to 0.62, respectively (Suppl. 2, Table S2). The Pr/Ph ratio varies from 0.25 to 0.51, suggesting anoxic conditions (DIDYK et al., 1978). A cross-plot of Ph/nC_{18} *versus* Pr/nC_{17} suggests mixed kerogen types II/III (Fig. 10b; CONNAN & CASSOU, 1980). The sterane/hopane ratio is lower than 1 (Suppl. 2, Table S3). The presence of hopane derivatives indicates a higher bacterial contribution (OURISSON et al., 1979; ROHMER, 1993). The C_{27} and C_{29} homologues in C_{27} – C_{29} regular steranes are equally present, suggesting an algal and microbial origin (VOLKMAN et al., 1986; VOLKMAN, 1988). The relative abundance on the ternary diagram suggests an open to shallow marine palaeoenvironment and a source biomass of phytoplankton origin with some contribution of terrestrial and bacterial organic matter (Fig. 12a; HUANG & MEINSHEIN, 1979). Diasteranes suggest more clastic facies.

Hopane and sterane maturity-related biomarker ratios generally indicate the mature bitumen (Fig. 13). The 22S/(22S+22R) 17α21β-C_{32} homohopane is in equilibrium, while 20S/(20S+20R) and ββ/(ββ+αα) are from 0.46 to 0.49 and 0.56 to 0.62, respectively (MACKENZIE et al., 1982; SEIFERT & MOLDOWAN, 1978, 1980, 1986; MACKENZIE & MAXWELL, 1981). Biomarker maturity parameters from the aromatic fraction also indicate mature bitumen (RADKE, 1988; RADKE et al., 1982a, b). The vitrinite reflectance calculated from MPI-1 ranges from $Rc_{(MPI-1)}$ 0.97 to 1.09% (RADKE & WELTE, 1983). Vitrinite reflectance values (VR 1.15% to 1.37%R_o in Upper Triassic; 1.55% to 1.83%R_o in Middle Triassic) also indicate higher thermal maturity, suggesting palaeotemperatures (T_p) of approximately 145 – 160 °C for Upper Triassic and 165 – 180 °C for Middle Triassic formations (BARKER & PAWLEWICZ, 1994; BOSTICK, 1979; RAINER et al., 2016). These rocks are within the main gas generation window. Despite the absence of observed hydrocarbon shows during drilling, the thermally altered Middle to Upper Triassic marls and limestones in the Glamoč-1 well retain characteristics of fair to good source rocks.

The varying thermal maturity observed in the Glamoč area underscores the importance of understanding the complex structural-tectonic relationships (DRAGIČEVIĆ, 2010).

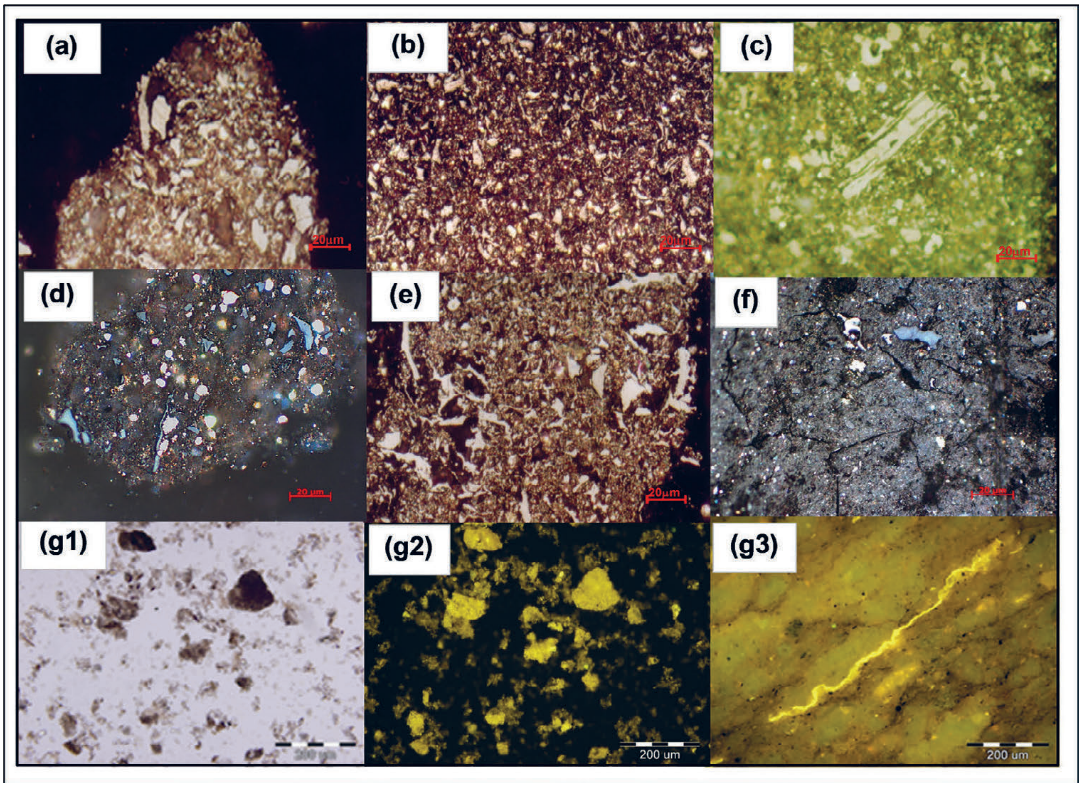

Figure 9. Photomicrographs illustrating the organic matter composition of Triassic carbonates and shales, featuring vitrinite and inertinite (fusinite) within amorphous organic matter. All reflected white light images are taken under oil immersion. **a** Fužine shale with vitrinite reflectance (VR) of 2.27%R_o; **b** Lokve – Homer silty shale (VR 1.99%R_o); **c** Donje Pazarište (Jovanović Draga) shale (VR 2.01%R_o); **d** Glamoč-1 well, Carnian shale from 2040 – 2042 m depth (VR 1.26%R_o); **e** Muć Sutine dark limestone exhibiting vitrinite reflectance of 2.29%R_o and the presence of pyrobitumen; **f** Zelovo – Sutinske Staje dark limestone containing chert (VR 1.26%R_o); **g** Vlasta-1 well (depth: 5433-5452 m), mudstone: **g1** Amorphous organic matter (isolated kerogen) under transmitted white light; **g2** Same field of view as g1 under blue-fluorescent light; **g3** Lamalginite in a whole rock section, oriented perpendicular to bedding and viewed under blue-fluorescent light.

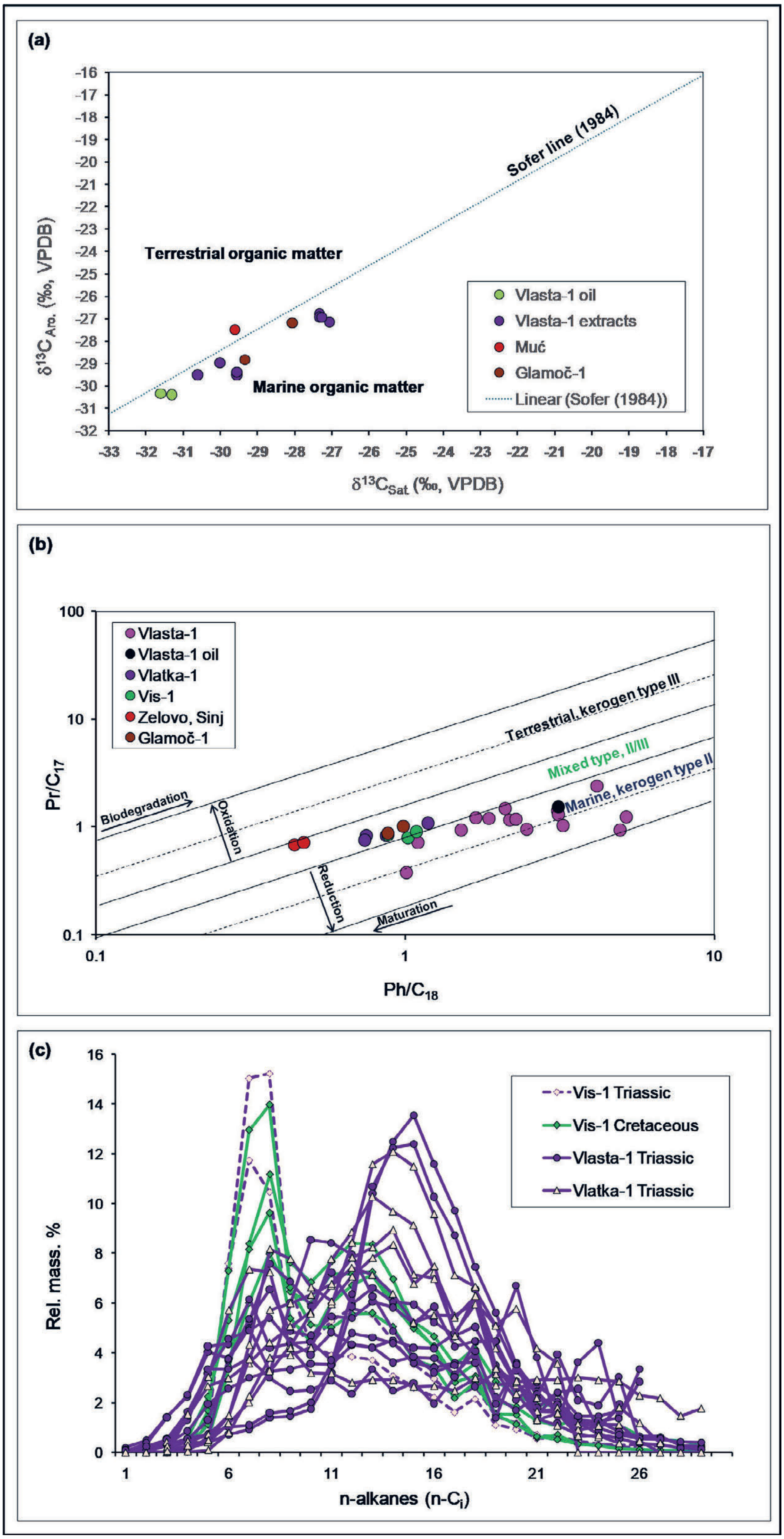

Figure 10. Source rock evaluation of Triassic carbonates and shales using biomarker and stable carbon isotope ratios: **a** Stable carbon isotope ratios ($\delta^{13}C$, VPDB) of saturated and aromatic hydrocarbon fractions of extracts, used to infer organic matter type (in the SOFER´s (1984) diagram). Remark: Statistical trends are based on n-alkanes greater than C_{15}, while our analysis included the entire saturated fraction; **b** Pristane (Pr)/nC_{17} *versus* Phytane (Ph)/nC_{18} crossplot illustrating organic matter type, depositional conditions (including oxygen levels), and thermal maturity trends (in the CONNAN & CASSOU´s (1980) diagram); **c** The distribution of n-alkanes in extracts from wells Vlasta-1, Vis-1, and Vlatka-1.

Intense tectonic activity, including uplift, in the Dinarides likely influenced burial depth and temperature history, ultimately rendering these rocks inactive source rocks today. Triassic source rocks in the Croatian part of the External Dinarides are predominantly depleted or overmature. Their maturation occurred either towards the end of the Triassic or in the Early Jurassic, prior to the formation of the current structural regime/setting. The results of vitrinite reflectance measurements have highlighted Middle Triassic volcanism as the most significant thermal event in the evolution of the area. As no other thermal events have been registered in the Dinarides region according to the analysis results, the calibration of this volcanism in heat flow analyses is particularly important. Thermal modelling has corroborated vitrinite reflectance data, specifically the maximum temperature to which organic matter was exposed (ŚRODOŃ et al., 2018; RAINER et al., 2016; BOSTICK, 1979; BARKER & PAWLEWICZ, 1994). According to ŚRODOŃ et al. (2018), maximum palaeotemperatures in the northwestern Dinarides region reached > 200 °C, but did not exceed 270 °C, while in the southeastern region they were slightly lower, down to 150 °C. The thermal climax was reached during the Late Cretaceous and Palaeocene. It is associated with the burial of sediments at significantly higher palaeogeothermal gradients (30 °C/km) than present-day gradients (10 – 20 °C/km). Cooling commenced between 80 and 35 Ma ago. The average exhumation rate ranged from 55 to 110 m/Ma. Estimates of the minimum thickness of the eroded sedimentary column vary from 6 to 6.3 km for Carboniferous deposits and from 3.5 to 4 km for Triassic deposits. Recent research further highlights this complexity. Further eastward, in Eastern Herzegovina, Upper Triassic (Carnian) marls and shales exhibit elevated organic carbon content and source rock characteristics, with kerogen type II of marine, algal origin, reaching the oil window (VR 0.66 – 0.78%R_o, T_p 100 to 120 °C; ALEKSIĆ et al., 2021). Conversely, further westward, Upper Triassic (Carnian, Julian) dark limestones of Drenov Grič (Lesno Brdo, Slovenia), deposited in shallow, calm lagoons and exhibiting mixed kerogen types II and III, are highly thermally altered (VR 2.71 to 3.89%R_o, T_p 210 to 245 °C; MALENŠEK ANDOLŠEK & MARKIČ, 2021).

The Vlasta-Komiža facies, a significant source rock formation within the Adriatic Burano facies, is identified in the Vlasta-1, Vlatka-1, and Vis-1 wells (COTA & BARIĆ, 1998; TROSKOT-ČORBIĆ et al., 2015; COTA et al., 2015; BARIĆ, 2006; VELIĆ, 2007). This Triassic (Ladinian – Carnian) volcano-sedimentary-evaporitic facies also outcrops on the islands of Palagruža and Vis, represented by the Žalo, Pištica, and Stara pošta units (KORBAR et al., 2009, 2012; OŠTRIĆ et al., 2014; BOROVIĆ et al., 1976, 1977). The Žalo and Pištica units correlate with the Ladinian deposits of the Vlasta-1 well (6519 – 6260 m), and the Stara pošta unit with the Carnian section (5440 – 5010 m).

Early to Middle Carnian (Cordevolian to Julian) deposits in the Vlasta-1 well (6225 to 5587 m) comprise a continuous sequence of subaqueous halite with thin layers of carbonate, anhydrite, and clay. This deposition occurred in an isolated

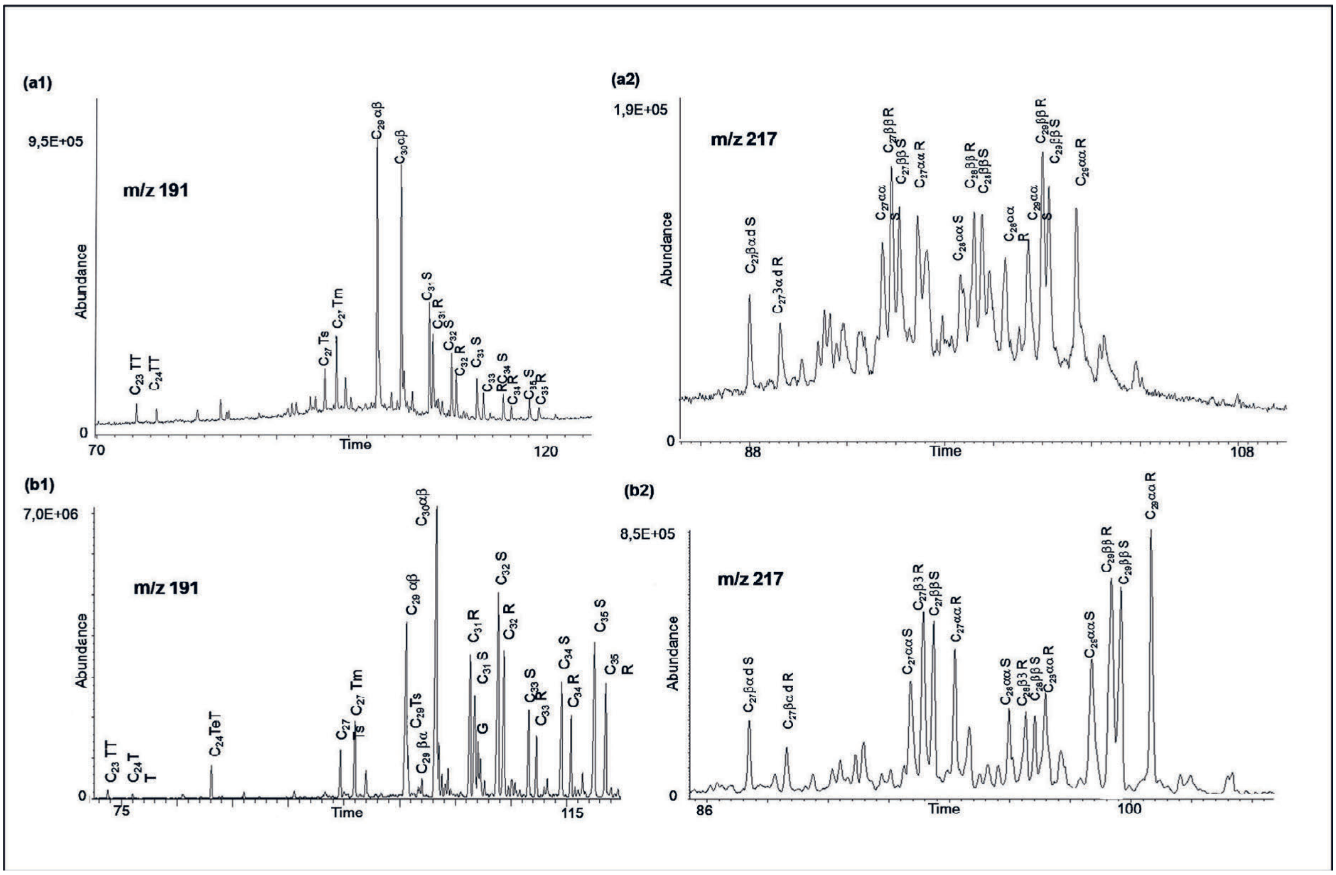

Figure 11. Mass chromatograms of extracts from Triassic carbonates, marls, and shales: **a** Sinj – Zelovo extract with mass chromatograms for **a1** terpanes (m/z 191) and **a2** steranes (m/z 217); **b** Vlasta-1 well extract with mass chromatograms for **b1** terpanes (m/z 191) and **b2** steranes (m/z 217).

marine bay or lagoon, likely due to tectonic activity or sea-level fluctuations. The restricted connection to the open sea, with seawater inflow through narrow channels, defines the sabkha facies (members of the sabkha cycle) in the Vlasta-1, Vlatka-1, and Vis-1 wells. While the Vlasta-1 well exhibits a complete sequence from lagoonal (subtidal) to supratidal cycles, the Vlatka-1 well only penetrated the lagoonal (subtidal) cycle. Notably, the Vlatka-1 well contains a few Norian laminated interlayers with source rock potential, characterized by type II kerogen and associated bitumen extending into adjacent layers (Suppl. 2, Table S2). In the Vlasta-1 well, oil (26.5 and 28.8 °API) was recovered from the Carnian intervals (5539 – 5510 and 5456 – 5402 m). Carnian laminated limestones and shales deposited between 5400 and 5600 m in the Vlasta-1 well have promising source rock characteristics (COTA & BARIĆ, 1998). They have a high total organic carbon (TOC) content, reaching up to 4% (Suppl. 2, Table S1). The organic matter is a mixture of kerogen and associated bitumen (petroleum). Hydrogen indices indicate an original HI≥500 mg HC/g TOC (Fig. 8c). The kerogen is type II, derived from algae and bacterially degraded material (Fig. 8a–c). These rocks demonstrate good to very good petroleum potential, with $S_1 + S_2$ values up to 23 mg HC/g rock (Fig. 8d; PETERS & CASSA, 1994). The organic-rich layers within the laminated limestones vary in thickness from laminae to several centimetres and are typically saturated with bitumen. The maceral composition is dominated by strongly yellow-fluorescing amorphous organic matter (Fig. 9g1, g2). Examination of polished rock surfaces perpendicular to bedding revealed laminated algal organic matter (alginite, mainly lamalginite) transitioning into bituminite or organic mineral mass (Fig. 9g3). These structural features support the algal and bacterial origin of the organic matter (TEICHMÜLLER & OTTENJANN, 1977; HUTTON et al., 1980; SENFTLE et al., 1987; HUTTON, 1987; LITTKE et al., 1988; TYSON, 1995; TAYLOR et al., 1998).

The bitumen yield is high, reaching up to 9310 ppm. The bitumen composition is dominated by asphaltenes and NSO-compounds (74 – 85%), reflecting the specific characteristics of the original sulphur-rich facies (Suppl. 2, Table S2). The n-alkane distribution is bimodal with maxima at C_{17} and nC_{27}. A cross-plot of Ph/nC_{18} *versus* Pr/nC_{17} indicates the presence of algal marine organic matter (CONNAN & CASSOU, 1980). The Pr/Ph ratio primarily suggests anoxic conditions during deposition (DIDYK et al., 1978). In the C_{27} to C_{35} $17\alpha,21\beta$(H)-type series of hopanes, $17\alpha,21\beta C_{30}$ hopane dominates (Fig. 11b1). Anoxic conditions during deposition, indicated by ratios Pr/Ph<0.8, prominent Ph peak, $C_{35}/\Sigma C_{31-35}$ 23 to 43%, $C_{35}S/C_{34}S$ 1.09 to 2.65, and G/H 0.12 to 1.09, played a crucial role in preserving the organic matter (Suppl. 2, Tables S2, S3; Figs. 10a–c, 11b1, b2, 12b, c, d; DIDYK et al., 1978; MOLDOWAN et al., 1992; CLARK & PHILP, 1989; PETERS & MOLDOWAN, 1991). The Sterane/Hopane ratio is low (St/Hop < 1). The

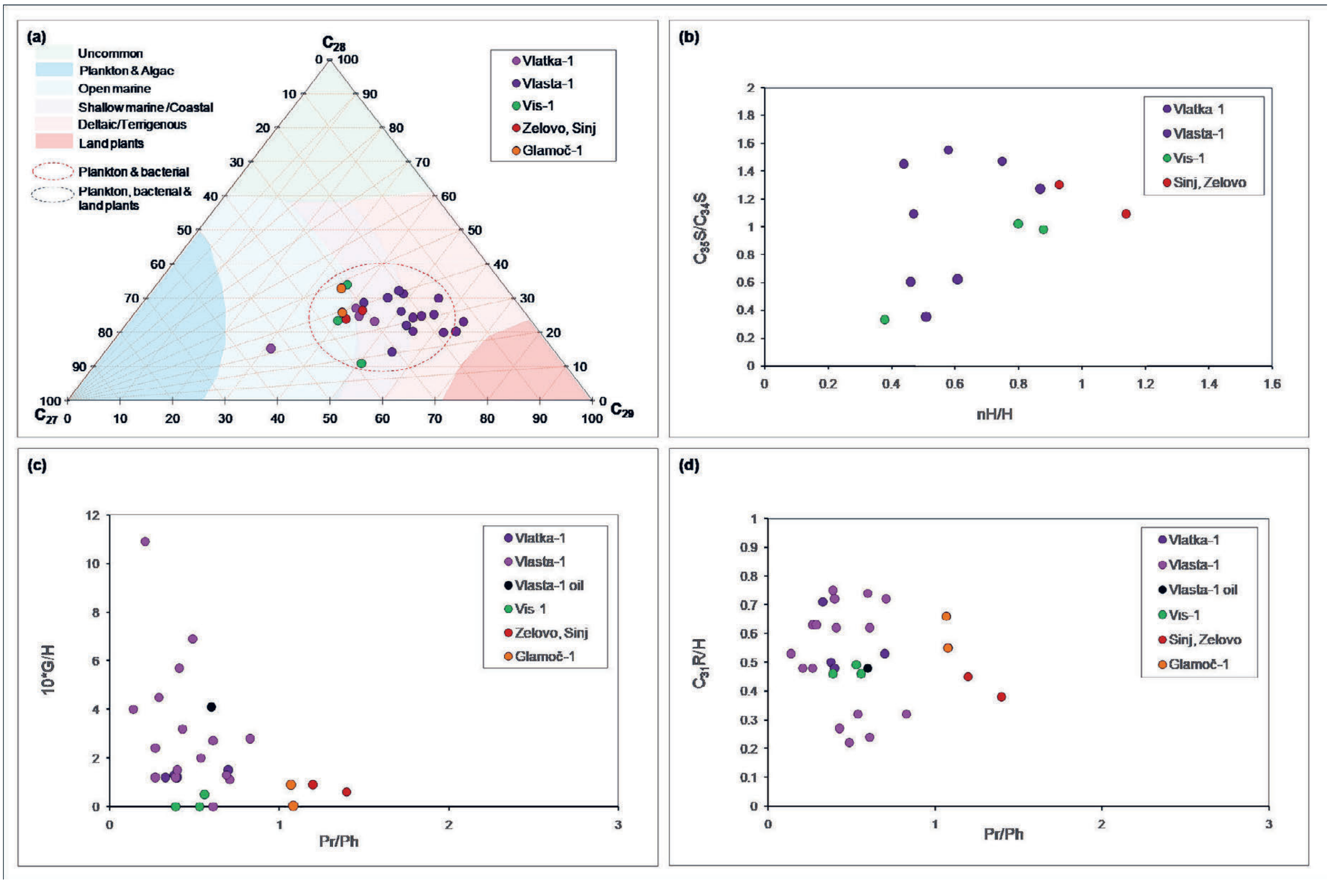

Figure 12. Source and depositional environment indicators for Triassic carbonates and shales: **a** Ternary plot illustrating the relative proportions of C_{27}, C_{28}, and C_{29} steranes in extracts from Triassic carbonates and shales (in the HUANG & MEINSHEIN´s (1979) diagram) indicative of source input and depositional setting; **b** Crossplot of $C_{35}S/C_{34}S$ homohopane ratio *versus* the nH/H ratio, providing insights into depositional conditions particularly redox potential and carbonate influence; **c** Crossplot of 10 * gammacerane concentration *versus* the pristane/phytane (Pr/Ph) ratio, indicating water column stratification and redox conditions; **d** Crossplot of the $C_{31}R/H$ ratio *versus* the pristane/phytane (Pr/Ph) ratio, reflecting specific environmental influences.

dominant homologues in C_{27}–C_{29} regular steranes are C_{29}, followed by C_{27} and C_{28} homologues (ranging from 50.6 to 63.98%, 15.85 to 31.04%, and 14.22 to 26.70%, respectively; Fig. 11b1). The relative abundance on the ternary diagram indicates a shallow marine depositional environment with a contribution of mainly phytoplanktonic and bacterial biomass (Fig. 12a; HUANG & MEINSHEIN, 1979). The organic matter was deposited in a marine carbonate environment, with an increasing shale component observed in deeper intervals (diasteranes/regular steranes (D/R) 0.11 to 0.58). All source-related biomarker ratios of both Triassic bitumen and oil point towards marine organic matter derived from algae and bacteria, with minimal influence from terrestrial sources (Suppl. 2, Table S3; Fig. 12). This is further supported by the consistent stable carbon isotope ratios in both kerogen and bitumen ($\delta^{13}C_{Ker.}$ -27.22 to -28.98‰ and $\delta^{13}C_{Bit.}$ -29.06 to -31.85‰, VPDB, respectively), and trends observed in their isotope profiles ($\delta^{13}C_{Sat.}$ -30.61 to -29.55‰, $\delta^{13}C_{Aro.}$ -29.51 to -28.97‰, $\delta^{13}C_{NSO}$ -29.25 to -28.39‰, and $\delta^{13}C_{Asph.}$ -28.09 to -27.35‰, VPDB; GALIMOV, 1974, 1980). Stable carbon isotope ratios confirm a positive correlation between kerogen, bitumen, and oil, implying that the oil likely originated from the identified source rock in its vicinity (COTA & BARIĆ, 1998). Similar stable carbon isotope ratios have been documented in Triassic sediments worldwide (KATZ et al., 2000; CHUNG et al., 1992).

Organic matter is in an immature to early mature stage (Fig. 8b, T_{max} 411 to 439 °C, TAI 1^+ to 2-2^+, VR 0.35 to 0.65%R_o). The estimated depth at which the organic matter enters the oil window is approximately 5200 ± 100 m. The maturity-related biomarker ratios confirm the immature to early mature stage of oil and source rock (Ts/(Ts+Tm) 0.16 to 0.59, 22S/(22S+22R) 0.51 to 0.60, bb/(bb+aa) 0.26 – 0.60, and 20S/(20S+20R) 0.30 – 0.45, respectively) (Suppl. 2, Table S3; Fig. 13; MACKENZIE et al., 1982; SEIFERT & MOLDOWAN, 1978, 1980, 1986; MACKENZIE & MAXWELL, 1981). Biomarker maturity parameters from the aromatic fraction, primarily methylphenanthrenes indices (MPI-1 and MPI-3), generally indicate early mature bitumen (RADKE et al., 1982a, b). The calculated vitrinite reflectance $Rc_{(MPI-1)}$ ranges from 0.60 to 0.83% (RADKE & WELTE, 1983).

Unfortunately, the surface rocks on the islands of Vis and Palagruža were found to lack promising source rock characteristics. The Triassic sediments drilled in the Vis-1 well exhibited a slightly elevated total organic carbon content (up to 0.88% TOC) in specific intervals (143.3 – 146.4 m and 195.1 – 199.1 m; Suppl. 2, Table S1). However, these rocks are not considered source rocks due to their degraded organic matter, which is dominated by non-fluorescent, detrital amorphous organic matter with varying amounts of inertinite (semifusinite and fusinite). The kerogen of types III and IV indicate a degraded organic matter of mixed origin with a possible minor presence of better-quality type II organic matter (Figs. 8, 10b). Thermal maturity parameters suggest that the organic matter in these rocks is immature transitioning to an early stage of catagenesis (VR 0.55 – 0.58%R_o). A small amount of mature, secondary bitumen is also present. Interestingly, biomarker data suggest that the bitumen in these Triassic sediments originated from a Cretaceous source rock, also identified within the Vis-1 well (Fig. 10c; Suppl. 2, Table S3; Suppl. 4, Table S3).

Surface exposures of Triassic rocks on the islands of Vis (near Komiža) and Palagruža yielded similar results. These rocks generally have a low total organic carbon content (up to 0.5% TOC) and degraded mixed kerogen types III and IV transitioning from diagenesis to early catagenesis (VR 0.55 to 0.61% R_o, TAI 2 to 2^+). The organic matter is primarily amorphous with traces of vitrinite and inertinite. Due to the low organic matter content, unfavourable type of organic matter, and degradation, these surface carbonates are not considered source rocks. However, a few shale fragments at the base of the dolomite-gypsum breccia (Stara pošta), with immature kerogen type II suggest the possibility of source rock characteristics related to the Vlasta-Komiža facies.

The Middle Triassic rocks in the Kornati more-1 and 1a wells exhibit variable total organic carbon contents, ranging from 0.50 to 0.87% TOC, observed in dolostones and tuffitic breccias (Suppl. 2, Table S1). The Upper Triassic (Norian) deposits also contain cracks filled with dark matter, but the overall organic matter content remains low, excluding them from being classified as source rocks. Microscopic examination revealed bitumen within pores and fractures of these rocks. Only the heavier bitumen components are present, suggesting the loss of lighter components. This bitumen suggests that Triassic limestones or shales in the vicinity have potentially generated this bitumen and/or hydrocarbon. These rocks have undergone early catagenesis (T_{max}>436 °C). The thermal maturity parameters of these deposits may be influenced by faulting.

Geochemical analysis of Triassic sedimentary rocks sheds light on the broader geological picture, aligning with existing conceptual models (ZAPATTERRA, 1994; CALDARELLI et al., 2013). This analysis has confirmed the presence of the intraplatform troughs within the Dinarides and the Adriatic (SMIRČIĆ, 2017; SMIRČIĆ et al., 2018, 2020; KORBAR et al., 2009, 2012). By using source rock characterization and source rock-to-hydrocarbon correlation, COTA et al. (2015) were able to map the distribution of the Vlasta-Komiža (Burano) facies across the wider Adriatic region by integrating seismic data with geochemical analysis.

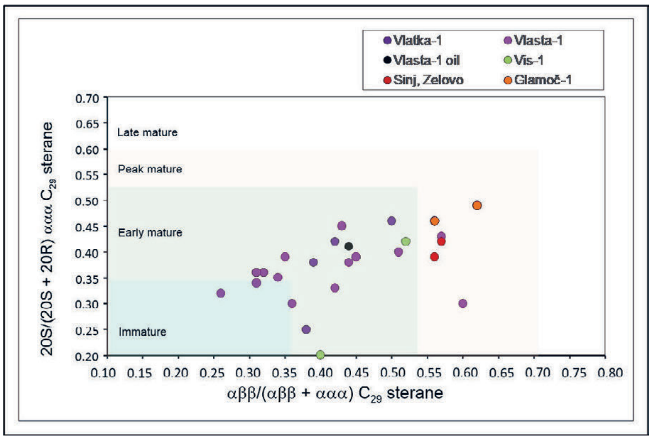

Figure 13. A crossplot illustrating the range of thermal maturity in extracts from Triassic carbonates and shales, using the ratios 20S/(20S+20R) and αββ/(αββ+ααα) of C_{29} steranes.

4.4. Jurassic source rocks characterisation

4.4.1. Early Jurassic

Research by ZAPPATERRA (1994), JENKYNS (1985, 1988, 1991, 2002) and JENKYNS & CLAYTON (1986) suggests that the Toarcian anoxic event created ideal conditions for source rock formation in particular regions. While this event has been identified on the Adriatic carbonate platform (VLAHOVIĆ et al., 2005), it did not result in the formation of significant source rocks. Early Jurassic deposits with higher organic carbon content have been identified in the Rovinj-1 well and in outcrops located in Gorski kotar and Velebit Mt. (sample locations 107, 27, 56 respectively on Figs. 4 and 15).

Liassic laminated carbonates in Gorski kotar (Jasenak) exhibit elevated organic carbon content (0.43 – 0.91% TOC; Suppl. 3, Table S1). The maceral composition is dominated by unstructured amorphous organic matter with rare vitrinite particles (Fig. 14). The amorphous organic matter is thermally altered, reaching a higher stage of catagenesis and transitioning into metagenesis (VR>1.80%R_o, TAI>3$^+$). Similarly, the TOC content of Liassic lithiothid limestones in Velebit Mt. (Kubus) rarely exceeds 0.50% TOC, with a maximum of 0.94% TOC. The kerogen is primarily amorphous and highly thermally altered. Vitrinite reflectance measurements on rare clasts indicate higher catagenesis transitioning into metagenesis (VR 2.12 to 2.48%R_o, TAI 4$^-$). All these findings suggest that the outcropping Lower Jurassic carbonates in this area have undergone significant thermal alteration.

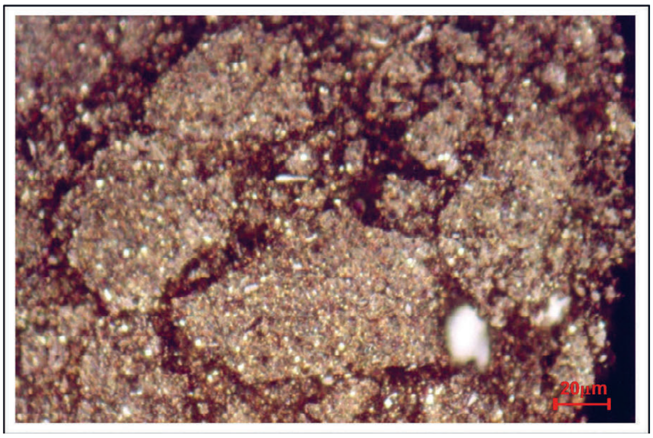

Figure 14. Photomicrograph of thermally altered amorphous organic matter (isolated kerogen) from Lower Jurassic laminated mudstone, Jasenak, observed under reflected white light with oil immersion.

Several Lower Jurassic carbonate layers in the Rovinj-1 well demonstrate good source rock potential (Suppl. 3, Table S1), with organic matter content ranging from 1.03% to 1.43% TOC (COTA & BARIĆ, 1998). The organic matter is classified

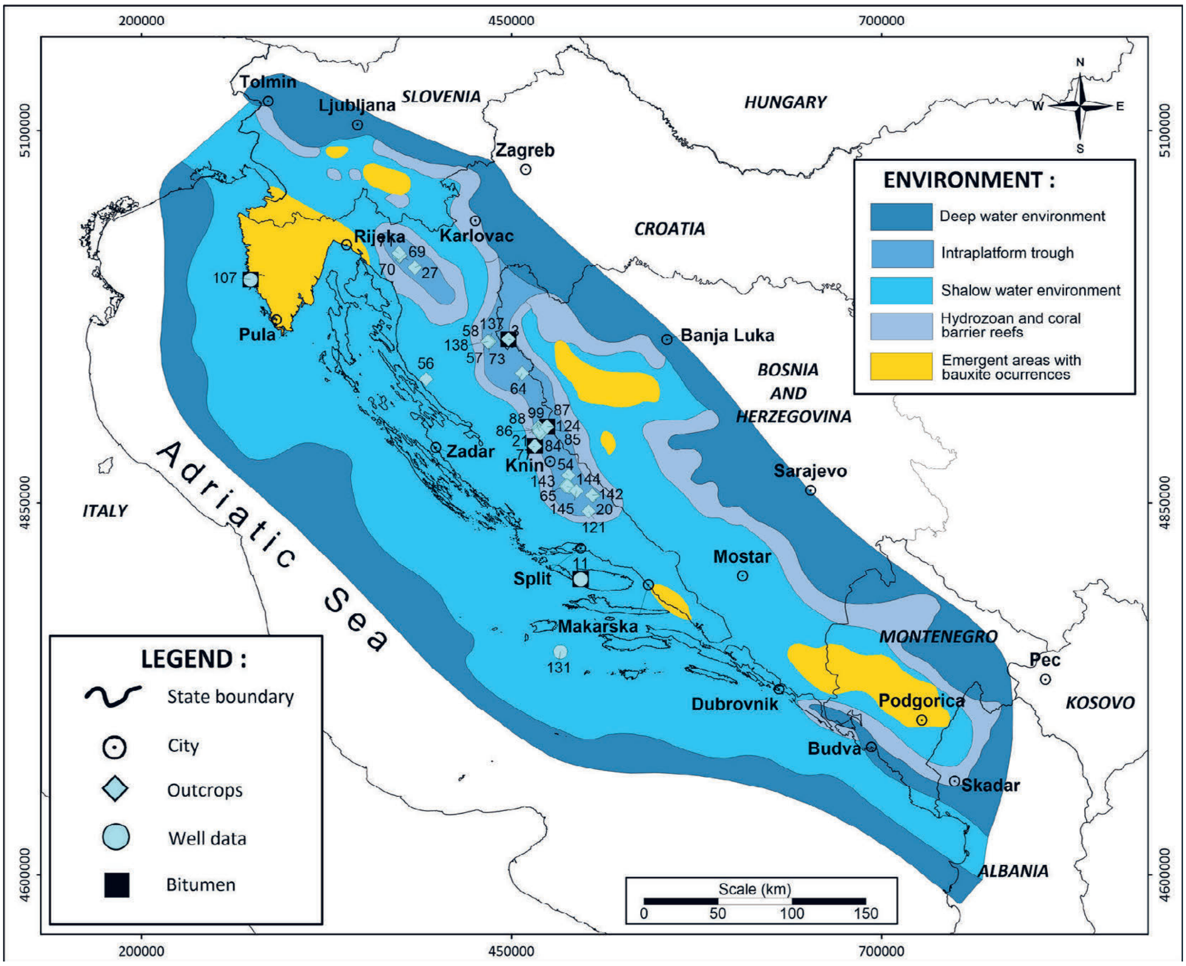

Figure 15. The spatial distribution of the sample locations of organic-rich carbonates and shales on a schematic Kimmeridgian – Early Tithonian palaeogeographical map of the AdCP (Adriatic Carbonate Platform) showing the main environments (modified after VELIĆ et al., 2002b). Sample location names correspond to the list provided in Figure 4.

as kerogen type II of algal and bacterial origin (Fig. 16a, b). It is in the early stage of catagenesis (VR 0.62 to 0.68%R_o; TAI 2$^+$).

4.4.2. Late Jurassic

The Adriatic Carbonate Platform (AdCP) was a very dynamic entity, and during its history, numerous events influenced this predominantly shallow marine platform depositional system (VLAHOVIĆ et al., 2005; Fig. 15). During the Late Jurassic (the Late Oxfordian and Early Kimmeridgian) in the central part of the platform, deeper depositional environments formed in the area of today's Gorski kotar (Gorski kotar Trough/Basin) and Lika, towards Western Bosnia and Herzegovina and Northern Dalmatia (Lemeš Trough/Basin). VELIĆ et al.

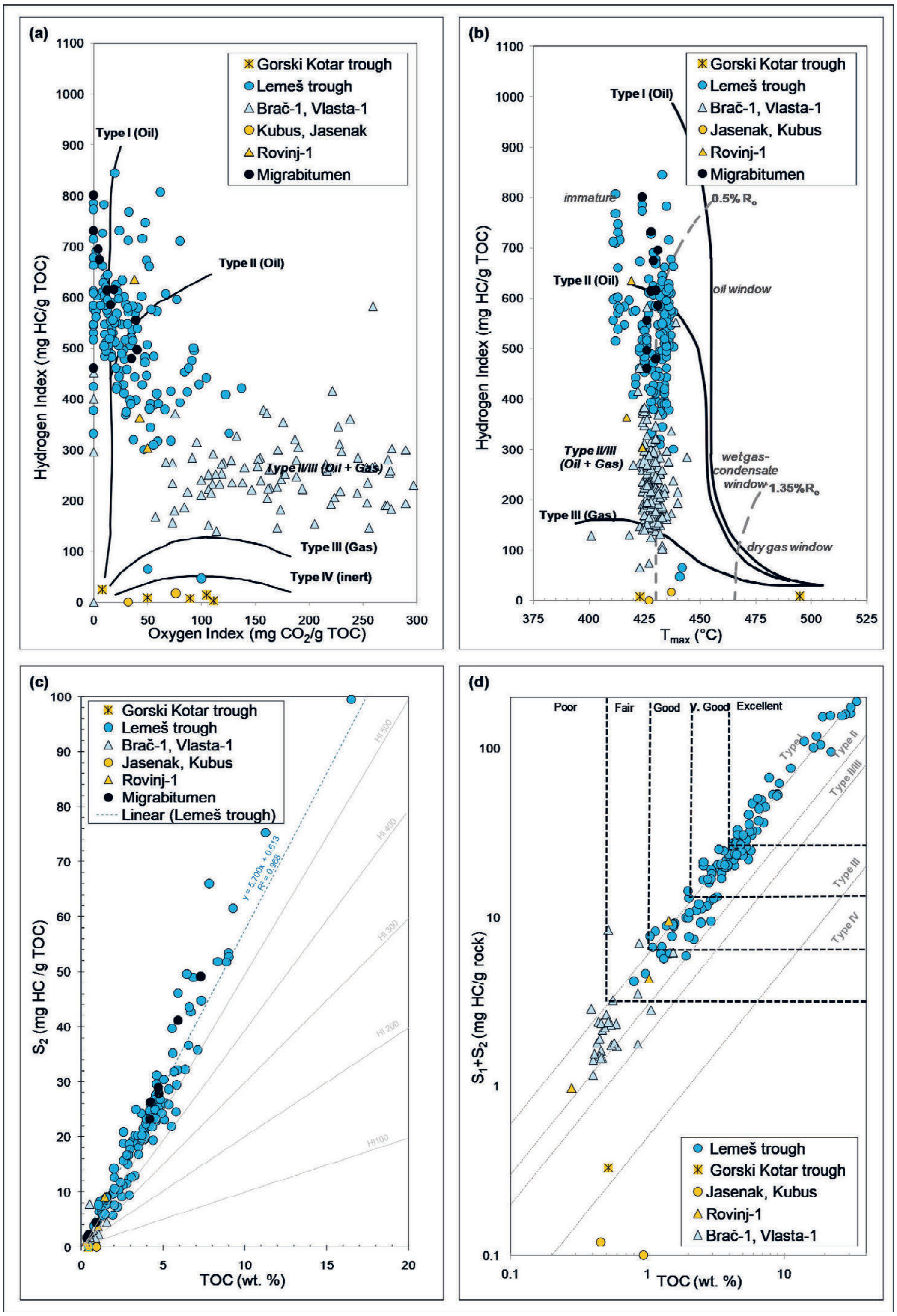

Figure 16. Source rock characterization of Jurassic carbonates, marls, and shales using Rock-Eval pyrolysis data: **a** Hydrogen Index (HI) *versus* Oxygen Index (OI) crossplot showing organic matter type classification; **b** Hydrogen Index (HI) *versus* T_{max} crossplot illustrating thermal maturity levels and trends; **c** Generative Potential (S_2) *versus* Total Organic Carbon (TOC) crossplot with superimposed average Hydrogen Index (HI) trends, indicating hydrocarbon generation potential; **d** Source rock quality assessment using a crossplot Petroleum potential (S_1+S_2) *versus* Total Organic Carbon (TOC).

(2002a, 2002b) attributed the formation of these relatively shallow intraplatform troughs/basins to compressional forces and the subsidence of the AdCP. Conversely, BUCKOVIĆ et al. (2004) proposed, following HERAK (1986), the interpretation of an extensional origin of the Lemeš Basin due to oceanic spreading, while VITZTHUM et al. (2021) propose a novel hypothesis suggesting that the Lemeš Basin formed through the westward obduction of ophiolites onto the Adriatic Plate.

VELIĆ et al. (2002a, 2002b) emphasized the palaeogeographic, depositional, and facies variations within these troughs. Coral-hydrozoan reefs developed along the trough edges, while deeper areas accumulated thin-layered mud carbonates with offshore fauna and volcanic ash-derived chert interlayers (ŠĆAVNIČAR & NIKLER, 1976; KRKALO et al., 1995; ŠEGVIĆ et al., 2006). Kimmeridgian reefs gradually filled the troughs with reef debris, leading to shallow platform deposition by the early Tithonian. The Gorski kotar trough, unlike the Lemeš Trough, lacked an open connection to the Tethys Ocean, functioning as a "sea tongue" within the AdCP. The relationship between these two troughs remains uncertain (Fig. 15). Due to their potential for organic-rich rock deposition, deep-water troughs with open sea connections, especially the Lemeš Basin, have been the subject of intensive geochemical research (BLAŽEKOVIĆ SMOJIĆ et al., 2009; TROSKOT-ČORBIĆ, 2011; VITZTHUM et al., 2021).

Gorski kotar Trough/Basin

Analysis of Upper Jurassic marls and carbonates in the Gorski kotar Trough reveals the generally low total organic carbon content (Suppl. 3, Table S1). Only dark, micrite-rich limestones in Matić Poljana exhibit slightly elevated values (TOC>0.5%, sample locations 69 – 71 on Figs. 4 and 15), but these lack significant source rock potential (Fig. 16). Organic matter maceral analysis indicates a predominance of non-fluorescent, amorphous organic matter, suggesting significantly decomposed and highly degraded organic material from various sources. A marine origin for the organic matter is suggested by palynofacies analysis. The favourable conditions for organic matter deposition might have existed locally in shallower environments, but they were not widespread in the Gorski kotar Trough (VELIĆ et al., 2002a). Small traces of bitumen initially suggest an algal and bacterial origin (kerogen type II). However, this organic matter has undergone significant oxidation and/or thermal degradation, evidenced by the high bitumen reflectance ($BR>2\%R_b$), which corresponds to a vitrinite reflectance of $VR>1.6\%R_o$ (calculated using the conversion of JACOB, 1989).

The organic matter of all the analysed Upper Jurassic rocks of the Gorski kotar Trough is highly altered and lacks the necessary characteristics to be considered a true source rock (TROSKOT-ČORBIĆ, 2011).

Lemeš Trough/Basin

The Lemeš Trough/Basin is an elongated deep-water marine trough, extending over a 4000 km² area, in which the 250 to 450 m thick Upper Jurassic Lemeš Formation (also called the Lemeš Deposits, Lemeš Beds, Lemeš Layers, Lemeš Facies, *Die Lemeš schichten*) was deposited (SCHUBERT, 1909; FURLANI, 1910). The Formation is subdivided into mappable "groups" (Lemeš Beds/Layers), with "group 4" identified as being organic-rich (BLAŽEKOVIĆ SMOJIĆ et al., 2009).

Carbonate rocks along the edges of the trough (near Jošani, Udbina, and Srb in Lika, and on the Kozjak and Svilaja mountains in Dalmatia) exhibit low total organic carbon content (TOC) and lack source rock potential. These rocks primarily contain oxidized, inert organic matter (kerogen type IV) (TROSKOT-ČORBIĆ, 2011).

In contrast, the central regions of the trough near Bihać, Korenica, Lapac in Lika, and Poštak Mt., Vrlika, and Dabar in Dalmatia revealed dark, laminated carbonates with higher total organic carbon content (sample locations 3, 11, 20 – 21, 54, 57 – 58, 64 – 65, 73, 84 – 88, 99, 121, 131, 137 – 138, 142 – 145, on Figs. 4, 15; Suppl. 3, Table S1). The most complete sequence of Kimmeridgian deep-sea deposits is found on the slopes of Poštak Mt. (BLAŽEKOVIĆ SMOJIĆ et al., 2009; TROSKOT-ČORBIĆ, 2011; VITZTHUM et al., 2021). This 250 to 280 m thick succession is composed of three members: the Rastičevo, Dimići, and Lemeš (VESELI et al., 2012). The middle Dimići member is characterized by alternating light grey and greenish-grey limestones containing *Radiolaria*, alongside dark grey, thinly bedded to laminated limestones enriched in organic matter and often recrystallized (VESELI et al., 2012; TROSKOT--ČORBIĆ, 2011; VITZTHUM et al., 2021).

Organic-rich dark, laminated limestones with interbedded cherts are the oldest deposits in the Lemeš Trough (Fig. 17). They contain kerogen type II (HI>450 mg HC/g TOC), characterized by good to excellent oil-generating potential ($S_1+S_2>6$ mg HC/g rock; Suppl. 3, Table S1; Fig. 16). The organic matter originates from marine algae and bacteria. The concentration of organic sulphur varies within the trough, with higher values observed in the shallower areas ($S_{Ker.}$ 3.71 to 11.25%, S_{Bit}. 3.32 to 10.45%; Suppl. 3, Table S2). This variation classifies the kerogen as type IIS (ORR, 1986; ORR & SINNINGHE DAMSTE, 1990). The presence of sulphur in the kerogen structure allows for hydrocarbon generation to begin earlier, during diagenesis. The amount of extractable organic matter (EOM) is significant, ranging from 88 to 90378 ppm. The EOM/TOC ratio remains consistent within the range typical for source rocks (up to 0.25). Asphaltenes and NSO-compounds (resins) constitute the dominant portion of the bitumen group composition, generally ranging from approximately 80% to 98.48% (with a minimum of 69.31% observed in one instance; Suppl. 3, Table S2). Gas chromatography analysis reveals the presence of low molecular weight hydrocarbons and a predominance of normal alkanes over corresponding isoprenoids (Pr/nC_{17}, $Ph/nC_{18}<1$; Suppl. 3, Table S2). The prominent nC_{17} peak and the crossplot of Ph/nC_{18} *versus* Pr/nC_{17} suggest a marine, algal origin for the organic matter (Fig. 18a, b, c1; CONNAN & CASSOU, 1980). Early-stage hydrocarbon generation was influenced by the presence of sulphur in kerogen molecules. Despite partial degradation, the bitumen still reflects the source rock's characteristics, especially its algal and microbially degraded origin. The domination of hopanes over steranes (St/Hop<1) and an elevated $C_{34}S/C_{35}S$ hopane ratio ($C_{34}S/C_{35}S \geq 1$) point towards a bacterial contribution to the organic matter (Figs. 18c1, c2, 19b, c; Suppl. 3, Table S3; OURISSON et al., 1979; ROHMER, 1993; MOLDOWAN et

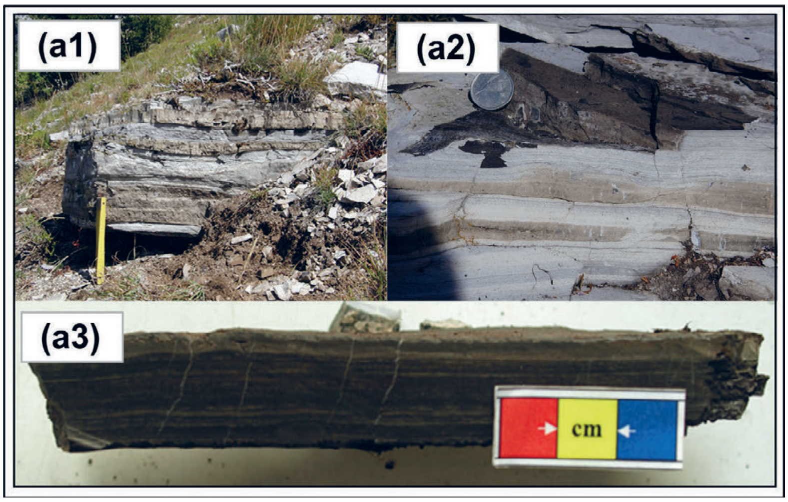

Figure 17. Outcrop photographs of Jurassic carbonates and shales from the Lemeš Trough. **a1**, **a2** Poštak Mt., illustrating the Upper Jurassic Dimići member: an alternation of light grey and greenish-grey limestones containing *Radiolaria*, and dark grey, thin-bedded to laminated radiolarian limestones that are mostly recrystallized and enriched in organic matter; **a3** Close-up view of an organic-rich dark laminated mudstone (6.38% TOC) (modified after TROSKOT-ČORBIĆ, 2011).

al., 1992). Stable carbon isotope analysis reveals values ranging from $\delta^{13}C_{Ker.}$ -27.79 to -24.65‰, VPDB for kerogen and $\delta^{13}C_{Bit.}$ -29.53 to -25.55‰, VPDB for bitumen (Fig. 20a). The isotope profile for Poštak Mt (Fig. 20b; after GALIMOV, 1974, 1980) shows positive correlations between the $\delta^{13}C$ of various organic fractions. These isotope ratios are comparable to those

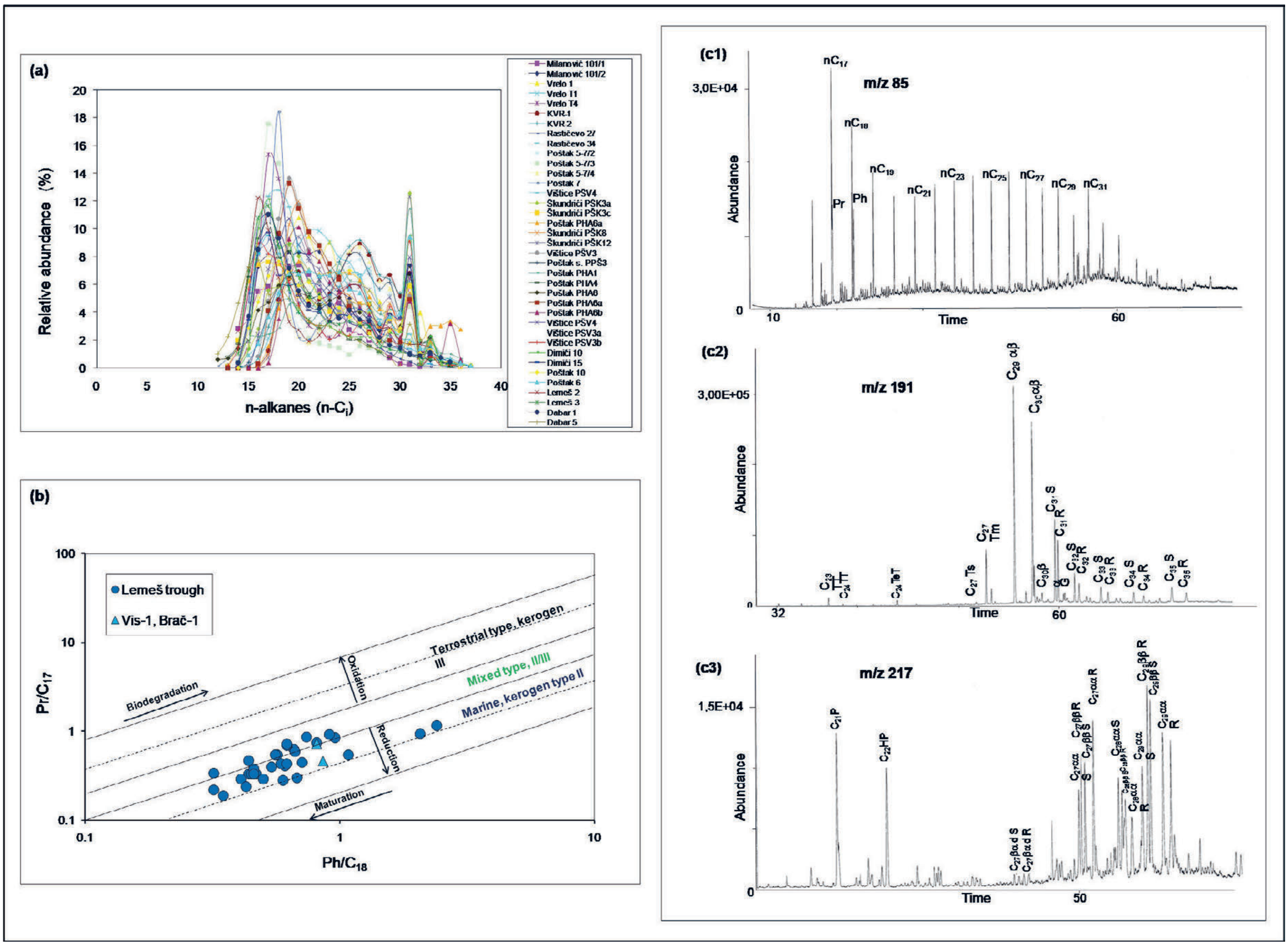

Figure 18. Source and depositional environment of Jurassic carbonate and shale extracts. **a** Distribution of n-alkanes in extracts from the Lemeš Trough, illustrating the relative abundance of different chain lengths; **b** Pristane (Pr)/nC_{17} *versus* phytane (Ph)/nC_{18} crossplot, used to infer organic matter type, depositional environment (redox conditions), and thermal maturity trends (in the CONNAN & CASSOU´s (1980) diagram); **c** Representative mass chromatograms from Poštak Mt. mudstone extracts: **c1** Mass chromatogram of n-alkanes (m/z 85); **c2** Mass chromatogram of terpanes (m/z 191); **c3** Mass chromatogram of steranes (m/z 217).

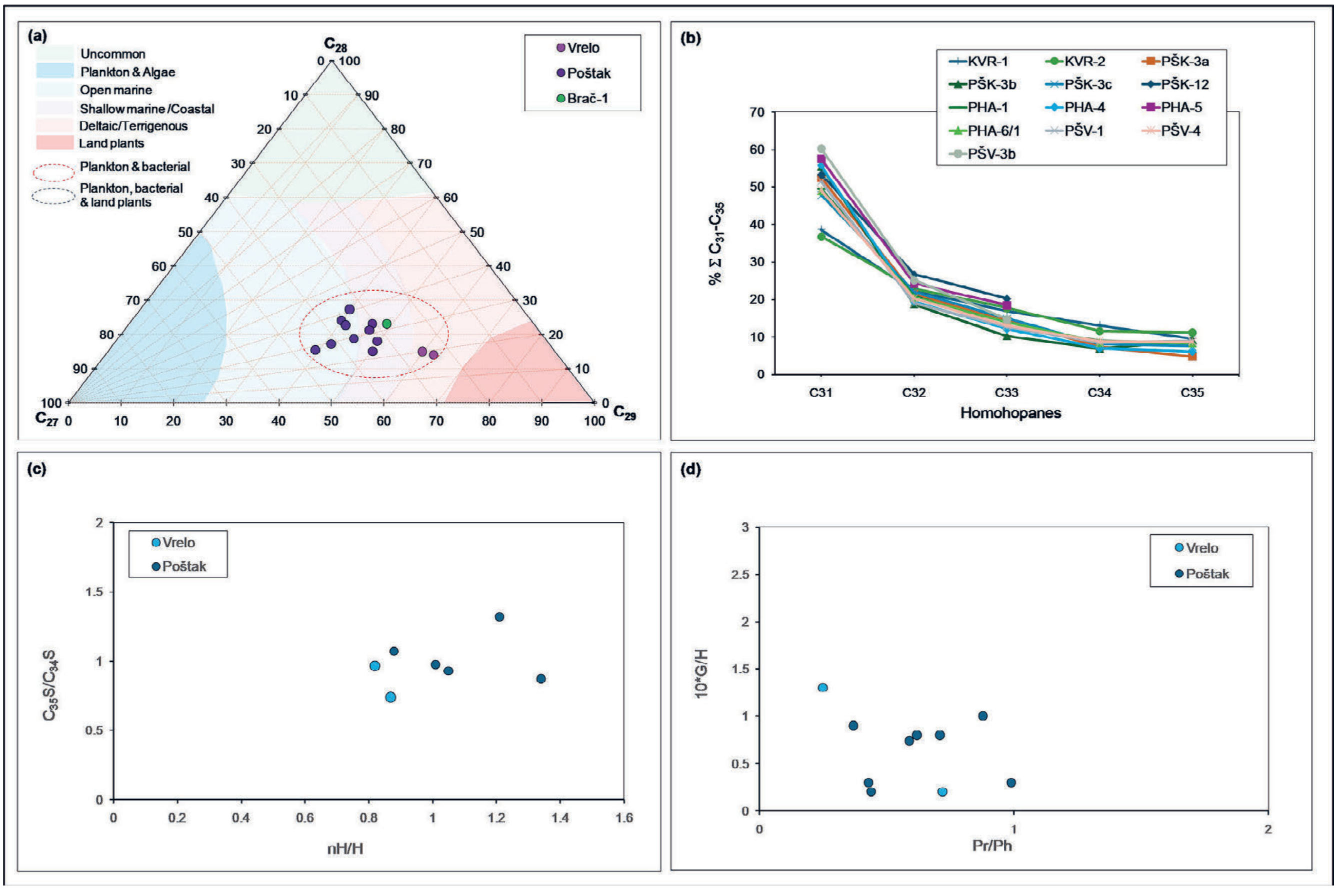

Figure 19. Source and depositional environment indicators for Jurassic carbonates and shales: **a** Ternary plot illustrating the relative proportions of C_{27}, C_{28}, and C_{29} steranes in extracts from Jurassic carbonates and shales (in the HUANG & MEINSHEIN´s (1979) diagram), indicative of source input and depositional setting; **b** Relative distribution of C_{31}-C_{35} homohopanes (m/z 191), showing the relative abundance of extended hopane homologues, providing insights into bacterial input and depositional conditions; **c** Crossplot of $C_{35}S/C_{34}S$ *versus* nH/H ratios, providing insights into redox conditions and carbonate influence during deposition; **d** Crossplot of 10 * Gammacerane *versus* Pr/Ph ratio, reflecting water column stratification and oxygen levels.

found in other Jurassic sediments, such as the Toarcian source rocks of Italy ($\delta^{13}C$ < -26 ‰, VPDB; KATZ et al., 2000). Additionally, the data fall within the expected range for Mesozoic carbonates with elevated sulphur content, as shown in the Chung´s diagram (the Pr/Ph *versus* $\delta^{13}C$ diagram; CHUNG et al., 1992).

It is interpreted that these sediments formed under low-energy conditions with distinct water layering, minimally disturbed by external water inflow. Biomarker analysis indicates anoxic bottom water conditions, but not extreme salinity, indicated by low gammacerane values (Figs. 18c2, 19d). Elevated nH/H ratios in extracts suggest a carbonate

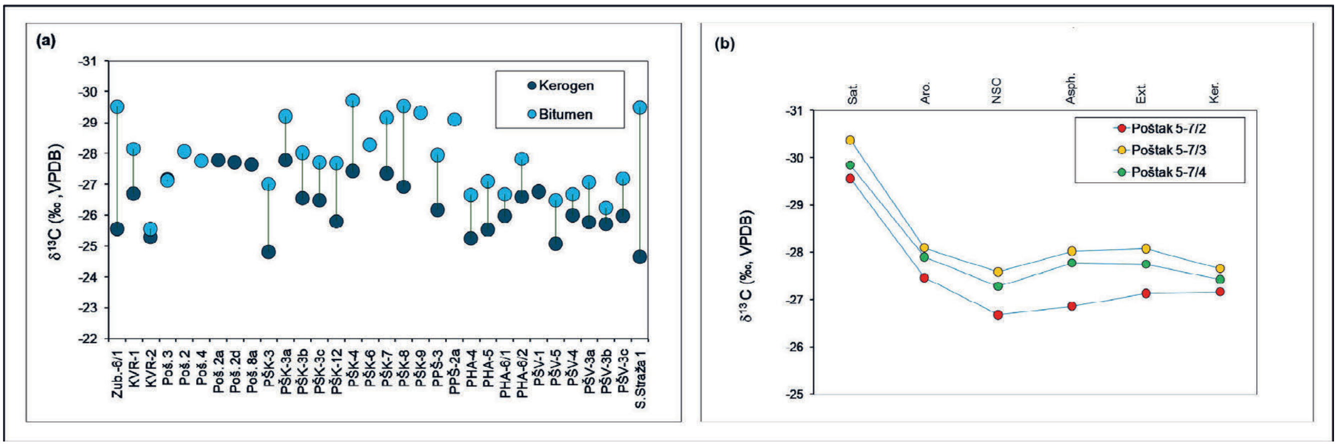

Figure 20. Stable carbon isotope ratios ($\delta^{13}C$, VPDB) of Upper Jurassic carbonates in the Lemeš Trough. **a** Stable carbon isotope ratios ($\delta^{13}C$, VPDB) of kerogen and bitumen extracted from Upper Jurassic carbonates; **b** Stable carbon isotope ratios profile of various organic fractions (kerogen, extract, saturated hydrocarbons, aromatic hydrocarbons, NSO compounds/resins, asphaltenes) from Poštak Mt. (in the GALIMOV´s (1974, 1980) diagrams). Key: Ker. = kerogen, Bit. = bitumen, Ext. = extract, VPDB = Vienna Pee Dee Belemnite standard, Sat. = saturated hydrocarbons, Aro. = aromatic hydrocarbons, NSO = nitrogen, sulphur, and oxygen-bearing compounds (resins), Asph. = asphaltenes.

marine depositional environment. The homohopane distribution and related ratios (C_{31}R/H, $C_{35}S/C_{34}S$ hopane) suggest isolated, enclosed anoxic depositional settings (Fig. 18c2). The favourable, calm, and stable conditions facilitated the deposition of layered organic matter, starting as lamalginite and gradually transitioning to bituminite type I and finally to a finely dispersed organic-mineral matrix bituminite (Figs. 21, 22; TEICHMULLER & OTTENJANN, 1977; HUTTON et al., 1980, 1987; SENFTLE et al., 1987; LITTKE et al., 1988; TYSON, 1995; TAYLOR et al., 1998). Notably, conditions within the Lika portion of the trough were more favourable and stable compared to the Dalmatian side (TROSKOT-ČORBIĆ, 2011). This difference is likely attributed to factors such as palaeogeography or the subsea depth profile of the trough.

The Lika section within the Lemeš Trough (Bihać – Korenica – Donji Lapac area, Figs. 4, 15) exhibits a highly prospective organic facies for hydrocarbon generation. This is evidenced by its elevated total organic carbon (TOC) content, ranging from 0.51 to 45.90% with an average of 10% (Suppl. 3, Table S1), which translates to a significant petroleum potential (S_1+S_2 values reaching up to 200 mg HC/g rock, averaging 60 mg HC/g rock, Fig. 16d). The organic matter is predominantly composed of type II kerogen, with subordinate occurrences of type I kerogen (Fig. 16a–c), indicating a primary algal and bacterial source. Microscopically, the organic matter is largely amorphous, characterized by the incorporation of liptinite macerals, specifically liptodetrinite and dinoflagellates, alongside minor amounts of inertinite (fusinite), vitrinite, and solid bitumen (Fig. 21a1–a4). The laminated structure of the amorphous material allows for its classification as lamalginite (Fig. 21a5–a6; HUTTON et al., 1980; HUTTON, 1987; TAYLOR et al., 1998), a known precursor for oil-prone kerogen. Furthermore, the presence of vitrinite-like particles exhibiting low solubility suggests they likely represent solid bitumen (Fig. 21a4; NOWAK, 2007), further contributing to the hydrocarbon potential.

Molecular organic geochemistry, specifically the analysis of the C_{27} – C_{29} regular steranes, reveals a predominance of the C_{29} and C_{27} homologues, with C_{29} steranes being the most

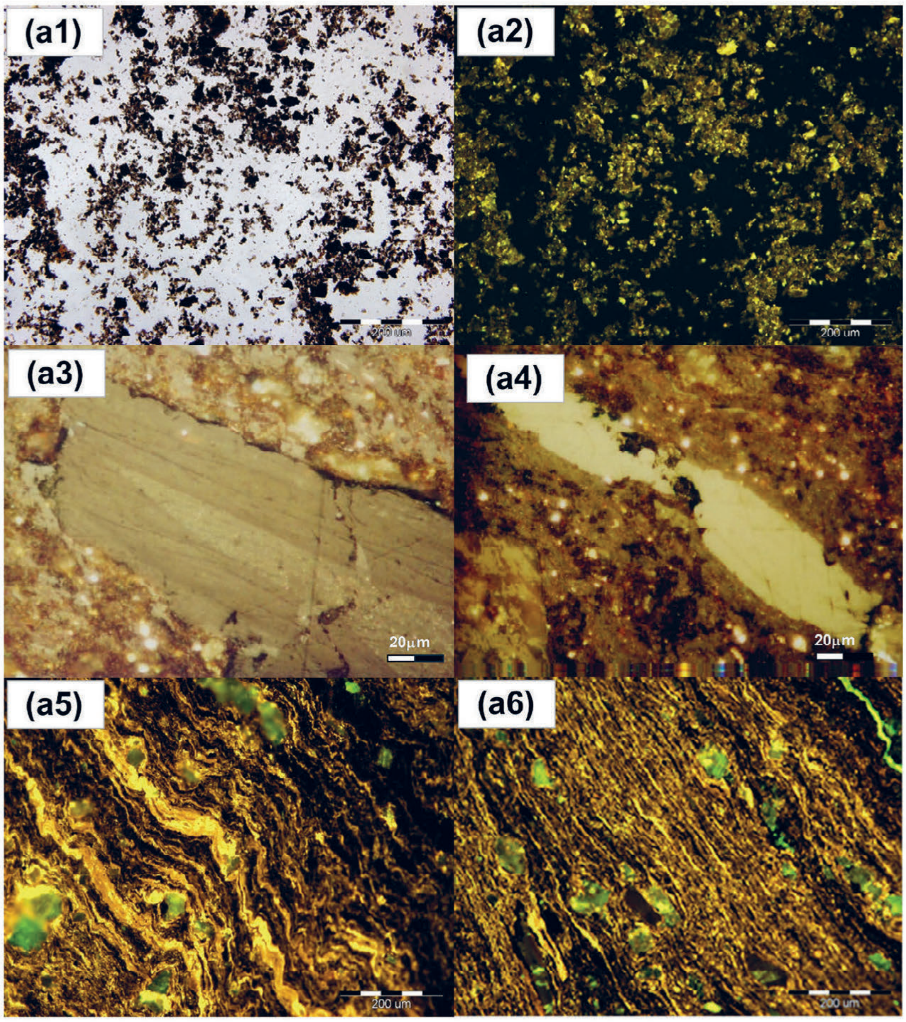

Figure 21. Photomicrographs of organic matter from Jurassic carbonates and shales, Lemeš Trough, Lika area (Vrelo and Zubović draga): **a1** Amorphous organic matter (AOM) observed in transmitted white light; **a2** Same field of view as a1 showing the fluorescence of AOM under blue light; **a3** Huminite/Vitrinite maceral (VR 0.45 to 0.48%R_o) embedded within amorphous organic matter, viewed under reflected white light with oil immersion; **a4** Vitrinite-like bitumen (BR ranging from 0.29 to 0.66%R_b) dispersed in amorphous organic matter, observed under reflected white light with oil immersion; **a5**, **a6** Lamalginite and associated bitumen within the whole rock, oriented perpendicular to bedding and imaged under blue-fluorescent light (modified from TROSKOT-ČORBIĆ, 2011).

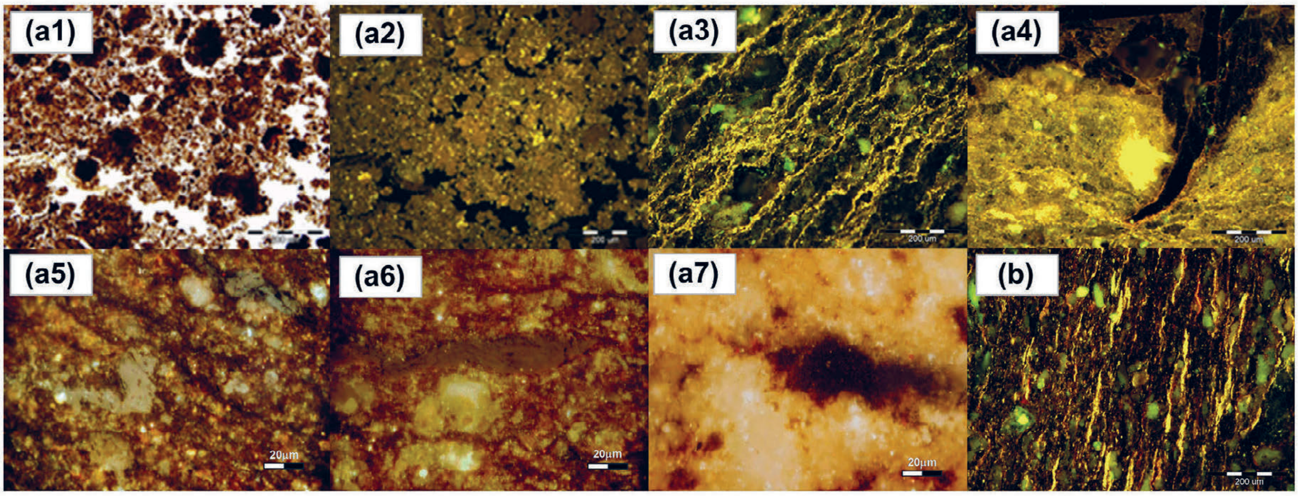

Figure 22. Photomicrographs of organic matter from Jurassic carbonates and shales, Lemeš Trough, Dalmatia, Poštak Mt.: **a** Škundrići mudstone: **a1** Amorphous organic matter (AOM, isolated kerogen, transmitted white light); **a2** Same view as a1 (blue-fluorescent light); **a3** Lamalginite; **a4** Bitumen (asphaltite, BR 0.25%R_b) in a fracture within lamalginite (whole rock, perpendicular to bedding, blue-fluorescent light); **a5** – **a7** Laminated dark organic matter and vitrinite-like bitumen (BR 0.20 – 0.47%R_b) (whole rock, perpendicular to bedding, reflected white light, oil immersion); **b** Dabar calcareous shale: Lamalginite (whole rock, perpendicular to bedding, blue-fluorescent light) (modified after TROSKOT-ČORBIĆ, 2011).

abundant (59-62%; Fig. 18c3). This high abundance of C_{29} steranes suggests a significant contribution from bacterial biomass to the original organic matter (VOLKMAN et al., 1986; VOLKMAN, 1988). The ternary diagram of the C_{27} – C_{29} regular steranes further supports a shallow to coastal marine depositional environment characterized by significant input from both phytoplanktonic and bacterial biomass, with only a minor influence from terrestrial organic matter (HUANG & MEINSHEIN, 1979). The elevated C_{29} sterane content is likely derived from the lipid/liptodetrinite remnants of algal taxa such as *Leiospheridia,* cyanobacteria, or other specific microbial communities prevalent in such environments.

The Dalmatian part of the Lemeš Trough (Poštak Mt., Vrlika, Dabar) exhibits a comparatively lower, yet still significant, potential for hydrocarbon generation compared to the Lika region. Total organic carbon (TOC) content ranges from 0.35 to 11.9%, averaging 3%. Despite this lower concentration, the petroleum potential remains favourable, with $S_1 + S_2$ values ranging from 1.17 to 67 mg HC/g rock and averaging 18 mg HC/g rock (Fig. 16d). The dominant kerogen type is II (Figs. 16a–c), indicative of a primary algal and bacterial source. Microscopically, the organic matter is predominantly amorphous, displaying an alternation between laminated and finely dispersed forms (Fig. 22). Distinct layers of lamalginite progressively transit into the more abundant bituminite I, eventually merging into an organic-mineral matrix bituminite (Fig. 22; TEICHMÜLLER & OTTENJANN, 1977; HUTTON et al., 1980; SENFTLE et al., 1987; HUTTON, 1987; TAYLOR et al., 1998). This textural evolution likely reflects the microbial degradation of primary producers, including algae, phytoplankton, zooplankton, and bacteria, under anaerobic conditions within the depositional environment.

Consistent with the Lika region, molecular biomarker analysis reveals a higher abundance of hopanes relative to steranes (Suppl. 3, Table S3; OURISSON et al., 1979; ROHMER, 1993), suggesting a significant contribution from bacterial organic matter. Only trace amounts of inertinite (semifusinite and fusinite) and vitrinite particles are observed. Vitrinite-like bitumen particles, exhibiting variable solubility, are also present (Fig. 22a4–a7; NOWAK, 2007). Bitumen reflectance (BR) values predominantly fall within the range of 0.18 to 0.26%R_b, with occasional higher measurements up to 0.40%R_b, indicating an early stage of thermal maturation. Corresponding vitrinite reflectance (VR) values range between 0.49 and 0.69%R_o. The distribution of cyanobacterial and liptinite/liptodetrinite organic matter shows variability within the Dalmatian part of the trough. The presence of the prasinophycean algae *Leiosphaeridia* and dinosporine cysts within the phytoplankton communities suggests deposition during the Late Jurassic. Variations in the distribution of C_{27} – C_{29} regular steranes (C_{27}: 30.53 – 49.88%; C_{28}: 15.08 – 22.63%; C_{29}: 32 – 52.67%, respectively), further support these observations (Suppl. 3, Table S3; VOLKMAN et al., 1986; VOLKMAN, 1988). Further biomarker ratios, including the diasterane/sterane ratio, homohopane distribution pattern, and nH/H, $C_{31}R/C_{30}H$, and $C_{35}S/C_{34}S$ hopane ratios, collectively confirm deposition in a marine carbonate environment characterized by organic matter rich in sulphur and accumulation under reducing (anoxic) conditions. In the C_{27} – C_{29} regular steranes, the dominant homologues are generally either C_{29} or C_{27}, with C_{29} typically being the most abundant, followed by C_{27} and C_{28} (Fig. 18c3). The absence of oleanane (Ol) indicates a lack of significant input from angiosperm-derived organic matter (EKWEOZOR et al., 1979; MOLDOWAN et al., 1994). The ternary diagram of the C_{27} – C_{29} regular steranes points towards a shallow to open marine depositional setting, primarily influenced by marine algal organic matter, predominantly phytoplanktonic, with a notable contribution from bacterial biomass (Fig. 19a; HUANG & MEINSHEIN, 1979).

The Upper Jurassic organic-rich deposits within the Lemeš Trough demonstrate excellent oil-generating potential, qualifying them as very good to excellent source rocks (Fig.

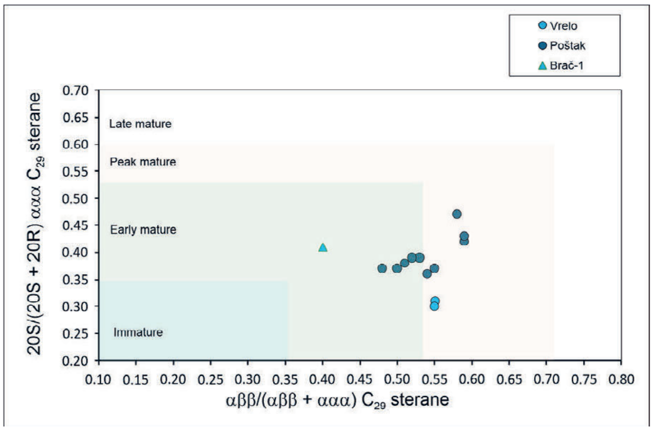

Figure 23. A crossplot illustrating the range of thermal maturity in extracts from Jurassic carbonates and shales, using the ratios 20S/(20S+20R) and αββ/(αββ+ααα) of C_{29} steranes.

16d). This exceptional potential is attributed to both the high abundance of organic matter and the presence of a particularly favourable kerogen type, (predominantly type II with some type I) and associated organic facies (JONES, 1984, 1987; PEPPER & CORVY, 1995a, b; PEPPER & DODD, 1995).

Based on a comprehensive suite of thermal maturity parameters, including T_{max} (411 to 439 ºC), Production Index (PI up to 0.37), Thermal Alteration Index (TAI 1^+ to 2-2^+), fluorescence colour (yellow to yellow-orange), vitrinite reflectance (VR 0.40 to 0.49 $\%R_o$, rarely 0.60$\%R_o$), bitumen reflectance (BR 0.15 – 0.38$\%R_b$, corresponding to vitrinite reflectance VR 0.52 and 0.63$\%R_o$, calculated using the conversion of JACOB (1989)), Methylphenanthrene Index (MPI-1) derived vitrinite reflectance equivalent ($Rc_{(MPI-1)}$ 0.67 – 0.82%), Methyl Dibenzothiophene Ratio derived vitrinite reflectance equivalent ($Rm_{(MDR)}$ 0.54 – 0.62%), hopane isomerization ratio (22S/(22S+22R) 058 – 063), sterane isomerization ratios ((20S/(20S+20R) 0.30 – 0.47 and αββ/(αββ+ααα) 0.47 – 0.59), and the Ts/Tm ratio (0.03 – 0.22), the Lemeš Trough source rocks are classified as being immature to early mature (Suppl. 3, Tables S1, S3; Figs. 16b, 18b, 23; PETERS & CASSA, 1994; MACKENZIE et al., 1982; SEIFERT & MOLDOWAN, 1980, 1986; MACKENZIE & MAXWELL, 1981; RADKE, 1988; RADKE & WELTE, 1983).

Recent thermal modelling corroborates the vitrinite reflectance data, specifically constraining the maximum temperature to which the organic matter was exposed (ŚRODOŃ et al., 2018; RAINER et al., 2016; BOSTICK et al., 1979; BARKER & PAWLEWICZ, 1994). According to ŚRODOŃ et al. (2018), the minimum thickness of the eroded sedimentary column overlying the Jurassic deposits is estimated to range from 2.2 to 2.4 km. The organic matter from the Kozjak, Svilaja, and Dinara Mountains is primarily immature, while that from Poštak Mountain and the Bihać – Korenica area exhibits a range from immature to early mature. Notably, the elevated sulphur content within the kerogen macromolecular structure suggests that these source rocks might be considered to have reached an initial stage of thermal maturity due to the specific catalytic effects of sulphur on early hydrocarbon generation (BASKIN & PETERS, 1992; ORR, 1986; ORR & SINNINGHE DAMSTE, 1990). This implies that the Upper Jurassic deposits underwent an initial phase of thermal transformation prior to uplift during the Late Cretaceous and Palaeogene (ŚRODOŃ et al., 2018). These spatial variations in source rock maturity (immature to early mature) are consistent with the observed differences in the amounts of generated bitumen.

Migrated bitumen (migrabitumen) is observed within pores, fractures, and vugs of the Upper Jurassic dolostone formations adjacent to the source rock, indicating localized, short-distance migration of early-stage petroleum-derived products, expelled from the sulphur-rich kerogen (sample locations 3, 77, 124 on Figs. 4, 15; Suppl. 3, Tables S1, S2). These migrabitumens are characterized by high to exceptionally high total organic carbon, (TOC contents between 6 and 11%). Based on their optical properties, the bitumen reflectance (BR) 0.10 – 0.28$\%R_b$, exhibiting strong to moderate yellow-orange-brown fluorescence and variable solubility characteristics, these migrabitumens are classified within the asphaltite group (encompassing a spectrum from wurtzilite to albertite, gilsonite, and glance pitch, JACOB, 1989; Fig. 24), suggesting a progression towards solid or semi-solid forms. Notably, these migrated bitumens display evidence of significant biodegradation. Despite their allochthonous nature, the migrabitumens retain geochemical signatures indicative of their Upper Jurassic source rock, including elevated sulphur content (S > 6%) and stable carbon isotope ratio ($\delta^{13}C$) values of the bulk bitumen and its fractions generally lower than $\delta^{13}C$ -26‰, VPDB ($\delta^{13}C_{Bit.}$ from -25.63 to -27.60‰, VPDB, and for the Palanka $\delta^{13}C_{Sat.}$ -28.30‰, $\delta^{13}C_{Aro}$.-27.29‰, $\delta^{13}C_{NSO}$ -27.21‰, $\delta^{13}C_{Asph.}$ -26.29‰, $\delta^{13}C_{Bit.}$-27.06‰, VPDB). However, their capacity for further migration appears limited due to a relative depletion in saturated hydrocarbon components and a corresponding enrichment in higher molecular weight, polar resinous and asphaltene fractions. These observations collectively suggest that the early-stage hydrocarbon products underwent short-range migration and were subsequently transformed into solid or semi-solid bitumen through processes of biodegradation and polymerization within the adjacent reservoir rock.

4.5. Cretaceous source rocks characterisation

During the Late Jurassic and Early Cretaceous, the AdCP was characterized by extensive shallow marine environments. Subsequent synsedimentary tectonic activity resulted in the development of deeper intra-platform troughs (Fig. 25; VELIĆ et al., 2002b; VLAHOVIĆ et al., 2005). Superimposed on this tectonic framework were episodes of global Oceanic Anoxic Events (OAE 1a, OAE 2), which caused periods of relative sea-level rise and platform drowning. These events facilitated the deposition of offshore pelagic and hemipelagic fauna and the accumulation of laminated, organic-rich, dark to black, highly bituminous limestones and dolomites (Fig. 27a1, c1; JENKYNS, 1980, 1985, 1991). These key periods of organic matter preservation primarily occurred during the Albian – Cenomanian, Late Santonian – Early Campanian, and Maastrichtian stages. The formation of these organic-rich deposits was favoured in low-energy, restricted environments, such as shallow subtidal lagoons or the deeper, more stagnant portions of the intra-platform troughs (Fig. 25). Evidence of

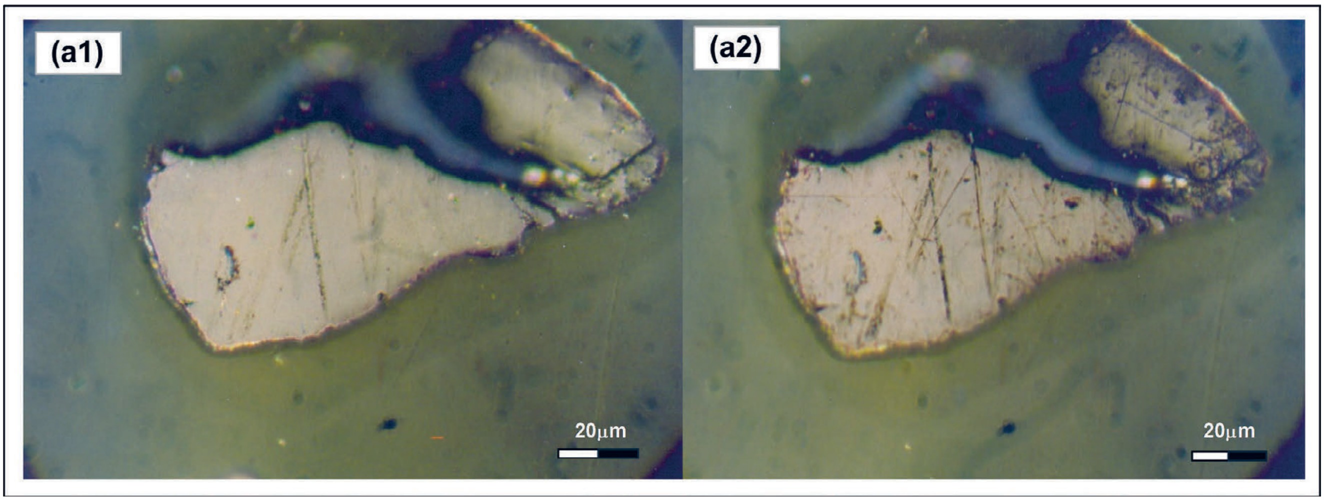

Figure 24. Photomicrographs illustrating migrabitumen (gilsonite) in dolostone from Zavalje, Bihać area. **a1** Initial view of vitrinite-like solid bitumen under reflected light with oil immersion; **a2** The same area after 15 minutes, demonstrating partial dissolution of the bitumen in the immersion oil.

these bituminous facies is widespread across the AdCP, documented along the Adriatic coast in surface outcrops and encountered in numerous exploration wells, including Premuda-1, Dugi otok-1, Ravni kotari-1, Ravni kotari-3, Jadran-3, Jadran-9, Jadran-13, Kate-1, Vis-1, Melita-1, and Boraja-1 (sample locations 1, 4 – 10, 12 – 13, 22, 24, 26, 28 –

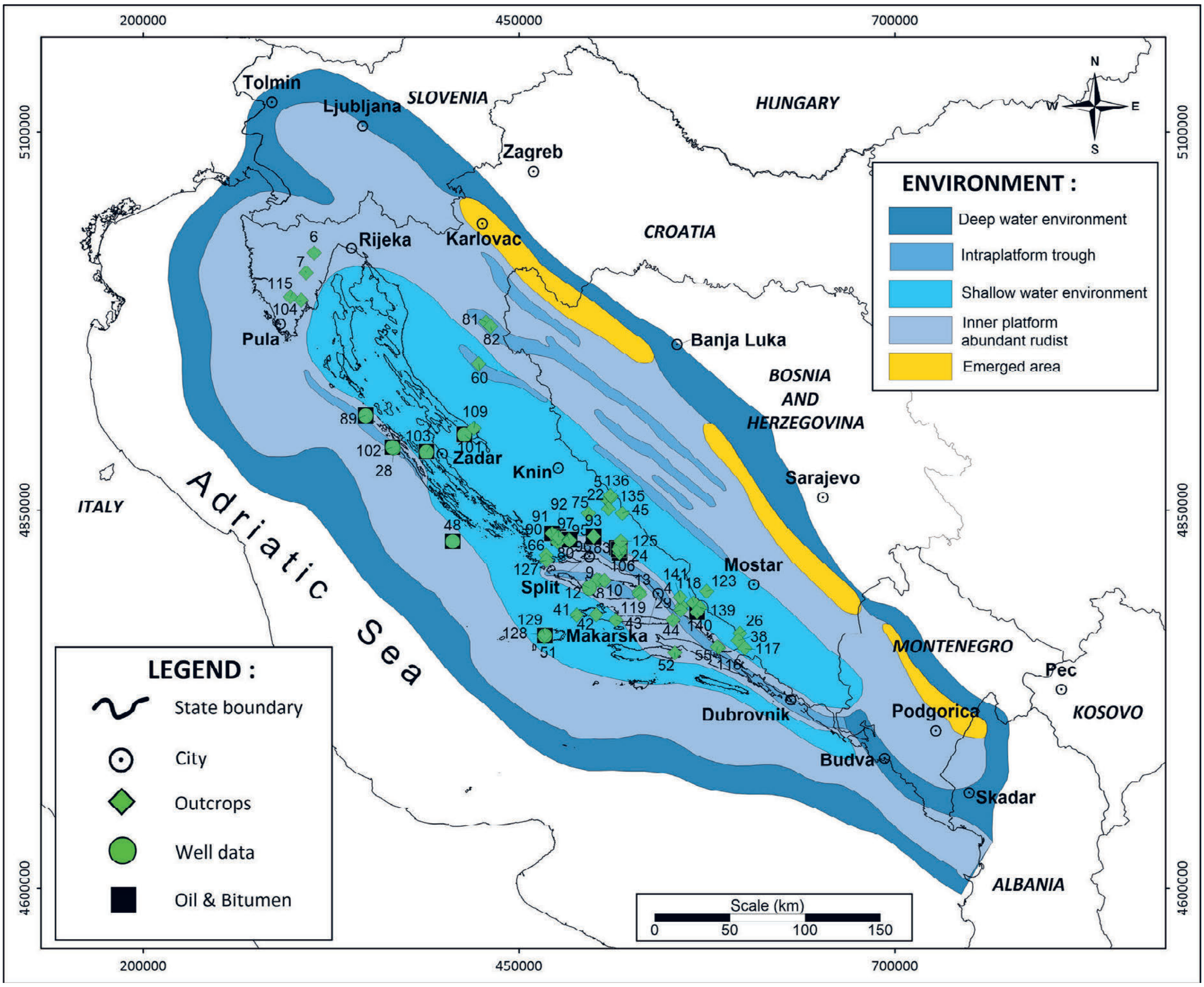

Figure 25. The spatial distribution of the sample locations of organic-rich carbonates and shales on a schematic Latest Cretaceous palaeogeographical map of the AdCP (Adriatic Carbonate Platform) showing the main sedimentary environments (modified after VELIĆ et al., 2002b). Sample location names are provided in Figure 4.

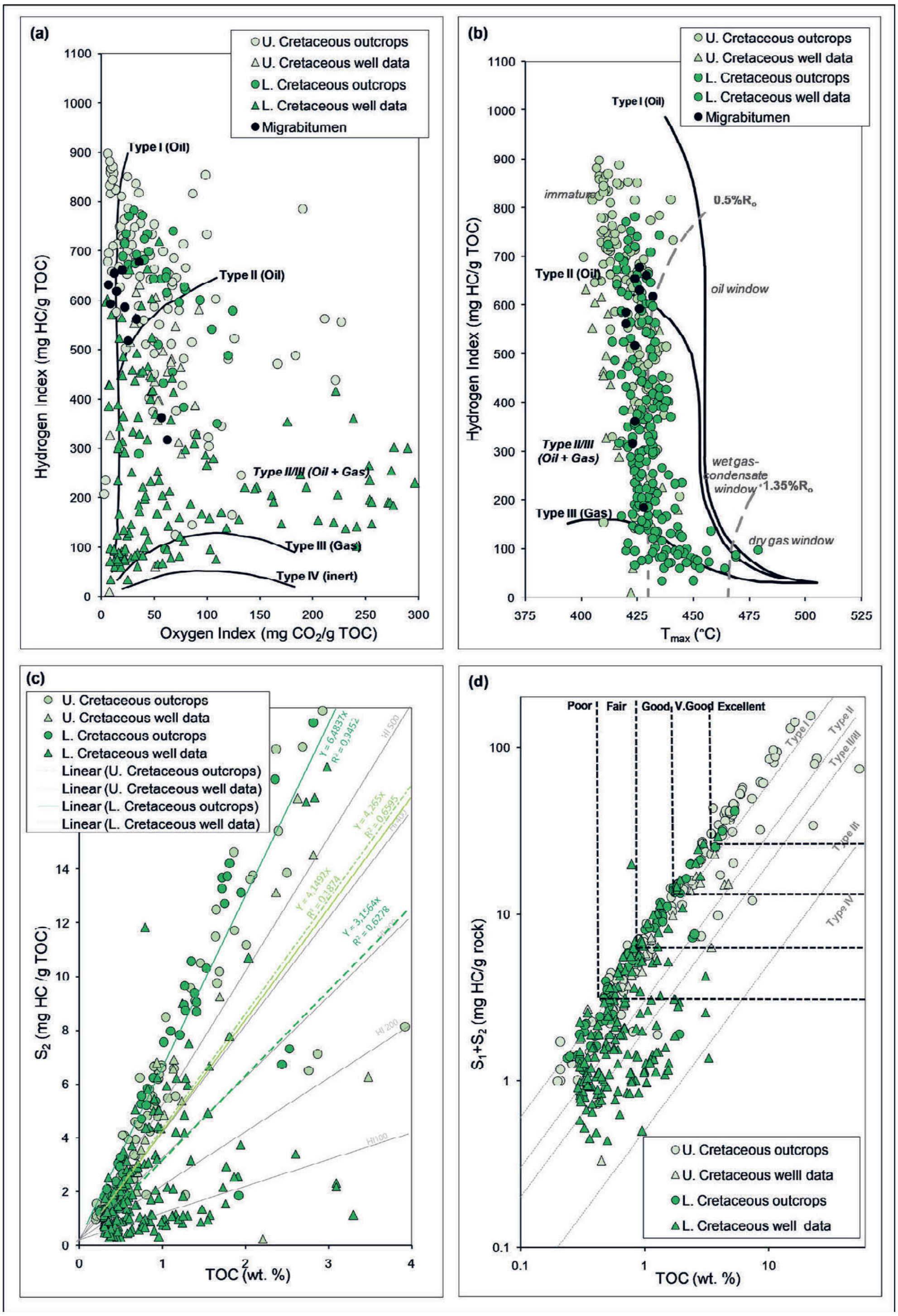

Figure 26. Source rock evaluation of Cretaceous carbonates, marls, and shales using Rock-Eval pyrolysis data: **a** Hydrogen Index (HI) *versus* Oxygen Index (OI) crossplot showing organic matter type classification; **b** Hydrogen Index (HI) *versus* T_{max} crossplot illustrating thermal maturity levels and trends; **c** Generative Potential (S_2) *versus* Total Organic Carbon (TOC) crossplot with superimposed average Hydrogen Index (HI) trends, indicating hydrocarbon generation potential; **d** Source rock quality assessment using a crossplot Petroleum potential (S_1+S_2) *versus* Total Organic Carbon (TOC).

29, 38, 41 – 45, 48, 51 – 52, 55, 60, 66, 75, 80 – 83, 89 – 93, 95 – 97, 101 – 106, 109, 115 – 119, 123, 125, 127 – 129, 135 – 136, 139 – 141 on Figs. 4, 25; ŠEBEČIĆ et al., 1988, 1989, 1990; JACOB et al., 1983; BARIĆ et al., 1988; JERINIĆ et al., 1994; ŠPANIĆ et al., 1995; COTA & BARIĆ, 1998; FIKET et al., 2008). The thickest accumulations of these Cretaceous carbonate-evaporite facies are observed in the central parts of the platform (GRANDIĆ et al., 1997). This spatially coincides with areas where the oil seeps and asphalt occurrences have also been reported (ŠEBEČIĆ et al., 1988, 1989, 1990; JACOB et al., 1983; MOLDOWAN et al., 1992; FIKET et al., 2008), suggesting a genetic link between these organic-rich deposits and hydrocarbon generation and migration.

The Cretaceous laminated carbonates and calcareous shales of the AdCP represent significant petroleum source rocks, exhibiting substantial organic enrichment of up to 25% TOC and demonstrating excellent oil-generating potential (S_1

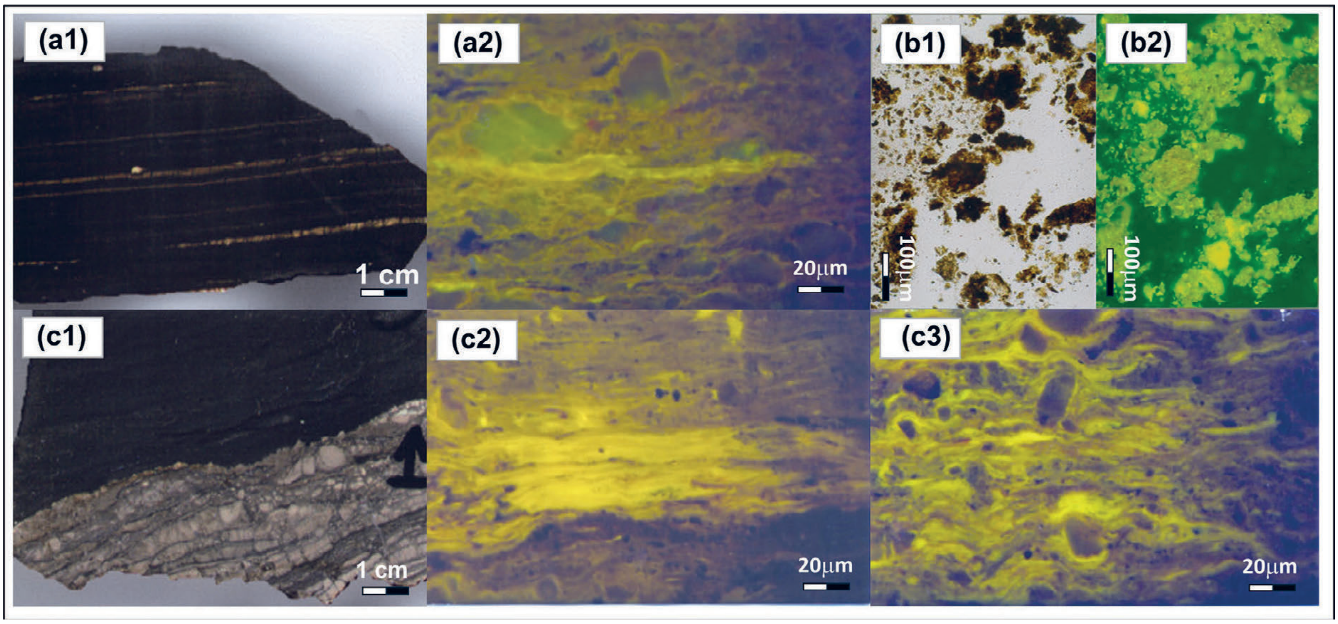

Figure 27. Photographs of Cretaceous carbonates and shales alongside photomicrographs of their organic matter. **a** Mirca, Brač: **a1** Upper Cretaceous (Maastrichtian) laminated limestone (7.31% Total Organic Carbon); **a2** Photomicrograph of lamalginite in the same rock (whole rock section, perpendicular to bedding, blue-fluorescent light); **b** Premuda-1 well, 1770 m, mudstone (2.72% TOC): **b1** Photomicrograph of amorphous organic matter (isolated kerogen) under transmitted white light; **b2** Same view under blue-fluorescent light; **c** Kremena, Ljubić creek: **c1** Upper Cretaceous laminated limestone (35.7% TOC) and breccia; **c2**, **c3** Photomicrographs of lamalginite in the same rock (whole rock sections, perpendicular to bedding, blue-fluorescent light).

+ S_2 up to 84.13 mg HC/g of rock; Suppl. 4, Table S1; Figs. 26d, 27a1, c1). These source rocks are characterized by their oil-prone organic facies, with dominant type II kerogen and subordinate occurrences of type I kerogen (Fig. 26a–c). Several key geochemical properties define these organic facies. Both the kerogen and bitumen fractions display elevated sulphur content ($S_{Ker.}$ > 3.66 to 18%; $S_{Bit.}$ 3.11 to 10.60%; Supplement 4, Table S2), classifying the kerogen as predominantly type IIS and locally type IS (ORR, 1986; BASKIN & PETERS, 1992). The organic matter is primarily of algal and bacterial origin, predominantly amorphous in maceral composition (Fig. 27b1, b2). Organic petrographic analysis reveals that the organic matter within these carbonates is mainly microbial and algal, with lamalginite and bituminite as the dominant macerals, and occasional occurrences of telalginite (Fig. 27a2, c2, c3; TEICHMÜLLER & OTTENJANN, 1977; HUTTON et al., 1980; HUTTON, 1987; TAYLOR et al., 1998). Telalginite, often found incorporated within bituminite or the organic-mineral matrix, is more prevalent in deeper sections of intra-platform basins, particularly those formed during the Late Cretaceous transgressions. Microscopic examination confirms the widespread presence of solid bitumen particles (JACOB, 1985). Along the margins of the intra-platform, facies changes indicate the presence of coaly, terrestrial facies characterized by predominantly huminite macerals (e.g., Brač-Sumartin), highlighting dynamic lateral and vertical variations in depositional conditions and primary biomass production. The highest quality kerogens are dominated by amorphous organic matter of algal and bacterial origin. In more coastal influenced areas (the Premuda-1, Ravni kotari-3, and Boraja-1 wells), a slightly lower quality organic facies is observed, characterized by an increased proportion of vitrinite and inertinite macerals. Stable carbon isotope ratios ($\delta^{13}C$) of kerogen, bitumen, and saturated and aromatic hydrocarbons predominantly indicate a marine algal source for the organic matter (Suppl. 4, Table S2; Fig. 28a; SOFER, 1984). The $\delta^{13}C$ values in both kerogens and bitumens are generally higher than -26‰ VPDB and exhibit a positive correlation. However, exceptions to this trend are observed in the coastal areas, with the Premuda-1 well showing significant deviation from the consistent values observed elsewhere (Fig. 28b; GALIMOV, 1974, 1980).

The extractable organic matter (EOM) content ranges from 383 to 124,027 ppm. The bitumen composition is dominated by polar NSO-compounds and asphaltenes, ranging from 60% to 95% (Suppl. 4, Table S2). The n-alkane distributions are characterized by a strong predominance of short-chain n-alkanes, particularly nC_{17}, suggesting a significant contribution from algal lipids (Fig. 29a1; BRAY & EVANS, 1961; TISSOT & WELTE, 1984). The Pr/nC_{17} and Ph/nC_{18} ratios are typically below 1, while the Pr/Ph ratio exhibits variability but is generally also below 1, indicating fluctuating but predominantly anoxic depositional conditions (DIDYK et al., 1978). A cross-plot of Ph/nC_{18} *versus* Pr/nC_{17} further confirms the presence of algal-derived marine organic matter (Fig. 30a; CONNAN & CASSOU, 1980). The Sterane/Hopane ratio is consistently below 1, implying significant microbial reworking of the organic matter and an enhanced contribution from bacterial biomass (TISSOT & WELTE, 1984; OURISSON et al., 1979; ROHMER, 1993). Elevated nH/H and $C_{31}R/C_{30}H$ values suggest deposition in an isolated, enclosed, carbonate shallow marine environment (Suppl. 4, Table S3). The homohopane distribution pattern and the $C_{35}S/C_{34}S$ homohopane ratio are indicative of reducing (anoxic) conditions during deposition (MOLDOWAN et al., 1992; CLARK & PHILP, 1989; PETERS & MOLDOWAN, 1991). The presence of elevated gammacerane concentrations (0.11 to

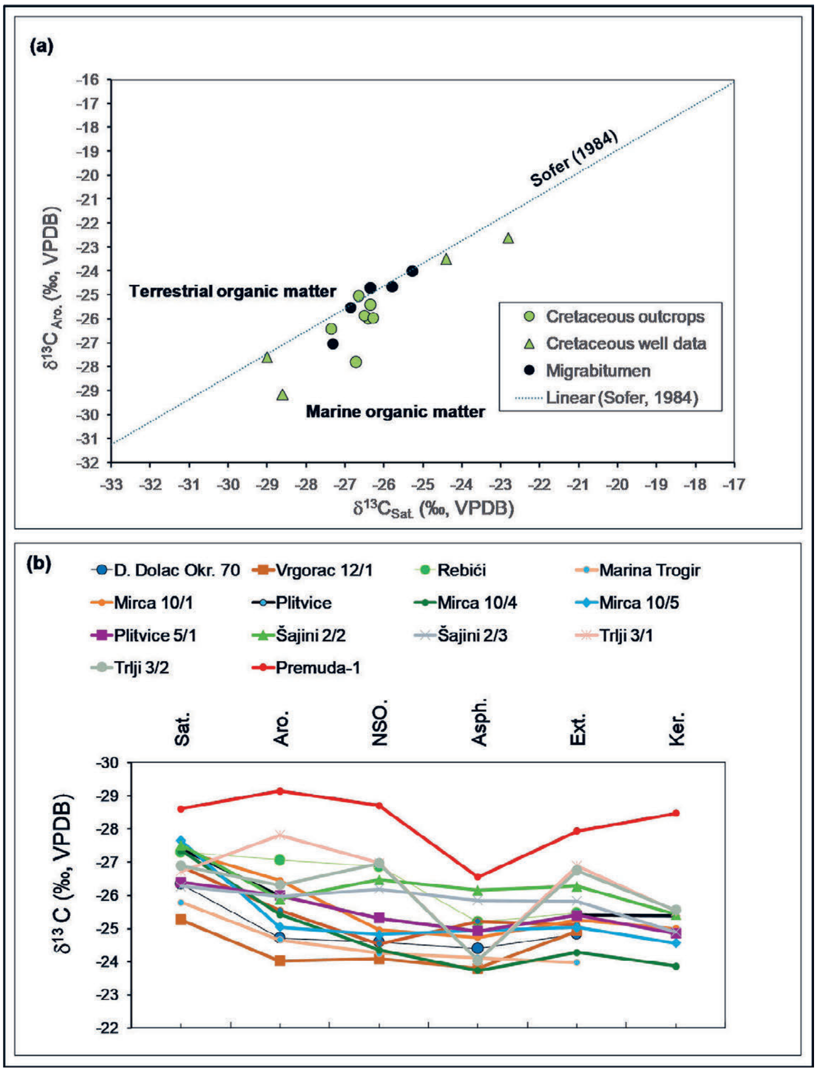

Figure 28. Stable carbon isotope ratios ($\delta^{13}C$, VPDB) characterization of organic matter from Cretaceous carbonates and shales: **a** A crossplot of $\delta^{13}C$ values for saturated and aromatic hydrocarbon fractions of extracts, used to infer organic matter type (in the SOFER´s (1984) diagram). Remark: Statistical trends are based on n-alkanes greater than C_{15}, while our analysis included the entire saturated fraction. **b** Stable carbon isotope ratios profiles of Cretaceous kerogen and its bitumen and bitumen fractions (saturated hydrocarbons, aromatic hydrocarbons, nitrogen, sulphur, and oxygen-bearing compounds/resins, and asphaltenes) (in the GALIMOV´s (1974, 1980) diagram). Key: Sat. = saturated hydrocarbons, Aro. = aromatic hydrocarbons, NSO = nitrogen, sulphur, and oxygen-bearing compounds (resins), Asph. = asphaltenes, Ext. = extract/bitumen, Ker. = kerogen, VPDB = Vienna Pee Dee Belemnite standard.

0.33) further supports deposition in stratified, isolated water column settings (SINNINGHE DAMSTE et al., 1995). In the C_{27} – C_{29} regular sterane distribution, C_{29} steranes are the dominant homologues, followed by C_{27} steranes (Fig. 29a3), suggesting a marine algal origin, with contributions from brown and green algae (VOLKMAN et al., 1986, VOLKMAN, 2003). The ternary diagram of C_{27} – C_{29} regular steranes points towards a shallow to open marine depositional environment with a source biomass comprising both phytoplankton and bacterial organic matter (Fig. 30b; HUANG & MEINSHEIN, 1979).

Collectively, the source rock and palaeoenvironmental parameters discussed above consistently indicate deposition within carbonate-evaporite environments under anoxic conditions, with the primary organic matter input derived from algae and bacteria. These findings agree with previous studies on the AdCP Cretaceous source rocks (MOLDOWAN et al., 1992; COTA & BARIĆ, 1998).

Geochemical analyses of the Cretaceous sediments reveal a thermal maturity gradient, with organic matter remaining immature down to approximately 4500 metres. Below this depth, a transition into the oil window is observed, as indicated by a range of optical and biomarker maturity parameters: T_{max} (401 – 479 °C), Thermal Alteration Index (TAI 1^+ to 3^-), fluorescence colour (yellow to yellow-orange), vitrinite reflectance (VR 0.30 – 0.50%R_o), bitumen reflectance (BR 0.06 – 0.73%R_b, corresponding to 0.43 to 0.84%R_o), Methylphenanthrene Index (MPI-1) derived vitrinite reflectance equivalent ($Rc_{(MPI-1)}$ 0.44 – 0.52%), sterane isomerization ratios (20S/(20S+20R) 0.18 – 0.52 and αββ/(αββ+ααα) 0.40 – 0.69), hopane isomerization ratio (22S/(22S+22R) 0.34 – 0.56), and the Ts/Tm ratio (0.02 – 0.06) (Suppl. 4, Tables S1, S3; PETERS & CASSA, 1994; MACKENZIE et al., 1982; SEIFERT & MOLDOWAN, 1980, 1986; MACKENZIE & MAXWELL, 1981; RADKE & WELTE, 1983). Despite this relatively low overall thermal maturity, the elevated sulphur

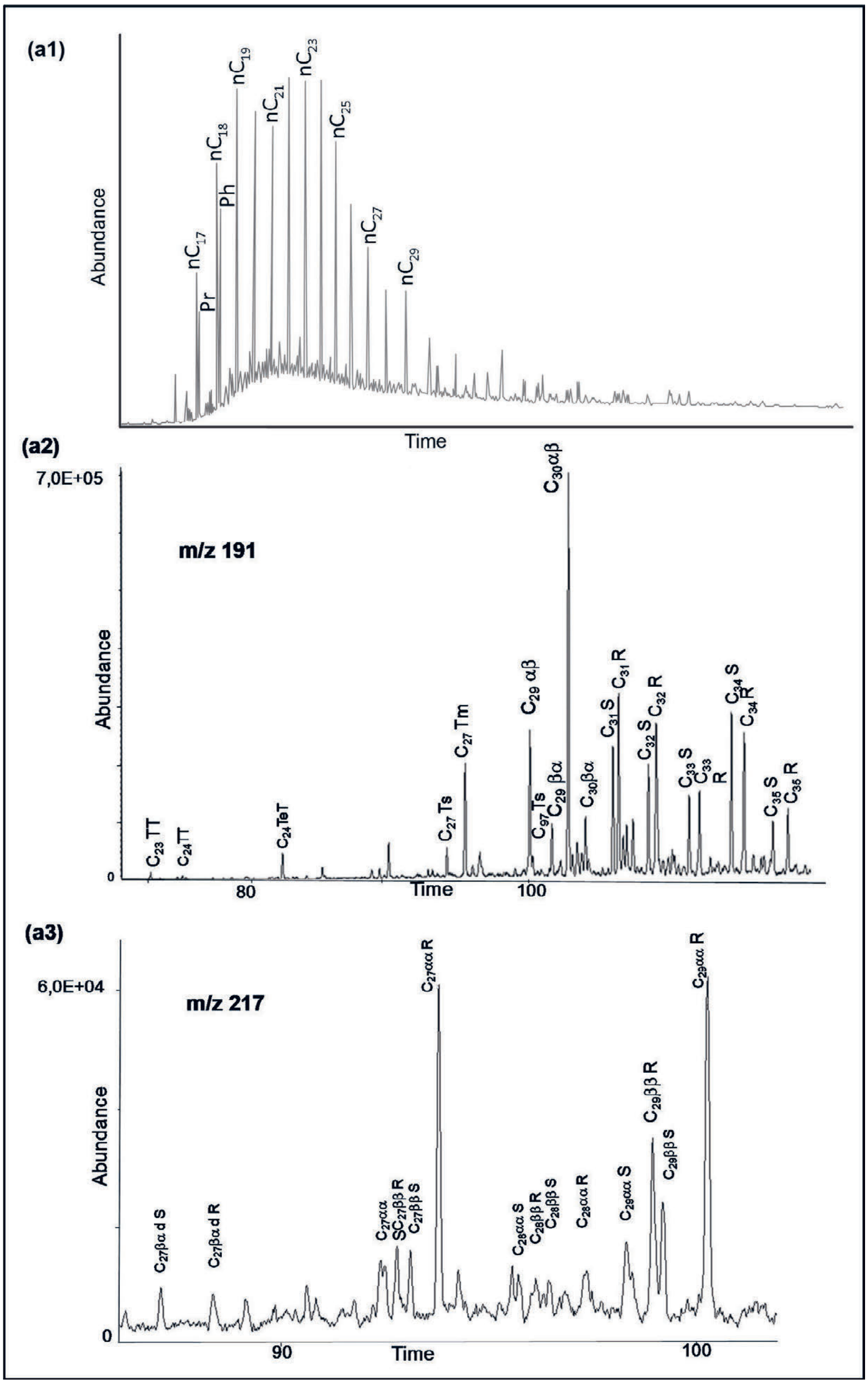

Figure 29. Chromatograms of Cretaceous carbonate extract (Vis-1 well, 2135.6 – 2138.6 m, mudstone): **a1** Gas chromatogram of bitumen; **a2** Mass chromatogram of terpanes (m/z 191); **a3** Mass chromatogram of steranes (m/z 217).

content within the kerogen matrix of these Cretaceous source rocks plays a crucial role in facilitating hydrocarbon generation at lower maturity levels (ORR, 1986; BASKIN & PETERS, 1992; RULLKÖTTER et al., 1990; ORR & SINNINGHE DAMSTE, 1990; SINNINGHE DAMSTE & LEEUW, 1990). This effect is evidenced by the exceptionally high bitumen content (extractable organic matter (EOM) often exceeding 20,000 ppm) and the increased microscopic observation of solid bitumen within the source rock lithologies.

Migrabitumen occurrences are widespread throughout the Dinarides (sample locations 1, 10, 24, 93, 95 – 97, 106, 109, 127 – 129, 139 – 141 on Figs. 4, 25), manifesting as fillings of cracks, cavities, and pores with oil, bitumen, asphalt, and other hydrocarbons, often appearing as coatings or stains (Fig. 31a, b1). Both onshore and offshore occurrences of oil and bitumen have been documented (JACOB et al., 1983; COTA & BARIĆ, 1998; MOLDOWAN et al., 1992; FIKET et al., 2008). While oil was encountered in the Ravni kotari-3 and Kate-1 wells, commercial viability was not achieved (COTA & BARIĆ, 1998). Oil samples from these wells exhibit low API gravity, ranging from 2 to 22°, and high sulphur content, a characteristic likely inherited from the sulphur-rich source rock kerogen. The content of heavy, polar resinous (NSO) compounds and asphaltene fractions is also elevated, contributing to the oil's

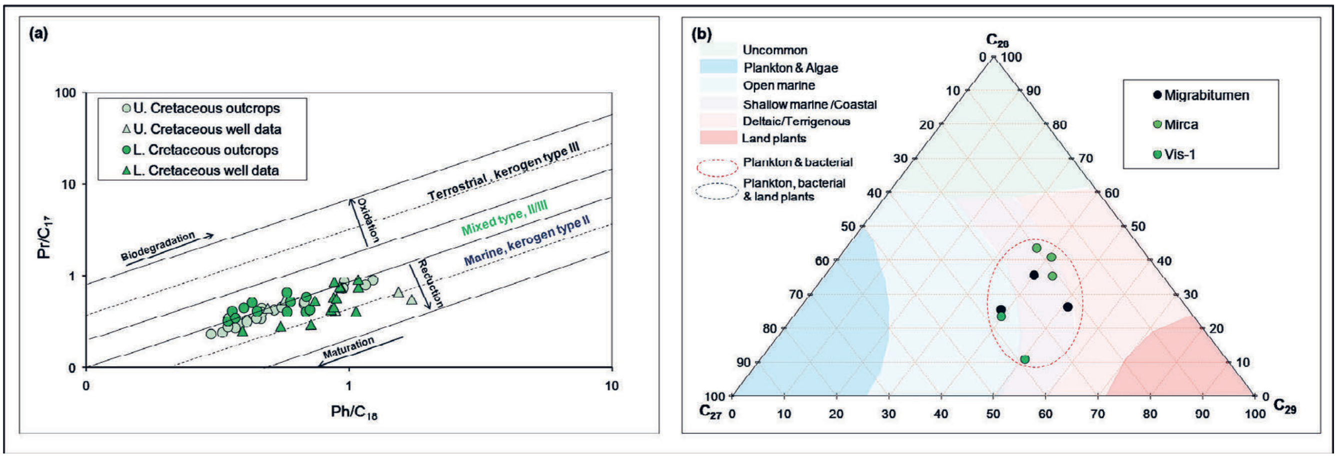

Figure 30. Source and depositional environment indicators for Cretaceous carbonates and shales: **a** Pristane (Pr)/nC_{17} *versus* Phytsne (Ph)/nC_{18} crossplot for organic matter type, depositional environment, oxygen exposure, and maturity (in the CONNAN & CASSOU´s (1980) diagram); **b** Ternary plot illustrating the relative proportions of C_{27}, C_{28}, and C_{29} steranes in extracts from Jurassic carbonates and shales (in the HUANG & MEINSHEIN´s (1979) diagram), indicative of source input and depositional setting.

increased viscosity and density. The predominantly naphthenic character of the oil suggests a relatively lower level of thermal maturity compared to paraffinic oils. Biomarker analysis and stable carbon isotope compositions consistently point towards an algal-bacterial origin of the organic matter, deposited in marine, carbonate, and potentially locally hypersaline environments under anoxic conditions. These integrated findings, along with the analytical data, establish a positive genetic correlation between the identified Cretaceous source rocks, the observed bitumen, and the encountered oil, indicating a common origin (COTA & BARIĆ, 1998).

The migrabitumens found throughout the region are classified as natural asphalts (JACOB et al., 1983), universally displaying low API gravity (less than 10°), indicative of a heavy, viscous nature and high sulphur content directly linked to the sulphur-rich source rock kerogen. The original organic compounds within these migrabitumens have undergone extensive biological alteration, signifying significant biodegradation. Their optical properties, characterized by orange to brown fluorescence and reflectance values below BR 0.2% R_o, classify them as a mixture of asphaltite, insoluble forms like wurtzilite and albertite, and soluble forms ranging from asphalt to glance pitch (Fig. 31b2, b3, c1, c2).

The stable carbon isotope ratios of kerogen ($\delta^{13}C_{Ker.}$ -23.86 to -26.10‰, VPDB) and bitumen ($\delta^{13}C_{Bit.}$ -24.27 to -23.43‰, VPDB) strongly support a genetic relationship between these

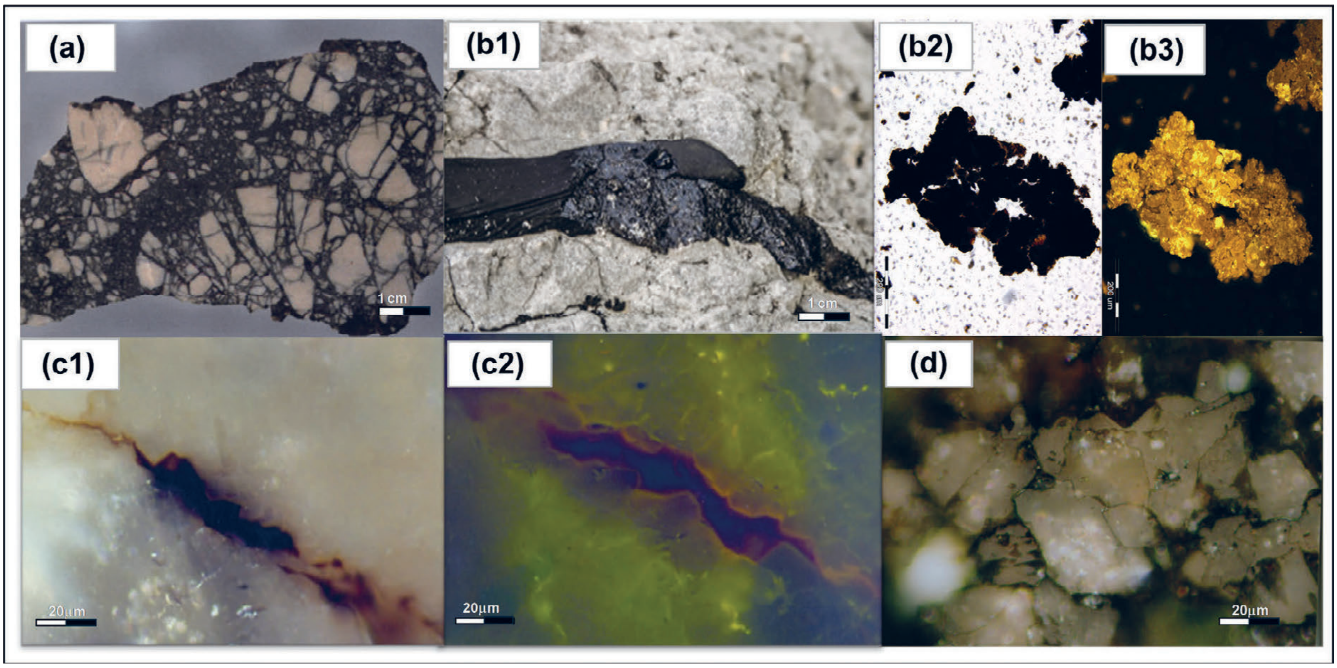

Figure 31. Photographs of Cretaceous carbonates and shales containing migrabitumen, and corresponding photomicrographs of bitumen. **a** Rošca: Upper Cretaceous bituminous limestone breccia containing 5.27% Total Organic Carbon; **b** Vrgorac: **b1** Photograph of Upper Cretaceous limestone with asphalt-wurtzilite (12.20% TOC, Bitumen Reflectance (BR) 0.10%R_b); **b2** Photomicrograph of solid bitumen (isolated organic matter) under transmitted white light; **b3** Same field of view under blue-fluorescent light; **c** Radošići: Upper Cretaceous limestone showing **c1** a fracture filled with asphalt (note visible dissolution in immersion oil, reflected light, oil immersion); **c2** a detailed view of c1 under blue-fluorescent light; **d** Škrip: Photomicrograph illustrating pores, fissures, and cavities within the rock filled with bitumen (reflected light, oil immersion).

migrabitumens and the Cretaceous source rocks (Fig. 28a; SOFER, 1984). The migrabitumens, particularly those found in the Split hinterland, are interpreted as early-stage products generated from the sulphur-rich kerogen. Following short-distance migration, they accumulated within cavities, pores, and fractures. Subsequent weathering and degradation processes transformed them from a dense liquid state into their current solid or semi-solid form (ŠPANIĆ et al., 1995; MOLDOWAN et al., 1992). While the Jurassic and Cretaceous source rocks may share some general characteristics, their stable carbon isotopic signatures allow for geochemical differentiation ($\delta^{13}C$ values around -26‰ VPDB can serve as a distinguishing factor; KATZ et al., 2000; CHUNG et al., 1992). Thermally immature Cretaceous source rocks, characterized by a specific sulphur-rich organic facies, generated heavy oils. These oils were encountered in non-commercial quantities within wells and as seeps throughout the Dinarides (Fig. 4). Their limited migration potential is likely attributable to their early-stage formation and subsequent in-reservoir transformation from a dense liquid to a solid state.

4.6. Palaeogene and Neogene source rocks characterisation

Palaeogene and Neogene sediments within the Dinarides generally exhibit a scarcity of strata with significantly elevated total organic carbon (sample locations 2, 14, 17 – 18, 46, 53, 72, 76, 94, 108, 114, 130, 134 on Fig. 4). In contrast to the Cretaceous, the Palaeogene depositional environments were predominantly freshwater to brackish, favouring the accumulation of terrestrial organic matter, primarily in the form of coal (coaly particles and distinct layers) within the Liburnian strata (VELIĆ et al., 2015). These Palaeogene coals range in rank from lignite to sub-bituminous coals and are classified as humic based on their maceral composition (STACH et al., 1982; TAYLOR et al., 1998). They are dominated by huminite macerals (including humotelinite, ulminite, humocollinite, and corpohuminite) with varying, generally lesser, amounts of liptinite macerals (such as cutinite, resinite, sporinite, and liptodetrinite) (Fig. 32a1–a3, b1–b2; SÝKOROVÁ et al., 2005; TAYLOR et al., 1998). This maceral assemblage typically renders these coals less favourable for significant liquid hydrocarbon generation (Suppl. 5, Table S1; Fig. 33). Furthermore, the organic matter in most Palaeogene sediments is thermally immature, with vitrinite reflectance (VR) values generally remaining below 0.5%R_o. A notable exception occurs in the Istrian basin, where the Raša coals exhibit exceptionally high TOC values ranging from 61.10 to 68%. These coals display VR values ranging from 0.52 to 0.60%R_o (n=50, standard deviation 0.03), indicating a higher level of thermal maturity compared to other Palaeogene occurrences. The Raša coals are primarily composed of telocollinite macerals (Fig. 32b1, b2) and are classified as high volatile bituminous C coal (*Glanzbraunkohle*) according to international coal classification standards (STACH et al., 1982; TAYLOR et al., 1998). A key characteristic of the Raša coals is their remarkably high sulphur content, on average 11.2% as cited by HAMRLA (1959) and between 10.29 and 11.07% as highlighted by MEDUNIĆ et al. (2016), respectively. This elevated sulphur content, primarily organically bound within the coal matrix, may potentially facilitate the generation of heavy oil or bitumen due to the relative weakness of carbon-sulphur bonds compared to carbon-carbon bonds during thermal maturation (ORR, 1986; BASKIN & PETERS, 1992). While JACOB et al. (1983) characterized extracts from these coals as asphalt, the overall volume and migration potential of any generated hydrocarbons are considered limited, making these coals unlikely to represent significant sources for conventional hydrocarbon accumulations.

Marls within the flysch series contain low concentrations of thermally immature organic matter (TOC ranging from 0.3 to 1%, vitrinite reflectance VR < 0.5%R_o). This organic matter is classified as terrestrial kerogen types III and IV, indicating negligible potential for hydrocarbon generation (Suppl. 5, Table S1; Fig. 33). Conversely, Palaeogene carbonates deposited in subtidal and lagoonal environments contain relatively higher amounts of marine-derived, amorphous organic matter originating from algae and bacteria (Fig. 32c1, c2). This organic matter is classified as type II kerogen and exhibits source rock characteristics. However, similar to the flysch marls, it remained thermally immature (Fig. 33).

During the Early and Middle Miocene, the Dinarides were characterized by an extensive system of lakes known as the Dinaride Lake System (DLS) (DE LEEUW et al., 2012). The sedimentary deposits associated with the DLS frequently contain coal, primarily lignite (JIMÉNEZ-MORENO et al., 2008, 2009; MANDIĆ et al., 2009). The maceral composition of these lignites is predominantly composed of huminite macerals, with subordinate amounts of liptinite and inertinite also present (Fig. 34a1; SÝKOROVÁ et al., 2005; TAYLOR et al., 1998). The occurrence of alternating layers of coal and limestone within the DLS deposits reflects cyclical periods of swamp formation and temporary subaqueous conditions, with the occasional presence of alginite and telalginite indicative of algal contributions to the organic matter (Fig. 34a2, a3).

The Upper Cretaceous/Palaeogene sediments along the northeastern edge of the AdCP (Karlovac – Petrinja – Glina area, Zrinska gora) exhibit elevated total organic carbon content (TOC > 1%). Low hydrogen index values suggest a predominance of terrestrial kerogen types III and IV (Suppl. 5, Table S1; Fig. 33). Detailed microscopic analysis confirms that these sediments are primarily composed of terrestrial plant material, ranging from finely dispersed amorphous detritus to larger inertinite and vitrinite particles (TAYLOR et al., 1998). This dominance of kerogen types III and IV is characteristic of turbidite deposits, where the original plant matter has undergone significant degradation. The organic matter in these sediments shows evidence of higher catagenesis (T_{max} > 450 ºC, vitrinite reflectance VR 0.92 to 1.40%R_o). This reworked organic matter is generally considered unfavourable for hydrocarbon generation. However, a few exceptional samples (e.g., from the Petrinjčica area, Karlovac-2 and Karlovac-3 exploration wells) exhibit higher generative potential due to a larger proportion of terrestrial liptinite macerals within the vitrinite-rich organic matter (Fig. 33). Maturity parameters indicate that these Palaeogene sediments are in transition from late diagenesis to the oil window, typically in the initial phase (T_{max} 433 to 438 ºC, VR 0.40 to 0.57 %R_o). The presence of solid bitumen in deep boreholes in the Karlovac area (Karlovac-2 and Karlovac-3 wells) suggests entry into the early oil window. Deep drilling in the Karlovac region also confirms that conditions for significant gas generation were not established.

Palaeogene (Palaeocene – Oligocene?) dark laminated shales and limestones from the Buzeta area, (Glina area, edge of Karlovac subbasin), demonstrate promising source rock characteristics. These sediments contain elevated organic

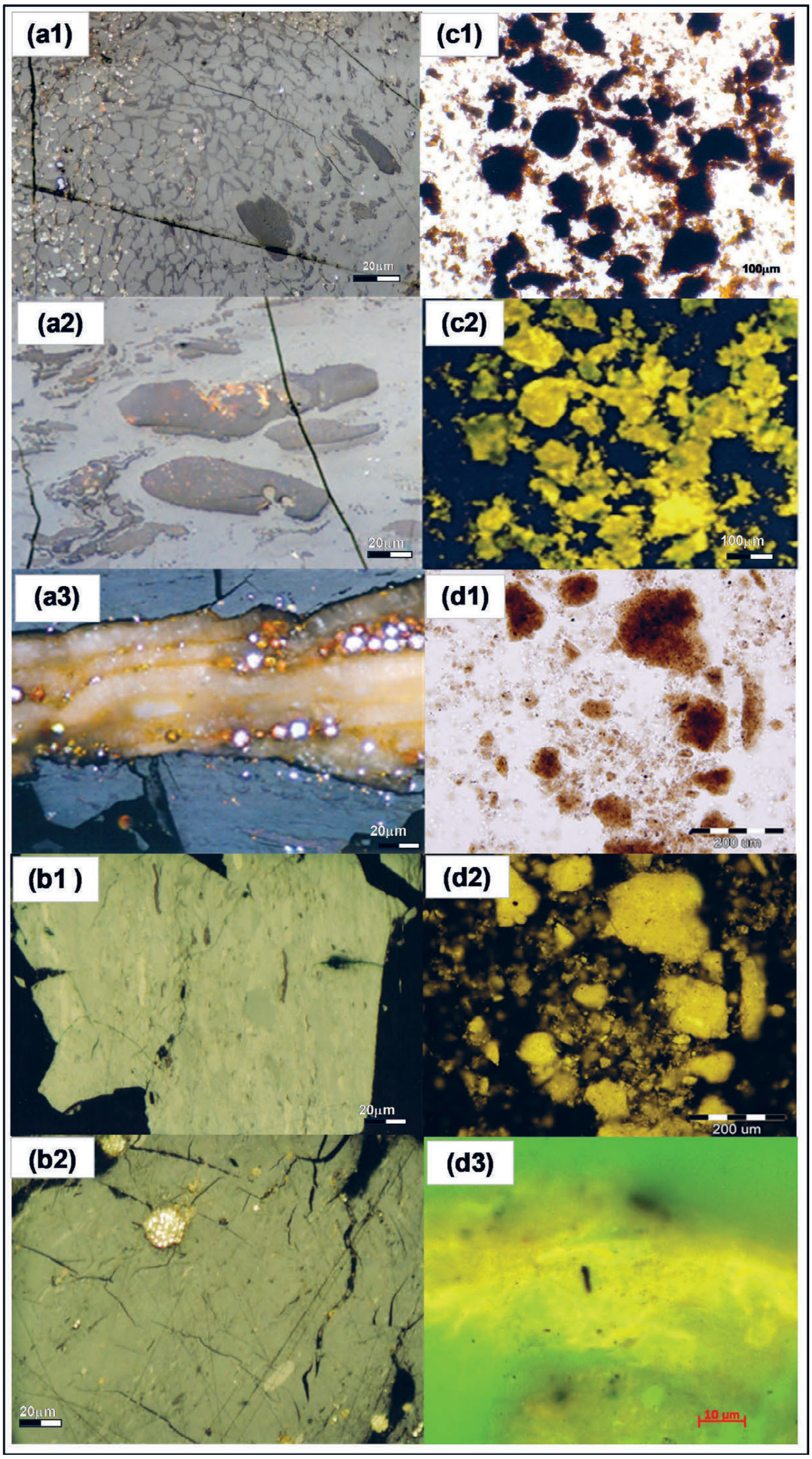

Figure 32. Photomicrographs illustrating organic matter types in Palaeogene carbonates, marls, coals, and shales. Reflected white light with oil immersion was used for coal and coaly shale samples; other techniques are specified. **a** Baška coaly shale (VR 0.44%R_o): **a1** – **a3** Huminite macerals (textinite and corpohuminite); **b** Raša coal and coaly shales (VR 0.60%R_o): **b1**, **b2** Telocollinite maceral and framboidal pyrite; **c** Koromačno carbonates: **c1** Impregnated (bituminous) amorphous organic matter (isolated organic matter) under transmitted white light; **c2** Same view as c1 under blue-fluorescent light; **d** Buzeta shales: **d1** Amorphous organic matter (isolated kerogen) under transmitted white light; **d2** Same view as d1 under blue-fluorescent light; **d3** Lamalginite in a whole rock section, oriented perpendicular to bedding and viewed under blue-fluorescent light.

carbon content (TOC up to 13%) and good generative potential ($S_1 + S_2 > 6$ mg HC/g of rock; Suppl. 5, Table S1; Fig. 33). The kerogen is classified as type II to II/I, indicating a mixed algal and bacterial origin. Microscopic analysis reveals that the organic matter is predominantly amorphous with traces of alginite, dinoflagellates, liptodetrinite, and rare low reflectance vitrinite. The relatively high negative values of stable carbon isotope ratios in kerogen ($\delta^{13}C_{Ker.}$ -26 to -30‰ VPDB; Suppl. 5, Table S2)

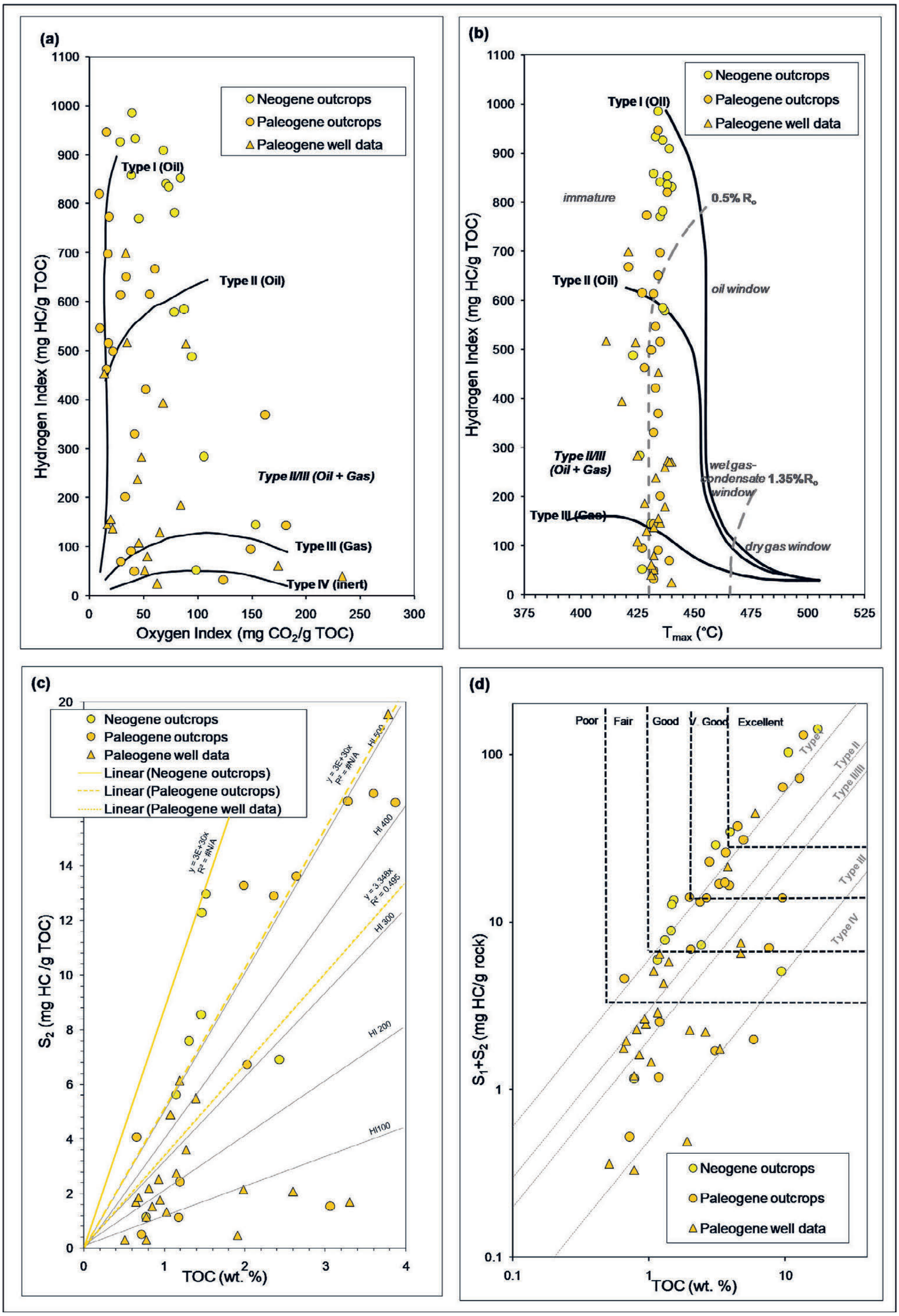

Figure 33. Source rock characterization of the Palaeogene and Neogene carbonates, marls, and shales using Rock-Eval pyrolysis data: **a** Hydrogen Index (HI) *versus* Oxygen Index (OI) crossplot showing the organic matter type classification; **b** Hydrogen Index (HI) *versus* T_{max} crossplot illustrating thermal maturity levels and trends; **c** Generative Potential (S_2) *versus* Total Organic Carbon (TOC) crossplot with superimposed average Hydrogen Index (HI) trends, indicating hydrocarbon generation potential; **d** Source rock quality assessment using a crossplot of Petroleum potential (S_1+S_2) *versus* Total Organic Carbon (TOC).

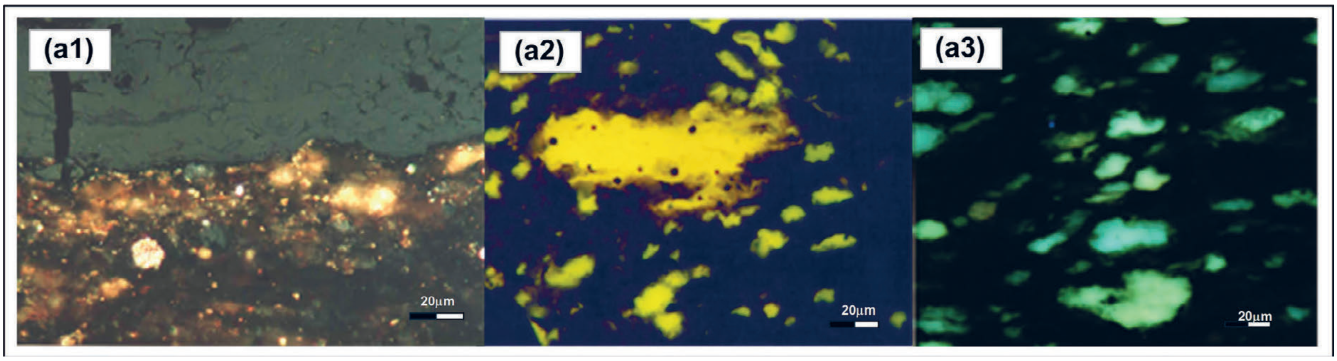

Figure 34. Photomicrographs illustrating organic matter in Neogene marls, coals, and shales from the Sinj Ruda coaly shales. **a1** Huminite maceral (textoulminite, VR 0.26%R_o) in whole rock, observed under reflected light with oil immersion; **a2** Alginite (telalginite type) in a whole rock section perpendicular to bedding, viewed under blue-fluorescent light; **a3** Same alginite as in a2, viewed under ultraviolet light.

could suggest a significant bacterial contribution rather than a solely terrestrial input. The organic matter is thermally immature, residing in the late diagenesis stage (T_{max} 430 to 435 ºC). While the kerogen type suggests a calm, possibly freshwater-influenced depositional environment, the diverse molecular distributions (variations in Pr/Ph, Pr/nC_{17}, Ph/nC_{18}; Fig. 35; DIDYK et al., 1978; CONNAN & CASSOU, 1980) indicate a mix of organic matter sources (algae, cyanobacteria, dinoflagellates, zooplankton) or fluctuating depositional conditions. The thickness of Palaeogene deposits in the Glina subbasin is estimated to range from 250 to 450 metres. However, the precise age and lateral extent of these sediments remain uncertain.

Additionally, thin interlayers of Palaeogene (Eocene) carbonates encountered in the Adriatic Sea (Melita-1 and Mirjana-1 wells) exhibit excellent source rock potential, with $S_1 + S_2$ values reaching up to 42 mg HC/g of rock. These interlayers contain immature, algal and bacterial organic matter classified as type II kerogen. Notably, their enrichment in sulphur (S 5 – 6%) allows for hydrocarbon generation at a lower maturity level compared to typical type II kerogen. The heavy oil (13° API) discovered in the Melita-1 well displays a positive genetic correlation with these thin-layered source rocks, as supported by biomarker and isotopic analyses ($\delta^{13}C$ -14 to -23‰ VPDB; Suppl. 5, Tables S1, S2), further substantiating their hydrocarbon potential.

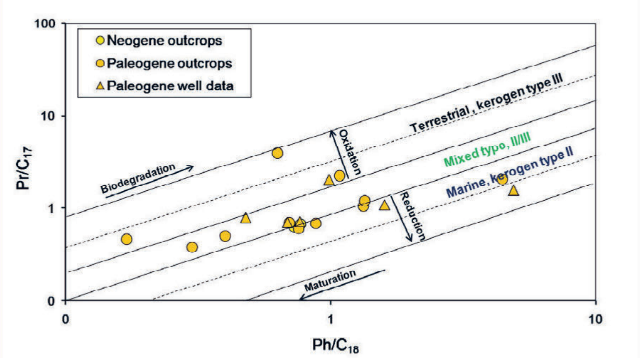

Figure 35. Source and depositional environment of Palaeogene and Neogene carbonate and shale extracts: Pristane (Pr)/nC_{17} *versus* Phytane (Ph)/nC_{18} crossplot for organic matter type, depositional environment, oxygen exposure, and maturity (in the CONNAN & CASSOU´s (1980) diagram).

5. CONCLUSIONS

Based on the comprehensive analysis of over 5,000 borehole and outcrop samples, this study provides a robust evaluation of the source rock potential across multiple stratigraphic levels within the External Dinarides. Our findings reveal the following key insights into the petroleum systems of the region:

a) Carboniferous and Permian organic-rich siliciclastics and carbonates are consistently overmature, having surpassed the oil and gas generation windows.

b) Triassic organic-rich shales and carbonates exhibit high levels of thermal alteration, with the presence of pyrobitumen indicating past hydrocarbon generation. Notably, the Upper Triassic Vlasta-Komiža Facies laminated limestones, outcropping on the islands of Vis and Palagruža in the Adriatic Sea, represent excellent oil-prone source rocks characterized by type II to IIS kerogen. These facies have reached the onset of oil generation, and geochemical data strongly correlate generated oil with these specific source rocks.

c) Lower Jurassic shales and carbonates are also highly thermally altered, suggesting limited remaining petroleum potential.

d) Upper Jurassic dark, organic-rich limestones and shales of the Lemeš Trough constitute excellent oil-prone source rocks, featuring type II and IIS kerogen. Their high sulphur content has enabled hydrocarbon generation at relatively lower thermal maturity levels, with observed bituminous coatings and seeps indicating short-distance migration of early-stage products.

e) Cretaceous laminated carbonates, deposited within restricted lagoons and intraplatform troughs, represent excellent, oil-prone source rocks containing immature type IIS kerogen. These sulphur-rich facies can generate hydrocarbons at lower maturity levels and have reached the oil window at depths exceeding 4,500 metres in the central Adriatic Sea. They are linked to non-commercial heavy hydrocarbons and oil shows, highlighting an active but potentially constrained petroleum system.

f) Palaeogene and Neogene coaly shales and carbonates are generally immature and occur only locally, suggesting limited regional significance as primary source rocks.

In summary, the most prospective source rocks within the External Dinarides are predominantly carbonate and calcareous shale lithologies enriched in high-quality, marine-derived (algal and microbial) organic matter with elevated sulphur content (kerogen type I/IIS). The deposition of these key source rock units was intrinsically linked to the evolving palaeoenvironmental conditions and depositional settings on the Adriatic Carbonate Platform (VELIĆ et al., 2002a, b; VLAHOVIĆ et al., 2005). The highest quality source rocks are identified within Middle Triassic intraplatform troughs, the Late Jurassic Lemeš Trough, and Cretaceous carbonate-evaporite and deep-water intraplatform facies.

Thermal maturity parameters clearly delineate the varying maturation histories of these source rocks. Triassic source rocks in the hinterland are largely in late catagenesis to metagenesis (Velebit, Svilaja Mt.), rendering them predominantly post-generative, whereas their offshore counterparts (Vlasta-Komiža facies) have reached initial maturity at significant depths (>5000 m). Source rocks within the Lemeš Trough range from immature to initially mature, while Cretaceous source rocks are generally immature across the explored areas. Thermal modelling confirms the maximum temperature exposure of organic matter, with Middle Triassic volcanism identified as the most significant thermal event influencing the region's petroleum evolution. This event likely caused early maturation and depletion in older Triassic sequences.

A defining characteristic of the carbonate-hosted organic facies is their elevated sulphur content, which demonstrably lowers the thermal maturity threshold for hydrocarbon generation. This explains the widespread occurrences of bitumen, migrabitumen, oil stains, asphalt, and oil and wet gas throughout the broader Dinarides. Isotopic analyses provide compelling evidence for positive genetic correlations between these allochthonous hydrocarbons and the identified Jurassic and Cretaceous source rocks, with further comparisons suggesting potential links to Italian oils, collectively confirming the presence of an active petroleum system.

However, the ultimate viability of these petroleum systems hinges on the critical temporal alignment of hydrocarbon generation, expulsion, and migration with the formation and preservation of suitable structural and stratigraphic traps, processes intimately linked to the complex structural evolution of the Dinarides. The prevalence of overmature Triassic source rocks, with generation occurring prior to significant structural development, underscores the importance of this temporal relationship.

The Upper Jurassic carbonates and calcareous shales of the Lemeš Formation, particularly the high-quality occurrences in the Lika part of the trough (TROSKOT-ČORBIĆ, 2011), and the Cretaceous carbonates of evaporitic and deep-water facies represent the most promising remaining source rock intervals in the External Dinarides. Recognizing that these Jurassic and Cretaceous organic facies likely attained maximum burial depths during the Late Cretaceous and Palaeocene, prior to major structural deformation, future onshore exploration efforts should prioritize ascertaining their subsurface distribution and thermal maturity at depths exceeding 3,000 metres. Consequently, detailed structural-tectonic interpretations will be crucial for effectively delineating the migration pathways and potential trap geometries, thereby enhancing our understanding of the petroleum system linkages and informing future exploration strategies within the External Dinarides.

Acknowledgement

We gratefully acknowledge the generous funding provided by INA-*Industrija nafte d.d.* This project would not have been possible without the continuous support and invaluable guidance of Josip BUBNIĆ, the operating director of INA Group Exploration and Production. A special thank you is extended to Dr. Jasmina JELIĆ-BALTA and our dedicated colleagues from INA's Exploration and Production Laboratory, whose contributions were essential to this work. We also wish to express our deep appreciation to our colleagues from the geochemistry laboratory for their expertise and commitment throughout this research. We sincerely thank the reviewers for their thoughtful and constructive feedback, which was instrumental in improving the quality of this manuscript.

REFERENCES

ALEKSIĆ, N., KOSTIĆ, A. & RADONJIĆ, M. (2021): Composition of organic matter and thermal maturity of Mesozoic and Cenozoic sedimentary rocks in East Herzegovina (External Dinarides, Bosnia and Herzegovina).– Annales Societatis Gelogorum Poloniae, 91, 369–382. https://doi.org/10.14241/asgp.2021.16

ANDERSON, H. & JACKSON, J. (1987): Active tectonics of the Adriatic Region.– Geophysical Journal of the Royal Astronomical Society, 91, 937–983. https://doi.org/10.1111/j.1365-246X.1987.tb01675.x

BALLING, P., TOMLJENOVIĆ, B., SCHMID, S.M. & USTASZEWSKI, K. (2021): Contrasting along-strike deformation styles in the central external Dinarides assessed by balanced cross-sections: Implications for the tectonic evolution of its Paleogene flexural foreland basin system.– Elsevier, Global and Planetary Change, 205, 4, 1–24. https://doi.org/10.1016/j.gloplacha.2021.103587

BARIĆ, G. (1988): Rezultati geokemijskih ispitivanja stijena Dinaridsko-jadranskog područja i rubnih dijelova Panonskog bazena [*Results of geochemical analyses of the rocks of the Dinaric-Adriatic area and the peripheral parts of the Pannonian basin* – in Croatian].– Nafta, 39, 9, 527–535.

BARIĆ, G. (2006): Naftna geokemija [*Petroleum geochemistry* – in Croatian].– INA-Industrija nafte d.d., Zagreb, 228 p.

BARIĆ, G. & COTA, L. (1999): Cretaceous source rock of the Adriatic offshore.– Nafta, 50, 5, 467–173.

BARIĆ, G. & COTA, L. (2003): Geochemical correlation of the Cenomanian/Turonian source rock sequences in the Mediterranean, North Africa-Adriatic/Dinaric area.– In: 1st North Africa/Mediterranean Petroleum & Geoscience Conference & Exhibition, Tunis, Extended Abstracts, 1030. https://doi.org/10.3997/2214-4609-pdb.8.T030

BARIĆ, G. & TARI, V. (2005): Upper Jurassic/Lower Cretaceous Anoxic Event of Adriatic-Dinaridic Domain.– In: GONZÁLEZ-VILA, F.J., GONZÁLEZ-PEREZ, J.A. & ALMEDROS, G. (eds.): 22nd International Meeting on Organic Geochemistry, Spain, Book of Abstracts, 804–805.

BARIĆ, G., MARIČIĆ, M. & RADIĆ, J. (1988): Geochemical characterization of organic facies in the Dugi Otok Basin, Adriatic Sea.– Organic Geochemistry, 13, 343–349.

BARIĆ, G., TARI, V. & IVKOVIĆ, Ž. (2003): Petroleum system in the southern part of the Pannonian Basin and in the Adriatic Offshore, Croatia.– Nafta, 54, 7–8, 299–307.

BARKER, C.E. & PAWLEWICZ, M.J. (1994): Calculation of Vitrinite Reflectance from Thermal Histories and Peak Temperatures A Comparison of Methods.– In: MUKHOPADHYAY, P. & DOW, W.G (eds.): Vitrinite Reflectance as a Maturity Parameter. ACS Symposium Series; American

Chemical Society: Washington, D, 216–229. https://pubs.acs.org/doi/book/10.1021/bk-1994-0570

BASKIN, D.K. & PETERS, K.E. (1992): Early Generation Characteristic of a Sulphur-Rich Monterey Kerogen.– American Association of Petroleum Geologists Bulletin, 76, 1–13.

BATTAGLIA, M., MURRAY, M.H., SERPELLONI, SERPELLONI, E. & BÜRGMANN, R. (2004): The Adriatic region: An independent microplate within the Africa-Eurasia collision zone.– Geophysical Research Letters, 31, L09605. https://doi.org/10.1029/2004GL019723

BERNOULLI, D. (1971): Redeposited pelagic sediments in the Jurassic of the central Mediterranean area.– Annales Instituti Geologici Publici Hungarici, 54/2, 71–90.

BERNOULLI, D. (2001): Mesozoic-Tertiary carbonate platforms, slopes and basins of the external Apennines and Sicily.– In: VAI, G.B. & MARTINI, I.P. (eds.): Anatomy of an Orogen: The Apennines and Adjacent Mediterranean Basins. Kluwer Academic Publishers, 307–327. https://doi.org/10.1007/978-94-015-9829-3_18

BLAŽEKOVIĆ SMOJIĆ, S., SMAJLOVIĆ, J., KOCH, G., BULIĆ, J., TRUTIN, M., OREŠKI, E., ALAJBEG, A. & VESELI, V. (2009): Source potential and palynofacies of Late Jurassic ''Lemeš facies", Croatia.– Organic Geochemistry, 40, 833–845. https://doi.org/10.1016/j.orggeochem.2009.05.005

BOROVIĆ, I., MARINČIĆ, S., MAJCEN, Ž., RAFAELI, P. & MAMUŽIĆ, P. (1976): Osnovna geološka karta SFRJ 1:100 000, list Vis K 33–33 (Jabuka K 33-31, Svetac K 33-32, Biševo K 33-45) [*Basic Geological Map of SFRY 1:100 000, Vis sheet K 33-33 (Jabuka K 33-31, Svetac K 33-32, Biševo K 33-45)* – in Croatian].– Institut za geološka istraživanja, Zagreb, Savezni geološki zavod, Beograd.

BOROVIĆ, I., MARINČIĆ, S., MAJCEN, Ž., RAFFAELLI, P. & MAMUŽIĆ, P. (1977): Osnovna geološka karta SFRJ 1:100.000. Tumač za list Vis K 33-33 (Jabuka K 33-31, Svetac K 33-32, Biševo K 33-45) [*Basic Geological Map of SFRY 1:100 000. Explanatory notes for the Vis sheet K 33-33, Jelsa sheet K 33-34, Biševo sheet K 33-45, Svetac K 33-32, and Jabuka K 33-31* – in Croatian].– Institut za geološka istraživanja, Zagreb, Savezni geološki institut, Beograd, 67 p.

BOSELLINI, A. (2002): Dinosaurs "re-write" the geodynamics of the eastern Mediterranean and the paleogeography of the Apulia platform.– Earth-Science Reviews, 59, 211–234. https://doi.org/10.1016/S0012-8252(02)00075-2

BOSTICK, N.H. (1979): Microscopic measurements of the level of catagenesis of solid organic matter in sedimentary rocks to aid exploration for petroleum and to determine former burial temperatures – a review.– SEPM Special Publication, 26, 17–43. https://doi.org/10.2110/pec.79.26.0017

BRAY, E.E. & EVANS, E.D. (1961): Distribution of n-paraffins as a clue to recognition of source beds.– Geochimica et Chosmochimica Acta, 22, 2–15. https://doi.org/10.1016/0016-7037(61)90069-2

BUCKOVIĆ, D., CVETKO TEŠOVIĆ, B. & GUŠIĆ, I. (2004): Late Jurassic paleoenvironmental evolution of the Western Dinarides (Croatia).– Geologia Carpathica, 55, 3–18.

BUSER, S. (1987): Osnovna geološka karta SFRJ 1:100 000, list Tolmin i Videm L 33-64 [*Basic geological map of SFRY 1:100 000, Tolmin and Videm sheet L 33-64* – in Slovenian].– Geološki zavod, Ljubljana, Savezni geološki zavod, Beograd.

CALAIS, E., NOCQUET, J.-M., JOUANNE, F. & TARDY, M. (2001): Current strain regime in the Western Alps from continuous Global Positioning System measurements, 1996–2001.– Geology, 30/7, 651–654. https://doi.org/10.1130/0091-7613(2002)030<0651:CSRITW>2.0.CO;2

CALDARELLI, C., MARTINI, P. & SMITH, D. (2013): Source Rock Potential and Maturity Modelling in the Southern Adriatic Sea Area: Key Controls for Predicting Hydrocarbon Distribution.– Search and Discovery, 50833.

CARMINATI, E. & DOGLIONI, C. (2005): Mediterranean Tectonics.– In: Encyclopaedia of Geology. Elsevier academic press, 136–146.

CARMINATI, E., LUSTRINO, M. & DOGLIONI, C. (2012): Geodynamic evolution of the central and western Mediterranean: Tectonics vs. igneous petrology constraints. Elsevier academic press.– Tectonophysics, 579, 173–192. https://doi.org/10.1016/j.tecto.2012.01.026

CAVAZZA, W. & WEZEL, C. (2003): The Mediterranean region–a geological primer.– Episodes, 26, 3, 160–168. https://doi.org/10.18814/epiiugs/2003/v26i3/002

CAVAZZA, W., ROURE, F. & ZIEGLER, P.A. (2004): The Mediterranean area and the surrounding regions: Active processes, remnants of former Tethyan oceans and related thrust belts.– In: CAVAZZA, W. ROURE, F.M., SPAKMAN, M., STAMPFLI, G.M. & ZIEGLER, P.A. (eds.): The TRANSMED Atlas–The Mediterranean region from crust to mantle. Berlin and Heidelberg, Springer, 1–29. https://doi.org/10.1007/978-3-642-18919-7_1

CHAMOT-ROOKE, N., RABAUTE, A. & KREEMER, C. (2005): Western Mediterranean Ridge mud belt correlates with active shear strain at the prism-backstop geological contact.– Geology, 33, 861–864. https://doi.org/10.1130/G21469.1

CHANNELL, J.E.T., D'ARGENIO, B. & HORVÁTH, F. (1979): Adria, the African promontory, in Mesozoic Mediterranean palaeogeography.– Earth-Science Reviews, 15/3, 213–292. https://doi.org/10.1016/0012-8252(79)90083-7

CHOROWICZ, J. (1975): Mechanics of Split-Karlovac transversal structure in Yugoslavian Dinarides.– Comptes Rendus Hebdomadaires séances l'Académie Sciences, 280, 20, 2313–2316.

CHOROWICZ, J. & GEYSSANT, J. (1972): Présence des couches de Lemeš (calcaires à Ammonites subméditerranéennes du Malm) dans le Lika (Croatie, Yougoslavie).– Comptes rendus de l'Académie des Sciences Paris, 275, 731–734.

CHUNG, H.M., ROONEY, M.A., TOON, M.B. & CLAYPOOL, G.E. (1992): Carbon isotope composition of marine crude oils.– American Association of Petroleum Geologists Bulletin, 76, 1000–1007. https://doi.org/10.1306/BDFF8952-1718-11D7-8645000102C1865D

CITA, M.B. & McKENZIE, J.A. (1986): The terminal Miocene event.– In: HSÜ, K.J., (ed.): Mesozoic and Cenozoic Oceans: Geodynamics Series 15, American Geophysical Union, 123–140. http://doi.org/10.1029/GD015p0123

CLARK, J.P. & PHILP, R.P. (1989): Geochemical characterization of evaporite and carbonate depositional environments and correlation of associated crude oils in the Black Creek Basin, Alberta.– Canadian Petroleum Geologists Bulletin, 37, 401–416. https://doi.org/10.35767/gscpgbull.37.4.401

CLAYTON, J.L. & SWETLAND, P.J. (1978): Subaerial weathering of sedimentary organic matter.– Geochimica et Cosmochimica Acta, 42/3, 30–5-312. http://doi.org/10.1016/0016-7037(78)90183-7

CONNAN, J. & CASSOU, A.M. (1980): Properties of gases and petroleum liquids derived from terrestrial kerogen at various maturation levels.– Geochemica et Cosmochimica Acta, 44, 1–23. https://doi:10.1016/0016-7037(80)90173-8

COTA, L. & BARIĆ, G. (1998): Petroleum Potential of the Adriatic offshore, Croatia.– Organic Geochemistry, 29, 1–3, 559–570. https://doi.org/10.1016/S0146-6380(98)00130-2

COTA, L., TROSKOT-ČORBIĆ, T., KOCH, G. & PANDŽIĆ, M. (2015): "Burano" facijes kao ključni element u istraživanju ugljikovodičnog potencijala srednjeg i južnog Jadrana [*"Burano" facies as a key element in the exploration of the hydrocarbon potential of the central and southern Adriatic* – in Croatian].– Naftaplin, 35/143–144, 71–78.

COWARD, M. & DIETRICH, D. (1989): Alpine tectonics–An overview.– In: COWARD, M.P., DIETRICH, D. & PARK, R.G. (eds.): Alpine Tectonics. Geological Society of London Special Publication, 45, 1–29. http://doi.org/10.1144/GSL.SP.1989.045.01.01

ČADJENOVIĆ, D., KILIBARDA, Z. & RADULOVIĆ, N. (2008): Late Triassic to Late Jurassic evolution of the Adriatic Carbonate Platform and Budva Basin, Southern Montenegro.– Sedimentary Geology, 204, 1–17. https://doi.org/10.1016/j.sedgeo.2007.12.005

DE CAPOA, P., RADOIČIĆ, R. & D'ARGENIO, B. (1995): Late Miocene Deformation of the External Dinarides (Montenegro and Dalmatia): New Biostratigraphic Evidence.– Memorie Scienze Geologia, Department of Geosciences, University of Padova, 47, 157–172.

DE LEEUW, A., MANDIĆ, O., KRIJGSMAN, W., KUIPER, K. & HRVATOVIĆ, H. (2012): Palaeomagnetic and geochronologic constraints on the geodynamic evolution of the central Dinarides.– Tectonophysics, 530–531, 286–298. http://doi.org/10.1016/j.tecto.2012.01.004

DECIMA, A. & WEZEL, F.C. (1973): Late Miocene evaporites of the central Sicilian basin.– In: RYAN, W.B.F. & HSÜ, K.J. (eds.): Initial Reports of the Deep-Sea Drilling Project, Leg 13: Washington, D.C., U.S. Printing Office, 1234–1240.

DEMAISON, G.J. & HUIZINGA, B.J. (1994): Genetic classification of petroleum system using three factors: charge, migration and entrapment.– In: MAGOON, B. & DOW, W.G. (eds.): The Petroleum System – From Source to Trap. American Association of Petroleum Geologists Memoir, 60, 73–93.

DERCOURT, J., ZONENSHAIN, L.P., RICOU, L.E., KAZMIN, V.G., LE PICHON, X., KNIPPER, A.L., GRANDJACQUET, C., SBORTSHIKOV, I.M., GEYSSANT, J. & LEPVRIER, C. (1986): Geological evolution of the Tethys belt from the Atlantic to the Pamirs since the Lias.– Tectonophysics, 123, 241-315. https://doi.org/10.1016/0040-1951(86)90199-X

DERCOURT, J., GAETANI, M., VRIELYNCK, B., BARRIER, E., BIJU-DUVAL, B., BRUNET, M.F., CADET, J.P., CRASQUIN, S. & SANDULESCU, M. (2000): Atlas Peri-Tethys, Paleogeographical maps, CCGM/CGMW, Paris: 24 maps and explanatory notes: I–XX; 1–269.

DEVOTI, C., RIGUZZI, F., CUFFARO, M. & DOGLIONI, C. (2008): New GPS constraints on the kinematics of the Apennines subduction.– Earth and Planetary Science Letters, 273, 163–174. http://doi.org/10.1016/j.epsl.2008.06.031

DEWEY, J.F., HEMPTON, M.R., KIDD, W.S.F., ŞAROĞLU, F. & ŞENGÖR, A.M.C. (1986): Shortening of continental lithosphere: The neotectonics of Eastern Anatolia–A young collision zone.– In: COWARD, M.P. & RIES, A.C. (eds.): Collision zone tectonics: Geological Society of London Special Publication, 19, 3–36. http://doi.org/10.1144/GSL.SP.1986.019.01.01

DEWEY, J.F., HELMAN, M.L., TURCO, E., HUTTON, D.H. & KNOTT, S.D. (1989): Kinematics of the western Mediterranean.– In: COWARD, M.P., DIETRICH, D. & PARK, R.G. (eds.): Alpine tectonics. Geological Society of London Special Publication, 45, 265–283. http://doi.org/10.1144/GSL.SP.1989.045.01.15

DIDYK, B.M., SIMONEIT, B.R.T., BRASSELL, S.C. & EGLINTON, G. (1978): Organic geochemical indicators of paleoenvironmental conditions of sedimentation.– Nature, 272, 216–222, https://doi.org/10.1038/272216a0

DILEK, Y. (2006): Collision tectonics of the Mediterranean region: Causes and consequences.– Special Paper 409. The Geological Society of America. https://doi.org/10.1130/2006.2409(01)

DILEK, Y. & MOORES, E.M. (1990): Regional tectonics of the Eastern Mediterranean ophiolites.– In MALPAS, J., MOORES, E.M., PANAYIOTOU, A. & XENOPHONTOS, C. (eds.): Ophiolites, oceanic crustal analogues: Proceedings of the symposium "Troodos 1987". Geological Survey Department, Nicosia, Cyprus, 295–309.

DILEK, Y., THY, P., HACKER, B. & GRUNDVIG, S. (1999): Structure and petrology of Tauride ophiolites and mafic dike intrusions (Turkey): Implications for the Neo-Tethyan ocean.– Bulletin of the Geological Society of America, 111, 8, 1192–1216. https://doi.org/10.1130/0016-7606(1999)1112.3.CO;2

DIMITRIJEVIĆ, M.D. (1997): Geology of Yugoslavia.– Geological Institute GEMINI Special Publication, Belgrade, 187 p.

DOGLIONI, C., GUEGUEN, E., HARABAGLIA, P. & MONGELLI, F. (1999): On the origin of west-directed subduction zones and applications to the western Mediterranean.– In: DURAND, B., JOLIVET, L., HORVÁTH, F. & SÉRANNE, M. (eds.): The Mediterranean basins: Tertiary extension within the Alpine orogen: Geological Society of London Special Publication, 156, 541–561. http://doi.org/10.1144/GSL.SP.1999.156.01.24

DRAGIČEVIĆ, I. (1987): Paleogeografska evolucija rubnog dijela mezozojske karbonatne platforme Dinarida između Vrbasa i Bosne [*Palaeogeographical evolution of the marginal zone of the Mesozoic carbonate platform of Dinarides in the area between Vrbas and Bosna rivers* – in Croatian, with an English Abstract].– Unpubl. PhD Thesis, University of Zagreb, 90 p.

DRAGIČEVIĆ, I: (2010): Sjeverni rub Jadranske karbonatne platforme [Northen margin of the Adriatic Carbonate Platform].– In: HORVAT, M. (ed.): Vodič ekskurzije 4. Hrvatski geološki kongres [Excursion Guidebook 4th Croatian Geological Congress]. Postaja 11 (Stop 11). Croatian geological survey, Zagreb, 61–72.

DRAGIČEVIĆ, I. & VELIĆ, I. (1994): Stratigraphical position and significance of reef facies at the northern margin of the Dinaric carbonate platform during the Late Jurassic and Cretaceous in Croatia and Bosnia.– Géologie Méditerranéenne, 21/3–4, 59–63.

DRAGIČEVIĆ, I. & VELIĆ, I. (2002): The northeastern margin of the Adriatic Carbonate Platform.– Geologia Croatica, 55/2, 185–232.

DROBNE, K., OGORELEC, B., PLENIČAR, M., BARATTOLO, F., TURNŠEK, D. & ZUCCHI-STOLFA, M.L. (1989): The Dolenja vas section, a transition from Cretaceous to Paleocene in the NW Dinarides, Yugoslavia.– Memorie Societa Geologica Italiana, 40, 73–84.

EKWEOZOR, C.M., OKOGUN, J.I., EKONG, D.E.U. & MAXWELL, J.R. (1979): Preliminary organic geochemical studies of samples from the Niger delta (Nigeria) I. Analyses of crude oils for triterpanes.– Chemical Geolology, 27, 11–28. https://doi:10.1016/0009-2541(79) 90100-1

ESPITALIÉ, J. & BORDENAVE, M.L. (1993): Rock Eval pyrolysis.– In: BORDENAVE, M.L. (ed.): Applied Petroleum Geochemistry. Éditions Technip, Paris, 237–261.

ESPITALIE, J., DEROO, G. & MARQUIS, F. (1985): Rock Eval pyrolysis and its applications.– Institut Francais du Petrole, 72 p.

FIKET, Ž., ALAJBEG, A., STRMIĆ PALINKAŠ, S., TARI-KOVAČIĆ, V., PALINKAŠ, L. & SPANGENBERG, H. (2008): Organic geochemistry of Jurassic-Cretaceous source rocks and oil seeps from the profile across the Adriatic-Dinaric carbonate platform.– Geologica Carpathica, 59, 3, 225–236.

FUČEK, L., JELASKA, V., GUŠIĆ, I., PRTOLJAN, B. & OŠTRIĆ, N. (1991): Padinski turonski sedimenti uvale Brbišnica na Dugom otoku [*Turonian slope deposits in the Brbišnica cove, Dugi Otok Island, Croatia* – in Croatian].– Geološki vjesnik, 44, 55–67.

FURLANI, M. (1910): Die Lemeš-schichten. Ein Beitrag zur Kenntnis der Juraformation in Mitteldalmatien.– Jahrbuch der Kaiserlich Königlichen Geologischen Reichsanstalt, 60/1, 67–98.

GAINA, C., TORSVIK, T.H., VAN HINSBERGEN, D.J.J., MEDVEDEV, S., WERNER, S.C. & LABAILS, C. (2013): The African Plate: a history of oceanic crust accretion and subduction since the Jurassic.– Tectonophysics, 604, 4–25. http://doi.org/10.1016/j.tecto.2013.05.037

GALIMOV, E. M. (1974): Organic geochemistry of carbon isotopes.– In: TISSOT, B. & BIENNER, F. (eds.): Advances in Organic Geochemistry, 1973, Editions Technip., 439–452.

GALIMOV, E. M. (1980): $^{13}C/^{12}C$ in kerogen.– In: DURAND, B. (ed.): Kerogen. Editions Technip, Paris, 271–299.

GARCIA-CASTELLANOS, D., ESTRADA, F., JIMÉNEZ-MUNT, I., GORINI, C., FERNÁNDEZ, M., VERGÉS, J. & DE VICENTE, R. (2009): Catastrophic flood of the Mediterranean after the Messinian salinity crisis.– Nature ,462, 778–781 (2009). https://doi.org/10.1038/nature08555

GAWLICK, H.J., ĐERIC, N., MISSONI, S., BRAGIN, N.Y., LEIN, R., SUDAR, M. & JOVANOVIĆ, D. (2017): Age and microfacies of oceanic Upper Triassic radiolarite components from the Middle Jurassic ophiolitic melange in the Zlatibor Mountains (Inner Dinarides, Serbia) and their provenance.– Geologica Carpathica 68, 350–365. https://doi.org/10.1515/geoca-2017-0024

GORIČAN, Š. (1994): Jurassic and Cretaceous radiolarian biostratigraphy and sedimentary evolution of the Budva zone (Dinarides, Montenegro).– Memoires de Geologie Lausanne 18, 176 p.

GRANDIĆ, S. (2010): Hydrocarbon potential assessment of the slope deposits along the SW Dinarides carbonate platform edge.– Nafta, 61/7–8, 191–195.

GRANDIĆ, S., BOROMISA-BALAS, E. & ŠUŠTERČIĆ, M. (1997): Exploration concept and characteristics of the Dinarides in Croatian offshore area.– Nafta, 48/8–9, 249–267.

GRANDIĆ, S., BOROMISA-BALAŠ, E., ŠUŠTERČIĆ, M. & KOLBAH, S. (1999): Hydrocarbon possibilities in the eastern Adriatic slope zone of Croatian offshore area.– Nafta, 50/2, 51–73.

GRANDIĆ S., BIANCONE, M. & SAMARŽIJA, J. (2001): Geophysical and Stratigraphic Evidence of the Triassic Rift Structuration in the Adriatic offshore area.– Nafta, 52/12, 383–396.

GRANDIĆ S., BIANCONE, M. & SAMARŽIJA, J. (2002a): Geophysical and Stratigraphic Evidence of the Adriatic Triassic Rift Structures.– Memorie Societa Geologia Italiana, 57, 315–325.

GRANDIĆ S., VESELI, V. & KOLBAH, S. (2002b): Hydrocarbon potential of Dugi Otok basin in offshore Croatia.– Nafta, 53/6–7, 215–224.

GRANDIĆ S., KRATKOVIĆ, I., KOLBAH, S. & SAMARŽIJA, J. (2004): Hydrocarbon potential of stratigraphic and structural traps of the Ravni Kotari area – Croatia.– Nafta, 55/7–8, 311–327.

GRANDIĆ, S., KRATKOVIĆ, I. & BALIĆ, D. (2013): Peri-Adriatic platforms Proximal Talus reservoir potential (part 1).– Nafta, 64/2, 147–160.

GRANDIĆ, S., KRATKOVIĆ, I., BALIĆ, D. & KOLBAH, S. (2014): Peri-Adriatic platforms Proximal Talus reservoir potential (part 2).– Nafta, 65/1, 29–40.

GRIMANI, I., ŠIKIĆ, K. & ŠIMUNIĆ, A. (1972): Osnovna geološka karta SFRJ 1:100 000, list Knin L 33-141. [*Basic Geological Map of SFRY 1:100 000; Knin sheet L 33-141* – in Croatian].– Institut za geološka istraživanja, Zagreb, Savezni geološki zavod, Beograd.

GRIMANI, I., JURIŠA, M., ŠIKIĆ, K. & ŠIMUNIĆ, A. (1975): Osnovna geološka karta SFRJ 1:100 000. Tumač za list Knin L 33-141 [*Basic Geological Map of SFRY 1:100 000. Explanatory notes for the Knin sheet L 33-141*].– Institut za geološka istraživanja, Zagreb, Savezni geološki zavod, Beograd, 61 p.

GUŠIĆ, I. & BABIĆ, LJ. (1970): Neke biostratigrafske i litogenetske osobine jure Žumberka [*Some biostratigraphic and lithogenetic characteristic of the Jurassic in Žumberak, northwest Croatia* – in Croatian].– Geološki vjesnik, 23, 39–54.

GUŠIĆ, I. & JELASKA, V. (1990): Stratigrafija gornjokrednih naslaga otoka Brača u okviru geodinamske evolucije Jadranske karbonatne platforme [*Upper Cretaceous stratigraphy of the Island of Brač within the geodynamic evolution of the Adriatic Carbonate Platform* – in Croatian].– JAZU i Institut za geološka istraživanja, Zagreb, 160 p.

GUŠIĆ, I. & JELASKA, V. (1993): Upper Cenomanian–Lower Turonian sea-level rise and consequences on the Adriatic–Dinaric carbonate platform.– Geologische Rundschau, 82/4, 676–686. http://doi.org/10.1007/BF00191495

HAMRLA, M. (1959): O pogojih nastanka premogišč na Krasu [*On the conditions of origin of the coal beds in the Karst region – in Slovenian, Summary in English*].– Geologija, 5, 180–264.

HANDY, M.R., SCHMID, S.M., BOUSQUET, R., KISSLING, E. & BERNOULLI, D. (2010): Reconciling plate-tectonic reconstructions of Alpine Tethys with the geological-geophysical record of spreading and subduction in the Alps.– Earth-Science Reviews, 102, 121–158. http://doi.org/10.1016/j.earscirev.2010.06.002

HANDY, M.R., USTASZEWSKI, K. & KISSLING, E. (2015): Reconstructing the Alps-Carpathians-Dinarides as a key to understanding switches in subduction polarity, slab gaps and surface motion.– International Journal of Earth Sciences, 104, 1–26. https://doi.org/10.1007/s00531-014-1060-3

HERAK, M. (1986): A new concept of geotectonics of the Dinarides.– Acta geologica, 16/1, 1–42.

HSÜ, K.J., CITA, M.B. & RYAN, W.B.F. (1973): The origin of the Mediterranean evaporites.– Initial Reports of the Deep Sea Drilling Project, 13, 1203–1231.

HUANG, W.Y. & MEINSHEIN, W.G. (1979): Sterols as ecological indicators.– Geochemica et Cosmochimica Acta, 43, 739–745, https://doi.org/10.1016/0016-7037(79)90257-6

HUNT, J.M. (1995): Petroleum Geochemistry and Geology.– W.H. Freeman and Company, San Francisco, 743 p.

HUTTON, A.C. (1987): Petrographic classification of oil shales.– International Journal of Coal Geology, 8, 203–231. http://doi.org/10.1016/0166-5162(87)90032-2

HUTTON, A.C., KANTSLER, A.J., COOK, A.C. & MCKIRDY, D.M. (1980): Organic matter in oil shales.– Australian Petroleum Exploration Association Journal, 20, 44–68. https://doi.org/10.1071/AJ79005

JACOB, H. (1985): Disperse solid bitumens as an indicator for migration and maturity in prospecting for oil and gas.– Erdöl und Kohle, 38, 365.

JACOB, H. (1989): Classification, structure, genesis and practical importance of natural solid bitumen („migrabitumen").– International Journal of Coal Geology, 11, 61–79. http://doi.org/10.1016/0166-5162(89)90113-4

JACOB, H., JENKO, K. & SPAIĆ, V. (1983): O disperznim, čvrstim do polučvrstim prirodnim naftnim bitumenima jadranskog obalnog područja (Vanjski Dinaridi) Jugoslavije [*About dispersed, solid to semisolid natural oil bitumens of the Yugoslav Adriatic coastal area (Outer Dinarides*) – in Croatian].– Nafta, 34/12, 693–700.

JELASKA, V. (1973): Paleogeografska i naftnogeološka razmatranja zapadnog dijela karbonatnog šelfa Dinarida [*Palaeogeographical and petroleum-geological considerations of the western part of the Dinaric carbonate shelfy* – in Croatian].– Geološki vjesnik, 25, 57–64.

JELASKA, V. (1987): Paleoambijentalna dinamika sjevero-istočnog rubnog prostora Vanjskih Dinarida u juri i kredi [*Jurassic and Cretaceous palaeoenvironmental dynamic of the northeastern margin of the Outer Dinarides* – in Croatian].– Geološki vjesnik, 40, 195–216.

JELASKA, V., GUŠIĆ, I., JURKOVŠEK, B., OGORELEC, B., ĆOSOVIĆ, V., ŠRIBAR, L. & TOMAN, M. (1994): The Upper Cretaceous geodynamic evolution of the Adriatic–Dinaric carbonate platform(s).– Geologie Mediterranee, 21/3–4, 89–91.

JELASKA, V., BENČEK, C., ĆOSOVIĆ, V., GUŠIĆ, I. & MATIČEC, D. (2000): Upper Cretaceous–Paleogene resedimented carbonates: their significance for the dynamics of the Adriatic–Dinarids carbonate platform.– In: Abstract book: Symposium Quantitative models on Cretaceous
carbonates and the Eastern margin of the Apulia platform. Vieste–Gargano, 12–12.

JENKYNS, H.C. (1980): Cretaceous anoxic events: from continents to oceans.– Journal of the Geological Society, 137, 171–188. http://doi.org/10.1144/gsjgs.137.2.0171

JENKYNS, H. C. (1985): The early Toarcian and Cenomanian-Turonian anoxic events in Europe: comparisons and contrasts.– Geologische Rundschau, 74, 505–518. http://doi.org/10.1007/BF01821208

JENKYNS, H.C. (1988): The Early Toarcian (Jurassic) anoxic event: Stratigraphic, sedimentary, and geochemical evidence.– American Journal of Science, 288, 101–151. http://doi.org/10.2475/ajs.288.2.101

JENKYNS, H.C. (1991): Impact of Cretaceous Sea level rise and anoxic events on the Mesozoic carbonate platform of Yugoslavia.– American Association of Petroleum Geologists Bulletin, 75, 1007–1017.

JENKYNS, H.C. & CLAYTON, C.J. (1986): Black shales and carbon isotopes in pelagic sediments from the Tethyan Lower Jurassic.– Sedimentology 33, 87–106. http://doi.org/10.1111/j.1365-3091.1986.tb00746.x

JENKYNS, H.C., JONES, C.E., GROCKE, D.R., HESSELBO, S.P. & PARKINSON, D.N. (2002): Chemostratigraphy of the Jurassic System: applications, limitations and implications for palaeoceanography.– Journal of the Geological Society, London, 159, 351–378. http://doi.org/10.1144/0016-764901-130

JERINIĆ, G., JELASKA, V. & ALAJBEG, A. (1994): Upper Cretaceous Organic-Rich Laminated Limestones of the Adriatic carbonate Platform, Island of Hvar, Croatia.– American Association of Petroleum Geologists Bulletin, 78, 8, 1313–1321.

JIMÉNEZ-MORENO, G., MANDIĆ, O., HARZHAUSER, M., PAVELIĆ, D. & VRANJKOVIĆ, A. (2008): Vegetation and climate dynamics during the early Middle Miocene from Lake Sinj (Dinaride Lake System, SE Croatia).– Review of Paleobotany and Palynology, 152/3, 237–245. https://doi.org/10.1016/j.revpalbo.2008.05.005

JIMÉNEZ-MORENO, G., DE LEEUW, A., MANDIĆ, O., HARZHAUSER, M., PAVELIĆ, D., KRIJGSMAN, W. & VRANJKOVIĆ, A. (2009): Integrated stratigraphy of the early Miocene lacustrine deposits of Pag Island (SW Croatia): Paleovegetation and environmental changes in the Dinaride Lake System.– Palaeogeography, Palaeoclimatology, Palaeoecology, 280/1, 193–206. https://doi.org/10.1016/j.palaeo.2009.05.018

JOLIVET, L., DE LAMOTTE, D.F., MASCLE, A. & SÉRANNE, M. (1999): The Mediterranean basins: Tertiary extension within the Alpine orogen– An introduction.– In: DURAND, B., JOLIVET, L., HORVÁTH, F. & SÉRANNE, M. (eds.): The Mediterranean basins: Tertiary extension within the Alpine orogen: Geological Society of London Special Publication, 156, 1–14. http://doi.org/10.1144/GSL.SP.1999.156.01.02

JONES, R.W. (1984): Comparison of carbonate and shale source rocks.– In: PALACAS, J.G. (ed.): Petroleum Geochemistry and Source Rock Potential of Carbonate Rocks. AAPG Studies in Geology, 18, 163–180, Tulsa. http://doi.org/10.1306/St18443C12

JONES, R.W. (1987): Organic facies.– In: BROOKS, J. & WELTE, D. (eds.): Advances in petroleum geochemistry 2. Academic Press, London, 90 p.

JONES, C.E. & JENKYNS, H.C. (2001): Seawater strontium isotopes, oceanic anoxic events, and seafloor hydrothermal activity in the Jurassic and Cretaceous.– American Journal of Science, 301, 112–149. http://doi.org/10.2475/ajs.301.2.112

JURKOVŠEK, B., TOMAN, M., OGORELEC, B., ŠRIBAR, L., DROBNE, K., POLJAK, M. & ŠRIBAR, LJ. (1996): Formacijska geološka karta južnega dela Tržaško–Komenske planote. Kredne in palaeogenske karbonatne kamnine, 1:50.000 (*Geological map of the southern part of the Trieste–Komen plateau, Cretaceous and Paleogene carbonate rocks*).– Institut za geologiju, geotehniku I geofiziku, Ljubljana, 143 p.

KASTENS, K.A. & MASCLE, J. (1990): The geological evolution of the Tyrrhenian Sea: an introduction to the scientific results of ODP LEG 107.– In: KASTENS, K.A., MASCLE, J., CITA, M.B. & MCCOY, F. (eds.): Proceedings ODP, Scientific Results, 107. College Station, TX (Ocean Drilling Program), 3–26. http://doi.org/10.2973/odp.proc.sr.107.187.1990

KATZ, B.J., DITTMAR, E.I. & EHRET, G.E. (2000): A geochemical review of carbonate source rocks in Italy.– Journal of Petroleum Geology, 23/4, 399–424. https://doi.org/10.1111/j.1747-5457.2000.tb00494.x

KORBAR, T. (2009): Orogenic evolution of the External Dinarides in the NE Adriatic region: a model constrained by tectonostratigraphy of Upper Cretaceous to Paleogene carbonates.– Earth-Science Reviews, 96, 296–312. http://doi.org/10.1016/j.earscirev.2009.07.004

KORBAR, T., MONTANARI, A., KOCH, G., MARIANI, S., DON DEPAOLO, A., TURCHYN, V., MIKNIĆ, M. & TARI, V. (2009): Geologic reconnaissance of the island of Velika Palagruža (central Adriatic, Croatia).– Geologia Croatica, 62/2, 75–94. https://doi.org/10.4154/GC.2009.07

KORBAR, T., BELAK, M., FUČEK, L., HUSINEC, A., OŠTRIĆ, N., PALENIK, D. & VLAHOVIĆ, I. (2012): Osnovna geološka karta Republike Hrvatske mjerila 1:50 000, list: Vis 3 i Biševo 1 [*Basic Geological Map of RH 1:50 000, Vis 3 and Biševo 1 sheets*].– Hrvatski geološki institut, Zagreb.

KRKALO, E., ŠUŠNJARA, A., ŠĆAVNIČAR, B. & GABRIĆ, A. (1995): Jurski silicijski sedimenti lemeškog facijesa (malm) u Dalmaciji i Lici [*Jurassic siliceous sediments of the Lemeš facies (Malmian) in Dalmatia and Lika* – in Croatian].– In: VLAHOVIĆ, I., VELIĆ, I. & ŠPARICA, M. (eds.): 1. Hrvatski geološki kongres, Zbornik radova (First Croatian Geological Congress, Proceedings), 1, 321–326, Zagreb.

LITTKE, R. (1993): Deposition, diagenesis and weathering of organic matter rich sediments.– Springer Nature, Lecture Notes in Earth Sciences, 47, 216 p.

LITTKE, R., BAKER, D.R. & LEYTHAUSER, D. (1988): Microscopic and sedimentologic evidence for the generation and migration of hydrocarbons in Toarcian source rock of different maturities.– In: MATTAVELLI, L. & NOVELLI, L. (eds.): Advances in Organic Geochemistry 1987, Organic Geochemistry, 13, 549–559. https://doi.org/10.1016/B978-0-08-037236-5.50061-0

LOWRENCE, S.R., TARI-KOVAČIĆ, V. & GJUKIĆ, B. (1995): Geological evolution model of the Dinarides.– Nafta, 46/2, 103–113.

MACKENZIE, A.S. & MAXWELL, J.R. (1981): Assessment of thermal maturation in sedimentary rocks by molecular measurements.– In: BROOKS, J. (ed.): Organic Maturation Studies and Fossil Fuel Exploration. Academic Press, London, 239–254.

MACKENZIE, A.S., BRASSELL, S.C., EGLINTON, G. & MAXWELL, J.R. (1982): Chemical fossils: the geological fate of steroids.– Science, 217, 491–504, https://doi.org/10.1126/science.217.4559.491

MAGOON, L.B. & DOW, W.G. (1994): The Petroleum System.– In: MAGOON, L.B. & DOW, W.G. (eds.): The Petroleum system – from Source to Trap.– American Association of Petroleum Geologists Memoir, 60, 3–25. http://doi.org/10.1306/M60585C1

MALENŠEK ANDOLŠEK, N. & MARKIČ, M. (2021): Organic petrological characterisation and facies interpretation of the Upper Triassic (Carnian – Julian) black limestone in the Lesno Brdo area (External Dinarides, Central Slovenia).– Marine and Petroleum Geology, 128, 105056. https://doi.org/10.1016/j.marpetgeo.2021.105056

MALVIĆ, T., ĐUREKOVIĆ, M., ŠIKONJA, Ž., ČOGELJA, Z., ILIJAŠ, T. & KRULJAC, I. (2011): Exploration and Production Activities in northern Adriatic Sea (Croatia), successful joint venture INA (Croatia) and ENI (Italy).– Nafta: exploration, production, processing, petrochemistry, 62, 9–10, 287–296.

MANDIĆ, O., PAVELIĆ, D., HARZHAUSER, M., ZUPANIĆ, J., REISCHENBACHER, D., SACHSENHOFER, R.F., TADEJ, N. & VRANJKOVIĆ, A. (2009): Depositional history of the Miocene Lake Sinj (Dinaride Lake System, Croatia): a long-lived hard-water lake in a pull-apart tectonic setting.– Journal of Paleolimnology 41, 431–452. https://doi.org/10.1007/s10933-008-9235-1

MARGETIĆ, M. (1950): Bituminozne stijene Dalmacije [*Bituminous rocks of Dalmatia* – in Croatian].– Geološki vjesnik, II–IV, 117–140.

MARINČIĆ, S. & MATIČEC, D. (1991): Tektonika i kinematika deformacija na primjeru Istre [*Tectonics and kinematic of deformations–an Istrian model* – in Croatian].– Geološki vjesnik, 44, 247–268.

MATIČEC, D. (1989): Strukturni sklop područja Rovinj–Poreč (zapadna Istra) [*Structural fabric of the Rovinj–Poreč area, Western Istria* – in Croatian].– Unpubl. MSc Thesis, University of Zagreb, 50 p.

MATIČEC, D., VLAHOVIĆ, I., VELIĆ, I. & TIŠLJAR, J. (1996): Eocene limestones overlying Lower Cretaceous deposits of western Istria (Croatia): did some parts of present Istria form land during the Cretaceous?– Geologia Croatica, 49/1, 117–127.

MATTAVELLI, L. & NOVELLI, L. (1990): Geochemistry habit of the oils in Italy.– American Association of Petroleum Geologists Bulletin, 74/10, 1623–1639.

MATTAVELLI, L., NOVELLI, L. & ANELLI, L. (1991): Occurrence of hydrocarbons in the Adriatic Basin.– In: SPENCER, A.M. (ed.): Generation accumulation, and production of Europe's hydrocarbons. Special Publication of the European Association of Petroleum Geoscientists, 1, 369–380.

MEDUNIĆ, G., RAĐENOVIĆ, A., BAJRAMOVIĆ, M., ŠVEC, M. & TOMAC, M. (2016): Once grand, now forgotten: what do we know about the superhigh-organic-sulphur Raša coal?– The Mining-Geology-Petroleum Engineering Bulletin, 2016, 27–45. https://doi.org/10.17794/rgn.2016.3.3

MICALLEF, A., CAMERLENGHI, A., GARCIA-CASTELLANOS, D., CUNARRO-OTERO, D., GUTSCHER, M.A., BARRECA, G., SPATOLA, D., FACCHIN, L., GELETTI, R., KRASTEL, S., GROSS, F. & URLAUB, M. (2018): Evidence of the Zanclean megaflood in the eastern Mediterranean Basin.– Scientific Reports, 8, 1078. https://doi.org/10.1038/s41598-018-19446-3

MOLDOWAN, J.M., SUNDARAMAN, P., SALVATORI, T., AJALBEG, A., GUKIC, B., LEE, C.Y. & DEMAISON, G. (1992): Source correlation and maturation assessment of select oils and rocks from the Central Adriatic basin (Italy and Yugoslavia).– In: MOLDOWAN, M., ALBRECHT, P. & PHILIP, R.P. (eds.): Biological Markers in Sediments and Petroleum. Prentice-Hall, New Jersey, 370–401.

MOLDOWAN, J.M., DAHL, J., HUIZINGA, B.J., FAGO, F.J., HICKEY, L.J., PEAKMAN, T.M. & TAYLOR, D.W. (1994): The molecular fossil record of oleanane and its relation to angiosperms.– Science, 265, 768–771. http://doi.org/10.1126/science.265.5173.768

MUTTONI, G., GARZANTI, E., ALFONSI, L., CIRILLI, S., GERMANI, D. & LOWRIE, W. (2001): Motion of Africa and Adria since the Permian: paleomagnetic and paleoclimatic constraints from Northern Libya.– Earth and Planetary Science Letters, 192, 159–174. http://doi.org/10.1016/S0012-821X(01)00439-3

NOWAK, G.J. (2007): Comparative studies of organic matter petrography of the Late Paleozoic black shales from Southwestern Poland.– International Journal of Coal Geology, 71, 568–585.

ORR, W.L. (1986): Kerogen/asphaltene/sulfur relationship in sulfur-rich Monterey oils.– Organic Geochemistry, 10, 499–516. http://doi.org/10.1016/0146-6380(86)90049-5

ORR, W.L. & SINNINGHE DAMSTE, J.S. (1990): Geochemistry of Sulphur in Petroleum System.– In: ORR, W.L. & WHITE, C.M. (eds.): Geochemistry of Sulphur in Fossil Fuels. American Chemistry Society, Washington, 2–30.

OŠTRIĆ, N., FUČEK, L., PRTOLJAN, B., JELASKA, V., KOROLIJA, B., GUŠIĆ, I., ŠPARICA, M., KORBAR, T. & HUSINEC, A. (2014): Osnovna geološka karta Republike Hrvatske mjerila 1:50 000, list Vis 4 [*Basic Geological Map of RH 1:50 000, Vis 4 sheet* – in Croatian].– Hrvatski geološki institut, Zagreb.

OURISSON, G., ALBRECHT, P. & ROHMER, M. (1979): The hopanoids.– Pure Applied Chemistry, 51, 709–729.

PALACAS, J.G. (1984): Carbonate rocks and sources of petroleum: geological and chemical characteristic and oil-source correlation.– In: Proceedings of the 11th World Petroleum Congress 1983, 2, 31–43. John Willey & Sons, Chichester.

PÁLFY, J. & SMITH, P.L. (2000): Synchrony between Early Jurassic extinction, oceanic anoxic event, and the Karoo–Ferrar flood basalt volcanism.– Geology, 28, 747–750. http://doi.org/10.1130/0091-7613(2000)28%3C747:SBEJEO%3E2.0.CO;2

PAMIĆ, J. (1993): Eoalpine to Neoalpine magmatic and metamorphic processes in the northwestern Vardar Zone, the easternmost Periadriatic Zone and the southwestern Pannonian Basin.– Tectonophysics, 226, 503–518. http://doi.org/10.1016/0040-1951(93)90135-7

PAMIĆ, J. (2002): The Sava-Vardar Zone of the Dinarides and Hellenides *versus* the Vardar Ocean.– Eclogae Geologicae Helvetiae, 95, 99–113.

PAMIĆ, J., GUŠIĆ, I. & JELASKA, V. (1998): Geodynamic evolution of the Central Dinarides.– Tectonophysics, 297, 251–268. http://doi.org/10.1016/S0040-1951(98)00171-1

PAMIĆ, J., TOMLJENOVIĆ, B. & BALEN, D. (2002): Geodynamic and petrogenetic evolution of Alpine ophiolites from the central and NW Dinarides: an overview.– Lithos, 65, 113–142. http://doi.org/10.1016/S0024-4937(02)00162-7

PEPPER, A.S. & CORVI, P.J. (1995a): Simple kinetic models of petroleum formation. Part I: Oil and Gas generation from kerogen.– Marine and Petroleum Geology, 12, 3, 291–319. http://doi.org/10.1016/0264-8172(95)98381-E

PEPPER, A.S. & CORVI, P.J. (1995b): Simple kinetic models of petroleum formatio. Part III: modelling an open system.– Marine and Petroleum Geology, 12, 417–452. https://doi.org/10.1016/0264-8172(95)96904-5

PEPPER, A.S. & DODD, T.A. (1995): Simple kinetic models of petroleum formation. Part II: oil-gas cracking.– Marine and Petroleum Geology, 12, 3, 321–340. http://doi.org/10.1016/0264-8172(95)98382-F

PETERS K.E. & CASSA, M.R. (1994): Applied source rock geochemistry.– In: MAGOON, L.B. & DOW, W.G. (eds.): The petroleum System – From Source to Trap.– American Association of Petroleum Geologists, Tulsa, 93–117.

PETERS, K.E. & MOLDOWAN, J.M. (1991): Effects of source, thermal maturity, and biodegradation on the distribution and isomerization of homohopanes in petroleum.– Organic Geochemistry, 17/1, 47–61. https://doi.org/10.1016/0146-6380(91)90039-M

PETERS K.E., WALTERS, C.C. & MOLDOWAN, J.M. (2005a): The Biomarker Guide 2nd Edition, Volume I. Biomarkers and Isotopes in the Environment and Human History.– Cambridge University Press, Cambridge, 472 p.

PETERS K.E., WALTERS, C.C. & MOLDOWAN, J.M. (2005b): The Biomarker Guide, 2nd Edition, Volume II. Biomarkers and Isotopes in Petroleum and Earth History.– Cambridge University Press, Cambridge, U.K., 473–1155.

PICOTTI, V. & COBIANCHI, M. (2017): Jurassic stratigraphy of the Belluno Basin and Friuli Platform: a perspective on far-field compression in the Adria.– Swiss Journal of Geoscience, 110, 833–850. https://doi.org/10.1007/s00015-017-0280-5

PINTER, N., GRENERCZY, G., WEBER, J., STEIN, S. & MEDAK, D. (2005): The Adria Microplate: GPS Geodesy, Tectonics and Hazards (NATO Science Series IV: Earth and Environmental Sciences).– Springer, 413 p.

POLŠAK, A., JURIŠA, M., ŠPARICA, M. & ŠIMUNIĆ, A. (1977): Osnovna geološka karta SFRJ 1:100 000, list Bihać L 33-116 [*Basic Geological Map of SFRY 1:100 000, Bihać sheet L 33-116* – in Croatian].– Institut za geološka istraživanja, Zagreb, Savezni geološki zavod, Beograd.

POLŠAK, A., ŠPARICA, M., CRNKO, J. & JURIŠA, M. (1978): Osnovna geološka karta SFRJ 1:100 000. Tumač za list Bihać L 33-116. [*Basic Geological Map of SFRY 1:100 000. Explanatory notes for the Bihać sheet L 33-116* – in Croatian].– Institut za geološka istraživanja, Zagreb, Savezni geološki zavod, Beograd.

PRIFTI, I. & MUSKA, K. (2013): Hydrocarbon occurrences and petroleum geochemistry of Albanian oils.– Italian Journal of Geoscience (Bolletino Societa Geologica Italiana), 132, 2, 228–235.

RADKE, M. (1988): Application of aromatic compounds as maturity indicators in source rocks and crude oils.– Marine and Petroleum Geology, 5/3, 224–236. http://doi.org/10.1016/0264-8172(88)90003-7

RADKE, M. & WELTE, D.H. (1983): The methylphenanthrene index (MPI): A maturity parameter based on aromatic hydrocarbons.– In: BJØROY, M., ALBRECHT, P., CORNFORD, C., DE GROOT, K., EGLINTON, G., GALIMOV, E., LEYTHAEUSER, D., PELET, R., RULLKÖTTER, J. & SPEERS, G. (eds.): Advances in Organic Geochemistry. Chichester, 504–512.

RADKE, M., WELTE, D.H. & WILLSCH, H. (1982a): Geochemical study of a well in the Western Canada Basin: relation of aromatic distribution pattern to maturity of organic matter.– Geochimica et Cosmochimica Acta, 46, 1–10. https://doi.org/10.1016/0016-7037(82)90285-X

RADKE, M., WILLSCH, H. & LEYTHAEUSER, D. (1982b): Aromatic components of coal: relation of distribution pattern to rank.– Geochimica et Cosmochimica Acta, 46, 1831–1848, https://doi.org/10.1016/0016-7037(82)90122-3

RADOIČIĆ, R., JOVANOVIĆ, D. & SUDAR, M. (2009): Stratigraphy of the Krs Gradac section (SW Serbia).– Annales Geologiques de la Peninsule Balkanique, 70, 23–41. https://doi.org/10.2298/GABP0970023R

RAINER, A.T., SACHSENHOFER, R.F., GREENB, P.F., RANTITSCHA, G., HERLEC, U. & VRABEC, M. (2016): Thermal maturity of Carboniferous to Eocene Sediments of the Alpine–Dinaric Transition Zone (Slovenia).– International Journal of Coal Geology, 157, 19–38. https://doi.org/10.1016/j.coal.2015.08.005

RIGAKIS, N. & KARAKITSIOS, V. (1998): The source rock horizons of the Ionian Basin, NW Greece.– Marine and Petroleum Geology, 15, 593–617. https://doi.org/10.1016/S0264-8172(98)00032-4

ROHMER, M. (1993): The biosynthesis of triterpenoids of the hopane series in the Eubacteria: a mine of new enzymatic reactions.– Pure Applied Chemistry, 65, 1293–1298, https://doi:10.1351/pac199365061293

RULLKÖTTER, J., LITTKE, R. & SCHAEFER, R.G. (1990): Characterization of organic matter in sulfur-rich lacustrine sediments of Miocene age (Nördlinger ries, Southern Germany).– In: ORR, W.L. & WHITE, C.M. (eds.): Geochemistry of Sulfur in fossil Fuels.– American Chemical Society Symposium Series, 429, 149–169. https://doi.org/10.1021/bk-1990-0429.ch008

RYAN, W.B.F, STANLEY, D.J., HERSEY, J.B., FAHLQUIST, D.A. & ALLAN, T.D. (1971): The tectonics and geology of the Mediterranean Sea.– In MAXWELL, A.E. (ed.): The Sea, 4. Wiley, New York, 387–492.

SCHEFER, S., EGLI, D., MISSONI, S., BERNOULLI, D., FÜGENSCHUH, B., GAWLICK, H.J., JOVANOVIĆ, D., KRYSTIN, L., LEIN, R., SCHMID, S.M. & SUDAR, M.N. (2010): Triassic metasediments in the internal Dinarides (Kopaonik area, southern Serbia): Stratigraphy, paleogeographic and tectonic significance.– Geologica Carpathica, 61, 2, 89–109. https://doi.org/10.2478/v10096-010-0003-6

SCHETTINO, A. & TURCO, E. (2011): Tectonic history of the western Tethys since the Late Triassic.– Geological Society of America Bulletin, 123, 89–105. https://doi.org/10.1130/B30064.1

SCHLANGER, S.O., ARTHUR, M.A., JENKYNS, H.C. & SCHOLLE, P.A. (1987): The Cenomanian–Turonian anoxic event: I. Stratigraphy and distribution of organic carbon-rich beds in the marine 13C excursion.– In: BROOKS, J. & FLEET, A.J. (eds.): Marine Petroleum Source Rocks. Special Publication of Geological Society of London, 26, 371–399.

SCHMID, S.M. & KISSLING, E. (2000): The arc of the Western Alps in the light of geophysical data on deep crustal structure.– Tectonics 19, 62–85. https://doi.org/10.1029/1999TC900057

SCHMID, S.M., BERNOULLI, D., FÜGENSCHUH, B., MATENCO, L., SCHUSTER, R., SCHEFER, S., TISCHLER, M. & USTASZEWSKI, K. (2008): The Alpine-Carpathian Dinaridic orogenic system: Correlation and evolution of tectonic units.– Swiss Journal of Geoscience, 101,139–183. https://doi.org/10.1007/s00015-008-1247-3

SCHMID, S.M., FÜGENSCHUH, B., KOUNOV, A., MATENCO, L., NIEVERGELT, P., OBERHÄNSLI, R., PLEUGER, J., SCHEFER, S., SCHUSTER, R., TOMLJENOVIĆ, B., USTASZEWSKI, K. & VAN HINSBERGEN, D.J. (2020): Tectonic units of the Alpine collision zone between Eastern Alps and Western Turkey.– Gondwana Research, 78, 308–374. https://doi.org/10.1016/j.gr.2019.07.005

SCHUBERT, R. (1909): Geologija Dalmacije [*Geology of Dalmatia* – in Croatian].– Matica Dalmatinska, Zadar, 183 p.

SEIFERT, W.K. & MOLDOWAN, J.M. (1978): Applications of steranes, terpanes and monoaromatics to the maturation, migration and source of crude oils.– Geochimica et Cosmochimica Acta, 42, 77–95. https://doi:10.1016/0016-7037(78)90219-3

SEIFERT, W.K. & MOLDOWAN, J.M. (1980): The effect of thermal stress on source-rock quality as measured by hopane stereochemistry.– Physical Chemistry Earth, 12, 229–23, https://doi.org/10.1016/0079-1946(79)90107-1

SEIFERT, W.K. & MOLDOWAN, J.M. (1986): Use of biological markers in petroleum exploration.– In: JOHNS, R.B. (ed.): Methods in Geochemistry and Geophysics 24. Elsevier, Amsterdam, 261–290.

SENFTLE, J.T., BROWN, J.H. & LARTE, S.R. (1987): Refinement of organic petrographic methods for kerogen characterization.– International Journal of Coal Geology, 7, 105–117. https://doi.org/10.1016/0166-5162(87)90015-2

SINNINGHE DAMSTE, J.S. & LEEUW, J.W. (1990): Analysis, structure and geochemical significance of organically-bound sulphur in the geosphere: State of the art and future research.– In: DURAND, B. & BEHAR, F. (eds.): Advances in Organic Geochemistry.– Organic Geochemistry, 16/4–6, 1077–1101. https://doi.org/10.1016/0146-6380(90)90145-P

SINNINGHE DAMSTE, J.S., KENIG, F., KOOPMAS, M.P., KOSTER, J., SCHOUTEN, S., HAYES, J.M. & DE LEEUW, J.W. (1995): Evidence for gammacerane as an indicator of water column stratification.– Geochimica et Cosmochimica Acta, 59, 1895–1900. https://doi.org/10.1016/0016-7037(95)00073-9

SMIRČIĆ, D. (2017): Geneza vulkanoklastičnih naslaga srednjeg trijasa Vanjskih Dinarida [*Genesis of Middle Triassic volcaniclastic deposits in the External Dinarides* – in Croatian].– Unpubl. PhD Thesis, University of Zagreb, Faculty of Mining, Geology and Petroleum.

SMIRČIĆ, D., KOLAR-JURKOVŠEK, T., ALJINOVIĆ, D., BARUDŽIJA, U., JURKOVŠEK, B. & HRVATOVIĆ, H. (2018): Stratigraphic Definition and Correlation of Middle Triassic Volcaniclastic Facies in the External Dinarides: Croatia and Bosnia and Herzegovina.– Journal of Earth Science, 29, 4, 864–878. https://doi.org/10.1007/s12583-018-0789-1

SMIRČIĆ, D., ALJINOVIĆ, D., BARUDŽIJA, U. & KOLAR-JURKOVŠEK, T. (2020): Middle Triassic syntectonic sedimentation and volcanic influence in the central part of the External Dinarides, Croatia (Velebit Mts.).– Geological Quarterly, 2020, 64/1, 220–239. http://doi.org/10.7306/gq.1528

SOFER, Z. (1980): Preparation of carbon dioxide for stable carbon isotope analysis of petroleum fractions.– Analytical Chemistry, 52, 1389–1391. http://doi.org/10.1021/ac50058a063

SOFER, Z. (1984): Stable carbon isotope compositions of crude oils: application to source depositional environments and petroleum alteration.– American Association of Petroleum Geologists Bulletin, 68, 31–49. https://doi:10.1306/ad460963-16f7-11d7-8645000102c1865d

SPAKMAN, W. & WORTEL, R. (2004): A tomographic view on western Mediterranean geodynamics.– In: CAVAZZA, W., ROURE, F.M., SPAKMAN, W., STAMPFLI, G.M. & ZIEGLER, P.A. (eds.): The TRANSMED Atlas– The Mediterranean region from crust to mantle: Springer, Berlin and Heidelberg, 31–52. http://doi.org/10.1007/978-3-642-18919-7_2

ŚRODOŃ, J., ANCZKIEWICZA, A.A., DUNKL, B.I., VLAHOVIĆ, I., VELIĆ, I., TOMLJENOVIĆC, B., KAWIAKA, T., BANAŚA, M. & VON EYNATTENB, H. (2018): Thermal history of the central part of the Karst Dinarides, Croatia: Combined application of clay mineralogy and low-T thermochronology.– Tectonophysics, 744, 155–176. https://doi.org/10.1016/j.tecto.2018.06.016

STACH, E., MACKOWSKY, M.T., TEICHMÜLLER, M., TAYLOR, G.H., CHANDRA, D. & TEICHMÜLLER, R. (1982): Coal Petrology.– Gebrüder Borntraeger, Berlin-Stuttgart, 535 p.

STAMPFLI, G.M. & BOREL, G.D. (2004): The TRANSMED Transects in space and time: Constraints on the Paleotectonic evolution of the Mediterranean domain.– In: CAVAZZA, W., ROURE, F.M., SPAKMAN, W., STAMPFLI, G.M. & ZIEGLER, P.A. (eds.): The TRANSMED Atlas– The Mediterranean region from crust to mantle. Springer, Berlin and Heidelberg, 53–80. http://doi.org/10.1007/978-3-642-18919-7_2

SÝKOROVÁ, I., PICKEL, W., CHRISTANISC, K., WOLF, M., TAYLORE, G.H. & FLORES, D. (2005): Classification of huminite ICCP System 1994.– International Journal of Coal Geology, 62, 85–106. http://doi.org/10.1016/j.coal.2004.06.006

ŠĆAVNIČAR, B. & NIKLER, L. (1976): Staklasti tuf u lemeškim naslagama Velike Kapele [*Vitriotuff in Upper Jurassic Lemeš-deposition of Mt. Velika Kapela, Croatia* – in Croatian].– Geološki vjesnik, 29, 269–275.

ŠEBEČIĆ, B. (1979a): Bituminozne pojave Dinarida [*Bituminous occurrences of Dinarides* – in Croatian].– Nafta, 2, 55–61.

ŠEBEČIĆ, B. (1979b): Rasjedni sistemi i bituminozne pojave u Vanjskim Dinaridima [*Fault systems and bituminous occurrences in the Outer Dinarides* – in Croatian].– Geološki vjesnik, 31, 383–386.

ŠEBEČIĆ, B. (1980): Problemi migracije i akumulacije ugljikovodika i naftnogeološke osobine karbonatnih naslaga Dinarida (hipotetski trendovi migracije ugljikovodika) [*Problems of migration and accumulation of hydrocarbons and geological properties of carbonate deposits of the Dinarides (hypothetical trends of hydrocarbon migration)* – in Croatian].– Nafta, 2, 59–70.

ŠEBEČIĆ, B. (1982): O naftomatičnom potencijalu i pokušaju njegove procjene iz kemijskih analiza bituminoznih stijena Vanjskih Dinarida [*On petroleum potential and an attempt to estimate it from chemical analyses of bituminous rocks of the Outer Dinarides* – in Croatian].– Nafta, 33, 537–544.

ŠEBEČIĆ, B. (1983.): Prijedlog novih naziva za "bituminozne škriljavce" s osvrtom na njihovo dosadašnje istraživanje u nas [*Proposal of new names for "bituminous shale" with reference to their research so far in our country* – in Croatian].– Geološki vjesnik, 36, 309–318.

ŠEBEČIĆ, B. (1984): Bituminozne pojave Vinisca kod Trogira [*Bituminous occurrences of Vinišće near Trogir* – in Croatian].– Geološki vjesnik, 37, 175–196.

ŠEBEČIĆ, B. (1995): Povijest istraživanja i eksploatacije bituminoznih i kerogenih nalazišta Hrvatske [*History of exploration and exploitation of bitumen and kerogen deposits in* Croatia – in Croatian].– Rudarsko-geološko-naftni zbornik, 7, 97–107.

ŠEBEČIĆ, B. (1996): O trgovini bitumenom u Dalmaciji od XIII do XVIII stoljeća [*About bitumen trade in Dalmatia from the 13th to the 18th century* – in Croatian].– Rudarsko-geološko-naftni zbornik, 129–138.

ŠEBEČIĆ, B. & ERCEGOVAC, M. (1983): Prilog poznavanju stupnja zrelosti kerogena nekih bituminoznih karbonatnih naslaga Vanjskih Dinarida [*A contribution to the knowledge of kerogen maturity in some bituminous carbonate deposits of the Outer Dinarides* – in Croatian].– Nafta, 34/4–5, 183–187.

ŠEBEČIĆ, B., ALAJBEG, A., VITEZIĆ, M. & OPIĆ, I. (1988): Sedimentološke i organsko-geokemijske spoznaje o bituminozno kerogenim pojavama Radošića kod Splita [*Sedimentological and organic-geochemical findings on bituminous kerogen occurrences in Radošić near Split* – in Croatian].– Geološki vjesnik, 41, 197–217.

ŠEBEČIĆ, B., VITEZIĆ, M. & ALAJBEG, A. (1989): Bituminozno-kerogene pojave Sjeverno trogirskog područja [*Bitumin and kerogen occurrences of the Northern Trogir area* – in Croatian].– Geološki vjesnik, 42, 103–119.

ŠEBEČIĆ, B., SLOVENEC, D. & ALAJBEG, A. (1990): Kerogeni sediment Zubovića drage iz Vrela Koreničkog [*Kerogenous sediments of Zubović draga, Vrelo Korenica* – in Croatian].– In: Zbornik radova IV. jugoslavenski simpozij o bitumenu i asfaltu [*Proceedings of the 4th Yugoslav Symposium on Bitumen and Asphalt Mixture*]. JAZU, Zagreb, 251–259.

ŠEGVIĆ, B., TOŠEVSKI, A., ŠTEVANIĆ, D., BIŠEVAC, V. & LUGOVIĆ, B. (2006): Altered tephra layers in the Upper Jurassic Lemeš deposits near Maovice (Dalmatia, Croatia): Clay mineralogy and basic soil mechanic properties.– In: VLAHOVIĆ, I., TIBLJAŠ, D., DURN, G. & BIŠEVAC, V. (eds.): Abstracts Book of the 3rd Mid-European Clay Conference (MECC 06). Faculty of Science, Faculty of Mining, Geology and Petroleum Engineering, Zagreb, 104–104.

ŠIKIĆ, K. & BASCH, O. (1975): Geološka zbivanja od paleozoika do kvartara u zapadnom dijelu zagrebačke regije [*Geological events from Paleozoic to Quaternary in the western part of Zagreb area* – in Croatian].– In: 2. Godišnji znanstveni skup sekcije za primjenu geologiju, geofiziku, geokemiju. Znanstveni savjet za naftu JAZU [2nd *Annual scientific meeting of the section for applied geology, geophysics, geochemistry. Scientific committee for oil at Yugoslavian Academy of Sciences and Arts*], 5. JAZU, Zagreb, 69–86.

ŠPANIĆ, D. & TROSKOT-ČORBIĆ, T. (2013): Organic petrology and geochemistry of the Oligocene source rocks in the Glina depression (Croatia).– In: Abstract book, 65th ICCP/30th TSOP Meeting, Sosnowiec, Poland, 25. 8. – 1.9.2013., 118.

ŠPANIĆ, D., TROSKOT-ČORBIĆ, T. & MARIČIĆ, M. (1995): Geochemical Study of Surface Bituminous Occurrences in Cretaceous Sediments of the Outer Dinarides.– In: VLAHOVIĆ, I., VELIĆ, I. & ŠPARICA, M. (eds.): Proceedings of the First Croatian Geological Congress, Opatija. Institute of Geology, Croatian Geological Society, Zagreb, 1995, 591–594.

ŠPARICA, M. (1981): Mezozoik Banije, Korduna i dodirnog područja Bosne [*Geology of the Mesozoic areas of Kordun, Banija and NW Bosnia, Yugoslavian* – in Croatian].– Nafta, Special Publication, 1–245.

ŠUŠNJARA, A., SAKAČ, K., JELEN, B. & GABRIĆ, A. (1992): Upper Permian evaporites and associated rocks of Dalmatia and borderline area of Lika and Bosnia.– Geologia Croatica 45, 95–115.

TAKAČ, D., BALIĆ, D., TROSKOT-ČORBIĆ, T. & MIKŠA, G. (2021): Povratak Dinaridima: nova strukturna koncepcija (*Return to the Dinarides: a new structural conception* – in Croatian).– Naftaplin, 41/168–169, 49–70.

TARI, V. (2002): Evolution of the northern and western Dinarides: a tectonostratigraphic approach.– Stephan Mueller Special Publication Series, 1, 223–236. http://doi.org/10.5194/smsps-1-223-2002

TAYLOR, G.H., TEICHMÜLLER, M., DAVIS, A., DIESSEL, C.F.K., LITTKE, R. & ROBERT, P. (1998): Organic Petrology.– Gebrüder Borntraeger, Berlin-Stuttgart, 704 p.

TEICHMÜLLER, M. & OTTENJANN, K. (1977): Art und Diagenese von Liptiniten und lipoiden Stoffen in einem Erdölmuttergestein auf Grund fluoreszenzmikroskopischer Untersuchungen.– Erdöl und Kohle, 30, 387–398.

TISSOT, B.P. & WELTE, D.H. (1984): Petroleum Formation and Occurrence. 2nd ed.– Springer, Berlin, 699 p.

TIŠLJAR, J. (1992): Origin and depositional environments of the evaporite and carbonate complex (Upper Permian) from the central part of the Dinarides (Southern Croatia and Western Bosnia).– Geologia Croatica, 45, 115–127.

TIŠLJAR, J., VELIĆ, I. & VLAHOVIĆ, I. (1994): Facies diversity of the Malmian platform carbonates in Western Croatia as a consequence of synsedimentary tectonics.– Géologie Méditerranéenne, 21/3–4, 173–176.

TIŠLJAR, J., VLAHOVIĆ, I., VELIĆ, I. & SOKAČ, B. (2002): Carbonate Platform Megafacies of the Jurassic and Cretaceous Deposits of the Karst Dinarides.– Geologia Croatica, 55/2, 139–170.

TROSKOT-ČORBIĆ, T (2011): Organski facijesi u gornjojurskim naslagama Gorskog kotare, Like i Dalmacije [Organic facies of the Upper Jurassic sediments in Gorski kotar, Lika and Dalmatia – in Croatian, with an English Abstract].– Unpubl. PhD Thesis, University of Zagreb, Faculty of Mining, Geology and Petroleum Engineering, 266 p.

TROSKOT-ČORBIĆ, T. (2019): Hydrocarbon Source Rock of the Dinarides: An Overview and Future Challenges.– In: HORVAT, M., MATOŠ, B. & WACHA, L. (eds.): Abstract book of the 6th Croatian geological Congress with international participation. Croatian Geological Survey, Zagreb, 8–9.

TROSKOT-ČORBIĆ, T. & ŠPANIĆ, D. (2010): Organic petrology of the External Dinarides, Croatia.– In: HORVAT, M. (ed.): Abstract book of the 4th Croatian geological congress, Šibenik, Croatian geological Survey, Zagreb, 300–301.

TROSKOT-ČORBIĆ, T., ŠPANIĆ, D., RUMENJAK, LJ., MARIČIĆ, M. & STANKOVIĆ, I. (2005): Organic Petrology and Geochemistry of the Jurassic Carbonates of the Karst Dinarides (Croatia).– In: Abstract Book of the 57th Annual Meeting of the International Committee for Coal and Organic Petrology. University of Patras, Patras, 48–48.

TROSKOT-ČORBIĆ, T., VESELI, V., COTA, L. & BUBNIĆ, J. (2015): New evidence for the Burano formation source rock facies in the Croatian sector of Central Adriatic.– In: PIMENTEL, N. & PENA DOS REIS, R. (eds.): Abstracts of the AAPG European Regional conference & exhibition: Tethys-Atlantic Interaction along the European-Iberian-African Plate Boundaries. Coast Geological Society, Lisbon, 95–95.

TYSON, R.V. (1995): Sedimentary organic matter. Organic facies and palynofacies.– Chapman and Hall, London, 591 p.

USTASZEWSKI, K., SCHMID, S. M., FÜGENSCHUH, B., TISCHLER, M., KISSLING, E. & SPAKMAN, W. (2008): A map-view restoration of the Alpine-Carpathian Dinaridic system for the Early Miocene.– Swiss Journal of Geoscience, 101/suppl. 1, 273–294. http://doi.org/10.1007/s00015-008-1288-7

USTASZEWSKI, K., KOUNOV, A., SCHMID, S.M., SCHALTEGGER, U., KRENN, E., FRANK, W. & FÜGENSCHUH, B. (2010): Evolution of the Adria-Europe plate boundary in the northern Dinarides: from continent-continent collision to back-arc extension.– Tectonics, 29, TC6017. http://doi.org/10.1029/2010TC002668

VAN HINSBERGEN, D.J., TORSVIK, T.H., SCHMID, S.M., MATENCO, L., MAFFIONE, M., VISSERS, R.L., GÜRER, D. & SPAKMAN, W. (2020): Orogenic architecture of the Mediterranean region and kinematic reconstruction of its tectonic evolution since the Triassic.– Gondwana Research. 81, 79–229. https://doi.org/10.1016/j.gr.2019.07.009

VAN UNEN, M., MATENCO, L., NADER, F.H., DARNAULT, R., MANDIĆ, O. & DEMIR, V. (2019): Kinematics of foreland-vergent crustal accretion: Inferences from the Dinarides evolution.– Tectonics, 38, 49–76, https://doi.org/10.1029/2018TC005066

VELIĆ, J. (2007): Geologija ležišta nafte i plina (*Geology of Oil and Gas Reservoirs* – in Croatian).– University of Zagreb, Faculty of Mining, Geology and Petroleum Engineering, 342 p.

VELIĆ, I. & SOKAČ, B. (1978): Biostratigraphic analysis of the Jurassic and Lower Cretaceous in the wider region of Ogulin, central Croatia.– Geološki vjesnik, 30/1, 309–337.

VELIĆ, I., VLAHOVIĆ, I. & TIŠLJAR, J. (1994): Late Jurassic lateral and vertical facies distribution: from peritidal and inner carbonate ramps to perireefal and peritidal deposits in SE Gorski Kotar (Croatia).– Geologie Mediteraneenne, 3–4, 177–180.

VELIĆ, I., TIŠLJAR, J., VLAHOVIĆ, I., VELIĆ, J., KOCH, G. & MATIČEC, D. (2002a): Palaeogeographic Variability and Depositional Environments of the Upper Jurassic Carbonate Rocks of Velika Kapela Mt. (Gorski Kotar area, Adriatic Carbonate platform, Croatia).– Geologia Croatica, 55/2, 121–138.

VELIĆ, I., VLAHOVIĆ, I. & MATIČEC, D. (2002b): Depositional sequences and palaeogeography of the Adriatic Carbonate Platform.– Memorie Societa Geologica Italiana, 57, 141–151.

VELIĆ, J., MALVIĆ, T., CVETKOVIĆ, M. & VELIĆ, I. (2015): Stratigraphy and petroleum geology of the Croatian part of the Adriatic basin.– Journal of Petroleum Geology, 38/3, 281–300. https://doi.org/10.1111/jpg.12611

VESELI, V., TROSKOT-ČORBIĆ, T., VELIĆ, I., VLAHOVIĆ, I., TOMLJENOVIĆ, B. & VELIĆ, J. (2012): Sedimentary dynamics in the central part of the Adriatic Carbonate Platform from the Late Oxfordian to the Earliest Tithonian (Poštak Mt., Croatia).– In: MISSONI, S. & GAWLICK, H. (eds.): Book of abstracts: 29th IAS Meeting of Sedimentology Schladming. Montan Universitaet Leoben, Schladming, 488–488.

VEZZANI, L., FESTA, A. & GHIZETTI, C.F. (2010): Geology and Tectonic Evolution of the Central-Southern Apennines, Italy.– The Geological Society of America, Special Paper, 469. https://doi.org/10.1130/SPE469

VISHNEVSKAYA, V.S., ĐERIĆ, N. & ZAKARIADZE, G.S. (2009): New data on Mesozoic Radiolaria of Serbia and Bosnia, and implications for the age and evolution of oceanic volcanic rocks in the Central and Northern Balkans.– Lithos, 108, 1–4, 72–105, https://doi.org/10.1016/j.lithos.2008.10.015

VITZTHUM, M.A.J., GAWLICK, H.J., SACHSENHOFER, R.F. & NEUMEISTER, S. (2021): Changing depositional environments in the semi-restricted Late Jurassic Lemeš Basin (Outer Dinarides; Croatia).– Facies, 68/2. https://doi.org/10.1007/s10347-021-00640-1

VLAHOVIĆ, I., TIŠLJAR, J., VELIĆ, I. & MATIČEC, D. (2005): Evolution of the Adriatic Carbonate Platform: Palaeography, main events and depositional dynamics.– Palaeogeography, Palaeoclimatology, Palaeoecology, 220, 333–360. https://doi.org/10.1016/j.palaeo.2005.01.011

VOLKMAN, J.K. (1988): Biological marker compounds as indicators of the depositional environments of petroleum source rocks.– In: FLEET, A.J., KELTS, K. & TALBOT, M.R. (eds.): Lacustrine Petroleum Source Rocks. Blackwell, London, 103–122.

VOLKMAN, J.K. (2003): Sterols in microorganisms. Applied Microbiology and Biotechnology, 60, 5, 496–506.

VOLKMAN, J.K., ALLEN, D.I., STEVENSON, P.L. & BURTON, H.R. (1986): Bacterial and algal hydrocarbons in sediments from a saline Antartic lake, Ace Lake.– Organic Geochemistry, 10, 671–681. https://doi.org/10.1016/S0146-6380(86)80003-1

WAPLES, D.W. (1985): Geochemystry in Petroleum Exploration.– IHRD, Boston, 232 p.

WEBER, J., VRABEC, M., STOPAR, B., PAVLOVIC-PRESEREN, P. & DIXON, T. (2006.): The PIVO-2003 experiment: a GPS study of Istria Peninsula and Adria microplate motion, and active tectonics in Slovenia.– In: PINTER, N., GRENERCZY, G., WEBER, J., STEIN, S. & MEDAK, D. (ed.): The Adria Microplate: GPS Geodesy, Tectonics and Hazards. Springer, 305–320. https://doi.org/10.1007/1-4020-4235-3_21

ZAPPATERRA, E. (1994): Source-Rock Distribution Model of the Periadriatic region.– American Association of Petroleum Geologists Bulletin, 78, 3, 333–354.

Web source:

INA Annual Financial Reports (2024–2025): INA Annual Financial Reports. Available at: https://www.ina.hr/investitori/financijska-izvjesca/godisnji-izvjestaji. Accessed on February 15th 2025:

Geologia Croatica

Supplement 1

Table S1. Rock eval pyrolysis data, vitrinite reflectance and thermal alteration index from Carboniferous marls and shales.

Sample ID Well/Outcrop	Well/Depth (m) Outcrop (OUT)	TOC (%)	S_1 (mg HC/g rock)	S_2 (mg HC/g rock)	S_1+S_2 (mg HC/g rock)	S_3 (mg CO_2/g rock)	T_{max} (°C)	HI (mg HC/g TOC)	OI (mg CO_2/g TOC)	PI	S_2/S_3	R_o (%)	TAI
Bruvno-1	316	4.08	0.39	0.28	0.67	0.21		7	5	0.58	1.33	2.02	4^-
Bruvno-1	546	0.57	0.13	0.06	0.19	0.08		11	14	0.68	0.75		4^-
Bruvno-1	584	0..48	0.11	0.03	0.14	0.08		6	17	0.79	0.38		4^-
Bruvno-1	689	0.49	0.18	0.07	0.25	0.16		14	33	0.72	0.44		4^-
Bruvno-1	833	0.62	0.16	0.05	0.21	0.08	552	8	13	0.76	0.63		4^-
Bruvno-1	924	0.73	0.18	0.07	0.25	0.05		10	7	0.72	1.40		4^-
Bruvno-1	1002	0.59	013	0.05	0.18	0.04	574	8	7	0.72	1.25	2.42	4^-
Bruvno-1	1765	0.89	0.16	0.03	0.19			3		0.84		2.22	4^-
Bruvno-1	1838	0.87	0.07	0.01	0.08	0.02		1	2	0.88	0.50		4^-
Bruvno-1	2206	0.50	0.06	0.05	0.11	0.26		10	52	0.55	0.19	4.04	4
Bruvno-1	2206	0.60	0.02	0.01	0.03			3		0.66			4
Bruvno-1	2618	0.50	0.02	0.02	0.04			4		0.50		4.14	4
Marunovac	OUT	0.92	0.05	0.06	0.11	0.15		7	16	0.45	0.40		4
Klarića Vrelo	OUT	0.69	0.21	0.15	0.36			22		0.58			4
Ričice	OUT	0.82	0.12	0.11	0.23			13		0.52			4
Ličko Cerje 1	OUT	14.30	0.07	0.24	0.31	0.60	550	2	4	0.23	0.40		4
Sv Rok Lotići	OUT	1.30	002	0.09	0.11			0	1				4
Raduč	OUT	1.64	0.03	0.00	0.00	0.13		0	8				4
Pikovac 1	OUT	0.70	0.08	0.05	0.13	0.37		7	53	0.62	0.14	4.45	4
Pikovac 2	OUT	0.87	0.14	0.10	0.24	0.23		11	26	0.58	0.43	4.54	4
Pikovac A	OUT	2.17	0.01	0.01	0.02	0.16		0	7	0.50	0.06	4.41	4
Pikovac B	OUT	0.70	0.01	0.08	0.09	0.02	522	11	3	0.11	4.00	4.69	4
Pikovac C	OUT	1.19	0.00	0.01	0.01	0.65	553	1	55	0.00	0.02	4.50	4

OUT outcrops; TOC total organic carbon; S_1 the amount of free hydrocarbons; S_2 the amount of hydrocarbon generated through thermal cracking; S_3 the amount of CO_2 produced during pyrolysis; T_{max} the temperature of maximum hydrocarbon generation; PI production index; S_1+S_2 generative potential (PETERS & CASSA, 1994); %R_o vitrinite reflectance (VR); TAI thermal alteration index; TAI to VR (%R_o) correlation scale: 4^- 2.00 – 3.00%R_o, 4>3.00%R_o.

Table S2. Rock eval pyrolysis data, vitrinite reflectance and thermal alteration index from Permian marls and shales.

Sample ID Outcrop	TOC (%)	S_1 (mg HC/g rock)	S_2 (mg HC/g rock)	S_1+S_2 (mg HC/g rock)	S_3 (mg CO_2/g rock)	T_{max} (^oC)	HI (mg HC/g TOC)	OI (mg CO_2/g TOC)	PI	S_2/S_3	R_o (%)	TAI
Homer - 1	0.88	0.01	0.20	0.21	0.08	530	23	9	0.05	2.50	1.99	4^-
Lokve-Špičunak	4.30	0.01	0.70	0.71	1.46	531	16	34	0.01	0.48	1.65	3^+-4^-
Fužine PP	0.77	0.02	0.06	0.08	0.02	487	8	3	0.25	3.00	2.25	4^-
Gerovo Razloge	4.18	0.01	0.29	0.3	1.31	532	7	31	0.03	0.22	1.66	3^+-4^-
Ravna gora SS	1.58	0.01	0.06	0.07	0.60	466	4	38	0.14	0.10	2.30	4^-
Gerovo Klukov l.	6.24	0.01	0.31	0.32	2.48	551	5	40	0.03	0.13	1.94	4^-
Gerovo Tršće	2.18	0.01	0.65	0.66	0.06	520	30	3	0.02	10.83	1.66	3^+-4^-
Čabar Ravnice	2.03	0.01	0.19	0.20	0.25	567	9	12	0.05	0.76	2.32	4^-
Skrad Rasohe 2	0.95	0.03	0.08	0.11	0.11	484	8	12	0.27	0.73	2.70	4^-
Skrad most 3	1.30	0.01	0.02	0.03	1.00		2	77	0.33	0.02		4^-
Brušane 1	4.41	0.06	0.16	0.22	0.39	605	4	9	0.27	0.41	2.33	4^-
Brušane 2	4.35	0.09	0.28	0.37	0.41	605	6	9	0.24	0.68	2.12	4^-
Brušane 3	3.78	0.10	0.23	0.33	0.40	605	6	11	0.30	0.58	2.33	4^-
Brušane 4	4.04	0.03	0.13	0.16	0.36	605	3	9	0.19	0.36	2.30	4^-
Brušane 5	5.41	1.02	1.62	2.64			30		0.39			4^-
Brušane 6	4.51	0.60	0.70	1.30		597	16		0.46		2.07	4^-
Brušane 8	5.10	0.03	0.36	0.39		598	7		0.08		2.00	4^-
Brušane 9	4.14	0.07	0.15	0.22		591	4		0.32			4^-
Takalice 1	3.50	0.00			0.70		0	20				4^-
Takalice 2	3.38	0.10		0.10	0.80		0	24	1.00			4^-
Takalice 9	3.56	0.10		0.10	0.40		0	11	1.00			4^-
Takalice 10	2.51	0.10	0.10	0.20	0.70		4	28	0.50	0.14		4^-
Takalice 11	6.33	0.10	0.10	0.20	0.30		2	5	0.50	0.33		4^-
Takalice 12	5.63	0.00	0.10	0.10	0.30		2	5	0.00	0.33		4^-
Takalice 14	2.36	0.10	0.10	0.20	0.20		4	8	0.50	0.50	2.05	4^-
Takalice 15	6.49	0.10	0.10	0.20	0.20	482	2	3	0.50	0.50		4^-
Takalice 17	4.16	0.10	0.10	0.20	1.50		2	36	0.50	0.07		4^-
Takalice 18	7.61	0.10	0.10	0.20	0.50		1	7	0.50	0.20	2.12	4^-
Takalice 19	2.50	0.10		0.10	0.30		0	12	1.00			4^-
Takalice 22	3.05	0.00			1.10		0	36		0.00		4^-
Takalice 23	3.57	0.10		0.10	1.10		0	31	1.00	0.00	2.04	4^-
Paljež	2.08	0.17	0.14	0.31	0.59		7	28	0.55	0.24		4^-
Marunovac IVa	0.89	0.12	0.13	0.25	0.11		15	12	0.48	1.18		4^-
Velika Draga-1	1.68	0.06	0.14	0.20	0.31	574	8	18	0.30	0.45		4^-
Velika Draga-2	1.76	0.07	0.12	0.19	0.57	578	7	32	0.37	0.21	2.06	4^-
Griči 2	1.63	0.03	0.16	0.19	0.21	577	10	13	0.16	0.76		4^-
Griči 3	1.52	0.02	0.16	0.18	0.21	578	11	14	0.11	0.76		4^-
Griči 4	1.81	0.11	0.24	0.35	0.39	578	13	22	0.31	0.62	2.11	4^-

TOC total organic carbon; S_1 the amount of free hydrocarbons; S_2 the amount of hydrocarbon generated through thermal cracking; S_3 the amount of CO_2 produced during pyrolysis; T_{max} the temperature of maximum hydrocarbon generation; PI production index; S_1+S_2 generative potential (PETERS & CASSA, 1994); %R_o vitrinite reflectance (VR); TAI thermal alteration index; TAI to VR (%R_o) correlation scale: 3^+ 1.25 – 2.00%R_o, 4^- 2.00 – 3.00%R_o, 4>3.00%R_o.

Supplement 2

Table S1. Rock eval pyrolysis data, vitrinite reflectance and thermal alteration index from Triassic carbonates, marls and shales.

Sample ID Well/Outcrop	Outcrop Well/Depth (m)	TOC (%)	S_1 (mg HC/g rock)	S_2 (mg HC/g rock)	S_1+S_2 (mg HC/g rock)	S_3 (mg CO_2/g rock)	T_{max} (°C)	HI (mg HC/g TOC)	OI (mg CO_2/g TOC)	PI	S_2/S_3	R_o (%)	TAI
Fužine željeznička	OUT	0.80	0.01				535					2.27	4^-
Fužine Bajersko j.	OUT	0.62	0.01				547					2.51	4^-
Lokve Lazac	OUT	0.57	0.01				529					1.87	3^+-4^-
Lokve Homer	OUT	0.86	0.01				529					1.74	3^+-4^-
Donje Pazarište 14	OUT	0.84	0.02	0.03	0.05		561	4		0.40		2.52	4^-
Donje Pazarište 19	OUT	0.89	0.02	0.02	0.04		447	2		0.50		1.84	3^+-4^-
DP. Jovanović p. 1	OUT	1.25	0.27	0.03	0.30	0.08		2	6	0.90	0.38	2.32	4^-
DP. Jovanović p. 2	OUT	0.80	0.10	0.13				16				2.01	4^-
DP. Jovanović p. 3	OUT	0.95	0.20	0.13				14					4^-
Muć	OUT	1.46	0.23	0.48	0.71	0.41	492	33	28	0.32	1.17	1.32	3-3^+
Muć 1	OUT	1.26	0.03	0.60	0.63	0.50	454	48	40	0.05	1.20		3-3^+
Muć 3	OUT	1.27	0.00	0.20	0.20	1.10		16	87		0.18		3-3^+
Muć 4	OUT	1.67	0.00	0.10	0.10	1.10		6	66		0.09		3-3^+
Muć 5	OUT	1.80	0.70	0.30	1.00	0.30		17	17	0.70	1.00		3-3^+
Sutina 14/2	OUT	3.13	0.10	0.16	0.26		594	5		0.38		1.93*	3^+
Sutina 14/6	OUT	3.23	0.09	0.15	0.24		594	5		0.38			3^+
Sutina 14/34	OUT	4.21	0.46	0.36	0.82		594	9		0.56		1.81*	3^+
Sutina 14A	OUT	0.62	0.20	0.28	0.48		486	45		0.42			3^+
Sutina 28/2	OUT	1.07	0.22	0.64	0.86		465	60		0.26		1.42	3^+
Zelovo Sutin. s. 13/7	OUT	1.25										1.26	3
Zelovo Sutin. s.13/7a	OUT	1.36										1.14	3
Glamoč Busija	OUT	1.06	0.23	4.20	4.43		432	396		0.05		0.62	2^+
Glamoč 1A	OUT	2.25	0.20	3.40	3.60	1.80	430	151	80	0.06	1.89	0.60	2^+
Glamoč 3C	OUT	1.78	0.20	4.30	4.50	1.20	429	242	67	0.04	3.58	0.64	2^+
Glamoč 4D	OUT	2.07	0.20	5.10	5.30	1.50	428	246	72	0.04	3.40	0.59	2^+
Glamoč-1	1604	2.60	0.71	1.27	1.98	0.25	479	49	10	0.36	5.08	1.55	3^+
Glamoč-1	1605	1.40	0.21	0.86	1.07	0.20	458	61	14	0.20	4.30	1.83	3^+
Glamoč-1	1638	1.51	0.40	0.61	1.01	0.29	476	40	19	0.40	2.10		3^+
Glamoč-1	1660	0.90	0.28	0.32	0.60	0.13		36	14	0.47	2.46	1.60	3^+
Glamoč-1	1718	2.26	0.53	0.81	1.34	0.30	465	36	13	0.40	2.70	1.38	3^+
Glamoč-1	1720	0.99	0.36	0.46	0.82	0.25		46	25	0.44	1.84	1.61	3^+
Glamoč-1	1758	1.88	1.14	0.94	2.08	0.27	461	50	14	0.55	3.48		3^+
Glamoč-1	1792	2.11	1.15	2.04	3.19	0.46	458	97	22	0.36	4.43	1.69	3^+
Glamoč-1	1795	1.34	0.29	1.33	1.62	0.19	453	99	14	0.18	7.00	1.15	3-3^+
Glamoč-1	1798	1.53	0.57	0.7	1.27	0.29	462	46	19	0.45	2.41		3-3^+
Glamoč-1	1838	1.64	0.41	0.6	1.01	0.32	466	37	20	0.41	1.88		3-3^+
Glamoč-1	1878	1.07	0.25	0.38	0.63	0.29	462	36	27	0.40	1.31		3-3^+
Glamoč-1	1958	1.49	0.88	0.88	1.76	0.24	458	59	16	0.50	3.67		3-3^+
Glamoč-1	1998	1.04	0.34	0.47	0.81	0.23	463	45	22	0.42	2.04		3-3^+
Glamoč-1	2040	1.01	0.21	0.47	0.68	0.21	465	47	21	0.31	2.24	1.26	3-3^+
Glamoč-1	2078	1.03	0.27	0.38	0.65	0.24	465	37	23	0.42	1.58		3-3^+
Karlovac-2	3777	0.77	0.03	0.33	0.36	0.06		43	8	0.08	5.50	1.11	3
Komiža 2B	OUT	0.45	0.07	1.09	1.16	0.35	434	242	78	0.06	3.11	0.55	2-2^+
Komiža 8	OUT	0.59	0.05	0.79	0.84	0.19	447	134	32	0.06	4.16	0.61	2^+
Palagruža 4	OUT	0.48	0.02	0.13	0.15	1.07	437	27	223	0.13	0.12		2-2^+
Vis-1	145	0.88	0.04	0.23	0.27	0.07	431	26	8	0.15	3.29		2
Vis-1	195	0.88	0.03	0.22	0.25	0.04	438	25	5	0.12	5.50	0.55	2-2^+
Kornati More-1	2152	0.81	0.02	0.61	0.63	0.52	434	75	64	0.03	1.17		2-2^+
Vlatka-1	3830	0.74	0.18	3.14	3.32	0.40	422	424	54	0.05	7.85		2
Vlatka-1	4586	0.81	0.09	1.34	1.43	1.09	443	165	135	0.06	1.23		2-2^+
Vlasta-1	5410	1.00	2.03	4.30	6.33		430	430		0.32			2-2^+
Vlasta-1	5410	0.98	0.09	1.82	1.91		427	186		0.05			2-2^+
Vlasta-1	5410	0.89	1.78	2.62	4.40	0.00	428	294		0.40			2-2^+
Vlasta-1	5410	1.61	0.60	5.27	5.87	0.52	426	327	32	0.10	10.13	0.63	2-2^+
Vlasta-1	5419	1.07	0.34	3.12	3.46	0.42	427	292	39	0.10	7.43		2-2^+
Vlasta-1	5431	1.26	3.25	3.67	6.92		425	291		0.47			2-2^+
Vlasta-1	5432	1.22	1.26	4.81	6.07		430	394		0.21			2-2^+
Vlasta-1	5441	0.82	0.67	5.29	5.96	0.29	424	645	35	0.11	18.24		2-2^+
Vlasta-1	5442	1.08	0.67	5.43	6.10	0.01	436	503		0.11	543.00		2-2^+
Vlasta-1	5444	0.83	1.07	3.74	4.81	0.00	430	451		0.22			2-2^+
Vlasta-1	5445	0.91	0.56	5.06	5.62	0.28	423	556	31	0.10	18.07		2-2^+
Vlasta-1	5452	4.10	2.01	23.20	25.21	0.20	432	566	5	0.08	116.00		2-2^+
Vlasta-1	5452	0.84	0.45	3.49	3.94	0.31	421	415	37	0.11	11.26		2-2^+
Vlasta-1	5457	1.48	2.75	6.45	9.20	0.48	420	436	32	0.30	13.44		2-2^+
Vlasta-1	5458	1.08	0.87	5.43	6.30		428	503		0.14			2-2^+
Vlasta-1	5465	1.80	3.91	7.34	11.25	0.75	411	408	42	0.35	9.79		2-2^+
Vlasta-1	5466	0.97	2.58	5.53	8.11	0.67	422	570	69	0.32	8.25		2-2^+
Vlasta-1	5467	1.76	0.80	12.46	13.26	0.57	423	708	32	0.06	21.86		2-2^+

Geologia Croatica

Table S1. *Continued.*

Sample ID Well/Outcrop	Outcrop Well/Depth (m)	TOC (%)	S_1 (mg HC/g rock)	S_2 (mg HC/g rock)	S_1+S_2 (mg HC/g rock)	S_3 (mg CO_2/g rock)	T_{max} (°C)	HI (mg HC/g TOC)	OI (mg CO_2/g TOC)	PI	S_2/S_3	R_o (%)	TAI
Vlasta-1	5467	1.77	0.92	12.56	13.48	0.72	424	710	41	0.07	17.44		$2-2^+$
Vlasta-1	5467	0.95	0.69	5.57	6.26	0.44	423	586	46	0.11	12.66		$2-2^+$
Vlasta-1	5468	1.39	1.08	8.33	9.41	0.40	435	599	29	0.11	20.83		$2-2^+$
Vlasta-1	5551	1.02	1.22	3.63	4.85	0.36	418	356	35	0.25	10.08	0.54	$2-2^+$
Vlasta-1	5552	1.04	1.06	3.58	4.64	0.24	419	344	23	0.23	14.92		$2-2^+$
Vlasta-1	5552	1.04	1.63	4.69	6.32	0.27	420	451	26	0.26	17.37		$2-2^+$

OUT outcrops; TOC total organic carbon; S_1 the amount of free hydrocarbons; S_2 the amount of hydrocarbon generated through thermal cracking; S_3 the amount of CO_2 produced during pyrolysis; T_{max} the temperature of maximum hydrocarbon generation; PI production index; S_1+S_2 generative potential (PETERS & CASSA, 1994); $\%R_o$ vitrinite reflectance (VR); *$\%R_o$ Vitrinite reflectance measured on solid bitumen, bitumen reflectance (BR, $\%R_b$). The corresponding vitrinite reflectance is calculated using the equation $\%R_o = 0.61 * \%R_b + 0.40$ proposed by JACOB (1989), TAI thermal alteration index, TAI to VR ($\%R_o$) correlation scale: 2 0.45 – 0.55$\%R_o$, 2^+ 0.55 – 0.70$\%R_o$, 3^- 0.70 – 0.95$\%R_o$, 3 0.95 – 1.25$\%R_o$, 3^+ 1.25 – 2.00$\%R_o$, 4^- 2.00 – 3.00$\%R_o$, 4>3.00$\%R_o$. Well data published by COTA & BARIĆ (1998) are included in the table.

Table S2. Chemical data, gas chromatography parameters and stable carbon isotope ratios of extracts from Triassic carbonates, marls and shales and Vlasta-1 oil.

Sample ID Well/Outcrop	Outcrop Well/Depth (m)	Sat. (%)	Aro. (%)	NSO+Asph. (%)	Pr/nC_{17}	Ph/nC_{18}	Pr/Ph	$\delta^{13}C_{Ker.}$ (‰, VPDB)	$\delta^{13}C_{Bit.}$ (‰, VPDB)	$\delta^{13}C_{Sat.}$ (‰, VPDB)	$\delta^{13}C_{Aro.}$ (‰, VPDB)
DP Jovanović p. 2	OUT							-24.11	-25.88		
DP Jovanović p. 6	OUT							-22.87			
DP Popović p. 3	OUT							-23.52	-25.11		
DP Popović p. 9/1	OUT							-22.62	-23.51		
DP Popović p. 10/1	OUT							-24.43	-24.88		
Muć	OUT				0.39	0.48	0.39		-27.20	-29.60	-27.50
Zelovo s.s. 13/7	OUT							-27.07			
Zelovo s.s. 13/7a	OUT				0.72	0.47	1.40	-26.41			
Glamoč-1	1605				0.82	0.62	0.42		-27.90	-29.34	-28.84
Glamoč-1	1718				0.43	0.52	0.25				
Glamoč-1	1795				0.47	0.57	0.51		-28.90	-28.06	-27.18
Komiža1	OUT				1.61	3.06	0.53				
Vis-1	144				0.95	1.10	0.55				
Vis-1	197				0.79	1.02	0.39				
Vlatka-1	3830				0.76	0.74	0.40				
Vlatka-1	4586				0.84	0.87	0.33				
Vlasta-1 oil	5404	33.90	16.80	49.30	1.75	4.38	0.52		-30.60	-31.30	-30.40
Vlasta-1	5406				0.34	0.63	0.54				
Vlasta-1	5410	22.90	22.40	54.70	0.18	0.92	0.36	-27.99	-30.75		
Vlasta-1	5411	33.20	19.30	47.50	0.39	1.82	0.38	-28.98	-31.85		
Vlasta-1	5411.				0.42	1.01	0.31	-27.81	-30.55		
Vlasta-1	5418	31.20	12.90	55.90	2.61	4.78	0.34		-30.71		
Vlasta-1	5419				0.72	1.10	0.61	-27.76			
Vlasta-1	5419				1.48	2.11	0.83			-30.01	-28.97
Vlasta-1	5441	34.70	18.40	46.90				-27.22	-29.33	-29.55	-29.51
Vlasta-1	5445	29.50	19.60	50.90	3.80	3.28	0.69				
Vlasta-1	5452				0.57	0.94	0.47	-28.38	-29.06		
Vlasta-1	5452				1.17	2.28	0.54			-30.61	-29.51
Vlasta-1	5468	21.70	16.50	61.80	1.63	18.10	0.11				
Vlasta-1 oil	5490	50.50	15.30	34.20	0.89	2.38	0.41				
Vlasta-1	5535				2.42	4.18	0.43			-29.55	-29.39
Vlasta-1 oil	5551	44.60	16.60	38.80	1.68	6.62	0.37				
Vlasta-1 oil	5551-5556	32.80	19.40	47.80	1.55	3.13	0.60		-30.48	-31.60	-30.36
Vlasta-1	5552	22.30	16.60	61.60	1.25	5.18	0.21	-28.31	-31.22		
Vlasta-1	5615				1.21	1.87	0.39			-27.32	-26.79
Vlasta-1	6115				0.94	1.52	0.40			-27.05	-27.16
Vlasta-1	6285				1.22	1.69	0.71			-27.32	-26.93
Vlasta-1	6505				0.98	1.00	0.69			-27.26	-26.95

$\delta^{13}C$ stable carbon isotope ratio; VPDB Vienna Pee Dee Belemnite standard; Ker. kerogen; Bit. bitumen; Sat. saturated hydrocarbons; Aro. aromatic hydrocarbons; NSO nitrogen (N), sulphur (S), and oxygen(O)-bearing compounds; Asph. asphaltenes; Pr pristane; Ph phytane. Well data published by COTA & BARIĆ (1998) are included in the table.

Table S3. Source and maturity related biomarker and non-biomarker ratios of extracts from Triassic carbonates, marls and shales and Vlasta oil.

Sample ID Well/Outcrop	Outcrop Well/Depth (m)	a	b	c	d	e	f	g	h	i	j	k	l	m	n	o	p	r	s
Sinj-3	OUT	0.00	0.93	0.37	0.57	0.09	0.65	0.08	0.45	1.30	0.14	0.56	0.39	30.59	26.31	43.10	0.36	0.34	
Zelovo 10	OUT	0.00	1.14	0.35	0.58	0.06	0.83	0.07	0.38	1.09	9.15	0.57	0.42	34.99	23.80	41.21	0.39	0.42	
Glamoč-1	1604	0.04	1.19	0.39*	0.58	0.09						0.62	0.49	34.70	25.83	39.48	0.53	0.07	1.05
Glamoč-1	17920	0.16	0.68	0.75*	0.58							0.56	0.46	31.33	32.88	35.80	0.42	0.21	0.97
Vlatka-1	3830	0.00	0.61	0.27	0.54	0.13	0.58	0.03	0.50	0.62	16.65	0.39	0.38	29.84	23.20	46.95	0.03	0.25	
Vlatka-1	3830	0.00	0.46	0.25	0.53	0.15	0.60	0.02	0.53	0.60	16.78	0.42	0.42	32.08	24.67	43.26	0.11	0.11	
Vlatka-1	3835	0.06	0.87	0.33	0.56	0.12	0.54	0.19	0.48	1.27	17.09	0.50	0.46	31.55	26.96	41.49	0.47	0.23	
Vlatka-1	4586	0.00	0.51	0.33	0.22	0.12	0.41	0.04	0.71	0.35	4.87	0.38	0.25	53.67	15.13	31.21	0.35	0.96	
Vlasta-1	5414	0.00	0.58	0.37	0.60	0.12	0.45	0.02	0.32	1.55	23.01	0.60	0.30	31.04	14.22	54.75	0.17	0.13	
Vlasta-1	5419	0.00	0.79	0.58*	0.58	0.28			0.63			0.51	0.40	22.04	24.22	53.74	0.50	0.12	0.79
Vlasta-1	5419	0.00	0.75	0.40	0.58	0.27			0.32	1.47	28.51	0.43	0.45	23.33	26.07	50.60	0.18	0.31	
Vlasta-1	5441	0.00	0.65	0.53*	0.45	0.00			0.62			0.42	0.33	13.01	23.02	63.97	0.57	0.36	0.83
Vlasta-1	5441	0.00	0.44	0.45	0.54	0.69	0.57	0.02	0.24	1.45	29.13	0.32	0.36	24.38	22.04	53.57	0.11	0.88	
Vlasta-1	5445	0.00	0.47	0.49	0.55	0.57	0.50	0.02	0.22	1.09	24.46	0.31	0.36	15.85	20.16	63.98	0.09	0.95	
Vlasta-1	5452	0.00	0.50	0.48*	0.48	0.20			0.62			0.36	0.30	18.42	19.81	61.78	0.39	0.39	0.82
Vlasta-1	5464	0.00	0.53	0.45	0.54	0.40	0.62	0.04	0.32	2.22	39.95	0.32	0.36	24.38	22.04	53.57	0.11	0.88	
Vlasta-1	5467	0.00	0.54		0.51	0.24			0.53	2.65	40.06	0.26	0.32	24.02	20.26	55.72	0.28	1.38	
Vlasta-1	5467	0.00	0.50	0.16	0.51	0.45		0.00	0.48	2.04	36.19	0.31	0.36	15.85	20.16	63.98	0.09	0.95	
Vlasta-1	5535		0.71		0.53	0.32			0.63			0.45	0.39	14.34	29.84	55.83	0.21	0.45	0.71
Vlasta-1	5552	0.00	0.40	0.59	0.56	1.09		0.01	0.27	2.46	42.94	0.35	0.39	17.55	25.15	57.30	0.30	2.76	
Vlasta-1 oil	5551-5556	0.01	0.51	0.89*	0.58	0.41			0.48			0.44	0.41	20.13	24.76	55.11	0.58	0.19	0.81
Vlasta-1	5615	0.05	0.97	0.43*	0.57	0.12			0.74			0.57	0.43	29.17	28.66	42.17	0.51	0.10	0.83
Vlasta-1	6115		0.99	0.49*	0.59	0.15			0.75			0.44	0.38	23.91	30.09	46.00	0.42	0.17	
Vlasta-1	6285	0.04	0.92	0.48*	0.56	0.11			0.72			0.31	0.34	20.34	31.24	48.42	0.44	0.30	0.66
Vlasta-1	6505	0.05	0.99	0.49*	0.57	0.13			0.72			0.34	0.35	20.76	32.12	47.12	0.43	0.24	0.60
Vis-1	197	0.00	0.80	0.29	0.59	0.00	0.44	0.40	0.46	1.02	12.74	0.52	0.42	29.63	33.96	36.41	0.31	0.31	
Vis-1	1631	0.00	0.88	0.26	0.51	0.00	0.56	0.10	0.49	0.98	15.69	0.56	0.46	36.75	23.40	39.85	0.27	0.31	
Vis-1	2135	0.00	0.38	0.20	0.34	0.05	0.66	0.02	0.46	0.33	9.83	0.40	0.20	38.55	10.80	50.64	0.04	0.12	

a) oleanane/hopane (Ol/H); b) 17α,21β–C_{30} norhopane/17α,21β–C_{30} hopane (NH/H); c) 17α–C_{27} trisnorhopane/(17α–C_{27} trisnorhopane+18α–C_{27} trisnorneohopane) (Ts/(Ts + Tm)), *Ts/Tm; d) 22S/(22S + 22R) 17α,21β–C_{32} homohopane; e) gammacerane/hopane (G/H); f) C_{24}/C_{23}TT tricyclic terpane; g) C_{23}TT/17α,21β–C_{30} hopane (C_{23} TT/H); h) 17α,21β–C_{31} (22R) homohopane/17α,21β–C_{30} hopane (C_{31}(R)/H); i) 17α,21β–C_{35} (22S) homohopane/17α,21β–C_{34} (22S) homohopane (C_{35}(S)/C_{34}(S)); j) 17α,21β–C_{35} homohopane/17α,21β–C_{31-35} homohopane (C_{35}/C_{31-35}); k) αββ/(αββ+ααα) C_{29} sterane; l) 20S/(20S + 20R) ααα C_{29} sterane; m) ααα(20R) C_{27} steranes/Σ ααα(20R) regular steranes; n) ααα(20R) C_{28} steranes/Σ ααα(20R) regular steranes; o) ααα(20R) C_{29} steranes/Σ ααα(20R) regular steranes; p) diasteranes/regular steranes; r) steranes/hopanes; s) %$Rc_{(MPI\ 1)}$ (RADKE & WELTE, 1983).

Supplement 3

Table S1. Rock eval pyrolysis data, vitrinite reflectance and thermal alteration index from Jurassic carbonates and shales.

Sample ID Well/ Outcrop	Outcrop Well/Depth (m)	TOC (%)	S_1 (mg HC/g rock)	S_2 (mg HC/g rock)	S_1+S_2 (mg HC/g rock)	S_3 (mg CO_2/g rock)	T_{max} (^oC)	HI (mg HC/g TOC)	OI (mg CO_2/g TOC)	PI	S_2/S_3	**R_o** (%)	TAI
Lower Jurassic carbonates and shales													
Kubus	OUT	0.94	0.10	0.01	0.11	0.30			32	1.00	0.00	2.48	4^-
Drežnica Jasenak	OUT	0.46	0.04	0.08	0.12	0.35		17	76	0.33	0.23	1.88	3^+-4^-
Rovinj-1	1043	1.43	0.46	9.09	9.55	0.54	419	636	38	0.05	16.83	0.62	2^+
Rovinj-1	1044	1.03	0.6	3.74	4.34	0.44	417	363	43	0.14	8.50	0.68	2^+
Upper Jurassic carbonates and shales													
Gorski Kotar Trough/Basin													
Matić Poljana 1a	OUT	0.46	0.00	0.04	0.04	0.23	495	9	50		0.17	2.02*	
Matić Poljana 1b	OUT	0.44	0.00	0.01	0.01	0.49		2	111		0.02		
Matić Poljana 1c	OUT	0.52	0.20	0.13	0.33	0.04	527	25	8	0.61	3.25	2.32*	
Lemeš Trough/Basin													
Vrelo 1	OUT	45.90	4.95	243.20	248.15			530		0.02			2
Vrelo 2	OUT	6.69	1.86	42.70	44.56	0.73	427	638	11	0.04	58.49	0.77	2
Vrelo 3	OUT	5.83	1.03	29.50	30.53	2.89		506	50	0.03	10.21		2
Vrelo T1	OUT	22.08	3.31	152.44	155.75	0.51	429	690	2	0.02	298.90		2
Vrelo T2	OUT	19.31	1.43	151.48	152.91		424	784		0.01			2
Vrelo T3	OUT	34.36	1.94	186.78	188.72		424	544		0.01			2
Vrelo T4	OUT	39.61	4.15	228.50	232.65		433	577		0.02			2
Zubović d. 2R2	OUT	22.18	0.99	94.05	95.04		431	424		0.01			2
Zubović d. 6R2	OUT	31.00	5.20	169.30	174.50		426	546		0.03			2
Zubović d. 13R1	OUT	28.29	4.30	154.50	158.80		424	546		0.03			2
Zubović d. 100	OUT	26.75	1.85	153.12	154.97	0.51	438	572	2	0.01	300.24	0.45	2
Zubović d. 100/1	OUT	5.51	0.08	21.91	21.99	2.15	430	398	39		10.19		2
Zubović d. 5-6/1	OUT	22.08	3.31	152.44	155.75	0.51	429	690	2	0.02	298.90		2
KVR-1	OUT	16.49	1.04	99.48	100.52	0.51	434	603	3	0.01	195.06	0.48	2
KVR-2	OUT	11.26	0.80	75.24	76.04	0.50	430	668	4	0.01	150.48	0.45	2
Milanović d. 101/1	OUT	1.10	0.18	6.44	6.62	0.33	428	585	30	0.03	19.52	0.62	2-2^+
Milanović d. 101/2	OUT	6.35	0.25	32.25	32.50	0.91	425	508	14	0.01	35.44		2-2^+
Zavalje 5/1	OUT	2.03	0.35	12.57	12.92	0.40	430	619	20	0.03	31.43		2
Zavalje 8/1	OUT	1.39	0.21	8.68	8.89	0.29	429	624	21	0.02	29.93		2
Zavalje 18/1	OUT	1.28	0.02	6.66	6.68	0.45	426	520	35		14.80		2
Mamac 18R4	OUT	2.20	0.09	7.30	7.39		428	332		0.01			2
Mamac 2R5	OUT	3.16	0.29	19.32	19.61		427	611		0.01			2
Dimići A	OUT	4.61	1.70	31.21	32.91		437	677		0.05			2-2^+
Dimići B	OUT	9.28	0.25	61.49	61.74		438	663		0.00			2-2^+
Poštak 5-7/1	OUT	1.93	0.37	9.56	9.93	0.26	432	495	13	0.04	36.77		2
Poštak 5-7/2	OUT	4.65	0.14	25.62	25.76	0.76	434	551	16	0.01	33.71		2
Poštak 5-7/3	OUT	2.01	0.08	9.81	9.89	0.33	431	488	16	0.01	29.73		2
Poštak 5-7/4	OUT	2.42	0.17	11.66	11.83	0.40	432	482	17	0.01	29.15		2
Poštak 5	OUT	4.38	0.76	19.40	20.16	1.67	435	443	38	0.04	11.62		2-2^+
Poštak 6	OUT	3.87	0.23	20.50	20.73	0.69	436	530	18	0.01	29.71		2-2^+
Poštak 7	OUT	4.60	0.36	22.83	23.19	1.86	435	496	40	0.02	12.27		2-2^+
Poštak 9	OUT	4.25	1.39	25.93	27.32	0.94	437	610	22	0.05	27.59		2-2^+
Poštak 10	OUT	4.01	0.70	23.48	24.18	0.53	438	586	13	0.03	44.30		2-2^+
Poštak P1	OUT	3.44	0.20	18.80	19.00	0.90	431	547	26	0.01	20.89		2-2^+
Poštak P2	OUT	4.28	0.90	25.00	25.90		430	584	0	0.03			2-2^+
Poštak P3	OUT	6.86	0.20	49.00	49.20		436	714	0				2-2^+
Poštak P4	OUT	4.54	0.60	27.60	28.20		435	608	0	0.02			2-2^+
Dimići 1	OUT	3.50	0.10	18.10	18.20	0.60	436	517	17	0.01	30.17		2-2^+
Dimići2	OUT	3.78	0.10	21.50	21.60	0.50	437	569	13		43.00		2-2^+
Dimići 3	OUT	4.68	0.20	23.20	23.40	1.30	433	496	28	0.01	17.85		2-2^+
Dimići 4	OUT	2.90	0.10	12.40	12.50	0.80	434	428	28	0.01	15.50		2-2^+
Dimići5	OUT	3.51	0.10	16.80	16.90	1.00	433	479	28	0.01	16.80		2-2^+
Dimići 6	OUT	4.77	0.10	25.70	25.80	0.80	435	539	17		32.13		2-2^+
Dimići 7	OUT	3.86	0.20	19.50	19.70	0.90	437	505	23	0.01	21.67		2-2^+
Dimići 8	OUT	3.27	0.20	13.00	13.20	1.10	434	398	34	0.02	11.82		2-2^+
Dimići 9	OUT	1.93	0.10	5.80	5.90	0.90	438	301	47	0.02	6.44		2-2^+
Dimići 10	OUT	4.20	0.20	24.80	25.00	0.70	436	590	17	0.01	35.43		2-2^+
Dimići 11	OUT	3.69	0.30	19.40	19.70	0.60	437	526	16	0.02	32.33		2-2^+
Dimići 12	OUT	5.88	0.30	32.10	32.40	0.60	437	546	10	0.01	53.50		2-2^+
Dimići 13	OUT	4.57	0.40	23.40	23.80	0.90	436	512	20	0.02	26.00		2-2^+
Dimići 14	OUT	7.12	0.30	35.80	36.10	0.70	438	503	10	0.01	51.14		2-2^+
Dimići 15	OUT	4.05	0.20	23.30	23.50	0.50	437	575	12	0.01	46.60		2-2^+
Dimići 16	OUT	5.66	0.20	31.80	32.00	1.10	435	562	19	0.01	28.91		2-2^+
Dimići 17	OUT	4.78	0.80	26.30	27.10	1.00	434	550	21	0.03	26.30		2-2^+
Dimići 18	OUT	6.55	0.60	36.60	37.20	1.30	434	559	20	0.02	28.15		2-2^+
Dimići 19	OUT	4.52	0.20	25.00	25.20	0.70	435	553	15	0.01	35.71		2-2^+
Rastićevo 2	OUT	2.48	0.11	9.14	9.25	0.73	433	369	29	0.01	12.52		2-2^+
Rastićevo 3	OUT	5.15	0.11	26.05	26.16	0.66	436	506	13		39.47		2-2^+
Rastićevo 5	OUT	5.78	0.14	24.56	24.70	1.26	432	425	22	0.01	19.49		2-2^+
Rastićevo 6	OUT	3.07	0.17	12.62	12.79	0.86	434	411	28	0.01	14.67		2-2^+
Rastićevo 7	OUT	5.35	0.14	25.85	25.99	0.54	435	483	10	0.01	47.87		2-2^+
Rastićevo 8	OUT	2.94	0.05	9.40	9.45	1.08	432	320	37	0.01	8.70		2-2^+
Rastićevo 9	OUT	4.93	0.25	24.34	24.59	0.57	435	494	12	0.01	42.70		2-2^+

Table S1. *Continued.*

Sample ID Well/ Outcrop	Outcrop Well/Depth (m)	TOC (%)	S_1 (mg HC/g rock)	S_2 (mg HC/g rock)	S_1+S_2 (mg HC/g rock)	S_3 (mg CO_2/g rock)	T_{max} (°C)	HI (mg HC/g TOC)	OI (mg CO_2/g TOC)	PI	S_2/S_3	**R_o** (%)	TAI
Rastićevo 9a	OUT	3.88	0.03	19.64	19.67	0.53	435	506	14		37.06		2-2^{+}
Rastićevo 27	OUT	2.84	0.81	15.05	15.86	0.45	433	530	16	0.05	33.44		2-2^{+}
Rastićevo 30	OUT	9.00	0.27	53.39	53.66	1.04	435	593	12	0.01	51.34		2-2^{+}
Rastićevo 31	OUT	2.76	0.07	11.57	11.64	0.58	434	419	21	0.01	19.95		2-2^{+}
Rastićevo 34	OUT	4.33	0.11	21.82	21.93	0.43	435	504	10	0.01	50.74		2-2^{+}
Dimići PD2a	OUT	2.29	0.47	10.49	10.96	0.71	428	458	31	0.04	14.77		2
Dimići PD2d	OUT	8.34	1.12	51.88	53.00	0.91	432	622	11	0.02	57.01		2
Dimići PD8a	OUT	3.90	0.24	20.10	20.34	1.14	426	515	29	0.01	17.63		2
Škundrići PŠK3	OUT	5.90	0.84	46.15	46.99	0.57	435	782	10	0.02	80.96		2
Škundrići PŠK3a	OUT	1.57	0.20	8.62	8.82	0.30	433	549	19	0.02	28.73		2
Škundrići PŠK3b	OUT	2.59	1.02	15.63	16.65	0.27	432	603	10	0.06	57.89		2
Škundrići PŠK3c	OUT	7.82	0.98	66.02	67.00	1.53	433	844	20	0.01	43.15		2
Škundrići PŠK12	OUT	8.87	0.55	51.74	52.29	0.58	436	583	7	0.01	89.21		2
Škundrići PŠK8	OUT	1.26	0.10	5.94	6.04	0.60	429	471	48	0.02	9.90		2
Poštak h. PHA4	OUT	3.96	0.63	22.47	23.10	0.85	434	567	21	0.03	26.44		2
Poštak h. PHA6	OUT	4.60	1.20	29.63	30.83	0.59	433	644	13	0.04	50.22		2
Poštak h.PHA6a	OUT	3.30	0.13	20.24	20.37	0.40	435	613	12	0.01	50.60		2
Poštak h.PHA6b	OUT	6.59	0.23	43.59	43.82	0.56	434	661	8	0.01	77.84		2
Poštak s. PPŠ3	OUT	2.40	0.18	11.74	11.92	0.62	428	489	26	0.02	18.94		2
Vištice PŠV4	OUT	2.95	0.41	18.68	19.09	0.78	433	633	26	0.02	23.95		2
Vištice PŠV3a	OUT	2.98	0.34	17.72	18.06	0.38	435	595	13	0.02	46.63		2
Vištice PŠV3b	OUT	5.59	0.28	35.12	35.40	0.50	436	628	9	0.01	70.24		2
Vištice PŠV3c	OUT	4.25	0.18	26.32	26.50	0.48	436	619	11	0.01	54.83		2
Kozjak 7	OUT	4.01	0.39	23.23	23.62	1.64	414	579	41	0.02	14.16		1^{+}-2^{-}
Kozjak 8	OUT	1.59	0.06	9.11	9.17	0.93	420	573	58	0.01	9.80		1^{+}-2^{-}
Kozjak 9	OUT	2.92	0.16	16.66	16.82	0.94	413	571	32	0.01	17.72		1^{+}-2^{-}
Vrlika 9	OUT	1.15	0.07	8.18	8.25	0.37	411	711	32	0.01	22.11		1^{+}-2^{-}
Vrlika 2	OUT	3.48	0.23	20.27	20.50	1.25	416	582	36	0.01	16.22		1^{+}-2^{-}
Maovice 4	OUT	0.79	0.02	3.82	3.84	0.44	425	484	56	0.01	8.68		1^{+}-2^{-}
Lemeš-1	OUT	1.33	0.00	5.70	5.70	1.30	421	429	98	0.00	4.38		1^{+}-2^{-}
Lemeš-2	OUT	6.46	0.80	49.60	50.40	2.10	412	768	33	0.02	23.62		1^{+}-2^{-}
Lemeš-3	OUT	2.00	0.10	14.20	14.30	1.60	412	710	80	0.01	8.88		1^{+}-2^{-}
Lemeš-4	OUT	3.68	0.30	24.30	24.60	1.90	413	660	52	0.01	12.79		1^{+}-2^{-}
Lemeš-5	OUT	3.35	0.20	25.00	25.20	1.60	413	746	48	0.01	15.63		1^{+}-2^{-}
Lemeš-6	OUT	2.59	0.30	20.90	21.20	1.60	412	807	62	0.01	13.06		1^{+}-2^{-}
Lemeš-7	OUT	5.55	0.70	39.70	40.40	2.50	414	715	45	0.02	15.88		1^{+}-2^{-}
Lemeš-8	OUT	1.47	0.10	6.00	6.10	1.80	420	408	122	0.02	3.33		1^{+}-2^{-}
Svilaja 1	OUT	1.33	0.00	5.70	5.70	1.30	421	428	97	0.00	4.38		1^{+}-2^{-}
Svilaja 2	OUT	6.46	0.80	49.60	50.40	2.10	412	768	33	0.02	23.62		1^{+}-2^{-}
Svilaja 3	OUT	2.00	0.10	14.20	14.30	1.60	412	710	80	0.01	8.88		1^{+}-2^{-}
Svilaja 4	OUT	3.68	0.30	24.30	24.60	1.90	413	660	52	0.01	12.79		1^{+}-2^{-}
Svilaja 5	OUT	3.35	0.20	25.00	25.20	1.60	413	746	48	0.01	15.63		1^{+}-2^{-}
Svilaja 6	OUT	2.59	0.30	20.90	21.20	1.60	412	807	62	0.01	13.06		1^{+}-2^{-}
Svilaja 7	OUT	5.55	0.70	39.70	40.40	2.50	414	715	45	0.02	15.88		1^{+}-2^{-}
Svilaja 8	OUT	1.47	0.10	6.00	6.10	1.80	420	408	122	0.02	3.33		1^{+}-2^{-}
Dabar 1	OUT	4.49	0.33	26.80	27.13	1.03	411	597	23	0.01	26.02		1^{+}-2^{-}
Dabar 4	OUT	4.37	0.27	23.54	23.81	1.78	413	539	41	0.01	13.22		1^{+}-2^{-}
Dabar PL5/1	OUT	5.05	0.29	30.38	30.67	2.25	413	602	45	0.01	13.50		1^{+}-2^{-}
Dabar PL 5/2	OUT	1.55	0.04	8.97	9.01	0.49	414	579	32		18.31		1^{+}-2^{-}
Brač-1	4360	0.85	1.25	2.28	3.53	2.22	420	268	261	0.35	1.03		2^{-}
Brač-1	4380	0.56	0.90	2.33	3.23	1.24	422	416	221	0.28	1.88		2^{-}
Brač-1	4390	0.60	0.37	1.35	1.72	0.98	427	225	163	0.22	1.38		2^{-}-2
Brač-1	5830	1.07	0.53	2.30	2.83	5.28	440	215	493	0.19	0.44		2^{+}
Brač-1	5840	1.88	1.57	4.62	6.19	5.08	441	246	270	0.25	0.91		2^{+}
Brač-1	5870	0.85	0.14	1.64	1.78	1.87	440	193	220	0.08	0.88		2^{+}
Brač-1	5930	0.52	0.60	7.80	8.40	1.18	430	900	227	0.07	6.61		2^{+}
Brač-1	5950	0.52	0.60	1.80	2.40	1.18	430	346	227	0.25	1.53		2^{+}
Vlasta -1	2120	0.87	3.11	3.93	7.04			452		0.44			1^{+}
					Migrabitumen								
Bihać-Zavalje 2/1	OUT	4.71	1.58	28.92	30.5	0.59	428	614	13	0.05	49.02	0.08-0.27*	
Bihać-Zavalje 7/1	OUT	2.59	1.29	18.80	20.09	0.22	428	726	8	0.06	85.45		
Torbički Vagan 313	OUT	4.76	1.3	27.85	29.15	0.75	431	585	16	0.04	37.13	0.10-0.28*	
Palanka 1	OUT	17.50	2.11	140.14	142.25		424	801		0.01		0.09-0.25*	
Palanka 3	OUT	4.18	1.90	23.23	25.13	1.63	426	556	39	0.08	14.25	0.10-0.27*	
Palanka 4	OUT	7.30	4.83	49.19	54.02	0.4	429	674	5	0.09	122.98	0.09-0.20*	
Palanka 5	OUT	5.92	4.66	41.12	45.78	0.23	431	695	4	0.10	178.78	0.11-0.28*	
Palanka 6	OUT	18.40	1.73	134.50	136.23		428	731		0.01			

OUT outcrops; TOC total organic carbon; S_1 the amount of free hydrocarbons; S_2 the amount of hydrocarbon generated through thermal cracking; S_3 the amount of CO_2 produced during pyrolysis; T_{max} the temperature of maximum hydrocarbon generation; PI production index; S_1+S_2 generative potential (PETERS & CASSA, 1994); %R_o vitrinite reflectance (VR); *%R_o Vitrinite reflectance measured on solid bitumen, bitumen reflectance (BR, %R_b). The corresponding vitrinite reflectance is calculated using the equation %R_o=0.61 * %R_b+0.40 proposed by JACOB (1989), TAI thermal alteration index, TAI to VR (%R_o) correlation scale: 1^{+}<0.35%R_o, 2^{-} 0.35 – 0.45%R_o, 2 0.45 – 0.55%R_o, 2^{+} 0.55 – 0.70%R_o, 3^{-} 0.70 – 0.95%R_o, 3 0.95 – 1.25%R_o, 3^{+} 1.25 – 2.00%R_o, 4^{-} 2.00 – 3.00%R_o, 4>3.00%R_o. New data, alongside data from TROSKOT-ČORBIĆ (2011), have been integrated with selected published data from BLAŽEKOVIĆ SMOJIĆ et al. (2009) and COTA & BARIĆ (1998).

Table S2. Chemical data, gas chromatography parameters and stable carbon isotope ratios of extracts from Jurassic carbonates and shales.

Sample ID Well/Outcrop	Sat. (%)	Aro. (%)	NSO+Asph. (%)	n-alkanes (%)	$Pr/n\text{-}C_{17}$	$Ph/n\text{-}C_{18}$	Pr/Ph	CPI	$S_{Ker.}$ (%)	$S_{Bit.}$ (%)	$\delta^{13}C_{Ker.}$ (‰, VPDB)	$\delta^{13}C_{Bit.}$ (‰, VPDB)
Zubović d. 100	0.50	9.10	90.40	96.54	0.73	0.46	1.15	1.20	11.45			
Zubović d. 5-6/1	0.80	10.20	89.00	85.82	0.33	0.44	0.86	1.97	9.48	9.60	-25.56	-29.53
KVR-1	0.40	1.12	98.48	95.77	0.63	0.66	0.25	1.28	10.11	10.11	-26.71	-28.16
KVR-2	0.50	1.56	97.94	94.09	0.70	0.62	0.72	1.17	10.71	9.19	-25.30	-25.55
Milanović d. 1	9.10	7.50	83.40	71.53	1.17	2.41	0.39	0.93				
Milanović d. 2	8.90	7.10	84.00	91.51	0.40	0.54	0.62	1.19	7.98			
Rastičevo I 9	2.24	5.25	84.29	83.70	0.59	0.67	1.05	1.07	9.33			
Rastićevo 34	6.50	7.20	86.30	91.90	0.47	0.44	1.26	1.08	9.25			
Poštak 5-7/1	6.28	7.88	85.84	91.97	0.29	0.41	0.77	1.21	4.04			
Poštak 5-7/2	3.05	12.38	83.10	82.76	0.34	0.46	0.89	1.72	7.33	10.32	-27.16	-27.13
Poštak 5-7/3				92.25	0.33	0.47	0.92	1.17	4.57			-28.07
Poštak 5-7/4				96.44	0.33	0.45	0.82	1.06				-27.75
Poštak 2a	13.31	17.38	69.31	97.58	0.52	0.36	0.85	1.02	9.62		-27.79	
Poštak 2d	9.09	9.45	81.46	97.70	0.57	0.40	0.86	1.01	8.96		-27.72	
Poštak 8a	18.86	8.33	72.81	85.94	0.44	0.30	0.75	1.06	6.35		-27.66	
Škundrići PŠK3	2.31	10.66	87.04	95.76	0.07	0.14	0.47	1.25	10.87	8.74	-24.81	-27.01
Škundrići PŠK3a	3.13	15.38	81.49	90.84	0.45	0.71	0.59	2.08	8.96	9.22	-27.79	-29.22
Škundrići PŠK3b	5.29	22.89	71.83						5.82	6.18	-26.55	-28.03
Škundrići PŠK3c	1.54	8.09	90.38	91.83	0.22	0.32	0.71	1.49	7.01	7.71	-26.48	-27.72
Škundrići PŠK12	2.06	4.94	93.01	92.77	0.38	0.46	0.37	1.43	12.21		-25.80	-27.70
Škundrići PŠK4				97.20	0.29	0.50	0.22	1.18			-27.44	-29.71
Škundrići PŠK6									8.25			-28.29
Škundrići PŠK7				96.59	0.41	0.61	0.14	1.84	9.50		-27.36	-29.16
Škundrići PŠK8				94.75	0.85	0.96	0.13	1.75	5.08		-26.92	-29.54
Škundrići PŠK9										3.32		-29.33
Poštak s. PPŠ-2a												-29.10
Poštak s. PPŠ-3				96.65	0.19	0.35	0.37	1.30	6.41		-26.18	-27.96
Poštak h.PHA-1				93.38	0.93	0.91	0.88	1.44	6.34			
Poštak h.PHA-4				85.98	0.28	0.60	0.62	1.82	9.37	8.76	-25.25	-26.66
Poštak h.PHA-6/1									8.22	10.45	-25.97	-26.69
Poštak h.PHA-6/2				94.97	0.34	0.32	0.45	1.41	11.07	7.29	-26.60	-27.86
Vištice PŠV-1				93.20	0.24	0.43	0.44	1.66	5.45		-26.78	
Vištice PŠV-2				89.12	0.94	2.07	0.37	1.47	3.71			
Vištice PŠV-5				93.68	0.30	0.68	0.31	1.43	5.68	6.02	-25.08	-26.48
Vištice PŠV-4				82.43	0.54	1.08	0.43	1.44	6.32	5.55	-26.00	-26.68
Vištice PŠV-3a				88.50	0.43	0.59	1.05	2.37	10.65	10.43	-25.79	-27.08
Vištice PŠV-3a/1				83.98	0.74	0.81	0.99	1.88	12.25	7.21	-25.72	-26.25
Vištice PŠV-3b				89.44	0.33	0.46	0.99	2.33	11.19		-25.97	-27.18
Vištice PŠV-3c				88.88	0.43	0.62	1.00	1.48				
Vrlika 1	22.60	7.90	69.50	84.95	0.54	0.57	1.70	1.15				
Vrlika 2	12.00	5.20	82.80	86.42	0.54	0.56	1.46	1.12	9.78			
Dabar 1	6.30	4.50	89.20	78.79	0.87	0.74	1.57	1.12	9.98			
Dabar 4	7.50	4.00	88.50	83.32	0.72	0.62	1.37	1.14				
Bihać-Zavalje B2/1	1.70	0.50	97.80	92.69	0.77	0.84	0.56	1.10		6.62		
Torbički Vagan 313	39.50	0.30	60.20	66.95	1.20	2.44	0.45	1.70		10.25		
Palanka 3	1.48	6.81	91.72							10.41		-27.60
Palanka 4	5.90	24.80	69.30							11.31		-25.94
Palanka 5										9.61		-25.63
Vis-1. 3423 m				90.11	0.46	0.86	0.44	1.27				
Brač-1. 3425 m				74.54	0.72	0.81	0.87	1.03				

Sat. saturated hydrocarbons; Aro. aromatic hydrocarbons; NSO nitrogen (N), sulphur (S), and oxygen(O)-bearing compounds; Asph. asphaltenes; Pr pristane; Ph phytane; CPI carbon preference index (BRAY & EVANS, 1961); S sulphur; Ker. kerogen; Bit. bitumen; ^{13}C stable carbon isotope ratio; VPDB Vienna Pee Dee Belemnite standard.

Table S3. Source and maturity related biomarker and non-biomarker ratios of extracts from Jurassic carbonates, marls and shales.

Sample ID Outcrop Well/Depth (m)	a	b	c	d	e	f	g	h	i	j	k	l	m	n	o	p	r	s
Vrelo KVR-1	0.00	0.87	0.21	0.58	0.13	0.44	0.25	0.73	9.52	0.55	0.31	23.48	13.96	62.46	0.09	0.47	0.67	0.57
VreloKVR-2	0.00	0.82	0.22	0.60	0.02	0.41	0.27	0.96	11.15	0.55	0.30	25.23	14.89	59.88	0.08	0.43	0.71	0.58
Škundrići PŠK3a	0.00	1.69	0.08	0.63	0.07	0.52	0.12	0.65	4.70	0.54	0.36	32.93	27.22	39.87	0.22	0.31	0.73	0.62
Škundrići PŠK3b	0.00	1.21	0.04	0.60	0.05	0.23	0.04	1.32	8.97	0.59	0.42	30.69	22.98	46.32	0.06	0.19	0.71	0.57
Škundrići PŠK3c	0.00	1.92	0.05	0.62	0.08	0.53	0.06	0.93	7.43	0.59	0.43	32.16	21.23	46.62	0.08	0.44	0.82	0.54
Škundrići PŠK12	0.00	1.59	0.20	0.60	0.09	0.52	0.21			0.58	0.47	36.08	23.98	39.94	0.41	0.44	0.77	0.55
Poštak h.PHA-1	0.01	1.05	0.07	0.63	0.10	0.28	0.09	0.93	8.21	0.50	0.37	32.31	17.93	49.76	0.10	0.27		
Poštak h.PHA-4	0.01	1.34	0.06	0.62	0.08	0.24	0.20	0.87	6.02	0.53	0.39	45.36	15.44	39.21	0.13	0.38	0.71	0.59
Poštak h.PHA-5	0.00	2.19	0.03	0.63	0.12	0.75	0.07			0.57	0.37	30.53	16.80	52.67	0.12	0.62		
Poštak h.PHA-6/1	0.00	1.70	0.05	0.52	0.03	0.33	0.09	0.99	9.31	0.55	0.37	34.60	15.06	50.32	0.08	0.39		
Vištice PŠV-1	0.00	0.88	0.06	0.63	0.02	0.26	0.10	1.07	8.87	0.51	0.38	38.00	17.10	41.39	0.04	0.28	0.73	0.62
Vištice PŠV-4	0.00	1.01	0.07	0.63	0.03	0.31	0.13	0.97	8.63	0.52	0.39	36.41	18.67	44.92	0.00	0.34		
Vištice PŠV-3b	0.00	1.63	0.08	0.61	0.03	0.51	0.10			0.48	0.37	35.98	22.63	41.39	0.00	0.52	0.69	0.58
Brač-1 3425 m	0.00	0.80	0.20	0.58						0.40	0.41	28.00	23.00	49.00				

a) oleanane/hopane (Ol/H); b) 17α,21β–C_{30} norhopane/17α,21β–C_{30} hopane (NH/H); c) 17α–C_{27} trisnorhopane/18α–C_{27} trisnorneohopane (Ts/Tm); d) 22S/(22S + 22R) 17α,21β–C_{32} homohopane; e) gammacerane/hopane (G/H); f) C_{24}/C_{23}TT tricyclic terpane; g) C_{23}TT/17α,21β–C_{30} hopane (C_{23} TT/H); h) 17α,21β–C_{35} (22S) homohopane/17α,21β–C_{34} (22S) homohopane (C_{35}(S)/C_{34}(S)); i) 17α,21β–C_{35} homohopane/17α,21β–C_{31-35} homohopane (C_{35}/C_{31-35}); j) αββ/(αββ+ααα) C_{29} sterane; k) 20S/(20S + 20R) ααα C_{29} sterane; l) ααα(20R) C_{27} steranes/Σ ααα(20R) regular steranes; m) ααα(20R) C_{28} steranes/Σ ααα(20R) regular steranes; n) ααα(20R) C_{29} steranes/Σ ααα(20R) regular steranes; o) diasteranes/regular steranes; p) steranes/hopanes; r) %$Rc_{(MPI\ 1)}$ (RADKE & WELTE, 1983); s)%$Rm_{(MDR)}$ (RADKE, 1988).

Supplement 4

Table S1. Rock eval pyrolysis data, vitrinite reflectance and thermal alteration index from Cretaceous carbonates and shales.

Sample ID Well/Outcrop	Outcrop Well/Depth (m)	TOC (%)	S_1 (mg HC/g rock)	S_2 (mg HC/g rock)	S_1+S_2 (mg HC/g rock)	S_3 (mg CO_2/g rock)	T_{max} (°C)	HI (mg HC/g TOC)	OI (mg CO_2/g TOC)	PI	S_2/S_3	R_o (%)	TAI
Lower Cretaceous carbonates and shales													
Biokovo Duga Njiva5	OUT	0.74	0.54	5.25	5.79	0.28	421	709	38	0.09	18.75		1^{+-}
Biokovo Duga Njiva 6	OUT	1.39	0.62	9.38	10.00	0.70	425	675	50	0.06	13.40		1^{+-}
Bitelić Jelinjak 1	OUT	4.26	1.61	29.67	31.28	1.86	416	696	44	0.05	15.95	0.31	1^{+}
Bitelić Jelinjak 1a	OUT	3.74	0.46	24.63	25.09	1.65	418	659	44	0.02	14.93		1^{+}
Bitelić Jelinjak 6	OUT	1.75	0.71	12.71	13.42	0.51	413	726	29	0.05	24.92		1^{+}
Kamešnica Bili Brig 3	OUT	1.41	0.58	9.02	9.60	0.48	412	640	34	0.06	18.79		1^{+}
Kamešnica Bili Brig 9	OUT	1.81	0.46	14.19	14.65	0.52	422	784	29	0.03	27.29	0.34	1^{+-}
Kamešnica Bili Brig 10	OUT	1.02	0.50	7.55	8.05	0.41	420	740	40	0.06	18.41		1^{+-}
Kamešnica Bili Brig 11	OUT	1.72	0.70	13.67	14.37	0.51	423	795	30	0.05	26.80		1^{+-}
Kamešnica Bili Brig 12	OUT	1.72	0.53	13.27	13.80	0.67	419	772	39	0.04	19.81		1^{+-}
Kamešnica Bili Brig 9/1	OUT	2.36	2.32	17.33	19.65	0.56	416	734	24	0.12	30.95		1^{+-}
Kamešnica Bili Brig 14	OUT	1.35	1.14	10.55	11.69	0.42	412	781	31	0.10	25.12		1^{+-}
Ogorje Milešina 47	OUT	1.21	0.41	7.82	8.23	0.74	426	646	61	0.05	10.57		1^{+}
Tihaljina Zasjede 2a	OUT	1.41	0.30	8.67	8.97	0.87	410	615	62	0.03	9.97		1^{+}
Tihaljina Zasjede 3a	OUT	2.18	0.33	16.00	16.33	0.95	407	734	44	0.02	16.84		1^{+}
Tihaljina Zasjede 4a	OUT	1.10	0.26	7.96	8.22	0.45	405	724	41	0.03	17.69		1^{+}
Komiža	OUT	2.44	0.43	6.71	7.14		425	275		0.06		0.31	1^{+}-2-
Komiža 3	OUT	2.53	0.24	7.29	7.53	0.90	422	288	36	0.03	8.10	0.40	2^{-}
Komiža 7	OUT	1.92	0.07	1.83	1.90	1.16	414	95	60	0.04	1.58	0.35	2^{-}
Vrdovo Golo Brdo 100	OUT	2.82	1.56	19.43	20.99	0.58	424	689	21	0.07	33.50		1^{+}-2^{-}
Vrdovo Golo Brdo 101	OUT	5.36	2.84	38.32	41.16	1.20	422	715	22	0.07	31.93		1^{+}-2^{-}
Vrdovo Golo Brdo 102	OUT	1.53	0.75	10.30	11.05	0.49	425	673	32	0.07	21.02		1^{+}-2^{-}
Vrdovo Golo Brdo 104	OUT	1.78	0.16	13.72	13.88	0.47	427	771	26	0.01	29.19		1^{+}-2^{-}
Brač-1	4380	0.56	0.90	2.33	3.23	1.24	422	416	221	0.28	1.88		2^{-}
Dugi Otok-1	2515	0.94	0.80	6.24	7.04	0.41	430	664	44	0.11	15.22		2^{-}
Dugi Otok-1	2717	1.24	0.31	0.82	1.13	0.66	451	66	53	0.27	1.24		2^{-}-2
Dugi Otok-1	2717	1.16	0.28	1.15	1.43	0.47	447	99	41	0.20	2.45		2^{-}-2
Dugi Otok-1	3350	2.04	0.12	10.70	10.82	0.98	414	525	48	0.01	10.92		2
Dugi Otok-1	3556	2.83	0.22	16.65	16.87	1.07	418	588	38	0.01	15.56		2
Dugi Otok-1	3778	0.90	0.21	5.43	5.64	0.43	429	603	48	0.04	12.63		2
Dugi Otok-1	3857	0.82	0.46	5.81	6.27		431	709		0.07			2
Dugi Otok-1	3951	0.89	0.09	5.01	5.10		433	563		0.02		0.50	2
Dugi Otok-1	3953	0.92	0.08	3.36	3.44	0.19	434	365	21	0.02	17.68		2
Dugi Otok-1	3955	1.34	0.08	3.14	3.22	0.21	432	234	16	0.02	14.95		2
Dugi Otok-1	3957	0.92	0.08	3.36	3.44	0.19	434	365	21	0.02	17.68		2
Dugi Otok-1	3982	1.30	1.78	5.96	7.74	0.38	427	458	29	0.23	15.68		2
Kate-1	2439	2.73	7.91	16.48	24.39	0.15	431	604	5	0.32	109.87		2
Kate-1	2439	2.98	8.75	17.79	26.54	0.14	432	597	5	0.33	127.07		2
Kate-1	2440	0.84	2.41	4.40	6.81	0.14	433	524	17	0.35	31.43		2
Kate-1	2442	1.32	3.87	7.52	11.39	0.12	430	570	9	0.34	62.67		2
Kate-1	4383	1.94	12.32	3.73	16.05	3.16		192	163	0.77	1.18		2-2^{+}
Kate-1	5280	0.93	3.77	3.20	6.97	0.16	426	344	17	0.54	20.00		2^{+}
Kate-1	5281	1.26	5.27	4.85	10.12	0.09	427	385	7	0.52	53.89		2^{+}
Kate-1	5281	1.81	6.85	7.78	14.63	0.12	435	430	7	0.47	64.83		2^{+}
Kate-1	5290	1.56	1.51	6.67	8.18	0.12	438	428	8	0.18	55.58		2^{+}
Ravni Kotari-3	2624	1.16	0.88	4.22	5.10	0.40	428	364	34	0.17	10.55		2
Ravni Kotari-3	2666	0.98	2.07	4.35	6.42	0.46	427	444	47	0.32	9.46		2
Ravni Kotari-3	2667	0.95	2.40	4.42	6.82	0.42	425	465	44	0.35	10.52		2
Ravni Kotari-3	2709	1.05	2.88	5.93	8.81	0.34	427	565	32	0.33	17.44		2
Ravni Kotari-3	2713	0.83	0.54	3.07	3.61	0.42	430	370	51	0.15	7.31		2
Ravni Kotari-3	2716	1.26	1.08	4.16	5.24	0.45	430	330	36	0.21	9.24		2
Ravni Kotari-3	2920	1.48	0.24	1.34	1.58	0.31	445	91	21	0.15	4.32	0.71*	2^{+}
Ravni Kotari-3	2931	1.77	0.16	2.94	3.10	0.30	438	166	17	0.05	9.80		2^{+}-
Ravni Kotari-3	2931	1.91	0.39	2.57	2.96	0.40	433	135	21	0.13	6.43		2^{+}
Ravni Kotari-3	2931	1.30	0.40	1.09	1.49	0.22	469	84	17	0.27	4.95	0.73*	2^{+}
Ravni Kotari-3	2940	2.60	16.84	3.40	20.24		440	131		0.83			2^{+}-3^{-}
Ravni Kotari-3	2940	1.86	0.25	2.54	2.79		458	137		0.09			2^{+}-3^{-}
Ravni Kotari-3	2940	1.11	0.21	1.08	1.29	0.09	479	97	8	0.16	12.00		2^{+}-3^{-}
Ravni Kotari-3	2986	1.73	0.93	2.15	3.08	0.26	445	124	15	0.30	8.27		2^{+}-3^{-}

Table S1. *Continued.*

Sample ID Well/Outcrop	Outcrop Well/Depth (m)	TOC (%)	S_1 (mg HC/g rock)	S_2 (mg HC/g rock)	S_1+S_2 (mg HC/g rock)	S_3 (mg CO_2/g rock)	T_{max} (^{0}C)	HI (mg HC/g TOC)	OI (mg CO_2/g TOC)	PI	S_2/S_3	R_o (%)	TAI
Ravni Kotari-3	2988	1.76	0.31	1.55	1.86	0.29	443	88	16	0.17	5.34		2^{+}-3^{-}
Ravni Kotari-3	2989	1.25	0.34	1.82	2.16	0.35	443	146	28	0.16	5.20		2^{+}-3^{-}
Ravni Kotari-3	3107	3.30	0.25	1.12	1.37	0.29	436	34	9	0.18	3.86		2^{+}-3^{-}
Ravni Kotari-3	3107	0.96	0.24	1.75	1.99		442	182		0.12			2^{+}-3^{-}
Ravni Kotari-3	3107	1.17	3.71	6.22	9.93		422	532		0.37			2^{+}-3^{-}
Ravni Kotari-3	3108	0.79	7.97	11.82	19.79	0.50	425	1496	63	0.40	23.64		2^{+}-3^{-}
Ravni Kotari-3	3109	1.13	0.96	2.09	3.05	0.40	430	185	35	0.31	5.23		2^{+}-3^{-}
Ravni Kotari-3	3119	3.09	1.90	2.32	4.22	0.47	427	75	15	0.45	4.94		2^{+}-3^{-}
Ravni Kotari-3	3120	3.09	0.38	2.18	2.56	0.26	439	71	8	0.15	8.38		2^{+}-3^{-}
Ravni Kotari-4	2399	0.67	0.51	5.04	5.55		422	752		0.09			2^{-}
Susak more -1	1353	0.80	0.16	4.36	4.52		429	545		0.04			1^{+}
Vis-1	766	1.55	0.24	4.92	5.16	0.67	417	317	43	0.05	7.34		1^{+}
Vis-1	1217	0.96	0.17	5.03	5.20		419	524		0.03			1^{+}
Vis-1	1275	1.28	0.14	6.23	6.37	0.26	415	487	20	0.02	23.96		1^{+}
Vis-1	1632	0.51	0.12	2.33	2.45	0.20	418	457	39	0.05	11.65		1^{+}
Vis-1	2136	0.53	0.13	3.51	3.64	0.14	425	662	26	0.04	25.07		1^{+}
Upper Cretaceous carbonates and shales													
Bolobani 1/1	OUT	2.09	0.61	13.75	14.36	0.21	422	658	10	0.04	65.48		
Bolobani 1/2	OUT	1.14	0.34	6.56	6.90	0.16	426	576	14	0.05	41.00		
Bolobani 1/4	OUT	2.06	0.37	13.61	13.98	0.42	423	661	20	0.03	32.40		
Boljun 1	OUT	3.92	1.61	8.13	9.74	0.11	444	207	3	0.17	73.91		
Boljun 2	OUT	2.76	0.82	6.49	7.31	0.11	445	235	4	0.11	59.00		
Brač 50	OUT	5.31	2.37	39.77	42.14	0.91	411	749	17	0.06	43.70		
Brač 51	OUT	3.58	2.83	40.16	42.99	1.00	407	1122	28	0.07	40.16		
Brač 53	OUT	1.64	2.71	11.48	14.19	0.41	420	700	25	0.19	28.00		
Sumartin	OUT	8.57	2.63	29.18	31.81		432	340		0.08		0.48	
Dunj 3	OUT	0.84	0.29	5.80	6.09	0.39	419	690	46	0.05	14.87		
Dunj 4	OUT	0.95	0.26	6.19	6.45	0.61	420	652	64	0.04	10.15		
Dunj 5	OUT	1.86	0.48	14.62	15.10	0.47	414	786	25	0.03	31.11		
Seline 1	OUT	7.40	0.56	11.40	11.96		410	154		0.05			
Seline 2	OUT	24.55	4.33	80.77	85.10	21.80	414	329	89	0.05	3.71	0.47	
Seline 3	OUT	22.90	1.46	32.34	33.80		424	141		0.04			
Seline 4	OUT	23.58	3.55	75.80	79.35	23.87	418	321	101	0.04	3.18		
Hvar 1	OUT	5.32	1.24	43.74	44.98	0.65	405	822	12	0.03	67.29		
Hvar 3	OUT	54.05	6.75	66.85	73.60	37.77	425	124	70	0.09	1.77	0.20	
Hvar 108	OUT	0.95	0.57	4.77	5.34	0.22	434	502	23	0.11	21.68		
Krkmača 16a	OUT	3.11	0.97	22.54	23.51	0.63	416	725	20	0.04	35.78		
Krkmača 18a	OUT	4.25	1.34	28.19	29.53	1.05	413	663	25	0.05	26.85		
Kremena 1	OUT	6.17	2.30	54.79	57.09		417	888		0.04			
Kremena 105	OUT	28.45	9.81	234.49	244.30	3.85	408	824	14	0.04	60.91		
Kremena 105/1	OUT	5.16	1.40	37.79	39.19	1.44	412	732	28	0.04	26.24		
Ljubovo	OUT	2.37	1.34	18.45	19.79		410	778		0.07			
Glušci 74	OUT	1.66	1.26	9.75	11.01	0.59	415	587	36	0.11	16.53		
Glušci 76	OUT	1.40	1.52	9.08	10.60	0.51	409	649	36	0.14	17.80		
Dračevo 1	OUT	1.16	0.62	5.54	6.16		426	478		0.10			
Mirca 10/1	OUT	4.41	1.32	38.17	39.49	0.38	408	866	9	0.03	100.45		
Mirca 10/3	OUT	5.22	1.74	43.68	45.42	0.48	411	837	9	0.04	91.00		
Mirca 10/4	OUT	5.96	2.23	49.6	51.83	0.47	410	832	8	0.04	105.53		
Mirca 10/5	OUT	4.54	1.88	39.34	41.22	0.43	411	867	9	0.05	91.49		
Srijetež	OUT	2.50	1.05	13.84	14.89	0.88	421	554	35	0.07	15.73		
Plitvice 5/1	OUT	8.60	0.54	61.3	61.84	1.61	423	713	19	0.01	38.07		
Plitvice 5/2	OUT	11.11	1.17	79.24	80.41	1.69	424	713	15	0.01	46.89		
Plitvice	OUT	1.46	0.17	10.49	10.66		424	718		0.02			
Plitvice	OUT	16.32	1.94	138.90	140.84		425	851		0.01			
Primorski Dolac 2	OUT	5.01	0.17	11.16	11.33	4.56	429	555	227	0.02	2.45	0.35	
Upper Cretaceous carbonates and shales													
Bolobani 1/1	OUT	2.09	0.61	13.75	14.36	0.21	422	658	10	0.04	65.48		2^{-}
Bolobani 1/2	OUT	1.14	0.34	6.56	6.90	0.16	426	576	14	0.05	41.00		2^{-}
Bolobani 1/4	OUT	2.06	0.37	13.61	13.98	0.42	423	661	20	0.03	32.40		2^{-}
Boljun 1	OUT	3.92	1.61	8.13	9.74	0.11	444	207	3	0.17	73.91		2

Table S1. *Continued.*

Sample ID Well/Outcrop	Outcrop Well/Depth (m)	TOC (%)	S_1 (mg HC/g rock)	S_2 (mg HC/g rock)	S_1+S_2 (mg HC/g rock)	S_3 (mg CO_2/g rock)	T_{max} (^{0}C)	HI (mg HC/g TOC)	OI (mg CO_2/g TOC)	PI	S_2/S_3	R_o (%)	TAI
Boljun 2	OUT	2.76	0.82	6.49	7.31	0.11	445	235	4	0.11	59.00		2
Brač 50	OUT	5.31	2.37	39.77	42.14	0.91	411	749	17	0.06	43.70		1^{+}-2^{-}
Brač 51	OUT	3.58	2.83	40.16	42.99	1.00	407	1122	28	0.07	40.16		1^{+}-2^{-}
Brač 53	OUT	1.64	2.71	11.48	14.19	0.41	420	700	25	0.19	28.00		1^{+}-2^{-}
Sumartin	OUT	8.57	2.63	29.18	31.81		432	340		0.08		0.48	2^{-}
Dunj 3	OUT	0.84	0.29	5.80	6.09	0.39	419	690	46	0.05	14.87		1^{+}-2^{-}
Dunj 4	OUT	0.95	0.26	6.19	6.45	0.61	420	652	64	0.04	10.15		1^{+}-2^{-}
Dunj 5	OUT	1.86	0.48	14.62	15.10	0.47	414	786	25	0.03	31.11		1^{+}-2^{-}
Seline 1	OUT	7.40	0.56	11.40	11.96		410	154		0.05			1^{+}-2^{-}
Seline 2	OUT	24.55	4.33	80.77	85.10	21.80	414	329	89	0.05	3.71	0.47	2^{-}
Seline 3	OUT	22.90	1.46	32.34	33.80		424	141		0.04			1^{+}-2^{-}
Seline 4	OUT	23.58	3.55	75.80	79.35	23.87	418	321	101	0.04	3.18		1^{+}-2^{-}
Hvar 1	OUT	5.32	1.24	43.74	44.98	0.65	405	822	12	0.03	67.29		1^{+}-2^{-}
Hvar 3	OUT	54.05	6.75	66.85	73.60	37.77	425	124	70	0.09	1.77	0.20	1^{+}-2^{-}
Hvar 108	OUT	0.95	0.57	4.77	5.34	0.22	434	502	23	0.11	21.68		1^{+}-2^{-}
Krkmača 16a	OUT	3.11	0.97	22.54	23.51	0.63	416	725	20	0.04	35.78		1^{+}-2^{-}
Krkmača 18a	OUT	4.25	1.34	28.19	29.53	1.05	413	663	25	0.05	26.85		1^{+}-2^{-}
Kremena 1	OUT	6.17	2.30	54.79	57.09		417	888		0.04			1^{+}-2^{-}
Kremena 105	OUT	28.45	9.81	234.49	244.30	3.85	408	824	14	0.04	60.91		1^{+}-2^{-}
Kremena 105/1	OUT	5.16	1.40	37.79	39.19	1.44	412	732	28	0.04	26.24		1^{+}-2^{-}
Ljubovo	OUT	2.37	1.34	18.45	19.79		410	778		0.07			1^{+}-2^{-}
Glušci 74	OUT	1.66	1.26	9.75	11.01	0.59	415	587	36	0.11	16.53		1^{+}-2^{-}
Glušci 76	OUT	1.40	1.52	9.08	10.60	0.51	409	649	36	0.14	17.80		1^{+}-2^{-}
Dračevo 1	OUT	1.16	0.62	5.54	6.16		426	478		0.10			1^{+}-2^{-}
Mirca 10/1	OUT	4.41	1.32	38.17	39.49	0.38	408	866	9	0.03	100.45		1^{+}-2^{-}
Mirca 10/3	OUT	5.22	1.74	43.68	45.42	0.48	411	837	9	0.04	91.00		1^{+}-2^{-}
Mirca 10/4	OUT	5.96	2.23	49.6	51.83	0.47	410	832	8	0.04	105.53		1^{+}-2^{-}
Mirca 10/5	OUT	4.54	1.88	39.34	41.22	0.43	411	867	9	0.05	91.49		1^{+}-2^{-}
Srijetež	OUT	2.50	1.05	13.84	14.89	0.88	421	554	35	0.07	15.73		1^{+}-2^{-}
Plitvice 5/1	OUT	8.60	0.54	61.3	61.84	1.61	423	713	19	0.01	38.07		1^{+}-2^{-}
Plitvice 5/2	OUT	11.11	1.17	79.24	80.41	1.69	424	713	15	0.01	46.89		1^{+}-2^{-}
Plitvice	OUT	1.46	0.17	10.49	10.66		424	718		0.02			1^{+}-2^{-}
Plitvice	OUT	16.32	1.94	138.90	140.84		425	851		0.01			1^{+}-2^{-}
Primorski Dolac 2	OUT	5.01	0.17	11.16	11.33	4.56	429	555	227	0.02	2.45	0.35	1^{+}-2^{-}
Primorski Dolac 2	OUT	5.01	0.17	11.16	11.33	4.56	429	555	227	0.02	2.45	0.35	1^{+}-2^{-}
Primorski Dolac 3	OUT	0.71	1.06	4.52	5.58	0.48	423	637	68	0.19	9.42		1^{+}-2^{-}
Šajini 2/1	OUT	2.40	0.27	15.40	15.67	1.11	416	642	46	0.02	13.87		1^{+}-2^{-}
Šajini 2/2	OUT	2.89	0.51	20.56	21.07	0.84	413	711	29	0.02	24.48		1^{+}-2^{-}
Slivno Ravno 102	OUT	10.19	1.56	82.57	84.13	1.95	413	810	19	0.02	42.34		1^{+}-2^{-}
Stilja 48a	OUT	4.89	2.40	37.86	40.26	1.82	431	774	37	0.06	20.80		1^{+}-2^{-}
Stilja 48c	OUT	0.99	0.43	6.68	7.11	0.30	418	675	30	0.06	22.27		1^{+}-2^{-}
Stilja 1c	OUT	4.28	0.93	30.68	31.61	0.94	411	717	22	0.03	32.64		1^{+}-2^{-}
Trlji	OUT	5.32	1.24	43.74	44.98	0.65	405	822	12	0.03	67.29	0.30	1^{+}-2^{-}
Trlji 1	OUT	11.81	3.00	90.1	93.10	2.60	414	763	22	0.03	34.65		1^{+}-2^{-}
Trlji 2	OUT	21.84	4.20	149.3	153.50	5.40	410	684	25	0.03	27.65		1^{+}-2^{-}
Trlji 3	OUT	11.40	2.50	85.2	87.70	3.60	415	747	32	0.03	23.67		1^{+}-2^{-}
Trlji 3/1	OUT	6.10	0.72	54.73	55.45	0.37	408	897	6	0.01	147.92		1^{+}-2^{-}
Trlji 3/2	OUT	5.88	0.52	51.82	52.34	0.48	407	881	8	0.01	107.96		1^{+}-2^{-}
Trlji 4	OUT	10.93	2.60	92.9	95.50	2.70	416	850	25	0.03	34.41		1^{+}-2^{-}
Trlji 5	OUT	5.13	2.67	28.23	30.90	2.81	413	550	55	0.09	10.05	0.53	2^{-}
Trlji 6	OUT	2.69	1.30	18.54	19.84	1.03	413	689	38	0.07	18.00	0.49	2^{-}
Trlji 10	OUT	4.48	1.15	34.90	36.05		409	779		0.03			2^{-}
Premuda-1	1483	1.23	0.15	5.37	5.52	0.62	413	437	50	0.03	8.66		1^{+}
Premuda-1	1625	1.02	0.95	4.85	5.80	0.67		475	66	0.16	7.24	0.60*	2^{-}
Premuda-1	1625	2.82	0.84	14.52	15.36	0.77	431	515	27	0.05	18.86		2^{-}
Premuda-1	1765	1.69	0.53	9.25	9.78	1.18	435	547	70	0.05	7.84		2
Premuda-1	1770	1.14	0.13	6.91	7.04	0.59	406	606	52	0.02	11.71		2
Premuda-1	1770	3.68	0.78	24.42	25.20		407	664		0.03			2
Premuda-1	1770	2.63	0.32	16.62	16.94	0.95	402	632	36	0.02	17.49		2
Premuda-1	1771	3.66	0.36	22.57	22.93	1.20	409	617	33	0.02	18.81		2

Table S1. *Continued.*

Sample ID Well/Outcrop	Outcrop Well/Depth (m)	TOC (%)	S_1 (mg HC/g rock)	S_2 (mg HC/g rock)	S_1+S_2 (mg HC/g rock)	S_3 (mg CO_2/g rock)	T_{max} (^{0}C)	HI (mg HC/g TOC)	OI (mg CO_2/g TOC)	PI	S_2/S_3	R_o (%)	TAI
Ravni Kotari-3	529	0.96	0.14	4.37	4.51	0.60	410	455	63	0.03	7.28	0.30	1^+
Ravni Kotari-3	530	2.37	0.59	13.12	13.71	0.74	405	554	31	0.04	17.73		1^+
Ravni Kotari-3	1373	1.24	1.03	9.00	10.03		410			0.10			1^+
Ravni Kotari-3	1373	4.43	0.44	14.50	14.94	0.37	411	327	8	0.03	39.19		1^+
Ravni Kotari-3	1373	1.13	0.65	6.57	7.22	1.04	412	581	92	0.09	6.32		1^+
Ravni Kotari-3	1373	0.93	0.07	6.80	6.87		421			0.01			1^+
Ravni Kotari-3	1374	4.74	4.32	10.76	15.08		436	227		0.29			1^+
					Migrabitumen								
Akrap Duboki Dolac 75	OUT	6.50	26.20	38.06	64.26	1.45	420	586	22	0.41	26.25	0.08-0.16*	
Donji Dolac Okruglica 70	OUT	7.56	14.83	44.91	59.74	0.67	426	592	9	0.25	67.03	0.06-0.18	
Donji Dolac Okruglica 73	OUT	0.78	2.79	4.38	7.17	0.26	420	562	33	0.39	16.85		
Prugovo	OUT	12.56	19.31	79.25	98.56	0.86	426	631	7	0.20	92.15	0.06-0.12*	
Radošić Lastva 10	OUT	4.07	3.88	21.04	24.92	1.04	424	517	26	0.16	20.23		
Radošić Ninčevića 12	OUT	2.60	5.23	16.07	21.30	0.38	432	618	15	0.25	42.29	0.08-0.15*	
Radošić Tenderi 14	OUT	1.25	2.95	8.47	11.42	0.45	426	678	36	0.26	18.82		
Rošca 87	OUT	4.63	9.39	30.29	39.68	0.58	424	654	13	0.24	52.22	0.07-0.18*	
Vrgorac	OUT	1.32	0.12	2.43	2.55		428	184		0.05			
Vrgorac-Kozica 5a	OUT	2.93	7.06	19.87	26.93	0.18	427	678	6	0.26	110.39	0.08-0.20*	
Vrgorac -Kozica 5b	OUT	2.95	6.11	20.50	26.61	0.21	428	695	7	0.23	97.62		
Vrgorac 12/1	OUT	2.91	5.52	20.64	26.16	0.33	422	709	11	0.21	62.55	0.06-0.19*	

OUT outcrops; TOC total organic carbon; S_1 the amount of free hydrocarbons; S_2 the amount of hydrocarbon generated through thermal cracking; S_3 the amount of CO_2 produced during pyrolysis; T_{max} the temperature of maximum hydrocarbon generation; PI production index; S_1+S_2 generative potential (PETERS & CASSA, 1994); %R_o vitrinite reflectance (VR); *%R_o Vitrinite reflectance measured on solid bitumen, bitumen reflectance (BR, %R_b). The corresponding vitrinite reflectance is calculated using the equation %R_o = 0.61 * %R_b + 0.40 proposed by JACOB (1989); TAI thermal alteration index; TAI to VR (%R_o) correlation scale: 1^+<0.35%R_o, 2^- 0.35 – 0.45%R_o, 2 0.45 – 0.55%R_o, 2^+ 0.55 – 0.70%R_o, 3^- 0.70 – 0.95%R_o. New data have been integrated with representative outcrop data from ŠPANIĆ et al. (1995) and well data from BARIĆ et al. (1988), COTA & BARIĆ (1998) and BARIĆ & COTA (1999).

Table S2. Chemical data, gas chromatography parameters and stable carbon isotope ratios of extracts from Cretaceous carbonates, marls and shales.

Sample ID Well/Outcrop	Outcrop Well/Depth (m)	Sat. (%)	Aro. (%)	NSO+Asph. (%)	Pr/n-C_{17}	Ph/n-C_{18}	Pr/Ph	$S_{Ker.}$ (%)	$S_{Bit.}$ (%)	$\delta^{13}C_{Ker.}$ (‰, VPDB)	$\delta^{13}C_{Bit.}$ (‰, VPDB)	$\delta^{13}C_{Asph.}$ (‰, VPDB)	$\delta^{13}C_{NSO.}$ (‰, VPDB)	$\delta^{13}C_{Aro.}$ (‰, VPDB)	$\delta^{13}C_{Sat.}$ (‰, VPDB)
						Lower Cretaceous extracts									
Biokovo-Duga Njiva 5	OUT				0.40	0.69	1.68	3.66							
Dinara-Bitelić 15	OUT	5.42	8.46	86.14	0.44	0.40	1.71	16.20		-22.02					
Ogorje Milešina 38	OUT				0.42	0.71	0.78								
Tihaljina-Zasjede 2a	OUT				0.32	0.35	0.83	5.49							
Vis-Komiža 3	OUT				0.34	0.37	0.75	5.21							
Vis-Komiža 17	OUT				0.64	0.58	0.73								
Vrdovo Golo Brdo 103	OUT				0.40	0.58	2.67								
Dugi Otok-1	2515	12.20	16.60	71.20	0.43	0.86	0.37								
Dugi Otok-1	2965				0.46	0.88	0.56				-27.93				
Dugi Otok-1	3852	7.50	19.80	72.70	0.74	0.94	0.80				-26.91				
Premuda-1	2831										-25.78				
Ravni Kotari-3	2713				0.29	0.72	0.48							-22.60	-22.80
Ravni Kotari-3	2918				0.28	0.55	0.40								
Ravni Kotari-3	3107				0.25	0.40	0.67							-23.50	-24.40
Ravni Kotari-3	3143				0.41	1.06	0.38								
Ravni Kotari-4	2399	3.70	0.90	94.00	0.57	0.90	0.31								
Vis-1	766				0.76	0.93	0.33								
Vis-1	1217				0.75	1.09	0.35								
Vis-1	1632				0.90	1.09	0.53								
Vis-1	2136				0.85	0.88	0.56								
						Upper Cretaceous extracts									
Brač Mirca 50	OUT	5.21	9.84	84.95	0.84	0.96	1.57								
Brač Brizi 51	OUT	6.39	14.38	79.23	0.73	0.95	1.30								
Brač- Sumartin	OUT	5.30	22.90	71.80											
Hvar Sućuraj 108	OUT				0.48	0.68	1.31								
Korčula Krkmača 1a	OUT				0.44	0.47	2.65			-21.58					
Kremena Ljubić p. 105	OUT	5.90	7.50	86.60				17.40		-23.67					

Table S2. *Continued.*

Sample ID Well/Outcrop	Outcrop Well/Depth (m)	Sat. (%)	Aro. (%)	NSO+Asph. (%)	Pr/n-C_{17}	Ph/n-C_{18}	Pr/Ph	$S_{Ker.}$ (%)	$S_{Bit.}$ (%)	$\delta^{13}C_{Ker.}$ (‰, VPDB)	$\delta^{13}C_{Bit.}$ (‰, VPDB)	$\delta^{13}C_{Asph.}$ (‰, VPDB)	$\delta^{13}C_{NSO.}$ (‰, VPDB)	$\delta^{13}C_{Aro.}$ (‰, VPDB)	$\delta^{13}C_{Sat.}$ (‰, VPDB)
Mirca	OUT									-17.88					
Mirca 10/1	OUT				0.34	0.35	0.35	20.43	15.58		-25.25	-24.72	-24.95	-26.43	-27.35
Mirca 10/2	OUT	7.20	7.40	85.40	0.31	0.37	0.74			-26.02	-26.82				
Mirca 10/3	OUT				0.24	0.33	0.63	17.28		-23.86	-25.75				
Mirca 10/4	OUT				0.23	0.30	0.59	19.26			-24.27	-23.72	-24.34	-25.41	-26.34
Mirca 10/5	OUT				0.27	0.37	0.55	16.43			-25.02			-25.04	-26.64
Plitvice 5/1	OUT				0.30	0.39	0.71	9.57		-25.37	-25.39	-24.91	-25.30	-25.99	-26.39
Plitvice 5/2	OUT	1.70	12.00	86.30	0.33	0.41	0.69	10.46	11.60						
Plitvice Hajduk mlin 42	OUT	2.30	8.90	88.80	0.89	1.24	0.66			-29.12					
Primorski Dolac-Preslo 2	OUT				0.79	1.16	0.68								
Primorski Dolac-Preslo 3	OUT	6.28	11.64	82.08	0.50	0.68	2.61	7.11							
Šajini 2/1	OUT				0.34	0.46	0.76	7.92	6.37	-26.10	-26.85				
Šajini 2/2	OUT	3.70	7.40	88.90	0.34	0.44	0.71	9.10			-26.26	-26.14	-26.46	-25.87	-26.50
Šajini 2/3	OUT				0.38	0.46	0.62				-25.82	-25.84	-26.18	-25.96	-26.27
Slivno Ravno Kremena 102	OUT	3.10	6.30	90.60				18.20		-22.96					
Stilja -Vukmir 48a	OUT				0.45	0.56	1.57	5.99							
Trlji 3/1	OUT	0.60	1.50	97.90	0.32	0.41	0.96		13.27		-26.88	-24.03	-26.97	-27.81	-26.71
Trlji 3/2	OUT				0.28	0.35	0.83				-26.74	-24.03	-26.96	-26.30	-26.89
Premuda-1	1625				0.67	1.54	0.43				-31.10			-27.60	-29.00
Premuda-1	1625				0.54	0.57	0.38								
Premuda-1	1770	2.60	2.20	95.20	0.44	0.49	0.37	13.24		-28.47	-27.93	-26.55	-28.70	-29.14	-28.60
Premuda-1	1770				0.55	1.74	0.39			-27.07					
Ravni Kotari-3	1373										-25.01				
						Oil seep, migrabitumen									
Akrap Duboki Dolac 75	OUT	13.82	18.10	68.11					11.50		-22.95				
Donji Dolac Okruglica 70	OUT	8.88	19.22	71.90							-23.43	-24.39	-24.58	-24.71	-26.34
Prugovo 3	OUT	9.57	21.86	68.57							-23.99				
Radošić Lastva 10	OUT	2.99	3.38	93.63					10.60		-24.13				
Vrgorac	OUT	6.50	24.10	69.40							-23.29				
Vrgorac 12/1	OUT	6.10	15.20	78.70					9.75		-24.91	-23.78	-24.07	-24.02	-25.26
Vrgorac-Kozica 5a	OUT	14.11	22.99	62.90							-24.12				
Brač Škrip 53	OUT	5.97	10.78	83.25	0.46	0.57	2.43				-22.95				
Rebići	OUT										-25.46	-25.20	-26.86	-27.05	-27.30
Vinišće	OUT										-23.42				
Vinišće	OUT	10.80	37.80	51.40	0.70	0.76					-25.10	-25.21	-24.53	-25.54	-26.85
Marina Trogir	OUT	23.90	36.00	40.10	0.76	0.65	0.58		7.26		-23.97			-24.65	-25.78
Primorski Dolac	OUT	11.10	23.70	65.20					15.20		-24.10				

Sat. saturated hydrocarbons; Aro. aromatic hydrocarbons; NSO nitrogen (N), sulphur (S), and oxygen (O)-bearing compounds; Asph. asphaltenes; Pr pristane; Ph phytane; S sulphur; Ker. kerogen; Bit. bitumen; ^{13}C stable carbon isotope ratio; VPDB Vienna Pee Dee Belemnite standard.

Table S3. Source and maturity related biomarker and non-biomarker ratios of extracts from Cretaceous carbonates, marls and shales.

Sample ID Well/Outcrop	Outcrop Well/Depth (m)	a	b	c	d	e	f	g	h	i	j	k	l	m	n
Vrgorac 12/1	OUT	0.00	1.37	0.08*	0.56	0.16	0.61		0.62	0.39	24.47	35.54	40.00		
Rebići	OUT	0.00	0.92	0.03*	0.56	0.15	0.50		0.67	0.50	22.69	26.12	51.18		0.02
Vinišće	OUT	0.00	2.83	0.05*	0.53	0.33	0.63		0.62	0.40	35.83	25.43	38.74		0.03
Mirca 10/1	OUT	0.00	0.22	0.05*	0.41	0.11	0.45		0.50	0.17	19.92	43.54	36.55		0.13
Mirca 10/4	OUT	0.00	0.31	0.02*	0.41		0.63		0.52	0.18	14.45	40.87	40.68		0.09
Mirca 10/5	OUT	0.00	0.36	0.05*	0.43		0.75		0.54	0.19	18.10	35.24	43.67		
Ravni Kotari-3	2713	0.00	0.67	0.02*	0.50	0.23			0.69	0.52				0.05	
Ravni Kotari-3 oil	2856	0.00	0.52	0.02*	0.49	0.21			0.57	0.45				0.04	
Vis-1	1632	0.00	0.88	0.26	0.51		0.49	0.98	0.56	0.46	36.75	23.40	39.85	0.27	0.31
Vis-1	2136	0.00	0.38	0.20	0.34	0.05	0.46	0.33	0.40	0.20	38.55	10.81	50.64	0.04	0.12

a) oleanane/hopane (Ol/H); b) 17α,21β–C_{30} norhopane/17α,21β–C_{30} hopane (NH/H); c) 17α–C_{27} trisnorhopane/(17α–C_{27} trisnorhopane+18α–C_{27} trisnorneohopane) (Ts/(Ts + Tm)), *Ts/Tm; d) 22S/(22S + 22R) 17α,21β–C_{32} homohopane; e) gammacerane/hopane (G/H); f) 17α,21β–C_{31} (22R) homohopane/17α,21β–C_{30} hopane (C_{31}(R)/H); g) 17α.21β–C_{35} (22S) homohopane/17α,21β–C_{34} (22S) homohopane (C_{35}(S)/C_{34}(S)); h) αββ/(αββ+ααα) C_{29} sterane; i) 20S/(20S + 20R) ααα C_{29} sterane; j) ααα(20R) C_{27} steranes/Σ ααα(20R) regular steranes; k) ααα(20R) C_{28} steranes/Σ ααα(20R) regular steranes; l) ααα(20R) C_{29} steranes/Σ ααα(20R) regular steranes; m) diasteranes/regular steranes; n) steranes/hopanes.

Supplement 5

Table S1. Rock eval pyrolysis data, vitrinite reflectance and thermal alteration index from Palaeogene and Neogene marls and shales.

Sample ID Well/Outcrop	Outcrop Well/Depth (m)	TOC (%)	S_1 (mg HC/g rock)	S_2 (mg HC/g rock)	S_1+S_2 (mg HC/g rock)	S_3 (mg CO_2/g rock)	T_{max} (^oC)	HI (mg HC/g TOC)	OI (mg CO_2/g TOC)	PI	S_2/S3	R_o (%)	TAI
Neogene marls and shales													
Rude 27/3	OUT	48.10	16.66	399.60	416.26		440	831		0.04		0.26	1^+
Rude 1	OUT	17.40	6.83	133.95	140.78	7.98	435	770	46	0.05	16.79	0.26	1^+
Rude 3	OUT	49.82	23.70	461.50	485.20	14.30	436	926	29	0.05	32.27		1^+
Rude 4	OUT	37.00	13.20	364.30	377.50	14.70	434	985	40	0.03	24.78		1^+
Rude 5	OUT	10.57	3.80	98.60	102.40	4.50	433	933	43	0.04	21.91	0.22	1^+
Rude 11	OUT	44.16	7.79	345.05	352.84	34.77	436	781	79	0.02	9.92	0.26	1^+
Rude 137c	OUT	3.08	0.70	28.00	28.70	2.11	439	909	69	0.02	13.27		1^+
Rude 15	OUT	3.94	1.24	33.13	34.37	2.80	435	841	71	0.04	11.83		1^+
Rude 137b	OUT	1.47	0.34	12.27	12.61	1.08	438	835	73	0.03	11.36	0.22	1^+
Sutina 24	OUT	2.43	0.35	6.90	7.25	2.58	426	284	106	0.05	2.67	0.21	1^+
Sutina 28	OUT	9.41	0.17	4.89	5.06	9.30	427	52	99	0.03	0.53	0.27	1^+
Paleogene carbonates. marls and shales													
Buzeta-1	OUT	9.61	0.86	62.58	63.44	3.30	434	651	34	0.01	18.96		2^-
Buzeta-2	OUT	2.78	1.28	21.49	22.77	0.51	429	773	18	0.06	42.14		2^-
Ličke kuće-1	OUT	4.47	0.37	36.65	37.02	0.43	438	820	10	0.01	85.23		2
Ličke kuće-5	OUT	13.61	1.19	128.78	129.97	2.19	434	946	16	0.01	58.80		2
Vladića Mlin-1	OUT	2.64	0.22	13.60	13.82	0.47	435	515	18	0.02	28.94		2
Vladića Mlin-3	OUT	3.67	0.24	25.59	25.83	0.63	435	697	17	0.01	40.62		2
Vladića Mlin-4	OUT	3.87	0.18	16.31	16.49	2.02	433	421	52	0.01	8.07		2
Brezovo Polje-1	OUT	3.28	0.43	16.36	16.79	0.72	431	499	22	0.03	22.72		2^-
Brezovo p. Stupa m. 2	OUT	3.60	0.43	16.64	17.07	0.58	428	462	16	0.03	28.69		2^-
Koromačno II 33	OUT	0.66	0.51	4.06	4.57	0.37	427	615	56	0.11	10.97		2^-
Padr T-3-3/4	OUT	1.20	0.11	2.42	2.53	0.40	435	202	33	0.04	6.05		2
Baška 57	OUT	7.61	0.06	6.91	6.97	2.94	434	91	39	0.01	2.35		2
Baška 58	OUT	12.75	24.41	47.04	71.45	20.72		369	163	0.34	2.27	0.44	2
Karlovac-2	2472	0.51	0.05	0.31	0.36	0.89	431	61	175	0.14	0.35		2
Karlovac-2	2732	1.15	0.14	2.74	2.88	0.51	433	238	44	0.05	5.37		2
Karlovac-2	2793	4.69	0.08	6.43	6.51	1.00	432	137	21	0.01	6.43		2
Karlovac-2	2972	4.70	0.16	7.34	7.50	0.94	434	156	20	0.02	7.81		$2\text{-}2^+$
Karlovac-3	1557	1.08	0.19	4.89	5.08	0.15	434	453	14	0.04	32.60		2
Melita-1	2674	1.19	0.33	6.12	6.45	1.06	424	514	89	0.05	5.77		$2^-\text{-}2$
Melita-1	2676	3.78	1.71	19.54	21.25	1.31	411	517	35	0.08	14.92		$2^-\text{-}2$
Melita-1	2679	6.02	2.36	42.11	44.47	2.03	421	700	34	0.05	20.74		$2^-\text{-}2$
Melita-1	2872	1.39	0.31	5.48	5.79	0.95	418	394	68	0.05	5.77		$2^-\text{-}2$

OUT outcrops; TOC total organic carbon; S_1 the amount of free hydrocarbons; S_2 the amount of hydrocarbon generated through thermal cracking; S_3 the amount of CO_2 produced during pyrolysis; T_{max} the temperature of maximum hydrocarbon generation; PI production index; S_1+S_2 generative potential (PETERS & CASSA, 1994); %R_o vitrinite reflectance (VR); TAI thermal alteration index; TAI to VR (%R_o) correlation scale: 1^+<0.35%R_o, 2^- 0.35 — 0.45%R_o, 2 0.45 — 0.55%R_o, 2^+ 0.55 — 0.70%R_o.

Table S2. Gas chromatography parameters and stable carbon isotope ratios of extracts from Palaeogene and Neogene carbonates, marls and shales.

Sample ID Well/Outcrop	Outcrop Well/Depth (m)	Pr/nC_{17}	Ph/nC_{18}	Pr/Ph	$\delta^{13}C_{Ker.}$ (‰, VPDB)	$\delta^{13}C_{Bit.}$ (‰, VPDB)	$\delta^{13}C_{Sat.}$ (‰, VPDB)	$\delta^{13}C_{Aro.}$ (‰, VPDB)	$\delta^{13}C_{NSO}$ (‰, VPDB)	$\delta^{13}C_{Asph.}$ (‰, VPDB)
Neogene extracts										
Rude 1	OUT	0.63	0.73	2.02						
Rude 11	OUT	0.67	0.77	2.12						
Paleogene extracts										
Buzeta-1	OUT	1.06	1.33	0.66						
Ličke kuće-1	OUT	1.20	1.35	0.77	-30.56	-29.51				
Ličke kuće-4	OUT				-29.62	-30.95				
Vladića mlin-1	OUT				-25.16	-26.11				
Vladića Mlin-3	OUT				-28.61	-29.7				
Vladića Mlin-4	OUT	2.23	1.08	1.74						
Brezovo Polje-1	OUT				-27.87	-28.01				
Buzet Sovinjsko b. 19	OUT	0.60	0.76	0.69						
Koromačno II 33	OUT	2.08	4.45	0.40						
Padr T-3-3/4a	OUT	0.50	0.40	1.16						
Baška 57	OUT	0.69	0.88	0.90						
Rab Lopar	OUT	0.46	0.17	1.18						
Vodovađa	OUT	3.95	0.63	0.33						
G.Lukavac	OUT									
Dabrica	OUT	0.70	0.70	1.46						
Čičevo	OUT	0.38	0.30	1.55						
Karlovac-2	2472				-25.75					
Karlovac-2	2732	2.42		0.66						
Karlovac-2	2733	1.08	1.6	1.35						
Karlovac-2	2902	1.57	4.91	0.24	-27.11					
Karlovac-2	2972	2.05	0.99	0.37						
Melita-1	2676	0.70	0.69	0.90			-17.98	-18.09	-15.4	-14.16
Melita-1	2679	0.71	0.77	1.02			-18.34	-17.2	-15.9	-14.77
Melita-1	2872	0.80	0.48	1.70					-23.47	

Pr pristane; Ph phytane; ^{13}C stable carbon isotope ratio; VPDB Vienna Pee Dee Belemnite standard; Ker. kerogen; Bit. bitumen; Sat. saturated hydrocarbons; Aro. aromatic hydrocarbon; NSO nitrogen (N), sulphur (S), and oxygen (O)-bearing compounds; Asph. asphaltenes.